Stony Brook University

A common telomeric gene silencing assay is affected by nucleotide metabolism and the DNA damage response: implications for the role of PCNA in heterochromatin formation.

A Dissertation Presented

by

Marlies Petra Rossmann

to

The Graduate School

in Partial Fulfillment of the

Requirements

for the Degree of

Doctor of Philosophy

in

Genetics

Stony Brook University

August 2010

Stony Brook University

The Graduate School

Marlies Petra Rossmann

We, the dissertation committee for the above candidate for the
Doctor of Philosophy degree,
hereby recommend acceptance of this dissertation.

Bruce Stillman, Ph.D., President
Cold Spring Harbor Laboratory
Dissertation Advisor

Nancy Hollingsworth, Ph.D., Professor
Department of Biochemistry and Cell Biology, Stony Brook University
Chairperson of Defense

Bruce Futcher, Ph.D., Professor
Department of Molecular Genetics and Microbiology, Stony Brook University

Rolf Sternglanz, Ph.D., Professor
Department of Biochemistry and Cell Biology, Stony Brook University

Rodney Rothstein, Ph.D., Professor
Department of Genetics & Development, Columbia University Medical Center
Outside member

This dissertation is accepted by the Graduate School

Lawrence Martin, Ph.D.
Dean of the Graduate School

Abstract of the Dissertation

A common telomeric gene silencing assay is affected by nucleotide metabolism and the DNA damage response: implications for the role of PCNA in heterochromatin formation.

by

Marlies Petra Rossmann

Doctor of Philosophy

in

Genetics

Stony Brook University

2010

In budding yeast, telomere position effect variegation (TPEV) was discovered when prototrophic markers were placed near chromosome ends and was interpreted to reflect a reversible form of heterochromatin. Selection for or against these markers demonstrated roles for several proteins in telomeric heterochromatin formation; these include the SIR protein complex, chromatin assembly factors (CAF-1, Asf1), PCNA as a DNA replication factor as well as DNA damage checkpoint proteins.

PCNA (*POL30*) in particular as a component of the core DNA replication machinery has been shown to link DNA replication to the inheritance of nucleosomes and was, by extension, proposed to help maintain silenced chromatin. In analyzing the phenotype of the silencing defective *pol30-8* mutant using various TPEV reporter strains I found that this mutant exhibits only a very

subtle telomeric silencing defect in comparison to a *sir3Δ* mutant. Furthermore, employing the common *URA3* reporter at the telomere of chromosome VIIL that can be counter-selected with 5-FOA in a genetic screen, I identified high-copy suppressors of the *pol30-8*-dependent silencing defect. Interestingly, one of the suppressors, *CDC21*, the thymidylate synthase gene, also counteracted the telomeric silencing defect of a strain deleted for *DOT1*, encoding the only histone H3K79 methyltransferase in *S. cerevisiae*. Gene expression analysis of *pol30-8* mutant and *dot1* mutant strains surprisingly revealed that *dot1Δ* deletion results in repression of telomeric gene expression without an effect on Sir2/4 occupancy. On the other hand, the *pol30-8* mutation was linked to a general up-regulation of normally poorly expressed genes. Notably, the effect of *pol30-8* correlated with decreased histone levels. Among the affected genes were the ribonucleotide reductase (RNR) genes whose expression could be further induced by treatment with 5-FOA. Importantly, inhibition of RNR activity as well as mutations in the *RAD53* DNA damage response pathway rescued the sensitivity of *pol30-8 URA3*-VIIL cells to 5-FOA.

I speculate that in the context of low *URA3* expression such as in a *URA3*-VIIL strain a misbalance between Ura3, RNR and Cdc21 activity is responsible for a higher conversion rate of 5-FOA into its toxic metabolites which accounts for the 5-FOA sensitivity seen in *pol30-8* and *dot1Δ URA3*-VIIL mutants. In conclusion, while I found that Pol30 facilitates normal histone distribution with consequences for global gene expression, neither *pol30-8* nor *dot1Δ* mutants are defective in telomeric heterochromatin formation.

Für meine Eltern.

Für Michael †.

TABLE OF CONTENTS

ILLUSTRATIONS

TABLES

ABBREVIATIONS

aa	amino acid(s)
ACS	ARS consensus sequence
ALT	alternative lengthening of telomeres
ARS	autonomously replicating sequence
ASF1	anti-silencing function 1
3-AT	3-amino-1,2,4-triazole
ATP	adenosine triphosphate
BAH	bromo-adjacent homology
BLM	bleomycin
bp	base pair(s)
CAF-1	chromatin assembly factor 1
ChIP	chromatin immunoprecipitation
CsCl	cesium chloride
dATP	deoxyadenosine triphosphate
dCTP	deoxycytidine triphosphate
dGTP	deoxyguanosine triphosphate
D. melanogaster, *Dm*	*Drosophila melanogaster*
DNA	deoxyribonucleic acid
dNTP	deoxyribonucleoside triphosphate
DSB	double-strand break

dTMP	deoxythymidine monophosphate
dTTP	deoxythymidine triphosphate
dUMP	deoxyuridine monophosphate
E. coli	*Escherichia coli*
5-FOA	5-fluoroorotic acid
5-FU	5-fluorouracil
GO	Gene Ontology
HDAC	histone deacetylase
HU	hydroxyurea
LTR	long terminal repeat
MMS	methyl methanesulfonate
MTHF	N^5,N^{10}-methylenetetrahydrofolate
NAD^+	nicotinamide adenine dinucleotide
4-NQO	4-nitroquinoline 1-oxide
OMPdecase	orotidine-5'-phosphate decarboxylase
ON	overnight
ORC	origin recognition complex
ORF	open reading frame
PCI	phenol-chloroform-isoamyl alcohol
PCNA	proliferating cell nuclear antigen
PEV	position effect variegation
PIP box	PCNA-interacting protein box
pre-RC	pre-replication complex

qPCR	quantitative polymerase chain reaction
RFC	replication factor C
RNA	ribonucleic acid
RNR	ribonucleotide reductase
RT	room temperature
RT-qPCR	reverse transcription followed by quantitative polymerase chain reaction
SB	SDS sample buffer
SC	synthetic complete
S. cerevisiae	*Saccharomyces cerevisiae*, budding yeast
SIR	silent information regulator
S. pombe	*Schizosaccharomyces pombe*, fission yeast
TPEV	telomere position effect variegation
ts	temperature sensitive
UV	ultraviolet light
wt	wild type
YCp	yeast centromeric plasmid
YEp	yeast episomal plasmid

ACKNOWLEDGEMENTS

There are many people to thank. Foremost I am indebted to Dr. Bruce Stillman, for giving me the freedom and supporting me in my work on the role of DNA replication in heterochromatin formation, which was what I hoped to study after being inspired by the Graduate Genetics class at Stony Brook University. Despite his busy schedule his door was always open for helpful and stimulating discussions. I furthermore deeply thank him for his understanding when I was “out of service” for a long time due to two hip surgeries. Being in his laboratory over the past eight years, I had the opportunity to get a small glimpse of how a science environment like CSHL works. It was a fascinating experience and offered many opportunities to get to know other fields of research and the scientists involved in them.

I am grateful to Dr. Nancy Hollingsworth, my “scientific mother” and now chair of my thesis committee who took me on as an honorary member of her lab since my thesis proposal in Winter 2004/5, invited me to join her group meetings as well as journal clubs – and also lab lunches and annual holiday parties. She has tirelessly taught me how to try and think in a hypothesis-driven way, how to be concise and to the point.

I would like to thank all members of the Stillman laboratory, past (Kate Brown, Andrei Chabes, Viola Ellison, Patrick Finigan, Adriana Hemerly, Maarten Hoek, Juan Mendez, Supriya Prasanth, Khalid Siddiqui and Christian Speck) and present (Manzar Hossain, Jackie Jansen, Nihan Kara, Hiro Kawakami, Justin Kinney, Tony Mazurek, Sylvain Mitelheiser, Shuang Ni, Yi-Jun Sheu and Patty Wendel) for making the laboratory a pleasant environment to work in. My special thanks go to Patty Wendel who has had answers to any technical question in the lab; without her laboratory life would have been much more difficult and a lot less fun. Furthermore, I thank Anthony Mazurek, who joined the laboratory at the same time as I did and with whom I shared a bay for the last few years. He was always happy to critically discuss yeast metabolism even though he specializes in human DNA replication. Thanks, Tony! Furthermore I will keep happy memories of fun times late at night with Khalid Siddiqui, a former fellow Genetics graduate student from Stony Brook University, and with Adriana Hemerly who visited the Stillman lab for a sabbatical. My thanks also go to Maarten Hoek, the human CAF-1 specialist, and Juan Mendez for good times in the office and the laboratory. I am grateful to Delia King (for the first five years) and Karen Rodzenko (since three years) who were and are incredible at juggling the many demands to Bruce's time and making everything possible. My sincere thanks go to Karen for her tremendous support and for greatly aiding the transition to my next step in professional life.

I am grateful to my thesis committee: Dr. Bruce Futcher who with his critical insights has many times suggested crucial experiments that helped me along my way. Also, together with Dr. Janet Leatherwood and her laboratory he has helped me with a first microarray experiment leading to initial observations supporting the current working model. I am grateful to Dr. Rolf Sternglanz who, despite not being on my committee until recently, always followed my research and helped me back into heterochromatin research when I was struggling. I would like to further thank Dr. Rodney Rothstein from Columbia University, for coming out to CSHL for my committee meetings and helping me with advice and reagents. Lastly, I would like to thank Dr. Bill Tansey who until recently, before he moved to Vanderbilt University, was my thesis committee chair.

Ribonucleotide reductase is a complicated enzyme. The discussions I had with Dr. Andrei Chabes, a former post-doc from the Stillman laboratory, with his own laboratory at Umea University, Sweden, were vital to better understand what is important in the life of dNTPs. I also would like to thank his graduate student, Olga Tsaponina, for NTP and dNTP measurements. Chris Johns, at the Microarray Shared Resource, CSHL, performed the latest microarray and Dr. Weijun Luo, at the Bioinformatics Shared Resource, CSHL, analyzed the latest microarray data set and I am grateful for their help.

I would like to sincerely thank Dr. Arne Stenlund who was always happy to discuss any scientific problem that emerged. Moreover, I would like to thank Margaret Falkowski, Martha Daddario, Rodney Chisum and Vinney Meschan,

without whom things would run a lot less smoothly in James Building. My special thanks go to Carmelita Bautista for help with generating an antibody. Over the years many labs have had their home in James building, and I would like to thank the entire “James Building Gang” for making it a great place to study and work. Many people at CSHL helped me along my project and I am especially grateful to Cat Eberstark, Pamela Moody and Stephen Hearn.

My special thanks go to Drs. Gail Mandel, Scott Lowe and Nouria Hernandez and their groups for allowing me to rotate in their laboratories during my first year as a graduate student and to explore diverse questions as well as different techniques in molecular biology and biochemistry.

I would like to express my gratitude to the Genetics Program at Stony Brook University with its past and current directors Peter Gergen and Jerry Thomsen, respectively, for giving me the opportunity to widen my horizon and to learn about biology. Moreover, my sincere thanks go to the previous program coordinators Pam Sims and Robyn Fillinger, and foremost to Kate Bell who, since more than five years, has always been there with all her support and advice to overcome all sorts of administrative hurdles along the way.

When I joined the Stillman laboratory, I audited the Yeast Genetics Course at CSHL. From that time, I am especially grateful to Dr. Dan Burke, whose motto was “new screens, new genes” and who, as long as he taught the course, came back every year and gave me advice on my project. Furthermore, I am grateful to Drs. Dave Amberg, Beverly Erede, Frank Luca, Jeffrey Strathern and Malcolm Whiteway.

Many people have provided advice, reagents and protocols for my thesis work and would like to thank Drs. David Auble, Simon Avery, Steve Bell, Sue Biggins, Benjamin Böttner, Charlie Boone, Brenda Bourns, Dan Burke, Andrei Chabes, Sharon Dent, Anne Donaldson, Stephen Elledge, Andrew Emili, Marco Foiani, Bruce Futcher, Jeffrey Gerst, Dan Gottschling, Nancy Hollingsworth, Mark Johnston, Paul Kaufman, Richard Kolodner, Maria Longhese, Mark Longtine, Frank Luca, Danesh Moazed, Masashi Narita, Aaron Neiman, Jasper Rine, Adam Rosebrock, Sabine Rospert, Rodney Rothstein, Laura Rusché, Ali Shilatifard, David Shore, Arne Stenlund, Rolf Sternglanz, David Stillman, Bill Tansey, Mike Tyers, Jessica Tyler, Helle Ulrich, Chris Vakoc, Allain Verreault, Michael Weinreich, Michael Wigler, Virginia Zakian, Philip Zegerman and Zhiguo Zhang for that.

Before coming to Stony Brook University, I was fortunate to study with Dr. Detlev Ganten as an M.D. thesis student whose fascination with science and medicine was contagious and encouraged me to leave the clinical path.

My parents have fully supported my wish to work in basic science and take on a second graduate degree, for which I am very grateful. And lastly, probably the real reason of coming to Stony Brook University and then to CSHL was to find Benjamin Böttner; we both did our thesis at the same institute in Berlin, Germany, without knowing each other and only met here.

CURRICULUM VITAE AND PUBLICATIONS

Marlies Petra Rossmann

PERSONAL DATA

Date of Birth: October 20, 1971

Place of Birth: Berlin, Germany

Current Address: 1 Bungtown Road

Cold Spring Harbor, New York 11724, USA

Telephone: +1-631-827-3456

e-mail: rossmann@cshl.edu

EDUCATION

08/2002 - present Graduate Program in Genetics

Department of Microbiology, Stony Brook University, Stony Brook, USA

10/1991-11/1999 Medical studies at Free University and Humboldt University Berlin, Germany

11/1999 Qualified as physician by completing the *State Examination*

08/1982-06/1991 Protestant School Frohnau, Berlin, Germany

06/1991 School Leaving Examination (*Abitur*)

Advanced courses in Chemistry and Biology

RESEARCH/PROFESSIONAL EXPERIENCE

08/2003 – present Ph.D. thesis

A common telomeric gene silencing assay is affected by nucleotide metabolism and the DNA damage response: implications for the role of S. cerevisiae PCNA in heterochromatin formation.

Cold Spring Harbor Laboratory, Cold Spring Harbor, USA

Advisor: Dr. Bruce Stillman

01/1996-01/2003 M.D. thesis - *Summa cum laude*

Development of a hybridization based genetic marker system for the rat genome.

Max Delbrück Center for Molecular Medicine Berlin/

Max Planck Institute for Molecular Genetics Berlin, Germany

Advisor: Prof. Dr. Detlev Ganten

02/2001-02/2002 Medical House Officer

St. Bartholomew's / The Royal London Hospital, London, UK

Department of Medical Oncology, General Medical Inpatient Service

Leicester Royal Infirmary, Leicester, UK

Department of Integrated Medicine

02/2000-08/2000 *Ärztin im Praktikum* (Intern)

Ruprecht-Karls-University Hospital Heidelberg, Germany

Department of Neurology

- Emphasis on research in cerebrovascular disease with relevance to the role of nuclear factor-kappa B, interleukins and prostaglandins in cerebral ischemia
- Outpatient clinic with an interest in muscle diseases

06/1999-08/1999 Student

Université Pierre et Marie Curie (Paris VI), Paris, France

Department of Neurology (Faculté de médecine Pitié-Salpêtrière)

09/1998-01/1999 Biomedical Exchange Program Scholarship

***Post-ontogenic apoptosis in the cerebella of ataxic mouse mutants*.**

The Jackson Laboratory, Bar Harbor, USA

Advisor: Dr. Susan L. Ackerman

Student

Tufts University School of Medicine, Boston, USA

Depts. of Gastroenterology, Nephrology, Cardiology

PUBLICATIONS

Rossmann, M.P., Luo, W., Tsaponina, O., Chabes, A., Stillman, B. A common telomeric gene silencing assay is affected by nucleotide metabolism. ***Submitted***.

Klein, J.A., Longo-Guess, C.M., **Rossmann, M.P.**, Sebrun, K.L., Hurd, R.E., Frankel, W.N., Bronson, R.T., Ackerman, S.L. (2002). The harlequin mouse mutation down-regulates apoptosis-inducing factor. ***Nature*** 419, 367-374.

Mier, W., **Rossmann, M.**, Mohammed, A., Haberkorn, U., Eisenhut, M. (2001). 3'-End-labeling procedure for phosphorothioate oligonucleotides and oligonucleotide-conjugates. ***J. Lab. Comp. Radiopharm.*** 44 Suppl 1, 163-166.

Gösele, C., Hong, L., Kreitler, T., **Rossmann, M.**, Hieke, B., Gross, U., Kramer, M., Himmelbauer, H., Bihoreau, M.T., Kwitek-Black, A.E., Twigger, S., Tonellato, P.J., Jacob, H.J., Schalkwyk, L.C., Lindpaintner, K., Ganten, D., Lehrach, H., Knoblauch, M. (2000). High-throughput scanning of the rat genome using interspersed repetitive sequence-PCR markers. ***Genomics*** 69, 287-294.

1. INTRODUCTION

Most of our genomes carry around six billion base pairs in 46 units (GRCh37; Genome Reference Consortium, 2009), each 0.34 nm apart in the helical DNA structure (Franklin and Gosling, 1953; Watson and Crick, 1953; Wilkins et al., 1953), corresponding to 2 m (6' 6.74") which are fitted into an average nuclear volume of 180 μm^3 (Fujioka et al., 2006). This disproportion is more or less the same for all eukaryotic organisms which explains (1) the fascination with studying the molecular mechanisms that package genomes into higher-order structures and the processes that un-package genes when their function is required; (2) why a unicellular eukaryote such as budding yeast (*Saccharomyces* [*S.*] *cerevisiae*) with its unparalleled genetic accessibility can serve as a useful model organism.

How DNA is packaged into cells

Most of the negatively charged DNA in a cell does not exist as a naked molecule; rather, in all eukaryotes thus far examined it is negatively supercoiled as a result of its organization into chromatin, the smallest unit of which is the nucleosome. In this repeating unit, approximately 200 bp of DNA (or 146 bp in the core particle quite resistant to micrococcal-nuclease) are wound around a histone protein octamer, consisting of a tetramer of two highly conserved histone H3-H4 heterodimers flanked on either side by two histone H2A-H2B

heterodimers (Kornberg, 1974; Luger et al., 1997). The N-terminal tails protruding from all four histones are subject to extensive posttranslational modifications. In addition, linker histone H1 (Ushinsky et al., 1997) dynamically binds DNA in-between core nucleosomes, thereby facilitating chromatin folding (Schäfer et al., 2005) and modulating the activity of chromatin (Bustin et al., 2005).

The two different states of chromatin

Several mechanisms control the regulation of chromatin: methylation of cytosine in DNA in some species (but interestingly not in budding yeast and flies; reviewed by Suzuki and Bird, 2008), modifications of histones (Braunstein et al., 1993; Rea et al., 2000) or the replacement of canonical histones with functionally specialized histone variants (reviewed by Talbert and Henikoff, 2010) as well as nucleosome positioning through ATP-dependent chromatin remodeling (reviewed by Ho and Crabtree, 2010; Yuan et al., 2005) and finally, again with the exception of budding yeast, the crosstalk between chromatin and small RNAs (reviewed by Moazed, 2009). Also, the ordered nucleosome assembly by "molecular chaperones" (Laskey et al., 1978) after DNA replication or independently of it has been ascribed a regulatory role for chromatin which will be discussed in more detail below.

These mechanisms do not act equally across the genome. Rather, regions with lower condensed chromatin have been defined as euchromatin owing to their activities in RNA transcription, DNA replication, recombination and repair,

whereas higher condensed regions of the chromatin where factors involved in the above processes only have very limited access have been labeled as constitutive heterochromatin (reviewed by Dimitri et al., 2009). Initially, heterochromatin was identified cytologically, since it stained more deeply and remained condensed throughout the cell cycle (Heitz, 1928). However, with regard to the use of conventional transmission electron microscopy, heavy-atom salts for generating contrast might have exaggerated electrodense regions (Bazett-Jones et al., 2008), suggesting that the boundaries between eu- and heterochromatin might be more blurred. Still, it is thought that transcriptional silencing of large chromosomal domains involves assembly of the silenced regions into compact, heritable heterochromatin structures that repress gene expression in a promoter-independent fashion by blocking the interaction of RNA polymerase, or any other sequence-specific DNA-binding protein, with its recognition sequence (Pirrotta and Gross, 2005).

Heterochromatin-like regions with an emphasis on budding yeast

Other than for mammalian experimental systems, in *S. cerevisiae* much is already known about the assembly of silenced chromatin. In contrast to organisms like *Drosophila* (*D.*) *melanogaster* (for review see Schultz, 1947), heterochromatic regions in budding yeast are too small to be identified cytologically. However, like in the afore-mentioned organisms, heterochromatin-like regions in yeast appear to be condensed, since they prevent access to endonucleases (Loo and Rine, 1994), replicate late in S phase (Ferguson and

Fangman, 1992; McCarroll and Fangman, 1988) and are associated with foci that localize to the nuclear periphery (Gotta et al., 1996).

S. cerevisiae has been widely used as a model to study silencing at three loci: the two silent mating type loci hidden *MAT* right (*HMR*) and hidden *MAT* left (*HML*), telomeres and the rRNA-encoding DNA. Detailed studies of the assembly of silenced chromatin at all of these loci have revealed similarities between the *HM* loci and telomeres. Centromeres in budding yeast are just about 125 bp in length and, in contrast to fission yeast and metazoans, lack centromeric repeats and heterochromatin (Cherry et al., 1997).

Silent mating type loci

The mating type, specifying mating compatibility and thus required for sexual reproduction of budding yeast, is determined by the actively transcribed *MAT* locus which can harbor either of two alleles, **a** or α. Identical copies of these alleles are found in *HMR***a** and *HML*α, respectively, but are normally not expressed. The phenomenon in *S. cerevisiae* that an α cell can behave like an **a** cell (Hawthorne, 1963) founded genetic studies of the two silent mating type loci *HMR* and *HML* that led to the discovery that genetic information did not have to be deleted but could be silenced instead by the silent-information regulator (SIR) proteins (for review see Herskowitz, 1988). Repression of the *HM* loci requires the flanking cis-regulatory sites “E” (for essential) and “I” (for important) for silencing (Abraham et al., 1984; Feldman et al., 1984). While initially defined by

deletion studies using plasmids, only *HMR*-E has essential properties in the endogenous chromosomal context. The silencers contain binding sites for two or three different proteins (protein complexes), repressor activator protein 1 (Rap1) and/or autonomously replicating sequence (ARS)-binding factor 1 (Abf1) and - in all cases - an ACS (ARS consensus sequence) that binds the six-subunit origin recognition complex (ORC). The latter functions to assemble the pre-replication complex (pre-RC) which comprises the first step in initiation of DNA replication (Bell and Dutta, 2002). Interestingly, while all four silencers contain a functional origin of replication on plasmids, only *HMR*-E and *HMR*-I are *bona fide* chromosomal origins of replication (Dubey et al., 1991; Rivier et al., 1999; Rivier and Rine, 1992).

By studying the *HML* locus in *sir1Δ* mutants, Pillus and Rine (1989) first demonstrated three phases of silencing, establishment, maintenance and inheritance. Wild-type *MAT***a** cells when confronted with the mating pheromone α-factor usually arrest and shmoo. However, when a population of genetically identical *MAT***a** *sir1Δ* mutant cells was exposed to α-factor, only 20 % of the cells were in a silenced state at *HML* and indeed arrested, whereas in the other 80 % of cells *HML* was expressed leading them to continuously divide. Interestingly, both the silenced and the expressed states were stably heritable for more than 10 generations. Furthermore, since *HML* was expressed in 80 % of *sir1Δ* cells, Sir1 must promote the establishment of the silenced state. Finally, since 20 % of *sir1Δ* cells and their immediate descendants retained the silenced state, Sir1 is not directly required to maintain or inherit the silenced state. These experiments

thereby provide a sound example for the term “epigenetic” by referring to a trait that is mitotically heritable without accompanying DNA sequence alterations (Holliday, 1987).

Telomeres

Telomeres are the physical ends of chromosomes and protect against degradation and fusion (McClintock, 1938; Müller, 1938; Sandell and Zakian, 1993). Their highly conserved sequences consist of short G-rich tandem repeats in the strand that contains the 3’ end and that forms a single-stranded overhang. This “G-tail” is bound by Cdc13 in a heterotrimeric complex with Ten1 and Stn1, forming a replication protein A (RPA)-like complex (Gao et al., 2007). Proximal to telomeric repeats are subtelomeric regions that comprise several types of highly polymorphic repetitive elements.

The influence of heterochromatic repeat sequences on the expression of nearby genes was first demonstrated by mosaic repression of the *white* gene in flies, when “jumped” to the end of a chromosome via a transposable element (Levis et al., 1985). This phenomenon, termed position effect variegation (PEV) has also been observed in human cells (Baur et al., 2001; Koering et al., 2002). The importance of telomeric heterochromatin to chromosomal integrity is reflected by phenotypes associated with heterochromatin mutants that are characterized by shortened telomeres in yeast (Palladino et al., 1993), lengthened telomeres in mammalian cells (Garcia-Cao et al., 2004) as well as telomere fusion in flies (Fanti et al., 1998). Interestingly, the repressive effect of

telomeres might be influenced by their localization to the nuclear periphery (Andrulis et al., 1998; Mathog et al., 1984).

In *S. cerevisiae*, telomeres comprise 300 bp +/- 75 bp of ($C_{1-3}A/TG_{1-3}$) repeat DNA which is not bound by histones (Wright et al., 1992) but instead is bound by Rap1. The length of the repeat is determined by a balance between lengthening mechanisms such as DNA replication by telomerase (Lingner et al., 1997) or recombination by the ALT (alternative lengthening of telomeres) pathway (Lundblad and Blackburn, 1993) and shortening by nucleolytic degradation. Subtelomeric middle repetitive DNA sequences fall into two classes and vary between chromosome ends and strains: Y' elements of two main classes of 6.7 and 5.2 kb in size, short subtelomeric repeats (STRs; Louis et al., 1994) and 473-bp core X elements, the only repeat sequence found in all subtelomeric regions (Pryde and Louis, 1999).

Variegated gene expression, similar to PEV, was described in yeast as a telomere position effect (TPE; Gottschling et al., 1990) by studying a reporter *URA3* gene with its upstream regulatory sequences as well as a (TG_{1-3}) repeat that was placed at the telomere of chromosome VII-L. This construct also resulted in the truncation of the last 15.2 kb of VII-L. This artificial telomere could be silenced in a SIR-gene dependent manner over a 3.5-kb distance (Gottschling et al., 1990; Renauld et al., 1993). SIR proteins were thought to structurally exclude transcriptional activators from DNA in repressed chromatin (Gottschling, 1992; Loo and Rine, 1994). Upon overexpression of *SIR3* the silenced domain could be increased to 16 - 20 kb (Renauld et al., 1993).

SIR complex assembly

The step-wise assembly of silent chromatin has since been studied in detail by purification of native complexes and chromatin immunoprecipitation (ChIP) experiments (Figure 1; Hoppe et al., 2002; Rusche et al., 2002). SIR complex assembly is cooperative, that is, it involves the concerted action of many partially redundant recruiters. At *HM* loci, Orc1 recruits Sir1 via its bromo-adjacent homology (BAH) domain (Gardner et al., 1999; Triolo and Sternglanz, 1996; Zhang et al., 2002). While Sir1 is required along with Rap1 for recruitment of Sir4 to the silencers, it does not propagate beyond silencers (Moretti et al., 1994; Triolo and Sternglanz, 1996). At telomeres, with no described function for Sir1, Sir4 is recruited through Rap1 and Yku70 which directly bind to the nucleosome-free telomere repeats (Martin et al., 1999; Mishra and Shore, 1999; Tsukamoto et al., 1997). Sir4 assembles first Sir2 and then Sir3 at the silencers. Sir3 also contacts Rap1 and possibly binds Abf1. The NAD^+-dependent histone deacetylase activity of Sir2 (Imai et al., 2000; Landry et al., 2000; Smith et al., 2000) is not involved in the initial formation of the SIR complex on chromatin, however, it is required for spreading of the SIR complex. The proposed mechanism involves the sequential deacetylation of acetylated K16 and probably also K56 within the tails of histones H4 and H3, respectively, by Sir2 and thus creation of higher-affinity binding sites for Sir3 and the Sir2-Sir4 complex (Imai et al., 2000; Xu et al., 2007).

Figure 1: Silencing at *HM* loci and telomeres in *S. cerevisiae*.

Cartoon depicting the stepwise assembly of the silencing complex at *HMR*-E and at a telomere in *S. cerevisiae* (modified from Perrod and Gasser, 2003). A: Abf1, R: Rap1, 1: Sir1, 2: Sir2, 3: Sir3, 4: Sir4, Ac: acetyl group (ethanoyl), A, E and B (in DNA): binding sites for ORC, Rap1 and Abf1, respectively; for other abbreviations see text.

Silencing at *HM* loci

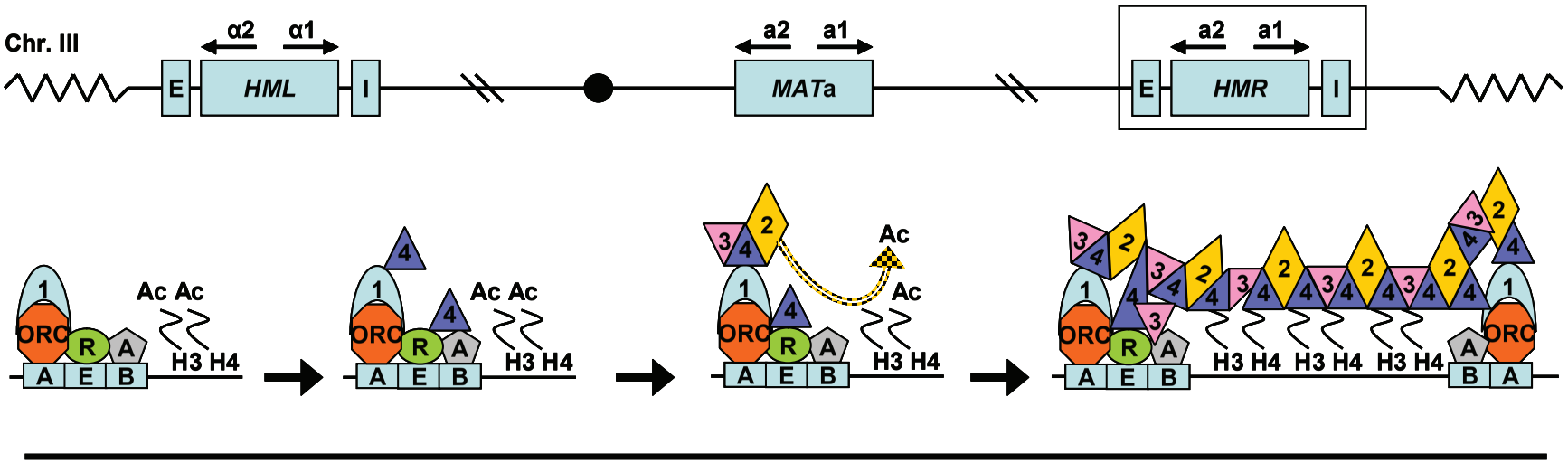

Silencing at telomeres

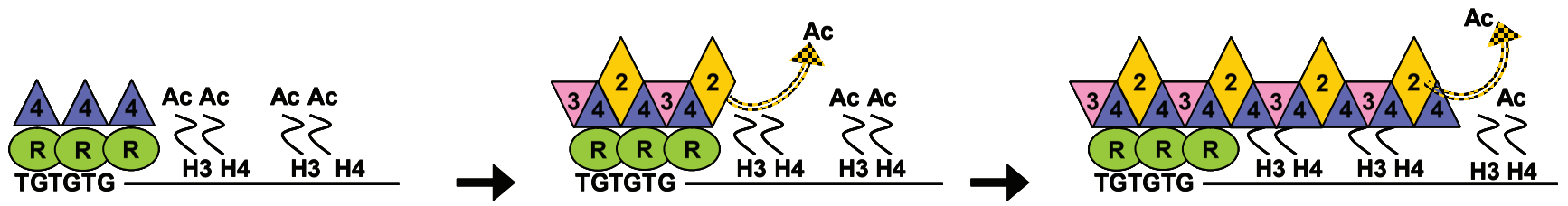

initiation deacetylation propagation of the SIR complex

Immunofluorescence studies have confirmed that Rap1 and the SIR proteins (except Sir1) form large macromolecular complexes which are thought to act as a structural barrier to transcription (Gotta et al., 1996; Hecht et al., 1995). Importantly, loss of Sir2, Sir3 or Sir4 function leads to complete derepression of the silent mating-type loci as well as loss of telomeric silencing. More recent studies suggest different mechanisms for SIR protein function. Transcription can be blocked by SIR proteins either at or downstream of RNA polymerase II occupying the promoter (Chen and Widom, 2005; Sekinger and Gross, 2001). Also, SIR protein requirements might vary between telomeres: Introduction of *URA3* at several positions within different native telomeres revealed discontinuous silencing, with a maximum at the ACS, required for initiation of DNA replication, contained within the subtelomeric 473-bp core X repeat sequence (Pryde and Louis, 1999).

DNA replication and gene silencing

A link between DNA replication and heterochromatin is suggested by the fact that euchromatin and heterochromatin display a different timing of their duplication within the cell cycle. With exceptions, heterochromatin is replicated late within S phase (Kim et al., 2003; Schubeler et al., 2002). Also the functions of telomerase, the reverse transcriptase that replicates telomeres, and DNA replication are coordinated (Diede and Gottschling, 1999; Marcand et al., 2000). Moreover, *TLC1*, the RNA component of telomerase has been found to participate in telomeric silencing (Singer and Gottschling, 1994).

A causal role for DNA replication in the establishment of transcriptional silencing suggested the requirement for S phase in the repression of *a1* transcription at the *HMR* locus in *S. cerevisiae*. The analysis of cells with initially derepressed *HM* loci that were arrested in G1, early S phase and mitosis during a single cell cycle demonstrated that silencing could be established only in mitosis after passage through S phase (Miller and Nasmyth, 1984). Assaying for SIR protein loading by ChIP and for *HMRa1* gene expression by quantitative PCR, Lau and colleagues (2002) found a requirement for M phase, in particular cleavage of Mcd1. However, lack of this cohesin subunit in S phase (hydroxyurea arrest) still did not lead to the establishment of silencing, suggesting separable requirements for S and M phase in this process. Both *bona fide* chromosomal origins of replication at *HMR*-E and *HMR*-I, when mutated, not only lost their origin function but also their silencing ability (McNally and Rine, 1991). Mutants in several factors involved in DNA replication, including PCNA, subunits of ORC, *CDC7*, *CDC45*, *RFC1*, *POL1* and subunits of polymerase ε, have been genetically linked to heterochromatin formation (Axelrod and Rine, 1991; Bell et al., 1993; Ehrenhofer-Murray et al., 1999; Foss et al., 1993; Micklem et al., 1993a; Smith et al., 1999; Zhang et al., 2000). To name a few examples, the *orc2-1* mutation resulted in derepression of *HMR* (Bell et al., 1993; Foss et al., 1993) and *D. melanogaster* (*Dm*) ORC2, 5 and 6 complexed *in vivo* with HP1 (Su[var]205), a chromodomain protein central to heterochromatin; furthermore, mutations in *Dm*ORC2 suppressed PEV in flies (Pak et al., 1997). A non-conserved H domain of the Orc1 N-terminal BAH domain was necessary and

sufficient for physical interaction with Sir1 and required for silencing function (Zhang et al., 2002). Interestingly, the recruitment of Sir1 by the Orc1 BAH domain was independent of a functional ORC complex (Triolo and Sternglanz, 1996), and thus, the establishment of silencing was separable from replication initiation. However, the S-phase requirement remained. Moreover, ORC was essential for telomeric silencing using a *TRP1* reporter (Fox et al., 1997). With the *URA3* reporter at the same telomere, however, the establishment of silenced chromatin required mitosis but not S phase (Martins-Taylor et al., 2004). These experiments cumulatively argued for an important and replication-initiation independent role of ORC subunits in heterochromatin formation both at *HM* loci and telomeres while the requirement of S phase was variable.

A definitive experiment addressing the requirement of DNA replication in the establishment of silencing was done by the Gartenberg and Rine groups (2001). The excision by FLP recombinase of a derepressed genomic *HMR* locus lacking any origin of replication still resulted in the establishment of silencing after passage through S phase. Although these experiments formally exclude a requirement for DNA replication fork passage in the establishment of silencing at the *HMR* locus, they still could involve some degree of recombinational DNA repair and thus proteins of the replication fork including PCNA, downstream of the involvement of ORC. Furthermore, they do not address a possible role of the DNA replication machinery in the maintenance or inheritance of a silenced state.

PCNA and its role in DNA replication and related cellular processes

PCNA stands for proliferating cell nuclear antigen. It was first discovered as a protein specific to proliferating cells recognized by antibodies from some patients with systemic lupus erythematosus, an autoimmune disease (Miyachi et al., 1978). Shortly thereafter, the same protein (Mathews et al., 1984), initially named “cyclin” was identified by 2-D gel electrophoresis in a search for cell cycle phase specific proteins in HeLa cells (Bravo and Celis, 1980; Bravo et al., 1981). Its direct role in DNA replication was demonstrated through its ability to stimulate DNA polymerase δ in replicating primed DNA templates (Prelich et al., 1987a; Prelich et al., 1987b; Tan et al., 1986).

Despite only little similarity in primary amino acid sequence of PCNA from different phyla, the three dimensional shape of human and yeast PCNA is almost identical (Gulbis et al., 1996; Krishna et al., 1994) and very similar to the functional homologs of *Escherichia* (*E.*) *coli* (β subunit of DNA polymerase III) and T4 bacteriophage (gp45; Kelman, 1997; Kong et al., 1992). This high degree of conservation underscores that the basic mechanism of processive DNA replication is conserved throughout prokaryotic and eukaryotic species. Each monomer of eukaryotic PCNA consists of two structurally similar domains which are linked by an interdomain connecting loop. The essential PCNA homologue in budding yeast, Pol30, forms a homotrimer of 29-kDa subunits (Bauer and Burgers, 1990; Krishna et al., 1994). It is assembled onto DNA by the five-subunit “clamp loader” replication factor C (RFC) in an ATP-dependent manner which threads onto the primer template junction like a screw-cap (Bowman et al.,

2004). The monomers are arranged head-to-tail to create two distinct faces of the ring as in the case of the prokaryotic β clamp (Krishna et al., 1994). Once loaded, PCNA forms a sliding clamp and, through interactions with DNA polymerases δ and ε at template-primer termini, it promotes processive DNA replication by these enzymes (more so of polymerase δ, see above). Both, the clamp loader and polymerases compete for the same C face of the ring (the side from which the C termini project). While the Pol30 ring only slowly dissociates from DNA by itself ($t_{1/2}$ = 24 min; Yao et al., 1996), RFC can also unload PCNA in an ATP-dependent manner (Bylund and Burgers, 2005). Importantly, this could provide a window for protein interactions required for the assembly of chromatin (see below). Due to the anti-parallel DNA double-helical structure, the semi-conservative replication process and the fact that DNA polymerase cannot synthesize DNA in a 3' to 5' direction, only the so-called leading strand which is oriented 3' to 5' relative to unwinding is replicated continuously in 5' to 3' direction, predominantly by polymerase ε (Pursell et al., 2007). In contrast, the lagging strand is synthesized predominantly by polymerases δ (Nick McElhinny et al., 2008) as 100 to 150-bp Okazaki fragments, onto each of which one PCNA molecule is loaded, leading to an uneven distribution of PCNA on both replicating strands.

Owing to its property to move along the replication fork, PCNA has been found to be a platform for proteins with functions in DNA replication and repair, chromatin assembly and regulation, sister chromatid cohesion, transposition,

transcription and cell cycle control (Lee et al., 2010; Li et al., 2009; Moldovan et al., 2007). In many of these proteins, specific motifs mediating the interaction have been found; above all a PCNA-interacting protein (PIP) box the consensus of which is Qxx(h)xx(a) (x = any, h = hydrophobic, a = aromatic; Warbrick et al., 1998). This structure docks into a hydrophobic pocket underneath the interdomain connecting loop (Gulbis et al., 1996). Additional motifs are a KA amino acid sequence in some proteins including polymerase δ (Xu et al., 2001) as well as a new motif named APIM (AlkB homologue 2 PCNA-interacting motif) after its prototype, hABH2, a human oxidative demethylase (Gilljam et al., 2009). Like DNA polymerases δ and ε, other partners of PCNA mostly interact with its C face; this and the homotrimeric structure of eukaryotic PCNA hints towards competition but possibly also co-existence of several proteins at the replication fork. In some cases such as Xenopus Cdt1 the interaction triggers the degradation of the PCNA-interactor (Arias and Walter, 2006). In other cases, modification of PCNA itself serves to create an interaction motif such as is the case for the very interesting modifications of PCNA by SUMO and ubiquitin at residue K164. K164 can be mono- or polyubiquitylated for error-prone synthesis by low-fidelity translesion polymerases and error-free bypass replication, respectively (Hoege et al., 2002), and also sumoylated, even in the absence of DNA damage. Sumoylated PCNA is preferentially recognized by Srs2, a helicase which is thought to prevent sister chromatid recombination during DNA replication by this interaction (Papouli et al., 2005; Pfander et al., 2005; Robert et al., 2006).

DNA replication-dependent chromatin assembly and gene silencing

Since any process involving DNA including transcription, replication and repair is partially disruptive to existing higher-order chromatin structures, these would subsequently need to be re-established. This process would start at the level of nucleosomes. Several histone chaperones have been identified to aid in nucleosome assembly and disassembly. These include CAF-1, Nap1, FACT, Asf1, Rtt106, Chz1 and Scm3/HJURP (for review see Ransom et al., 2010). One of them, chromatin assembly factor 1 (CAF-1) in particular prefers newly synthesized acetylated histones over recycled histones (Sobel et al., 1995). CAF-1 depends on DNA synthesis in its activity, either during DNA replication (Smith and Stillman, 1989; Stillman, 1986; Verreault et al., 1996) or nucleotide-excision repair (Gaillard et al., 1996). *In vitro*, CAF-1 deposits newly synthesized histones H3 and H4 onto DNA, whereas H2A and H2B bind subsequently to the H3-H4 tetramer (Smith and Stillman, 1991). *In vivo* studies have supported this role by localizing CAF-1 to replication foci (Krude, 1995) and heterochromatin (Taddei et al., 1999) and by assaying its recruitment to chromatin as a consequence of DNA damage in G1 or G2 phase (Martini et al., 1998). Human and budding yeast CAF-1 consists of three subunits - in yeast these are Cac1, Cac2 and Cac3. In contrast to human CAF-1 (Hoek and Stillman, 2003; Ye et al., 2003), deletion of one or all of the encoding yeast genes does not result in lethality (Game and Kaufman, 1999; Kaufman et al., 1997), suggesting that other chromatin assembly factors must be able to replace the function of CAF-1 in the assembly of nucleosomes during S phase. One good candidate is anti-silencing function 1

(Asf1). Its name stems from a genetic screen in which overexpression of *ASF1* rendered a strain carrying *TRP1* at the normally silenced *hml* locus prototroph for tryptophan (Le et al., 1997). Importantly, Asf1 from *D. melanogaster* embryos co-purifies with histone H3 and H4 and synergizes with CAF-1 in DNA replication-coupled nucleosome assembly *in vitro* (Tyler et al., 1999). Subsequently, this was also shown for budding yeast and human Asf1 (Sharp et al., 2001). CAF-1 and Asf1 might even assemble chromatin together in S phase: The second CAF-1 subunit physically interacts with Asf1 in several species, including budding yeast, flies and humans (Krawitz et al., 2002; Mello et al., 2002; Tyler et al., 2001). Furthermore, *in vitro*, Asf1 binds to the RFC clamp loader which recruits it to chromatin (Franco et al., 2005). Like CAF-1, Asf1 also localizes to replicated foci in cells cultured from flies (Schulz and Tyler, 2006).

The relevance of CAF-1 for heterochromatin formation became evident when a *cac1* mutant was isolated as a factor that causes Rap1 to localize in an altered punctuate, more diffuse nuclear pattern. This mutant did not, however, alter telomere length and the localization of telomeres to the nuclear periphery (Enomoto et al., 1997). This allele, as well as the *cac1Δ*, *cac2Δ* or *cac3Δ* mutants provoke a pronounced telomeric silencing defect in the *URA3*-VIIL reporter strain (Enomoto et al., 1997; Kaufman et al., 1997). The latter was interpreted to be due to an increased switching rate from the transcriptional “off” to the “on” state (Monson et al., 1997). Loss of *CAC1* has no consequences at the *HM* loci except at an already sensitized *hmr* locus (Enomoto et al., 1997; Kaufman et al., 1997; Sharp et al., 2001; Zhang et al., 2000).

The PCNA/CAF-1 pathway in silencing

During DNA replication, in particular PCNA has been suggested to be at the center of inheritance of distinct DNA methylation and posttranslational histone modification patterns from parental to daughter nucleosomes. Human and yeast PCNA have been shown to physically interact with CAF-1 (Rolef Ben-Shahar et al., 2009; Shibahara and Stillman, 1999; Zhang et al., 2000) and human PCNA associates also with other DNA or chromatin-modulating enzymes such as DNA methyltransferase 1 (DNMT1; Chuang et al., 1997), histone deacetylase 1 (HDAC1; Milutinovic et al., 2002) and Williams syndrome transcription factor (WSTF). The latter recruits an ISWI-nucleosome remodeling factor to replication foci (Poot et al., 2004). Replication-dependent chromatin assembly requires the loading of PCNA onto the DNA suggesting that PCNA marks replicated DNA; its asymmetry in number with respect to leading and lagging strand could offer an opportunity for passing different chromatin structures onto the two sister chromatids (Shibahara and Stillman, 1999).

Double-alanine scanning mutagenesis of *POL30* generated mutations with functional relevance at positions where charges were conserved from yeast to human (Ayyagari et al., 1995). One of these alleles, *pol30-8*, is characterized by a RD61,63AA mutation (Ayyagari et al., 1995) at the tip of the bulge of the homotrimer, distant from known protein-interacting regions (Krishna et al., 1994). Although Pol30-8 still associates with DNA polymerases δ and ε as well as RFC, this mutant shows increased sensitivity to UV, methyl methanesulfonate (MMS) and hydroxyurea (Ayyagari et al., 1995; Li et al., 2009; Linger and Tyler, 2005).

Interestingly, *pol30-8* also belongs to a class of PCNA mutants that are defective in silencing *HMR*, *HML* and telomeres (Ehrenhofer-Murray et al., 1999; Zhang et al., 2000); *pol30-8* exhibits a red-white sectoring phenotype at a modified *hmr*::*ADE2*, which resembles that of *sum1Δ* (Chi and Shore, 1996), *rap1Δ* or a deletion of the ACS in the *HMR*-E silencer (Sussel et al., 1993). This phenotype correlated with reduced binding of PCNA to Cac1 *in vitro* and a reduction in chromatin-bound Cac1 *in vivo*, although *cac1Δ hmr*::*ADE2* mutants exhibit little to no sectoring (Zhang et al., 2000; my own results). Deletion of *CAC1* does not exacerbate the *pol30-8* phenotype (Sharp et al., 2001; Zhang et al., 2000), supporting a role for both genes in the same heterochromatin assembly pathway. The sectoring phenotype of the *pol30-8* mutant has been suggested to indicate an unstable epigenetic inheritance of the transcriptional state at the *hmr*::*ADE2* locus which is in agreement with the previously described unstable telomeric silencing phenotype for *cac1Δ* mutants (Monson et al., 1997). Thus, a role for PCNA in the inheritance of heterochromatin structures during S phase was suggested.

With regard to silencing at *HM* loci and telomeres, Asf1 and Pol30/CAF-1 play a role in parallel and redundant pathways: *cac1Δ asf1Δ* or *pol30-8 asf1Δ* have synergistic silencing defects (Sharp et al., 2001; Tyler et al., 1999). Interestingly, other silencing-defective *POL30* alleles (*pol30-6*, *pol30-79*) act in a common genetic pathway with *ASF1*, hinting towards the central position of PCNA in coordinating the Asf1 and CAF-1 heterochromatin assembly pathways (Sharp et al., 2001). This genetic analysis has been extended to the *HIR* genes

(*HIR1*, *HIR2*, *HIR3*, *HPC2*), which encode proteins that repress histone transcription outside of S phase (Sherwood et al., 1993; Spector et al., 1997). *HIR* genes function in the same pathway as *ASF1* and the Hir proteins physically interact with Asf1 (Kaufman et al., 1998; Qian et al., 1998; Sharp et al., 2001). Deletion of another histone chaperone, *RTT106*, acts synergistically with *asf1Δ* but not with *pol30-8* or *cac1Δ* at *hmr*. In addition, Rtt106 also seems to be involved in replication-dependent nucleosome assembly, and facilitates heterochromatin formation through its interaction with Sir4 (Huang et al., 2005; Huang et al., 2007).

The role of histone modifications in budding yeast

Interestingly, silenced chromatin in budding yeast lacks histone modifications. In particular, methylation such as that of histone H3K9, which creates a binding site for the chromodomain-containing heterochromatin proteins Clr4 or HP1 in *S. pombe* and higher eukaryotes, respectively, is not present in *S. cerevisiae* (Bannister et al., 2001; Lachner et al., 2001; Nakayama et al., 2001). However, gene-activating methylation as well as acetylation and deacetylation are common between *S. cerevisiae* and higher eukaryotes. For instance, histone H3K4 trimethylation catalyzed by COMPASS, a complex consisting of seven proteins including the trithorax-family related catalytic subunit Set1, is recruited by RNA polymerase II, concentrates at 5' regions of euchromatic genes and is associated with gene activation in yeast (Miller et al., 2001; Ng et al., 2003b). Deacetylation has a repressive role in transcription: SIR proteins promote

silencing by deacetylating the amino-terminal tails of histones H3 (lysines 9, 14, 18, 23 and 27) and H4 (lysines 5, 8, 12 and 16; Suka et al., 2001) which allows their folding into a more compact structure (Luger et al., 1997). Interestingly, mutations in the histone acetyltransferases Gcn5 and Sas2 can weaken a tRNA gene barrier distal to the *HMR*-E locus and globally, *sas2Δ* and the histone H4K16R mutant lead to the spreading of the SIR complex beyond its natural barriers (Suka et al., 2002). SIR proteins are limiting in the cell (Renauld et al., 1993) and thus their "dilution" from heterochromatin to normally euchromatic regions is thought to result in a silencing defect, as proposed for *sas2Δ* mutants (Reifsnyder et al., 1996).

Like *SAS2*, *DOT1* (disruptor of telomeric silencing) belongs to a group of euchromatin-modifying proteins with "anti-silencing" properties (Tompa and Madhani, 2007 and references therein). *DOT1* was found in a screen for factors that when overexpressed disrupt silencing at two truncated telomeres, VI-R and VII-L, carrying the *ADE2* and *URA3* genes, respectively (Singer et al., 1998). Dot1 is the only known histone H3K79 methyltransferase in budding yeast (Feng et al., 2002; Lacoste et al., 2002; Ng et al., 2002; van Leeuwen et al., 2002) and its function is conserved in higher eukaryotes (Shanower et al., 2005). By methylating histone H3K79 in euchromatin, Dot1 is thought to prevent SIR proteins from promiscuously spreading from telomeric and *HM* loci into euchromatic regions (Ng et al., 2003a; van Welsem et al., 2008). Recently, a closer analysis of H3K79 di- and trimethylation identified these modifications in different genomic regions with only approximately 2 % overlap. Intriguingly,

H3K79 dimethylation fluctuates throughout the cell cycle and increases in S phase. This increase was dependent on the SBF transcription factor required for the expression of genes regulating G1/S transition (Schulze et al., 2009).

The DNA damage response in the context of DNA replication

S. cerevisiae is able to activate DNA damage checkpoints in the G1/S, S and G2/M phases of the cell cycle. In S phase, stalled replication forks can lead to double-strand breaks (DSBs). Also, DNA damage can be induced by intra- or extracellular sources such as free radicals or toxins, mutagenic chemicals as well as radiation. In both cases, an inhibitory pathway, the S phase checkpoint, is activated which slows down S phase, prevents mitosis and activates the DNA repair pathway to ensure accurate duplication of the genome and thus cell survival. The DNA damage response consists of a signal transduction cascade (Figure 2) with sensors, adaptors and effector kinases (Melo and Toczyski, 2002). However, rather than functioning in a unidirectional pathway these factors act in a complex network containing feedback loops (Putnam et al., 2009). Upon DNA damage, exposed single-stranded DNA is coated with RPA, which is recognized by the Ddc2 sensor protein (Byun et al., 2005; Zou and Elledge, 2003). Single-strand nicks in replication forks can also be converted into DSBs, the ends of which are bound by the Mre11-Rad50-Xrs2 (MRX) complex. These, together with other proteins including a heterotrimeric PCNA-like complex consisting of Ddc1, Mec3 and Rad17 are recognized by two protein kinases with homology to phosphatidylinositol 3-kinases (PI3K), Tel1 and Mec1. Tel1 and

Figure 2: The DNA damage response in *S. cerevisiae*.

Cartoon depicting some of the steps involved in the transcriptional response to cellular DNA damage in *S. cerevisiae* (modified from Sharp et al., 2005).

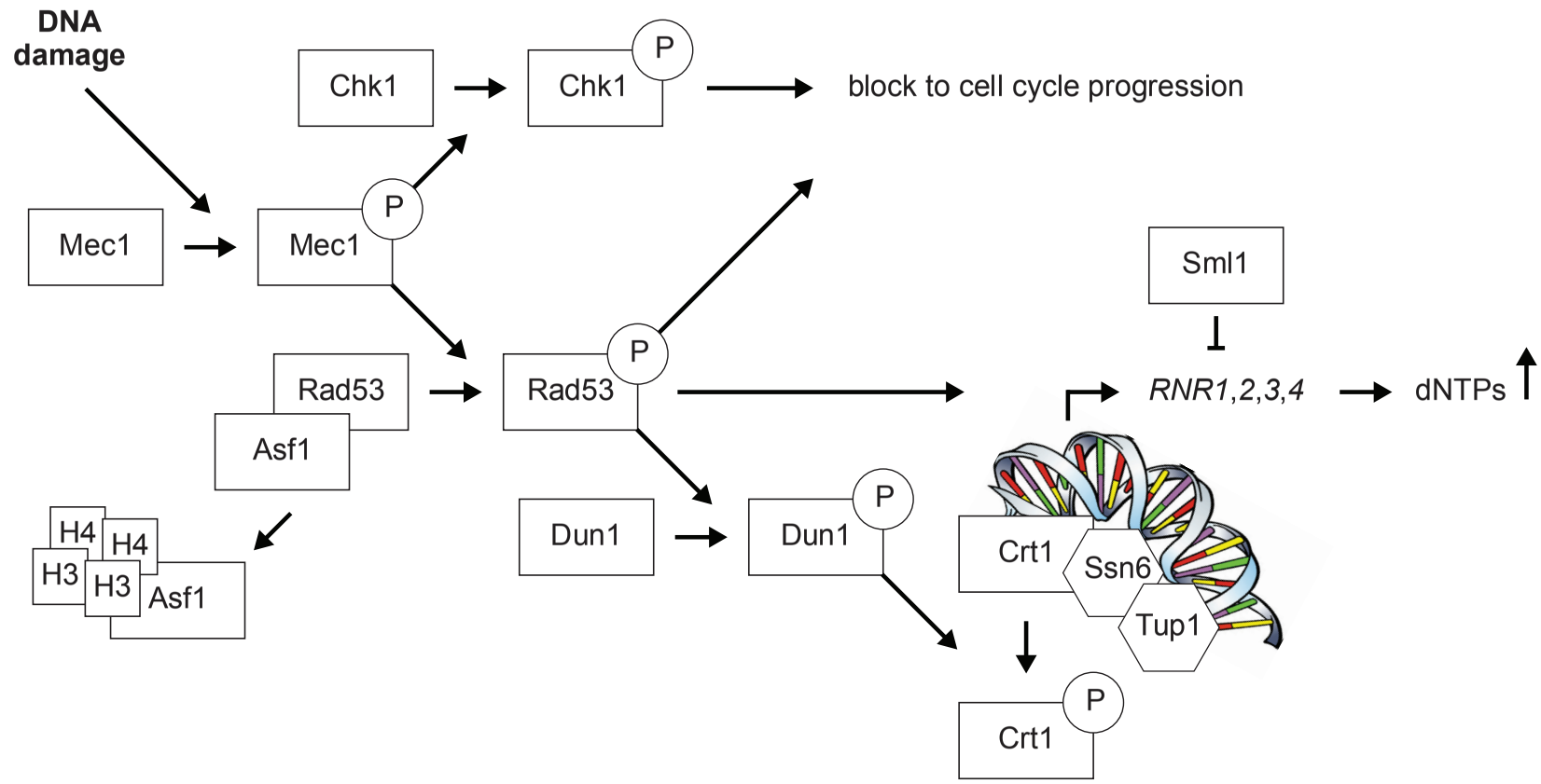
DNA damage
Chk1
P
Chk1
block to cell cycle progression
Mec1
P
Mec1
Sml1
Rad53
P
Rad53
RNR1,2,3,4
dNTPs
Asf1
H4
H4
H3
H3
Asf1
Dun1
P
Dun1
Crt1
Ssn6
Tup1
P
Crt1

Mec1 among many targets phoshorylate the central effector kinases Rad53 and Chk1. An adaptor, Rad9 (the first checkpoint gene identified; Weinert and Hartwell, 1988), acts as a scaffold to locally concentrate Rad53 (Gilbert et al., 2001). Interestingly, Rad9 contains two Tudor domains which have been shown to bind to methylated histones (Grenon et al., 2007). Phosphorylation and recruitment of Rad9 to a DSB are dependent upon histone H3K79 methylation by Dot1 which requires prior histone H2BK123 ubiquitylation by the Rad6/Bre1 E2/E3 enzyme complex (Giannattasio et al., 2005; Wysocki et al., 2005). Activation of Rad53 results in the direct phosphorylation and activation of the kinase Dun1 (Bashkirov et al., 2003; Lee et al., 2003). Dun1 directly phosphorylates the ribonucleotide reductase (RNR) inhibitor Sml1, thereby promoting its degradation (Zhao and Rothstein, 2002). Dun1 also phosphorylates and thus inhibits the transcriptional repressor Crt1 (Huang et al., 1998). Crt1 physically binds to the global Tup1-Ssn6 transcriptional co-repressor complex (DeRisi et al., 1997; Robyr et al., 2002) to suppress transcription of *RNR2*, *RNR3*, *RNR4* and that of itself in the absence of DNA damage (Huang et al., 1998). RNRs generate the four deoxyribonucleoside triphosphates (dNTPs) required for DNA synthesis in all organisms. In *S. cerevisiae*, this enzyme is a heterotetramer with the large catalytic R1 subunit comprising a homodimer of either Rnr1 or Rnr3, or their combination, and a small R2 subunit containing a heterodimer of Rnr2 and Rnr4 that harbors the radical cofactor required for reduction of ribonucleotides. After DNA damage dNTP pools increase 4-fold, thus

satisfying the higher nucleotide requirement by DNA polymerases during DNA repair (Chabes et al., 2003).

A connection between the DNA damage response and chromatin assembly is suggested by the interaction of Asf1 with Rad53 in its hypophosphorylated state (Emili et al., 2001; Hu et al., 2001). Subsequently, it was suggested that in the absence of DNA damage, Dun1 prevented dissociation of the Asf1-Rad53 complex, limiting the availability of Asf1 to mediate CAF-1-dependent heterochromatin assembly (Sharp et al., 2005). Rad53 also regulates histone levels at the protein level, by recruiting E2 (Ubc4 and Ubc5) and E3 (Tom1) enzymes to phosphorylated histones H3 and H4, enabling their ubiquitin-mediated degradation (Gunjan and Verreault, 2003; Singh et al., 2009). Such control of histone levels likely occurs in S phase and following DNA damage.

Dissertation scope and outline

In this dissertation, I studied the role of PCNA in regulating silent mating type silencing and telomere position effect variegation (TPEV) using *S. cerevisiae* as a model system. I initiated my work by asking which additional factors are required for PCNA-dependent telomeric gene silencing. For this purpose, I performed a high-copy suppressor screen for the silencing defect of the PCNA mutant *pol30-8* at an engineered *hmr* locus and telomere VII-L (Chapters 2.1, 2.2, 2.3, 2.4). To further characterize the isolated high-copy suppressors, I generated different telomeric reporter strains. These revealed a much weaker silencing phenotype exhibited by the *pol30-8* mutant than was

previously shown with the commonly used *URA3*-VIIL reporter in which *URA3* expression can be counter-selected for by 5-fluoroorotic acid (5-FOA; Chapters 2.5, 2.6, 2.7). None of the high-copy suppressors were obviously associated with heterochromatin formation or structure, but rather were involved in the DNA damage response and transcriptional regulation. At the same time, I found PCNA/CAF-1 dependent silencing to be limited to the transcriptional regulation of the telomeric *URA3*-VIIL reporter (Chapters 2.8, 2.9). Extending these studies, I identified a genetic and physical interaction between PCNA and Dot1, a histone H3K79 methyltransferase (Chapters 2.10, 2.11, 2.12). Re-analysis of the previously reported telomeric silencing phenotype of *dot1Δ* mutants using an alternative telomere reporter surprisingly revealed a complete absence of heterochromatin defects (Chapter 2.13). In addition, a microarray analysis of gene expression for both the *pol30-8* and *dot1Δ* mutants showed a genome-wide lack of a telomere-specific silencing defect (Chapters 2.14, 2.15). I further demonstrated that RNR, one of the downstream targets of the DNA damage response, which is also involved in 5-FOA metabolism, is up-regulated in *pol30-8* cells and further induced by the drug 5-FOA (Chapters 2.16, 2.17, 2.18, 2.19, 2.20, 2.21). Importantly, these results can explain the high sensitivity of *pol30-8* *URA3*-VIIL mutants to 5-FOA and suggest that the phenotype has little to do with silencing of gene expression by telomeric heterochromatin. Furthermore, I showed that cross-regulation of purine and pyrimidine biosynthesis is important for the *dot1Δ* phenotype at *URA3*-VIIL (Chapter 2.22). Finally, in light of these

results I discuss experiments with additional candidates obtained in the initial *pol30-8* screen (Chapter 2.23).

This work demonstrates that the widely used *URA3*-VIIL assay does not reflect a heterochromatin defect either in *pol30-8* or in *dot1Δ* mutants, but rather is a read-out of metabolic changes in these (and likely also other) mutants. In conclusion, the results suggest that TPEV in *S. cerevisiae* is not a ubiquitous model for the study of epigenetic inheritance of gene information, since it is influenced by subtle gene regulatory defects as seen in the *pol30-8* and *dot1Δ* mutants.

2. RESULTS

2.1 A genetic screen identifies five high-copy suppressors of the *pol30-8 URA3*-VIIL telomeric silencing defect.

The *S. cerevisiae* PCNA mutation *pol30-8* (RD61,63AA; Ayyagari et al., 1995) is reported to have a heterochromatin silencing defect at the *HMR* silent mating type locus marked with *ADE2* and at telomere VII-L marked with *URA3* adjacent to the 5' end of the truncated *ADH4* gene (Zhang et al., 2000). Pol30 has been shown to interact with CAF-1 *in vitro* and *in vivo* (Huang et al., 2005; Zhang et al., 2000); however, how this interaction specifically affects heterochromatin assembly has been unclear. To further elucidate the role of *pol30-8* in heterochromatin formation, a high-copy suppressor screen was performed. A yeast genomic library in a 2-μm plasmid (Vojtek et al., 1991) was transformed into a *pol30-8 hmr*::*ADE2 URA3*-VIIL strain (W303 background) in which *pol30-8* replaces *POL30* under its endogenous promoter. Transformants were first selected for presence of the 2-μm plasmid followed by counter-selection on 5-FOA-containing medium. 5-FOA selects for Ura^- auxotrophs, since the *URA3* gene product participates in conversion of 5-FOA into a lethally toxic metabolite (Boeke et al., 1984). High-copy suppressors of the *pol30-8* mutant had to both silence the *URA3*-VIIL (5-FOA resistant) and the *hmr*::*ADE2* loci (darker pink color than the *pol30-8* mutation transformed with a control 2-μm plasmid). 5-FOA resistant transformants were re-streaked onto plates containing

Table 1: A genetic screen identifies five high-copy suppressors of the *pol30-8 URA3*-VIIL telomeric silencing defect.

Summary of high-copy suppressor screen results for the *pol30-8 hmr*::*ADE2 URA3*-VIIL strain (MRY0041). The primary screen consisted of selection for 5-FOA resistant Leu^+ transformants; high-copy suppressors were kept as candidates when they were of mostly pink-red colony color after two re-streaks on -Leu medium containing 20 mg/l adenine. Genes in red also suppressed 5-FOA sensitivity of a strain with *URA3* at its endogenous locus.

Number of transformants screened	966,800
after primary screen	911
after secondary screen	356
POL30	157
empty vector	79
GFA1	33
MCM1	29
YCR023C	11
CDC21 (= *CRT9*)	10
SDT1	6
PPR1-DNA binding domain	3
CRT1 (= *RFX1*)	2
MSA2, *YKR078W*	1
ARL1, *UBS1*	1
not followed further (mostly 1 per hit)	24

20 mg/l adenine for color assessment. By screening 966,800 transformants I obtained 356 initial candidates that scored positive after the secondary screen (Table 1). Among these, *POL30* was isolated 157 times and five other genes were isolated: *CDC21*, *MCM1*, *YKR077W* and the weaker suppressing *CRT1* and *UBS1* (Table 1).

2.2 Some high-copy suppressors act in a telomere-non-specific manner.

To demonstrate that the effect of the high-copy suppressors was specific for telomeres, I tested their ability to suppress 5-FOA sensitivity of a strain wild-type for *URA3* at its endogenous locus on chromomosome V. For this experiment, 5-FOA concentrations were lowered to 0.2, 0.4 and 0.6 g/l to account for the higher expression of the endogenous *URA3* gene. Whereas *GFA1*, an essential gene for the synthesis of UDP-N-acetyl-D-glucosamine (Watzele and Tanner, 1989), *SDT1*, encoding a pyrimidine 5'-nucleotidase (Nakanishi and Sekimizu, 2002), and *YCR023C*, encoding a vacuolar membrane protein of unknown function (Albertsen et al., 2003), conferred at least 10,000-fold increased 5-FOA resistance as compared to empty vector (Figure 3), overexpression of *CDC21*, *MCM1*, *MSA2*, *CRT1* and *UBS1* did not cause a non-specific growth advantage on 5-FOA (Figure 3). I concluded that the latter five genes are high-copy suppressors of the telomeric silencing defect in *pol30-8 URA3*-VIIL cells. All these genes also suppressed the telomeric silencing defect of a *cac1Δ URA3*-VIIL but not that of a *sir3Δ URA3*-VIIL strain (data not shown) indicating that they were suppressors of the PCNA/CAF-1-dependent silencing

Figure 3: Some high-copy suppressors act in a telomere-non-specific manner.

10-fold serial dilution of three transformants each of a strain carrying *URA3* at its endogenous locus (AC437) transformed with the genomic library vector (YEp13M4) or genomic *GFA1* (1st panel), YEp13M4 or genomic *SDT1* (2nd panel), YEp13M4 or genomic *YCR023C* (3rd panel), the 2-µm origin containing cloning vector (pRS425) or *CDC21* (4th panel), pRS425 or *MCM1* (5th panel), YEp13M4 or genomic *MSA2* and the neighboring ORF *YKR078W* (6th panel), and (2 transformants each) YEp13M4, genomic *ARL1* and the neighboring ORF *UBS1* or genomic *CRT1* (7th panel). #1 - #11 indicate independent transformants.

URA3
+

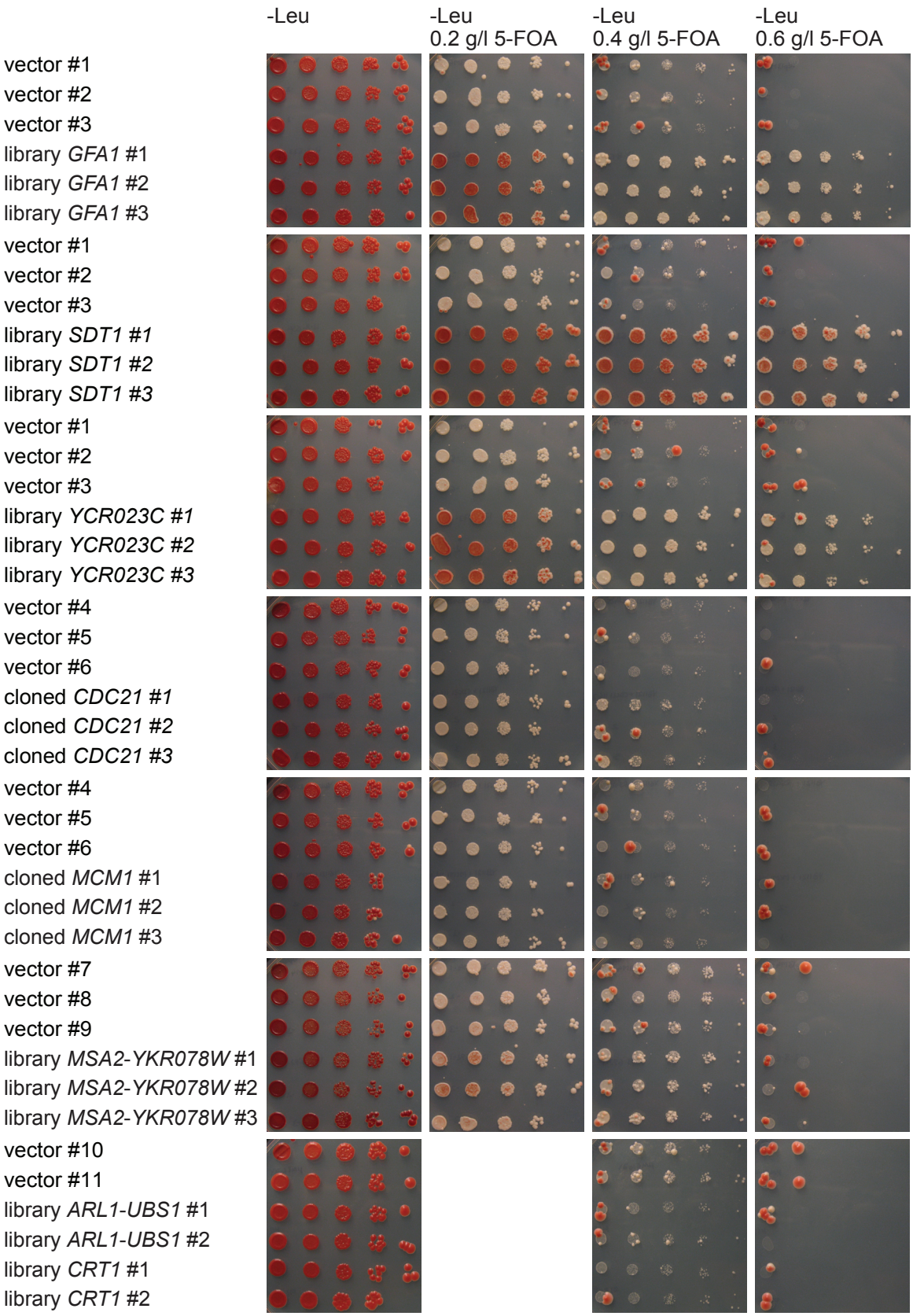
-Leu
-Leu
0.2 g/l 5-FOA
-Leu
0.4 g/l 5-FOA
-Leu
0.6 g/l 5-FOA
vector #1
vector #2
vector #3
library *GFA1* #1
library *GFA1* #2
library *GFA1* #3
vector #1
vector #2
vector #3
library *SDT1 #1*
library *SDT1 #2*
library *SDT1 #3*
vector #1
vector #2
vector #3
library *YCR023C #1*
library *YCR023C #2*
library *YCR023C #3*
vector #4
vector #5
vector #6
cloned *CDC21 #1*
cloned *CDC21 #2*
cloned *CDC21 #3*
vector #4
vector #5
vector #6
cloned *MCM1* #1
cloned *MCM1* #2
cloned *MCM1* #3
vector #7
vector #8
vector #9
library *MSA2-YKR078W* #1
library *MSA2-YKR078W* #2
library *MSA2-YKR078W* #3
vector #10
vector #11
library *ARL1-UBS1* #1
library *ARL1-UBS1* #2
library *CRT1* #1
library *CRT1* #2

pathway and required SIR proteins for their function. In the following I first focus on the role of *CDC21* and *POL30* in heterochromatin formation and then discuss experiments involving the other high-copy suppressors.

2.3 The function of *CDC21* as a high-copy suppressor of the *pol30-8 URA3*-VIIL telomeric silencing defect requires its catalytic activity.

CDC21 is an essential gene (Hartwell et al., 1970; Hartwell et al., 1973) encoding thymidylate synthase, required for synthesis of thymidine triphosphate (dTTP). Cdc21 catalyzes the addition of a methyl group to deoxyuridylate (dUMP) to form thymidylate (dTMP). N^5,N^{10}-methylenetetrahydrofolate (MTHF) serves as a methyl donor and is oxidized to dihydrofolate in this reaction. The *pol30-8 URA3*-VIIL 5-FOA sensitivity was suppressed by overexpressed wild-type *CDC21* over 1,000-fold (almost as well as the genomic insert, see Material and Methods), but not by fragments encompassing the 124 bp or 885 bp upstream of the *CDC21* ATG (Figure 4A). This result speaks in favor of *CDC21* itself being a high-copy suppressor rather than the 5' region titrating away an unknown factor involved in causing increased 5-FOA sensitivity of *pol30-8 URA3*-VIIL cells. A PROSITE motif search (Bairoch et al., 1997) predicts the Cdc21 active site to comprise amino acids 157 to 185 with a catalytic-site cysteine residue at position 177. Towards the N-terminus (Figure 4B), Cdc21 also contains a motif named EUK1. This motif is located within a surface loop important for substrate binding adjacent to the catalytic site. Notably, deletion of the EUK1 region of *S. cerevisiae CDC21* resulted in a decrease to 1 % of the

Figure 4: The function of *CDC21* as a high-copy suppressor of the *pol30-8 URA3*-VIIL telomeric silencing defect requires its catalytic activity.

(A) 10-fold serial dilution of a *pol30-8 hmr*::*ADE2 URA3*-VIIL strain (MRY0828) transformed with *POL30*, YEp13M4, pRS425, genomic *CDC21*, cloned *CDC21* or two fragments with the 885 bp or 124 bp upstream of the *CDC21* ATG.

(B) Cdc21 secondary structure (modified from Munro et al., 1999); aa = amino acid.

(C) 10-fold serial dilution of a *pol30-8 hmr*::*ADE2 URA3*-VIIL strain (MRY0828) transformed with *POL30*, pRS425, cloned *CDC21*, *cdc21-ΔEUK1* or *cdc21-C177A*.

(D) Western blot analysis of whole cell protein extracts from an experiment as in (C); “short” and “long” refer to exposure times.

(E) dCTP, dTTP, dATP and dGTP levels in two asynchronously growing *pol30-8 hmr*::*ADE2 URA3*-VIIL (MRY0041) strains transformed with pRS425 or genomic *CDC21* (2 transformants each). Values were normalized by NTP. Error bars denote the standard error of the mean (SEM).

A

pol30-8
hmr*::*ADE2
***URA3*-VIIL**
+

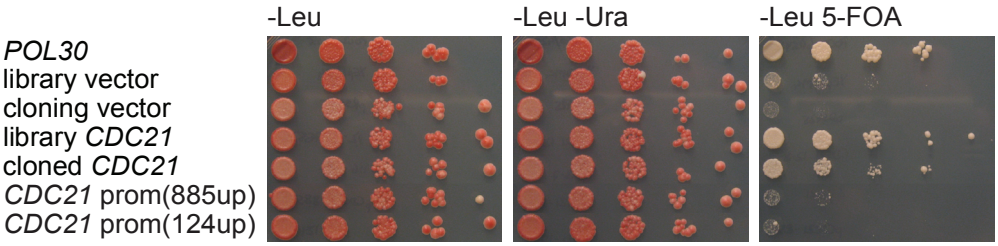

B

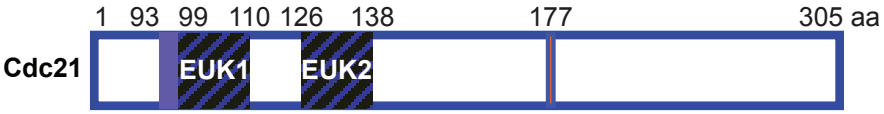

C

pol30-8
hmr*::*ADE2
***URA3*-VIIL**
+

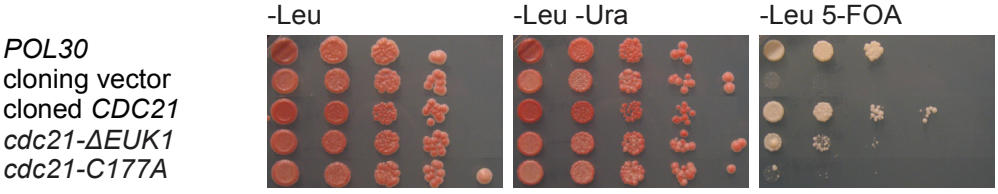

D

***pol30-8 hmr*::*ADE2 URA3*-VIIL**
+

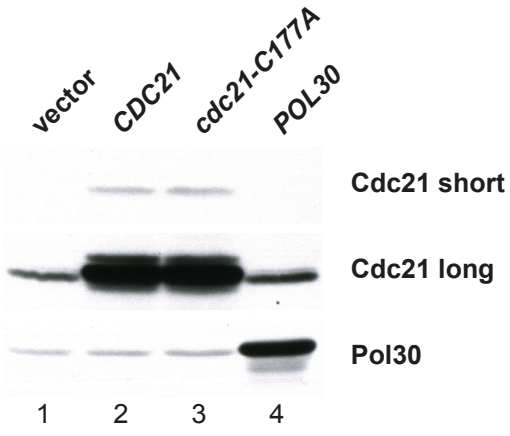

E

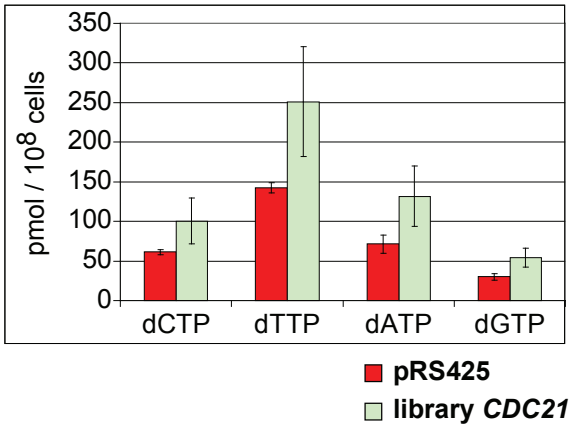

wild-type catalytic activity (Munro et al., 1999). To test whether the catalytic activity of Cdc21 is required for its suppressor function towards *pol30-8*, *cdc21-ΔEUK1* and *cdc21-C177A* expressing plasmids were generated. While *cdc21-ΔEUK1* suppressed the *pol30-8 URA3*-VIIL silencing defect more than 100-fold less well than wild-type *CDC21*, *cdc21-C177A* did not suppress it at all (Figure 4C) although it was expressed at levels comparable to the wild-type protein when tested with an antibody that was generated against full length Cdc21 (Figure 4D). These results demonstrate that the catalytic activity of Cdc21 is required for its suppressive function in *pol30-8 URA3*-VIIL cells.

The initial secondary screen required high-copy suppressors to be of dark pink colony color in two subsequent re-streaks, reflecting sustained silencing of *hmr*::*ADE2*, which ten clones of *CDC21* did (Table1). However, when serial dilutions of all such cultures were plated on SC -Leu, neither overexpression of the genomic insert containing *CDC21* nor that of cloned *CDC21* resulted in consistently darker pink colonies than those of *pol30-8 hmr*::*ADE2* alone (Figures 4A and 4C), except in transformations with two 2-μm plasmids, one of which containing *CDC21* and the other being empty vector (see below; Figures 9C and 23D). Moreover, colony colors of *pol30-8 hmr*::*ADE2 URA3*-VIIL strains from many different crosses including backcrosses to W303 also varied in the intensities (in tetrads and serial dilutions, e.g., Figures 4A, 5B, 10A). Weak repression of *ADE2* at the modified *hmr* locus (Sussel et al., 1993) has been previously described even for wild-type cells (Zhang et al., 2000). Due to lack of

robustness, I will not comment on effects on colony color with regard to *pol30-8* when discussing the suppressors except for notable differences.

Since the catalytic activity of Cdc21 is essential for dTTP synthesis, increased dTTP levels could be the cause of reduced *URA3*-VIIL expression. In collaboration with Olga Tsaponina, a graduate student in Dr. Andrei Chabes' laboratory (Umeå University, Umeå, Sweden), we found dTTP levels to be increased by 1.8-fold when the genomic library clone containing *CDC21* was overexpressed (Figure 4E), but not when cloned *CDC21* with 124-bp upstream sequence was overexpressed (data not shown). However, cloned *CDC21* also suppressed the *pol30-8 URA3*-VIIL 5-FOA sensitivity slightly less well (Figure 4A). Thus, *CDC21* overexpression modestly increases overall thymidylate synthase activity and thereby dTTP levels in the cell.

2.4 A *cdc21* mutant, *cdc21-216*, has a telomeric silencing defect at *URA3*-VIIL.

To test whether endogenous *CDC21* had a role in telomeric silencing, a loss-of-function allele needed to be analyzed. Mutant alleles of *CDC21* (*cdc21-216*), *CRT1* (or *RFX1*), *SSN6* and *TUP1* were identified in an EMS screen for mutants that constitutively express *RNR3* (constitutive *RNR3* transcription [CRT]; Huang et al., 1998; Zhou and Elledge, 1992). Sequencing this allele of *CDC21* revealed a GGT to GAT change at codon 139, substituting aspartic acid for glycine. To test whether this mutant was defective in heterochromatin formation, I

Figure 5: A *cdc21* mutant, *cdc21-216*, has a telomeric silencing defect at *URA3*-VIIL.

(A) Tetrads from a diploid strain heterozygous for *pol30-8*, *cdc21-216* (a ts allele), *hmr*::*ADE2* and *URA3*-VIIL (MRY1448) grown on YPD at room temperature (RT) and at 35˚C after replica-plating.

(B) 10-fold serial dilution of wild-type (MRY1655, 1657), *pol30-8* (MRY1653, 1652), *cdc21-216* (MRY1656, 1651) and *pol30-8 cdc21-216* (MRY1654, 1650) *hmr*::*ADE2 URA3*-VIIL segregants from MRY1448. Plates were incubated at RT.

A

YPD, RT

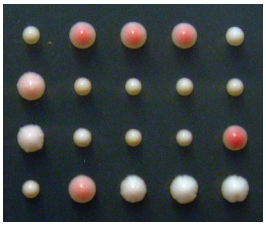

YPD, 35 ˚C

B

SC -Ura 5-FOA

*MAT***a**
*MAT*α
*MAT***a** *pol30-8*
*MAT*α *pol30-8*
*MAT***a** *cdc21-216*
*MAT*α *cdc21-216*
*MAT***a** *pol30-8 cdc21-216*
*MAT*α *pol30-8 cdc21-216*

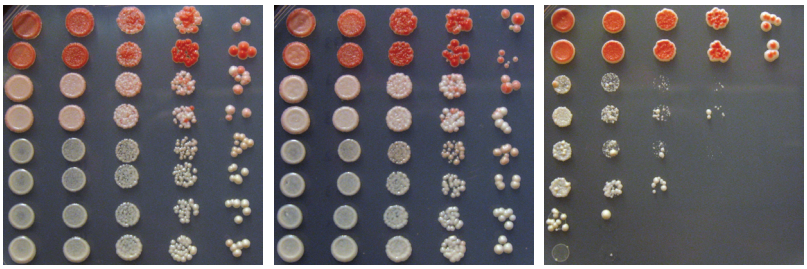

generated a *cdc21-216 hmr*::*ADE2 URA3*-VIIL strain. This strain was temperature-sensitive (ts) as described previously for the *cdc21-216* allele (Figure 5A; Zhou and Elledge, 1992). While the colony color and thus heterochromatin formation at *hmr*::*ADE2* could not be assessed due to the mutation conferring a petite phenotype (data not shown), this mutant strain was unable to grow in the presence of 5-FOA (Figure 5B), suggesting a role for *CDC21* in the TPEV phenotype.

2.5 An alternative telomeric marker, *HIS3*-VIIL, reveals differences in heterochromatic phenotypes.

In the original description of TPEV, four genes were placed at telomere VII-L and three were substantially silenced in their expression (Gottschling et al., 1990). To address the general effect of *CDC21* on TPEV, we asked whether its ability to suppress the telomeric silencing defect of *pol30-8* cells was specific to *URA3*-VIIL or applied to other markers inserted at the telomere (for schematic overview, see Figures 6A and 8A), I constructed *pol30-8*, *cac1Δ* or *sir3Δ* [as a control for this assay (Bourns et al., 1998)] mutant strains carrying *HIS3* at telomere VII-L. *HIS3* expression can be positively selected for on medium containing 3-amino-1,2,4-triazole (3-AT), a competitive inhibitor of the *HIS3* gene product, imidazoleglycerol-phosphate dehydratase (Brennan and Struhl, 1980). Surprisingly, *cac1Δ* and *pol30-8 HIS3*-VIIL mutant cells only had a slight growth advantage (less than 10-fold) compared to wild-type *HIS3*-VIIL cells on medium lacking histidine (Figure 6B). Moreover, addition of 3-AT did not result in a growth

Figure 6: An alternative telomeric marker, *HIS3*-VIIL, reveals differences in heterochromatic phenotypes.

(A) Schematic representation of (1) endogenous telomere VII-L, (2) telomere VII-L with *URA3* inserted adjacent to the 5' end of a truncated *ADH4*, (3) telomere VII-L carrying *HIS3* distal to *URA3*. Arrows above genes depict the direction of transcription.

(B) 10-fold serial dilution of wild-type (MRY0709, 0712), *cac1Δ* (MRY0704, 0713) and *pol30-8* (MRY0700) strains (upper panel) as well as wild-type (MRY1527) and *sir3Δ* (MRY1532) strains (lower panel). All strains carried *HIS3*-VIIL as depicted in (A3).

(C) *hmr*::*ADE2* and *URA3*-VIIL expression ratios, measured by RT-qPCR, in *pol30-8* (MRY1098, 1092), *sir3Δ* (MRY1084, 1080) and *pol30-8 sir3Δ* (MRY1088, 1102) compared to wild-type (MRY1081, 1097) strains. Strains of the same mating type were compared. All strains were deleted for the endogenous *ade2-1* and *ura3-1* alleles and carried *hmr*::*ADE2* as well as *URA3*-VIIL as depicted in (A2). The average result for three independent experiments with two primer pairs per gene is shown.

A

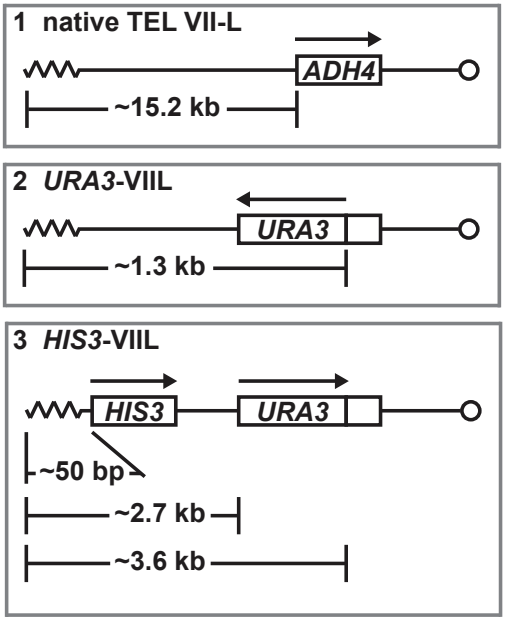

B

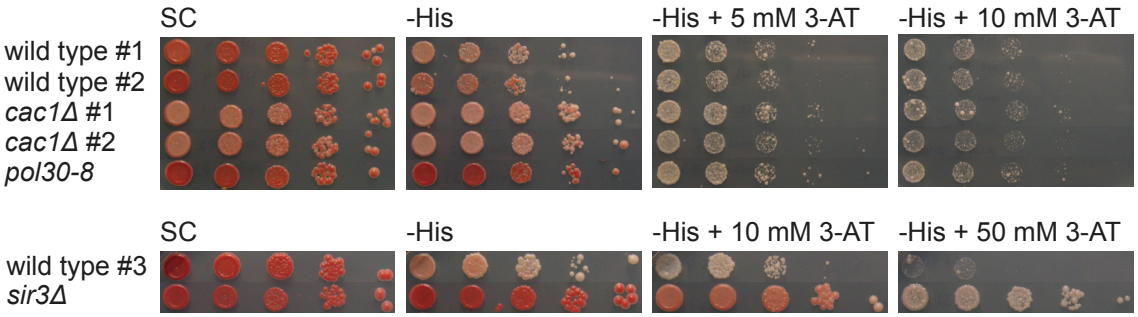

C

Mutant / wild-type expression ratios

		ADE2	*URA3*
pol30-8 / wild type	*MAT***a**	4.2	7.2
pol30-8 / wild type	*MAT*α	6.2	6.2
sir3Δ / wild type	*MAT***a**	41	354
sir3Δ / wild type	*MAT*α	46	187
pol30-8 sir3Δ / wild type	*MAT***a**	42	234
pol30-8 sir3Δ / wild type	*MAT*α	47	146

advantage of these mutants over wild type (Figure 6B). In striking contrast, *sir3Δ* mutants grew even in the presence of 50 mM 3-AT (Figure 6B). The stark difference between the telomeric effects at *URA3*-VIIL and *HIS3*-VIIL prompted me to assess the differences in *URA3*-VIIL expression levels between wild-type and *pol30-8*, *sir3Δ* and *pol30-8 sir3Δ* mutants. Reverse transcription followed by quantitative PCR (RT-qPCR) of RNA extracted from strains grown to logarithmic phase in rich medium revealed that *URA3*-VIIL expression was elevated by 6.2- to 7.2-fold in *pol30-8* compared to wild-type cells (Figure 6C). In contrast, in *MAT*α *sir3Δ* cells *URA3*-VIIL expression levels were at least 187 times above wild-type levels. For non-mating cells (*MAT***a** by inference from tetrad analysis) the ratio itself might be skewed due to alternative DSB repair pathway choice in the quasi-diploid *sir3Δ* mutant (Astrom et al., 1999; Lee et al., 1999). These data indicated that under non-selective conditions both reporter genes, *URA3* and *HIS3*, at telomere VII-L, were only mildly derepressed in *pol30-8* cells as compared to the larger effect conferred by a *SIR3* deletion.

2.6 *POL30* overexpression does not lower *URA3*-VIIL expression.

Unexpectedly, *POL30* overexpression only lowered elevated *URA3*-VIIL expression in *pol30-8* mutants by about 17 % (Figure 7A), while it suppressed their 5-FOA sensitivity very well (Figures 4A and 4C). This key observation suggested that *URA3* expression is not the sole determinant of 5-FOA sensitivity. In *pol30-8 HIS3*-VIIL strains, however, overexpression of *POL30* suppressed expression of *HIS3*-VIIL to below wild-type levels (Figure 7B). Interestingly,

Figure 7: *POL30* overexpression does not lower *URA3*-VIIL expression.

(A) Expression levels of *URA3*-VIIL, measured by RT-qPCR, in a wild-type strain (MRY1097) transformed with pRS425 or a *pol30-8* strain (MRY1092) transformed with pRS425, *POL30* or *CDC21*. Both strains were *ade2Δ ura3Δ hmr*::*ADE2 URA3*-VIIL. *ACT1*: reference. Results were normalized to wild-type *URA3*-VIIL levels. Error bars denote the SEM for two transformants, each tested with three primer pairs.

(B) Expression levels of *HIS3*-VIIL, measured as in (A), in a wild-type strain (MRY1418) transformed with pRS425 or *CDC21* or a *pol30-8* strain (MRY1414) transformed with pRS425, *POL30* or *CDC21*. Both strains were *his3Δ HIS3*-VIIL. Number of experiments and analysis as in (A).

A

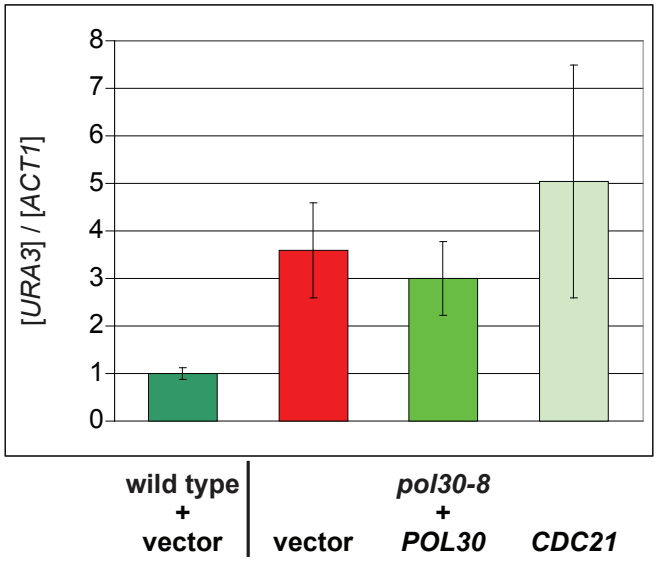
[URA3] / [ACT1]
8
7
6
5
4
3
2
1
0
wild type + vector
vector
pol30-8 + POL30
CDC21

B

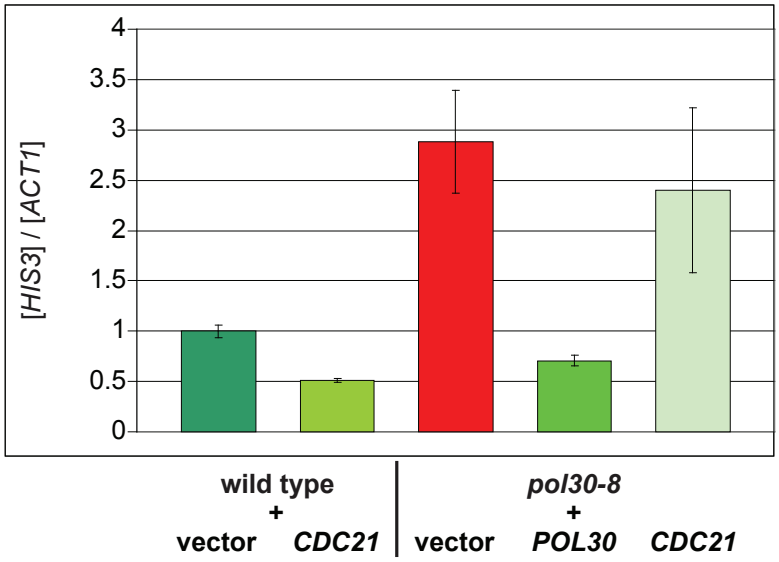
[HIS3] / [ACT1]
4
3.5
3
2.5
2
1.5
1
0.5
0
wild type + vector
CDC21
vector
pol30-8 + POL30
CDC21

overexpressed *CDC21* lowered expression of *HIS3*-VIIL in wild-type cells by 50 %, but did not alter *URA3*-VIIL or *HIS3*-VIIL expression in *pol30-8* cells; if anything it increased *URA3*-VIIL expression (Figure 7B and data not shown). These data (1) confirm the relatively small increase in gene expression of *URA3* or *HIS3* at telomere VII-L in *pol30-8* compared to a wild-type strain, (2) suggest differences between the regulation of expression at *URA3*-VIIL and *HIS3*-VIIL with regard to the role of *POL30* and *CDC21*, (3) suggest a function of *POL30* and *CDC21* as high-copy suppressors of *pol30-8 URA3*-VIIL distinct from regulation of *URA3*-VIIL expression, at least in the absence of 5-FOA.

2.7 *pol30-8* and wild-type cells do not differ in telomeric gene expression in the presence of a strong promoter.

The increase of telomeric expression in *pol30-8* compared to wild-type cells could be dependent on the promoters of the reporter genes being already weakened by their telomeric localization. To address this hypothesis, I replaced the *URA3* marker gene at telomere VII-L by the heterologous *kanMX6* cassette (Figure 8A; Longtine et al., 1998). This cassette contains the kanamycin resistance gene (*kan*^{r}) from *E. coli* under the strong promoter of the *Ashbya gossypii* translation elongation factor 1α as well as its terminator (Steiner and Philippsen, 1994; Wach et al., 1994). Interestingly, *kanMX6*-VIIL expression was repressed by 20 % in *pol30-8* compared to wild-type strains; in contrast, *kanMX6*-VIIL expression was still 1.5-fold up-regulated in *sir3Δ* cells (Figure 8B). The small effect even in *sir3Δ* cells is probably due to the strong promoter. These

Figure 8: *pol30-8* and wild-type cells do not differ in telomeric gene expression in the presence of a strong promoter.

(A) Schematic representation of (1) endogenous telomere VII-L, (2) telomere VII-L with *URA3* inserted adjacent to the 5' end of a truncated *ADH4*, (3) telomere VII-L with the *kanMX6* cassette replacing *URA3* in the construct shown in (2). Arrows above genes depict the direction of transcription.

(B) Box plot showing average *kanMX6*-VIIL expression levels (construct [A3]), measured by RT-qPCR, in wild-type (MRY1607, 1615, 1612, 1610), *pol30-8* (MRY1611, 1613, 1617, 1619), *sir3Δ* (MRY1609, 1622, 1614, 1620) and *pol30-8 sir3Δ* (MRY1616, 1618, 1621, 1608) strains. *ACT1*: reference. Error bars denote the SEM for four strains per genotype, each tested with three primer pairs.

(C) Expression levels of *URA3*, measured by RT-qPCR, averaged over four wild-type (MRY1551, 1556, 1549, 1554), four *pol30-8* (MRY1550, 1557, 1558, 1555), two *ppr1Δ* (MRY1547, 1552) and two *pol30-8 ppr1Δ* (MRY1548, 1553) strains carrying *URA3* at its endogenous locus grown in medium lacking uracil. *ACT1*: reference. Results were normalized to wild-type *URA3* levels. Error bars denote the SEM for all strains per genotype, each tested with three primer pairs.

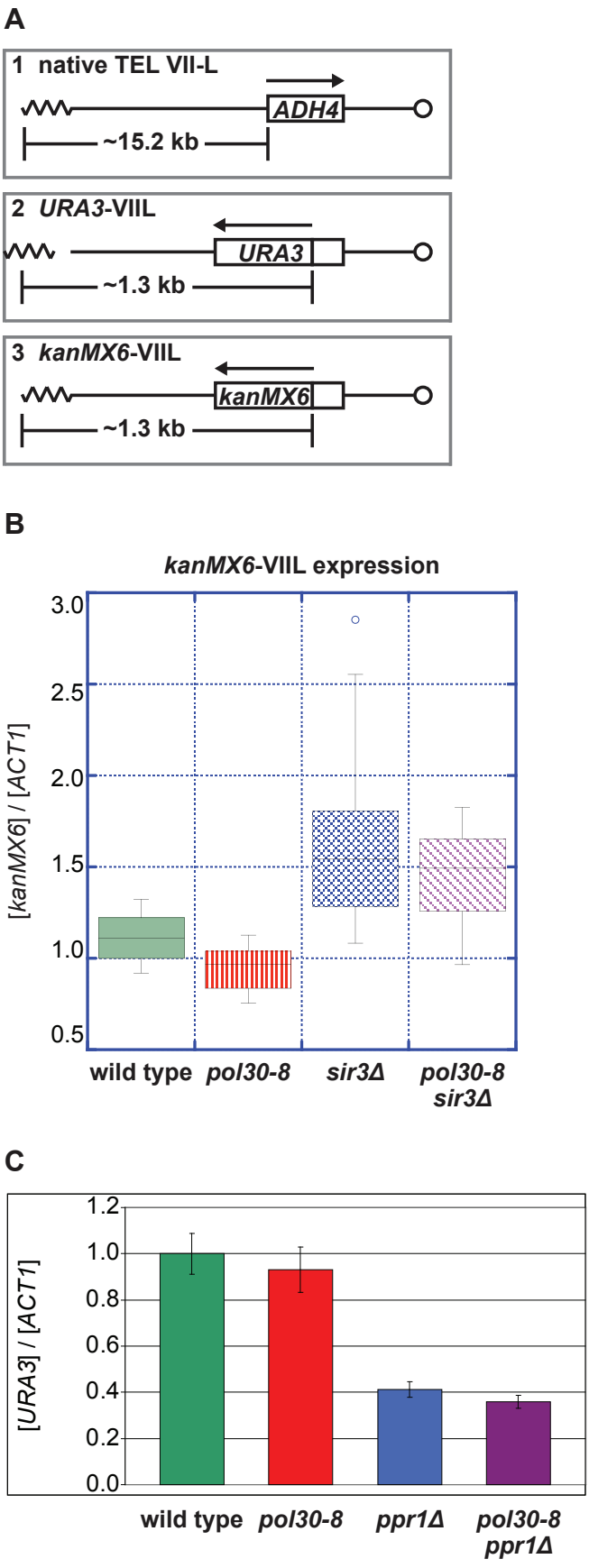
A
1 native TEL VII-L
ADH4
~15.2 kb
2 URA3-VIIL
URA3
~1.3 kb
3 kanMX6-VIIL
kanMX6
~1.3 kb
B
kanMX6-VIIL expression
[kanMX6] / [ACT1]
3.0
2.5
2.0
1.5
1.0
0.5
wild type
pol30-8
sir3Δ
pol30-8 sir3Δ
C
[URA3] / [ACT1]
1.2
1.0
0.8
0.6
0.4
0.2
0.0
wild type
pol30-8
ppr1Δ
pol30-8 ppr1Δ

data suggest a weak silencing defect in *pol30-8* mutants that can be completely overridden by a strong promoter, in contrast to the silencing defect of a *sir3Δ* mutation. In agreement with these results, the *pol30-8* mutation did not result in expression changes of *URA3* at its endogenous locus (Figure 8C), whereas deletion of a transcriptional activator of *URA3*, *PPR1* (which will be further discussed below), resulted in a 2-fold reduction in endogenous *URA3* levels, but only when strains were grown in medium lacking uracil (Figure 8C and data not shown).

2.8 The *POL30*/CAF-1 pathway genetically interacts with *PPR1*.

One possibility why *URA3*-VIIL expression is less susceptible to silencing in *pol30-8* cells could be a direct effect of *POL30* on *URA3*-VIIL transcription. That is, if *pol30-8* led to activation of *URA3*-VIIL transcription, it might do so in the absence of the transcriptional activator for *URA3*, Ppr1. *URA3* encodes the orotidine-5'-phosphate decarboxylase (OMPdecase), an inducible enzyme of the pyrimidine biosynthetic pathway (Lacroute, 1968). The regulation of *URA3* by pyrimidine pathway regulator 1 (*PPR1*) has been well studied as a model for the function of *cis*- and *trans*-acting regulatory elements of a yeast promoter. Basal endogenous *URA3* transcription is largely independent of Ppr1, although it has a role in the context of auxotrophic pressure (Figure 8C; Aparicio and Gottschling, 1994; Losson and Lacroute, 1983). In contrast, *ppr1Δ URA3*-VIIL cells grew only very poorly on medium lacking uracil (Figure 9A; Aparicio and Gottschling, 1994). However, *pol30-8 ppr1Δ* or *cac1Δ ppr1Δ* cells showed a 1,000- to 10,000-fold

Figure 9: The *POL30*/CAF-1 pathway genetically interacts with *PPR1*.

(A) 10-fold serial dilution of wild-type (MRY0814), *ppr1Δ* (MRY0811), *pol30-8* (MRY0041), *ppr1Δ pol30-8* (MRY0812), *cac1Δ* (MRY0813), *ppr1Δ cac1Δ* (MRY0815), *pol30-8 cac1Δ* (MRY0810) and triple mutant (MRY0816) *hmr*::*ADE2 URA3*-VIIL strains.

(B) 10-fold serial dilution of two *ppr1Δ* strains (MRY0191, 0731) transformed with pRS425 and pRS424, a *ppr1Δ hmr*::*ADE2 URA3*-VIIL strain (MRY0191) transformed with *POL30/pRS425* and pRS424*,* pR425 and *CAC1*/pRS424 or *POL30*/pRS425 and *CAC1*/pRS424 and a *ppr1Δ pol30-8* strain (MRY0180) transformed with pRS425 and pRS424. All strains carried *hmr*::*ADE2 URA3*-VIIL. #1 and #2 indicate independent transformants.

(C) 10-fold serial dilution of a *pol30-8 hmr*::*ADE2 URA3*-VIIL strain (MRY0041) transformed with pRS425 and pRS423, *POL30/pRS425* and pRS423*,* pR425 and *PPR1*/pRS423, *CDC21*/pRS425 and pRS423 or *CDC21*/pRS425 and *PPR1*/pRS423. #1 and #2 indicate independent transformants.

A

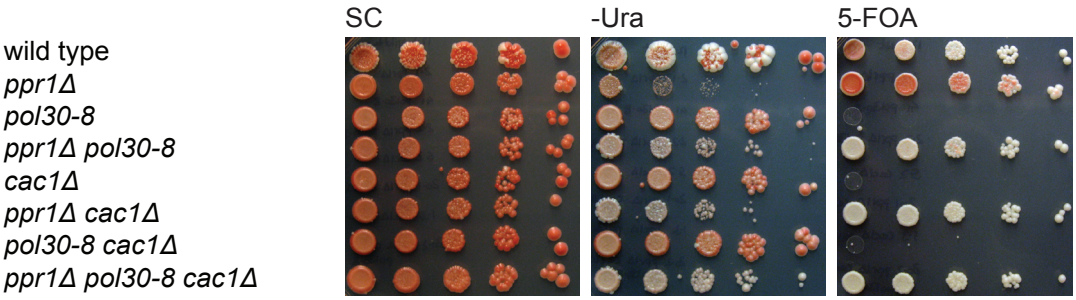

B

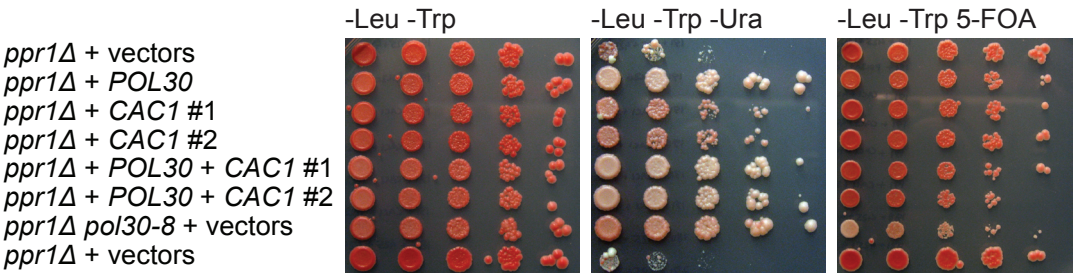

C

pol30-8
hmr*::*ADE2
***URA3*-VIIL**
+

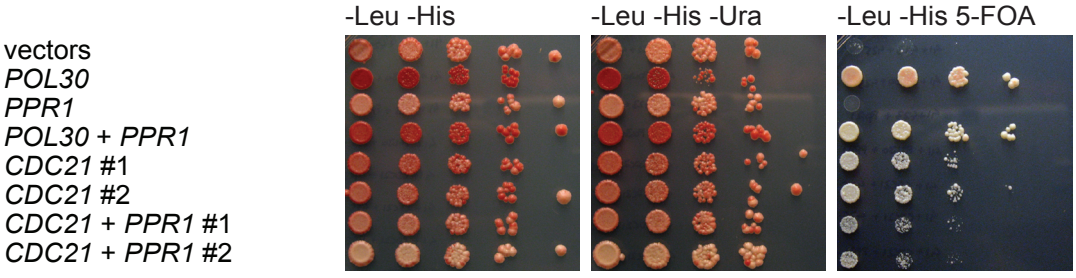

elevated growth rate on medium lacking uracil compared to *ppr1Δ* cells (Figure 9A). Interestingly, *POL30* overexpression had the same effect and was epistatic to *CAC1* (Figure 9B). Furthermore, whereas the suppressive effect of overexpressed *CDC21* on 5-FOA sensitivity in *pol30-8 URA3*-VIIL cells could be cancelled out by co-overexpression of *PPR1*, the suppressive activity of *POL30* was dominant over *PPR1* (Figure 9C).

2.9 5-FOA resistance does not correlate with Ura$^-$ auxotrophy.

Overexpression of *ASF1* causes derepression of silent mating type loci (Le et al., 1997) and telomeres V-R and VII-L marked with *ADE2* and *URA3*, respectively (Singer et al., 1998). Subsequently, Asf1 was found to be a histone chaperone aiding CAF-1 in the assembly of histones H3 and H4 onto replicating DNA (Tyler et al., 1999), but also to act independently of DNA replication (Sharp et al., 2001). Deletion of *ASF1* had no effect on 5-FOA sensitivity of a *URA3*-VIIL strain (Sharp et al., 2001 and Figure 10A), but like *pol30-8* could partially rescue a *ppr1Δ URA3*-VIIL strain on -Ura medium (Figure 10A). *pol30-8 asf1Δ ppr1Δ URA3*-VIIL cells grew even better on -Ura plates and were completely sensitive to 5-FOA, suggesting these two pathways are synergistic (Figure 10A).

For one of the SIR genes, *SIR1*, no role in silencing *URA3* at telomeres V-R and VII-L could be demonstrated, as assessed by 5-FOA sensitivity and *URA3* RNA levels (Aparicio et al., 1991). To test whether deletion of *SIR1* had a similar Ura$^+$ phenotype as *pol30-8* and *asf1Δ* in the context of *ppr1Δ*, I generated all genotype combinations from a *pol30-8 sir1Δ ppr1Δ* diploid. Like *asf1Δ*, *sir1Δ* also

Figure 10: 5-FOA resistance does not correlate with Ura$^-$ auxotrophy.

(A) 10-fold serial dilution of wild-type (MRY1510), *asf1Δ* (MRY1513), *pol30-8* (MRY1516), *ppr1Δ* (MRY1502), *asf1Δ pol30-8* (MRY1511), *asf1Δ ppr1Δ* (MRY1508), *pol30-8 ppr1Δ* (MRY1514) and triple mutant (MRY1505) *hmr*::*ADE2 URA3*-VIIL strains.

(B) 10-fold serial dilution of wild-type (MRY0183), *ppr1Δ* (MRY0191), *pol30-8* (MRY0181), *ppr1Δ pol30-8* (MRY0180), *sir1Δ* (MRY0178), *ppr1Δ sir1Δ* (MRY0182), *pol30-8 sir1Δ* (MRY0190) and triple mutant (MRY0185) *hmr*::*ADE2 URA3*-VIIL strains.

(C) 10-fold serial dilution of wild-type (MRY1022, 1024), *ppr1Δ* (MRY1025, 1023), *orc1-bah* (MRY1030, 1029) and *ppr1Δ orc1-bah* (MRY1028, 1034) *hmr*::*ADE2 URA3*-VIIL strains.

A

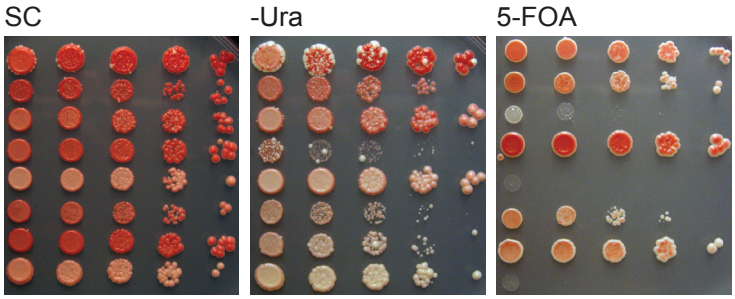
SC
-Ura
5-FOA
wild type
asf1Δ
pol30-8
ppr1Δ
asf1Δ pol30-8
asf1Δ ppr1Δ
pol30-8 ppr1Δ
asf1Δ pol30-8 ppr1Δ

B

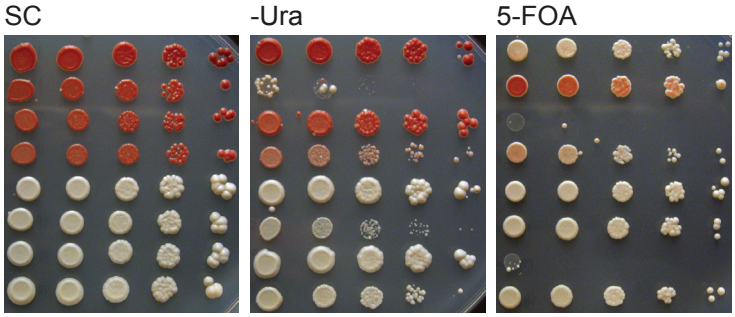
SC
-Ura
5-FOA
wild type
ppr1Δ
pol30-8
ppr1Δ pol30-8
sir1Δ
ppr1Δ sir1Δ
pol30-8 sir1Δ
ppr1Δ pol30-8 sir1Δ

C

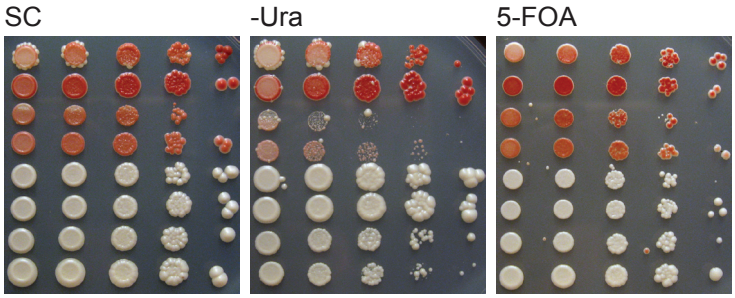
SC
-Ura
5-FOA
wild type MATa
wild type MATα
ppr1Δ MATa
ppr1Δ MATα
orc1-bah MATa
orc1-bah MATα
ppr1Δ orc1-bah MATa
ppr1Δ orc1-bah MATα

rescued the uracil auxotrophy of *ppr1Δ URA3*-VIIL strains (Figure 10B). This is likely dependent on its interaction with Orc1, since an *orc1* mutant lacking the N-terminal BAH domain responsible for the interaction with Sir1 (Triolo and Sternglanz, 1996; Zhang et al., 2002) recapitulated the *sir1Δ* phenotype with regard to *ppr1Δ* (Figure 10C). These results hint to a different cause, at least in some cases, for 5-FOA sensitivity than increased *URA3*-VIIL expression: while *asf1Δ* or *sir1Δ* cells display no or only marginally increased 5-FOA sensitivity, they activate *URA3*-VIIL as well as *pol30-8* does (Figures 10A and 10B).

2.10 *CDC21* also suppresses the 5-FOA sensitivity of a *dot1Δ URA3*-VIIL mutant.

Like *pol30-8*, *dot1Δ* also enables telomeric *URA3* expression in *ppr1Δ* cells (Singer et al., 1998). *DOT1* encodes the only known histone H3K79 methyltransferase in yeast (Ng et al., 2002; van Leeuwen et al., 2002) and was one of ten genes whose overexpression increased expression of *URA3* and *ADE2* in a *ppr1Δ ADE2*-VR *adh4*::*URA3*-VIIL strain (Singer et al., 1998). The similarity of the *pol30-8 ppr1Δ* and *dot1Δ ppr1Δ* phenotypes led me to test whether *CDC21* could also suppress the telomeric silencing phenotype of *dot1Δ URA3*-VIIL mutants. As shown in Figure 11A, this was the case.

However, *CDC21* did not suppress the *pol30-8 dot1Δ URA3*-VIIL (Figure 11A) or *pol30-8 asf1Δ URA3*-VIIL (Figure 11B) silencing defects. The synergism between *pol30-8* and *dot1Δ* on one side and *pol30-8* and *asf1Δ* on the other with regard to *CDC21* suppression led me to test for a genetic interaction between

Figure 11: *CDC21* also suppresses the 5-FOA sensitivity of a *dot1Δ URA3*-VIIL mutant.

(A) 10-fold serial dilution of wild-type (MRY1070), *pol30-8* (MRY1077), *dot1Δ* (MRY1063) or double mutant (MRY1062) *hmr*::*ADE2 URA3*-VIIL strains transformed with pRS425 or *CDC21*.

(B) 10-fold serial dilution of wild-type (MRY1237), *pol30-8* (MRY1224), *asf1Δ* (MRY1229) or double mutant (MRY1222) *hmr*::*ADE2 URA3*-VIIL strains transformed with pRS425 or *CDC21*.

(C) 10-fold serial dilution of wild-type (MRY1237), *dot1Δ* (MRY1242), *dot1Δ asf1Δ* (MRY1288) or *pol30-8 dot1Δ asf1Δ* (MRY1226) *hmr*::*ADE2 URA3*-VIIL strains transformed with pRS425 or *CDC21*.

A

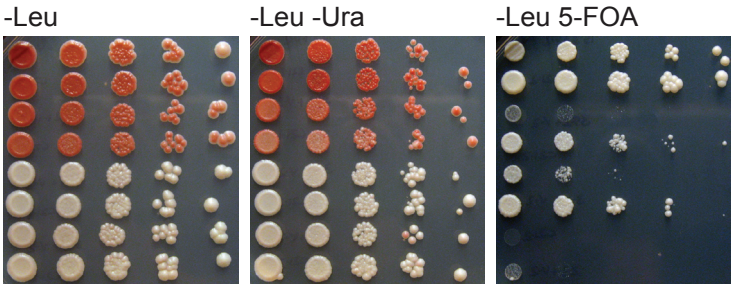
-Leu
-Leu -Ura
-Leu 5-FOA
wild type + vector
wild type + *CDC21*
pol30-8 + vector
pol30-8 + *CDC21*
dot1Δ + vector
dot1Δ + *CDC21*
pol30-8 dot1Δ + vector
pol30-8 dot1Δ + *CDC21*

B

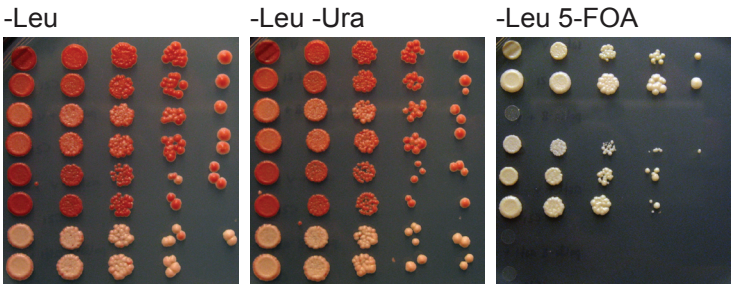
-Leu
-Leu -Ura
-Leu 5-FOA
wild type + vector
wild type + *CDC21*
pol30-8 + vector
pol30-8 + *CDC21*
asf1Δ + vector
asf1Δ + *CDC21*
pol30-8 asf1Δ + vector
pol30-8 asf1Δ + *CDC21*

C

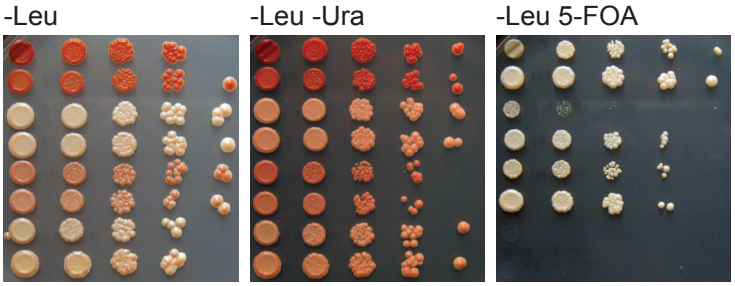
-Leu
-Leu -Ura
-Leu 5-FOA
wild type + vector
wild type + *CDC21*
dot1Δ + vector
dot1Δ + *CDC21*
dot1Δ asf1Δ + vector
dot1Δ asf1Δ + *CDC21*
pol30-8 dot1Δ asf1Δ + vector
pol30-8 dot1Δ asf1Δ + *CDC21*

DOT1 and *ASF1*. Unexpectedly, deletion of *ASF1* partially rescued the *dot1Δ* *URA3*-VIIL 5-FOA sensitivity, which could not be further alleviated by overexpressing *CDC21* (Figure 11C). I conclude that (genetically) *ASF1* is inhibitory to *DOT1* function at *URA3*-VIIL, and that *CDC21* might inhibit *ASF1*.

2.11 Pol30 and Dot1 interact directly.

Neither overexpression of *POL30* nor *DOT1* could rescue the mutation in the other gene (data not shown). These results underscore previous evidence of a genetic interaction between *CAC1* and *DOT1* (Zhou et al., 2006). This prompted me to ask whether these two proteins exist in a complex. The interaction of yeast, Xenopus and human PCNA with a number of proteins is mostly mediated by a hydrophobic pocket buried under the interdomain connecting loop (reviewed by Moldovan et al., 2007). A PIP box with the consensus sequence Qxx(h)xx(a) (x = any, h = hydrophobic, a = aromatic; Warbrick et al., 1998) has been found in many of the PCNA-interacting proteins, but also additional motifs can be involved. Dot1 contains a putative PIP box (Q_{516}INFY_{520}). Dot1 translated *in vitro* in the presence of [^{35}S]-methionine interacted with GST-Pol30, but not with GST (Figure 12, compare lane 5 with 6). Mutation of the aromatic amino acids within the putative PIP box in Dot1 resulted in a marked reduction in the interaction with GST-Pol30 (preliminary, data not shown).

Figure 12: Pol30 and Dot1 interact directly.

Top: Autoradiograph depicting a pull-down experiment of *in vitro* translated [^{35}S]-labeled Dot1 or a C-terminal Cac1(87-429) fragment with either 4 µg GST (G) or GST-Pol30 (G-P). Each lane contains 1 % input or 30 % pull-down reaction. Bottom: Coomassie Blue-staining of the same gel.

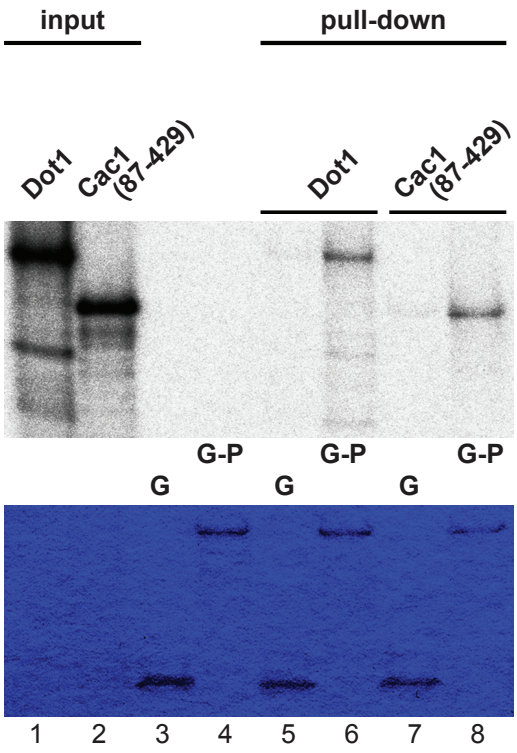
input
pull-down
Dot1
Cac1 (87-429)
Dot1
Cac1 (87-429)
G-P
G-P
G-P
G
G
G
1
2
3
4
5
6
7
8

2.12 The Pol30-Dot1 interaction is not required for telomeric silencing.

To test whether the interaction of Pol30 with Dot1 is relevant for the telomeric silencing phenotype seen in *dot1Δ* mutants, I expressed a mutant of *DOT1* in which the putative PIP box residues were mutated to alanine (*dot1-pip*) in *dot1Δ* cells. At telomeres, *dot1-pip* suppressed the defect of *dot1Δ URA3*-VIIL cells as well as *DOT1* (Figure 13A). In contrast, *dot1-pip* in either a centromeric or 2-µm based plasmid resulted in less repression of *hmr*::*ADE2* and therefore lighter pink colonies compared to wild-type *DOT1* (Figure 13A). Thus, the function of Dot1 to silence *hmr*::*ADE2* expression seems to partially depend on Pol30. It might also fully depend on Pol30, since this experiment does not address to which extent the Pol30-Dot1 interaction is affected by this mutation *in vivo*. A very small fraction of Pol30 could be co-immunoprecipitated with overexpressed 9Myc-Dot1 (preliminary, data not shown); however, co-immunoprecipitation experiments from an extract containing overexpressed 9Myc-Dot1-pip have not yet been performed. Interestingly, in the *dot1-pip* strain, global trimethylation of H3K79 was reduced compared to *DOT1*, with a concomitant increase in di- and monomethylation of H3K79, while total Dot1 protein levels were the same (Figure 13B, compare lanes 3 with 4 and 7 with 8). Thus, the Pol30-Dot1 interaction seems to have functional relevance at the *hmr*::*ADE2* locus and for trimethylation of H3K79, but not with regard to TPEV.

Figure 13: The Pol30-Dot1 interaction is not required for telomeric silencing.

(A) 10-fold serial dilution of wild-type (MRY1070) and *dot1Δ* (MRY1063) *hmr*::*ADE2 URA3*-VIIL strains transformed with vector, *DOT1* or *dot1-pip* (*dot1-QINFY516-520AANAA*) in either centromeric vector pRS415 (YCp; upper panel) or 2-µm origin containing vector pRS425 (YEp; lower panel).

(B) Western blot analysis of whole cell protein extracts from cultures used in (A); wt = wild type. Asterisks indicate cross-reacting bands; “short”, “medium” and “long” refer to exposure times.

A

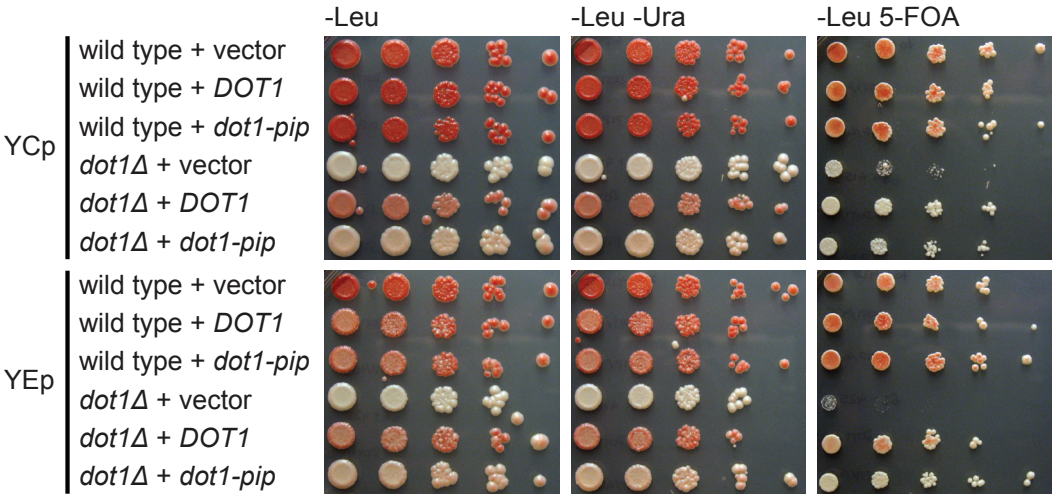
-Leu
-Leu -Ura
-Leu 5-FOA
YCp
wild type + vector
wild type + DOT1
wild type + dot1-pip
dot1Δ + vector
dot1Δ + DOT1
dot1Δ + dot1-pip
YEp
wild type + vector
wild type + DOT1
wild type + dot1-pip
dot1Δ + vector
dot1Δ + DOT1
dot1Δ + dot1-pip

B

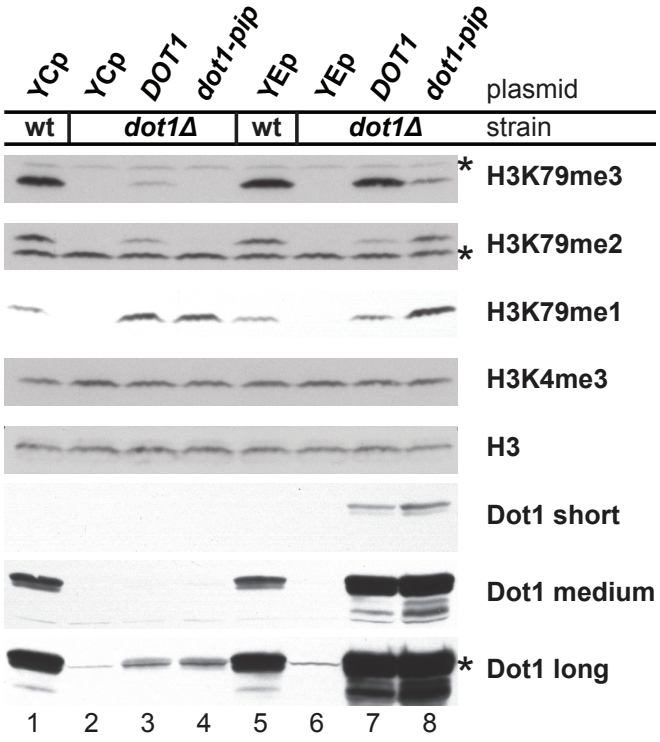
YCp
YCp
DOT1
dot1-pip
YEp
YEp
DOT1
dot1-pip
plasmid
wt
dot1Δ
wt
dot1Δ
strain
H3K79me3
H3K79me2
H3K79me1
H3K4me3
H3
Dot1 short
Dot1 medium
Dot1 long
1 2 3 4 5 6 7 8

2.13 The *dot1Δ* mutant exhibits maximal silencing of the *HIS3*-VIIL reporter.

On one hand, *dot1Δ pol30-8* cells seem to have a synergistic TPEV phenotype with the *URA3* reporter. On the other hand, a physical interaction between those two proteins did not seem to be required for TPEV as assayed by sensitivity of *URA3*-VIIL strains to 5-FOA. *dot1Δ hmr*::*ADE2* cells were almost completely white, and therefore must largely derepress expression at *hmr*::*ADE2*, similarly to *sir3Δ hmr*::*ADE2* but not like *pol30-8 hmr*::*ADE2* cells. Thus, I hypothesized that the *dot1Δ* telomeric silencing phenotype was also as robust as that of *sir3Δ* mutants. A difference in phenotype severity between *sir3Δ* and *pol30-8* or *cac1Δ* mutants was only visible using the *HIS3*-VIIL reporter since the *URA3*-VIIL reporter assay was maximally affected by both mutants. I therefore generated *dot1Δ*, *pol30-8* or *sir3Δ* strains with *HIS3*-VIIL. Surprisingly, in *dot1Δ* cells *HIS3*-VIIL was not expressed, in contrast to wild-type, *pol30-8* or *sir3Δ* cells which grew about 10,000-fold better on medium lacking histidine (Figure 14A). The *pol30-8* mutation partially rescued *HIS3*-VIIL expression only in the absence of 3-AT (Figure 14A), pointing to the ability of the *pol30-8* mutant to increase expression of a poorly expressed gene. As an aside, at high 3-AT concentrations, *pol30-8* seemed to impede *HIS3*-VIIL expression in *sir3Δ* mutants, reminiscent of a reduction of *URA3*-VIIL expression in the *pol30-8 sir3Δ* double mutant (Figure 6C). These data suggest that the *dot1Δ* mutation does not necessarily cause a telomeric silencing defect, at least not in the context of the *HIS3*-VIIL reporter.

Figure 14: The *dot1Δ* mutant exhibits maximal silencing of the *HIS3*-VIIL reporter.

(A) 10-fold serial dilution of wild-type (MRY1525), *dot1Δ* (MRY1530), *pol30-8* (MRY1521), *sir3Δ* (MRY1519) as well all double (MRY1529, 1528, 1523) and triple (MRY1533) mutant strains. All strains were *MATα his3Δ* and carried *HIS3*-VIIL as depicted in Figure 6 (A3).

(B) ChIP analysis for IgG, Sir2 (top) and Sir4 (bottom) followed by qPCR of wild-type (MRY1073) and *dot1Δ* (MRY1072) *ura3Δ URA3*-VIIL strains transformed with indicated 2-µm plasmids. Vector: pRS425. PCR primer pairs matched unique regions in *URA3* as well as sequences 200 bp, 600 bp and 11 kb away from telomere VI-R. Results were calculated as the fraction of immunoprecipitated sample of the input material. Error bars denote the SEM for two experiments.

A

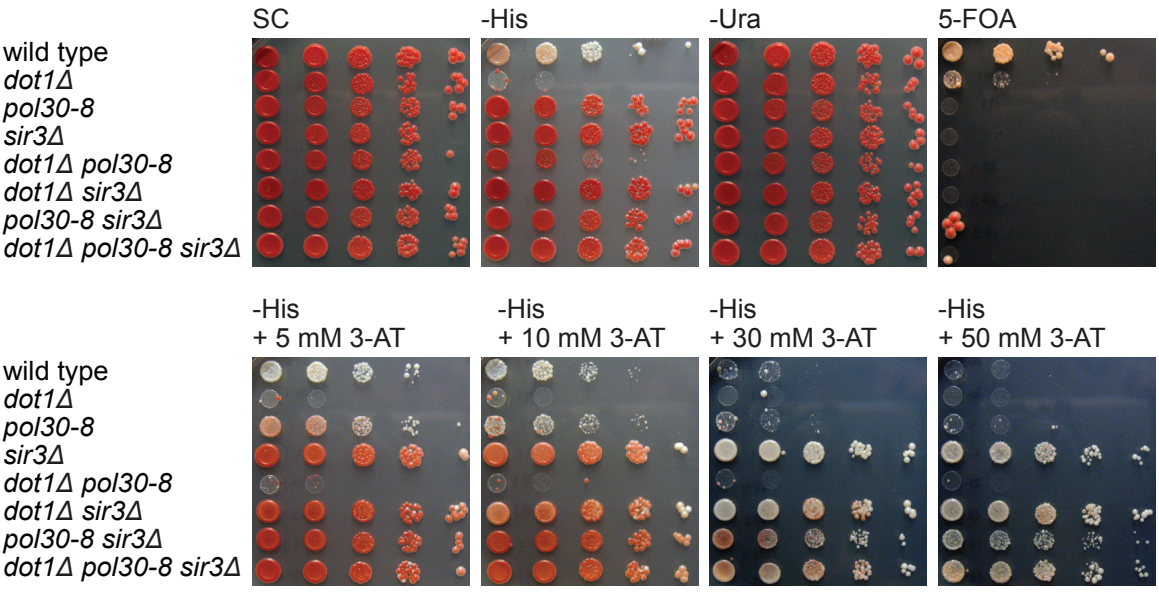
SC
-His
-Ura
5-FOA
wild type
dot1Δ
pol30-8
sir3Δ
dot1Δ pol30-8
dot1Δ sir3Δ
pol30-8 sir3Δ
dot1Δ pol30-8 sir3Δ
-His + 5 mM 3-AT
-His + 10 mM 3-AT
-His + 30 mM 3-AT
-His + 50 mM 3-AT
wild type
dot1Δ
pol30-8
sir3Δ
dot1Δ pol30-8
dot1Δ sir3Δ
pol30-8 sir3Δ
dot1Δ pol30-8 sir3Δ

B

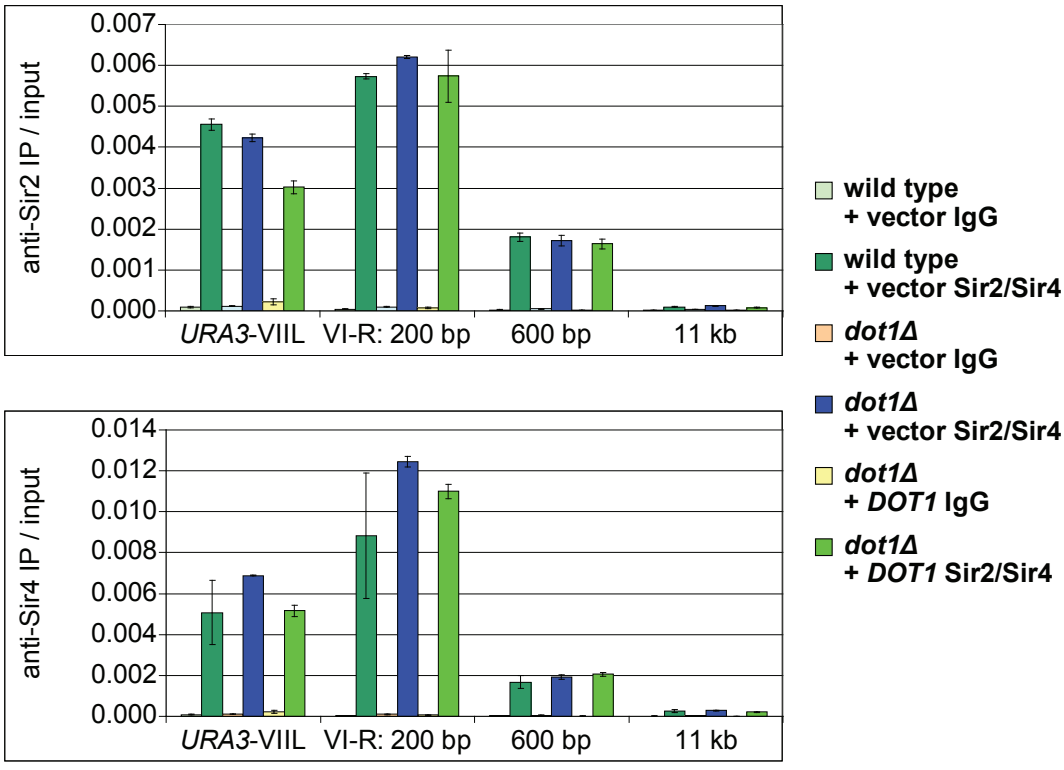
anti-Sir2 IP / input
0.007
0.006
0.005
0.004
0.003
0.002
0.001
0.000
URA3-VIIL
VI-R: 200 bp
600 bp
11 kb
anti-Sir4 IP / input
0.014
0.012
0.010
0.008
0.006
0.004
0.002
0.000
URA3-VIIL
VI-R: 200 bp
600 bp
11 kb
wild type + vector IgG
wild type + vector Sir2/Sir4
dot1Δ + vector IgG
dot1Δ + vector Sir2/Sir4
dot1Δ + DOT1 IgG
dot1Δ + DOT1 Sir2/Sir4

H3K79 trimethylation in euchromatin by Dot1 together with N-terminal acetylation of Sir3 by the NatA acetyltransferase complex reportedly acts as a barrier preventing SIR proteins from expanding from telomeric and *HM* heterochromatin into euchromatin (van Welsem et al., 2008). Hence, I expected the limiting SIR proteins to be less confined to telomeres in *dot1Δ* cells. However, performing ChIP I could not observe a reduced Sir2 and Sir4 occupancy at two telomeres in *dot1Δ* compared to wild-type cells (Figure 14B). This result stands in contrast to published work by the Gottschling, Struhl and Zhang groups, where a 50 % decrease in bound Sir2 and Sir3 at telomere VII-L (van Leeuwen et al., 2002), a 43 % and 40 % decrease in bound Sir2 and Sir3, respectively, at telomere VI-R (Ng et al., 2002) as well as a 37.5 % reduction in Sir4 occupancy at telomere VI-R (Zhou et al., 2006) was reported. Furthermore, Sir3-HA has been found to localize in mitotic nuclei more diffusely in *dot1Δ* compared to wild-type cells (San-Segundo and Roeder, 2000). However, from the presented data it is difficult to derive whether Sir3-HA was reduced specifically at telomeres.

In conclusion, genetic as well as ChIP data for SIR protein occupancy do not support the view of a telomeric silencing defect in *dot1Δ* cells caused by loss of SIR proteins.

2.14 *dot1Δ* and *pol30-8* cells do not have a general telomere-specific gene silencing defect.

To address in an unbiased fashion whether telomeric or other gene regions were derepressed in *pol30-8* and *dot1Δ* cells, mRNA levels were

measured using an Affymetrix-platform based microarray with help of Chris Johns at the microarray facility at Cold Spring Harbor Laboratory (CSHL, Cold Spring Harbor, NY). Three biological replicates of wild-type, *pol30-8*, *dot1Δ* and *pol30-8 dot1Δ* strains obtained from the same cross carrying the heterochromatin reporter constructs *hmr*::*ADE2* and *URA3*-VIIL while being deleted for the endogenous alleles *ade-1* and *ura3-1* in the W303 strain background were compared. A heatmap comparing *pol30-8*, *dot1Δ*, and *pol30-8 dot1Δ* to wild type, considering 20-kb segments from each of the 32 telomeres in yeast, confirmed the genetic results at *HIS3*-VIIL. For the *dot1Δ* mutant, no elevation but rather a mild down-regulation of telomeric gene expression was observed, except in the cases of *ADH4* (5.8-fold up-regulated) and *URA3* (2.9-fold up-regulated) at telomere VII-L (Figure 15 and Table 3). In the *pol30-8* mutant, gene expression within the distal 20 kb of each chromosome was significantly up-regulated (p value = 5.05×10^{-7}), with a maximum of 5.8-fold (*DAN3*, telomere II-R, Table 2). To analyze regional gene expression in the different mutants, Dr. Weijun Luo (Bioinformatics Shared Resource, CSHL) applied two different methods, “generally applicable gene-set enrichment” (GAGE; Luo et al., 2009) as well as “fold change” to plot the gene expression changes compared to wild type in 10-kb regions from all 32 pooled telomeres towards the pooled centers of all 16 chromosomes. This analysis demonstrated modest global up-regulation of gene expression in the telomere-proximal 50 kb in *pol30-8*, but not in *dot1Δ* cells (Figures 16A and 16B). Globally, the *pol30-8* mutation seemed to be dominant over the *dot1Δ* deletion (Figures 15, 16A and 16B, Tables 2, 3, 4 and 5). A

Figure 15: *dot1Δ* and *pol30-8* cells do not have a general telomere-specific silencing defect – part I.

log_2-based gene expression ratio in the regions 20 kb off each telomere (from top to bottom: I-L - XVI-R) for three biological replicates of *pol30-8* (MRY1071), *dot1Δ* (MRY1627) and *pol30-8 dot1Δ* (MRY1069) compared to wild-type (MRY1629) *ade2Δ ura3Δ hmr*::*ADE2 URA3*-VIIL strains. This array covered 125 genes from these regions. Genes at the engineered telomere VII-L are labeled.

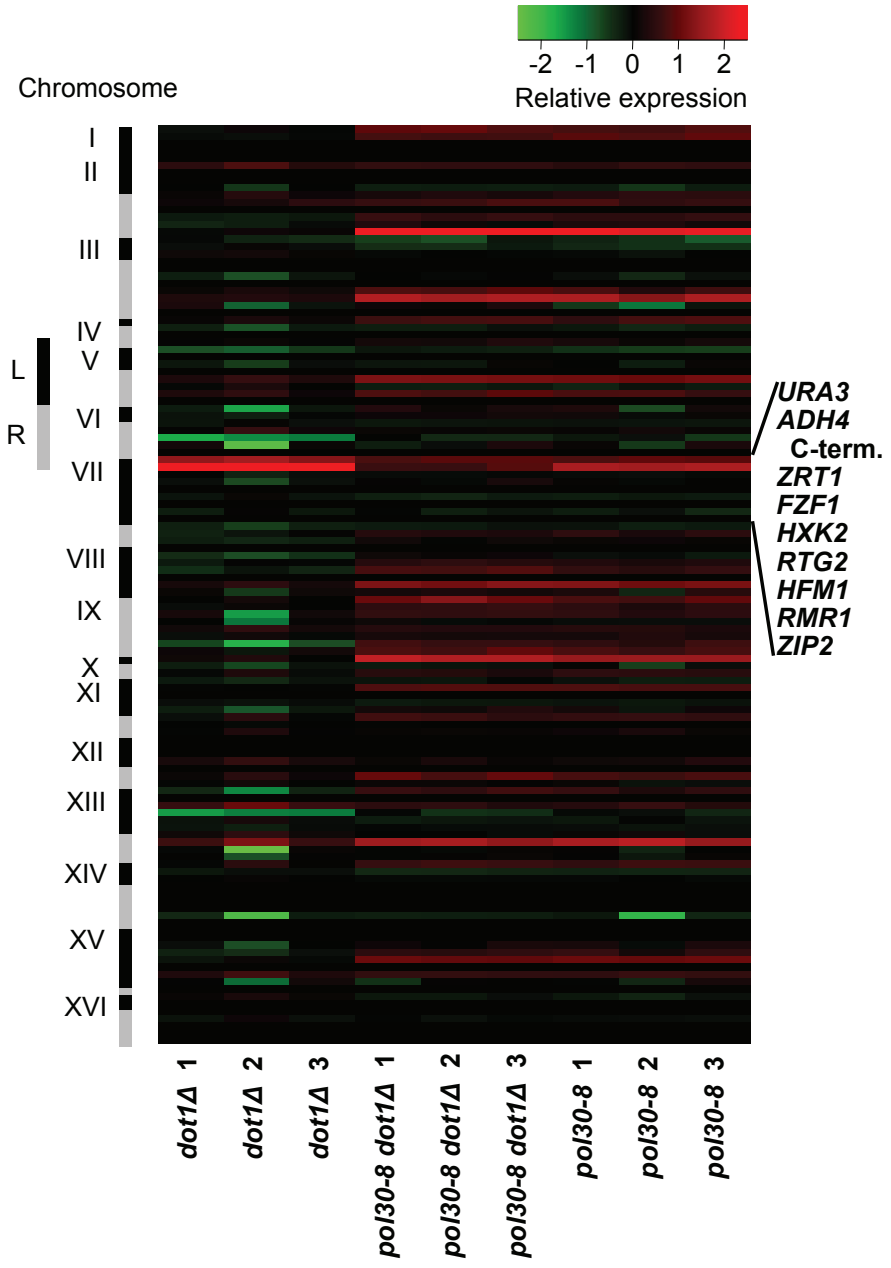
-2 -1 0 1 2
Relative expression
Chromosome
I
II
III
IV
V
VI
VII
VIII
IX
X
XI
XII
XIII
XIV
XV
XVI
L
R
URA3
ADH4
C-term.
ZRT1
FZF1
HXK2
RTG2
HFM1
RMR1
ZIP2
dot1Δ 1
dot1Δ 2
dot1Δ 3
pol30-8 dot1Δ 1
pol30-8 dot1Δ 2
pol30-8 dot1Δ 3
pol30-8 1
pol30-8 2
pol30-8 3

Figure 16: *dot1Δ* and *pol30-8* cells do not have a general telomere-specific silencing defect – part II.

(A) Average $\log_2$-based expression ratio for three biological replicates of *pol30-8* (MRY1071), *dot1Δ* (MRY1627) and *pol30-8 dot1Δ* (MRY1069) compared to wild-type (MRY1629) strains from all 32 telomeres to the center of chromosomes. Differential gene expression was determined using the fold change method. Each data point spans 10 kb of the corresponding regions in all 32 chromosome halves. Error bars denote the SEM.

(B) Overall gene expression level changes (mean t-statistics) in three biological replicates of *pol30-8*, *dot1Δ* and *pol30-8 dot1Δ* compared to wild-type strains as in (A) from all 32 telomeres to the center of chromosomes. Differential gene expression was measured by GAGE test statistics (Luo et al., 2009). Data points as in (A).

(C) Average $\log_2$-based expression ratio of two *asf1Δ* and *cac1Δ* compared to two wild-type strains. The raw data files were obtained from Dr. Jessica Tyler (Zabaronick and Tyler, 2005) and processed as in (A).

(D) Overall gene expression level changes of two *asf1Δ* and *cac1Δ* compared to two wild-type strains. Source of data as in (C). Analysis as in (B).

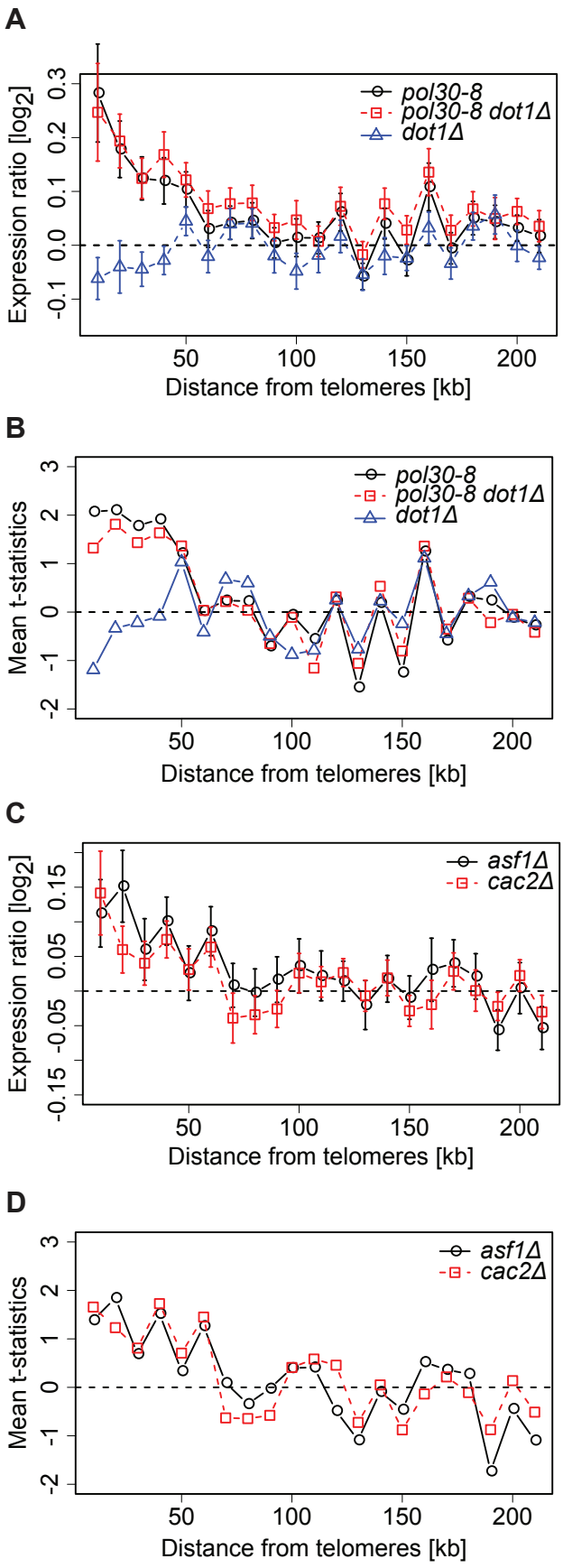
A
Expression ratio [log2]
-0.1
0.0
0.1
0.2
0.3
pol30-8
pol30-8 dot1Δ
dot1Δ
50
100
150
200
Distance from telomeres [kb]
B
Mean t-statistics
-2
-1
0
1
2
3
pol30-8
pol30-8 dot1Δ
dot1Δ
50
100
150
200
Distance from telomeres [kb]
C
Expression ratio [log2]
-0.15
-0.05
0.05
0.15
asf1Δ
cac2Δ
50
100
150
200
Distance from telomeres [kb]
D
Mean t-statistics
-2
-1
0
1
2
3
asf1Δ
cac2Δ
50
100
150
200
Distance from telomeres [kb]

Figure 17: *dot1Δ* and *pol30-8* cells do not have a general telomere-specific silencing defect – part III.

(A) Average $\log_2$-based expression ratio of all genes in *pol30-8* (MRY1071) compared to wild-type (MRY1629) strains versus baseline gene expression level in wild-type. Data points are for all three replicates of each strain. A local weighted polynomial smoothing (Loess) curve (in red) was fitted to the data.

(B) Same analysis as in (A) for three replicates of the *dot1Δ* strain (MRY1627).

(C) $\log_2$-based expression ratio of all genes in wild-type replicate 1 versus baseline expression level in wild-type replicate 2. Strains and analysis as in (A).

(D) $\log_2$-based expression ratio of all genes in wild-type replicate 1 versus baseline expression level in wild-type replicate 3. Strains and analysis as in (A).

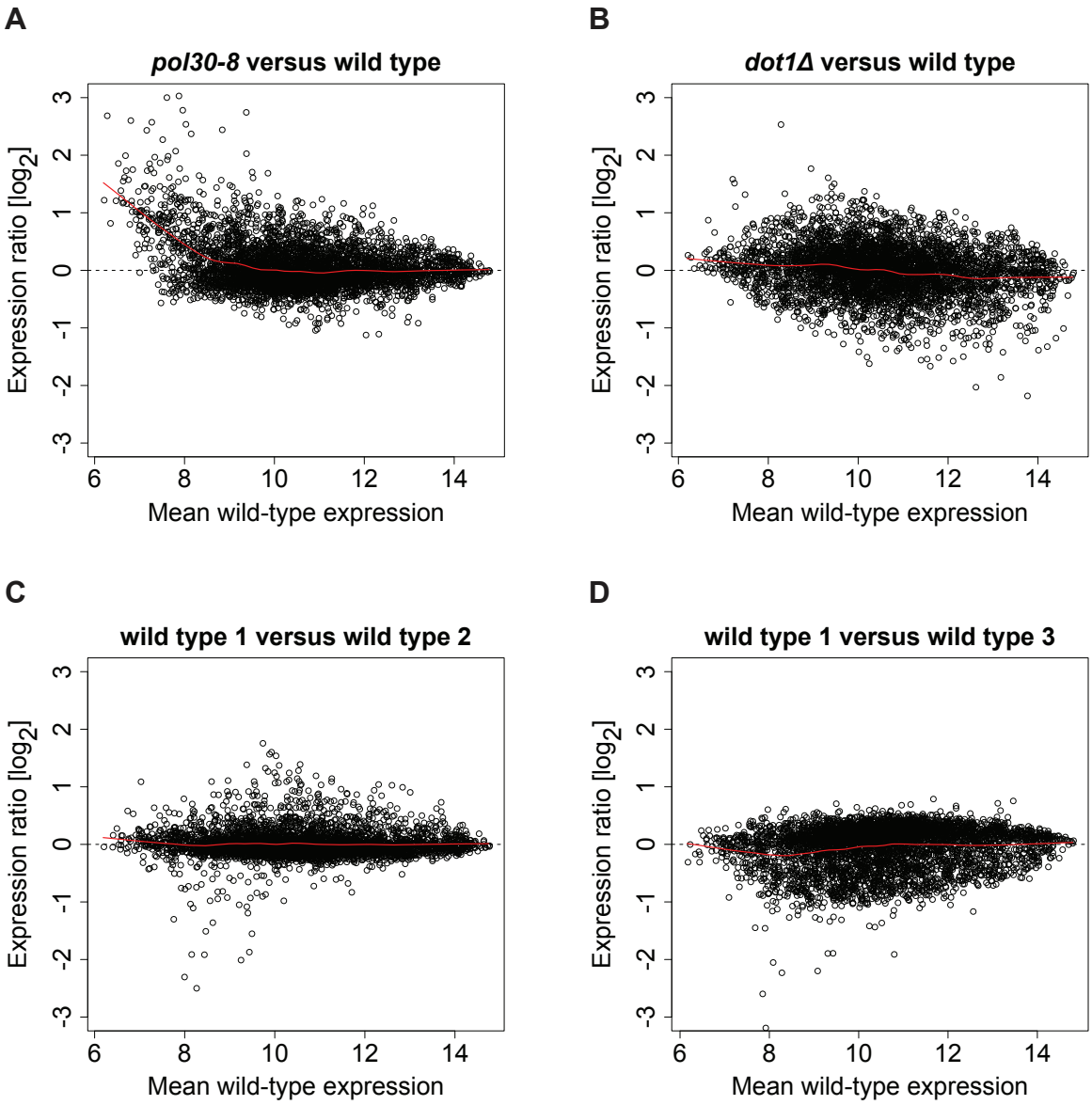
A
pol30-8 versus wild type
Expression ratio [log2]
Mean wild-type expression
B
dot1Δ versus wild type
Expression ratio [log2]
Mean wild-type expression
C
wild type 1 versus wild type 2
Expression ratio [log2]
Mean wild-type expression
D
wild type 1 versus wild type 3
Expression ratio [log2]
Mean wild-type expression

Figure 18: *dot1Δ* and *pol30-8* cells do not have a general telomere-specific silencing defect – part IV.

(A) Average $\log_2$-based expression ratio of all genes in *cac2Δ* compared to wild-type strains versus baseline expression level for wild-type. Data points are for all three replicates of each strain. A local weighted polynomial smoothing (Loess) curve (in red) was fitted to the data. The raw data files were obtained from Dr. Jessica Tyler (Zabaronick and Tyler, 2005).

(B) Same analysis as in (A) for *asf1Δ*. Source of data as in (A).

(C) $\log_2$-based expression ratio of all genes in wild-type replicate 1 versus baseline expression level in wild-type replicate 2 from dataset used in (A) and (B).

A

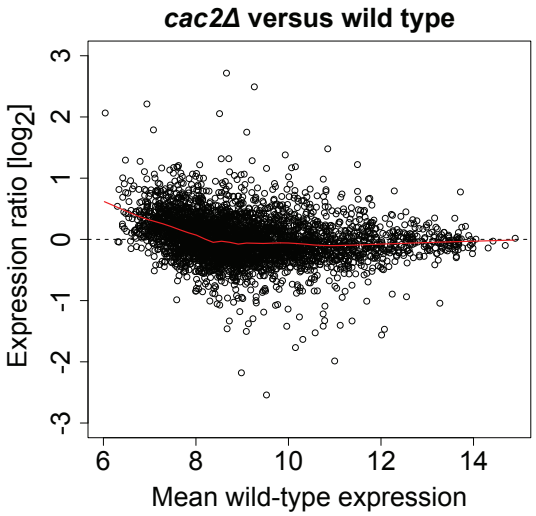
cac2Δ versus wild type
Expression ratio [log2]
3
2
1
0
-1
-2
-3
6
8
10
12
14
Mean wild-type expression

B

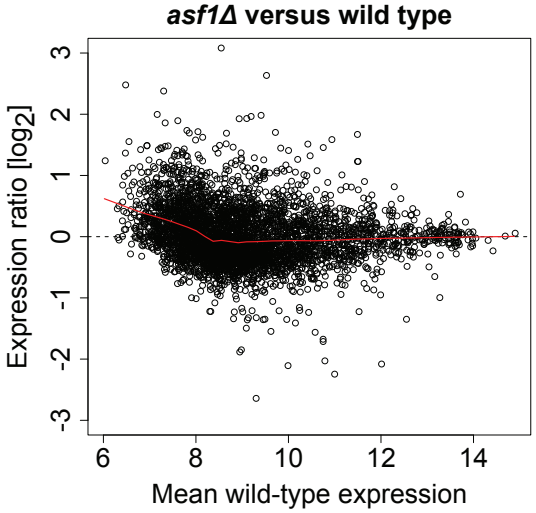
asf1Δ versus wild type
Expression ratio [log2]
3
2
1
0
-1
-2
-3
6
8
10
12
14
Mean wild-type expression

C

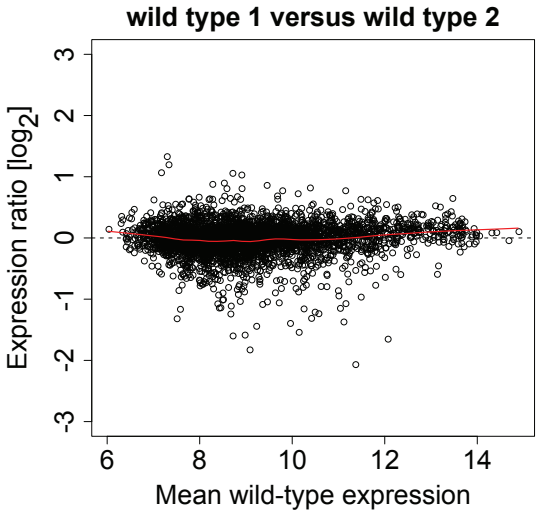
wild type 1 versus wild type 2
Expression ratio [log2]
3
2
1
0
-1
-2
-3
6
8
10
12
14
Mean wild-type expression

Table 2: Global expression level changes for the *pol30-8* mutant.

List of all up-regulated genes resulting from the comparison of three biological replicates of *pol30-8* (MRY1071) and wild-type (MRY1629) strains from the same diploid parent. For each gene, the relative expression level was defined as the $\log_2$-based expression level ratio of each mutant sample (the mean of three experiments) versus the mean of all three wild-type experiments. Both strains were *ade2Δ ura3Δ hmr*::*ADE2 URA3*-VIIL.

Symbol	ORF	stat. mean [log_2]	p value
HUG1	YML058W-A	3.82	0
ADH2	YMR303C	3.68	0
PAU5	YFL020C	3.03	5.2E-08
FRM2	YCL026C-A	3.00	7.5E-08
ANB1	YJR047C	2.78	1.9E-07
TIR1	YER011W	2.74	2.7E-07
IRC18	YJL037W	2.60	5.3E-07
YDR374C	YDR374C	2.68	5.6E-07
YNR064C	YNR064C	2.57	6.6E-07
DAN3	YBR301W	2.53	8.1E-07
FIT2	YOR382W	2.44	9.6E-07
YAL018C	YAL018C	2.43	1.5E-06
YDR034W-B	YDR034W-B	2.37	1.6E-06
YGR066C	YGR066C	2.07	5.1E-06
BNA2	YJR078W	2.02	5.8E-06
YLR307C-A	YLR307C-A	2.27	6.4E-06
SRX1	YKL086W	1.98	7.2E-06
GAS4	YOL132W	1.99	7.4E-06
YOR387C	YOR387C	1.96	9.3E-06
HXT9	YJL219W	1.86	1.3E-05
CDA1	YLR307W	1.85	1.7E-05
YHR126C	YHR126C	1.85	1.7E-05
FIG1	YBR040W	1.75	2.6E-05
ADH7	YCR105W	1.76	2.6E-05
GAL10	YBR019C	1.73	2.8E-05
YCR045C	YCR045C	1.76	3.4E-05
SPS2	YDR522C	1.72	3.6E-05
RNR3	YIL066C	1.70	4.4E-05
DTR1	YBR180W	1.69	4.5E-05
TAH1	YCR060W	1.68	4.8E-05
SPG4	YMR107W	1.92	5.1E-05
THI73	YLR004C	1.64	5.5E-05
YMR317W	YMR317W	1.61	5.6E-05
DMC1	YER179W	1.61	5.7E-05
MET16	YPR167C	1.59	6.4E-05
TIR2	YOR010C	1.60	6.9E-05
PAU2	YEL049W	1.56	8.8E-05
AAC3	YBR085W	1.56	8.9E-05
YOR214C	YOR214C	1.57	9.0E-05
DIT1	YDR403W	1.53	1.1E-04
SPO74	YGL170C	1.54	1.1E-04
SRD1	YCR018C	1.45	1.6E-04
MUC1	YIR019C	1.47	1.7E-04
YML083C	YML083C	1.45	1.8E-04
YMR244W	YMR244W	1.45	1.8E-04
PRM2	YIL037C	1.46	1.8E-04
YGL081W	YGL081W	1.45	2.0E-04
YDL218W	YDL218W	1.42	2.0E-04

Symbol	ORF	stat. mean [log_2]	p value
TIS11	YLR136C	1.43	2.2E-04
PRM1	YNL279W	1.42	2.2E-04
YMR118C	YMR118C	1.40	2.6E-04
YLR364W	YLR364W	1.36	2.6E-04
MAM1	YER106W	1.38	2.8E-04
YLR031W	YLR031W	1.38	2.9E-04
HES1	YOR237W	1.37	3.2E-04
PMA2	YPL036W	1.34	3.3E-04
THI4	YGR144W	1.35	3.4E-04
FMP46	YKR049C	1.29	3.5E-04
TSA2	YDR453C	1.32	3.7E-04
DAL1	YIR027C	1.32	3.9E-04
FMP23	YBR047W	1.29	4.7E-04
YHL042W	YHL042W	1.28	4.9E-04
FIT3	YOR383C	1.29	5.1E-04
HOT13	YKL084W	1.23	5.1E-04
TIR3	YIL011W	1.29	5.2E-04
YJL045W	YJL045W	1.27	5.6E-04
PAI3	YMR174C	1.23	6.3E-04
OSW1	YOR255W	1.25	6.4E-04
DAD4	YDR320C-A	1.26	6.4E-04
YNL195C	YNL195C	1.20	6.6E-04
MIP6	YHR015W	1.22	6.7E-04
DAK2	YFL053W	1.23	6.8E-04
SPS100	YHR139C	1.26	6.8E-04
PUG1	YER185W	1.24	7.0E-04
FKS3	YMR306W	1.21	7.4E-04
IMD2	YHR216W	1.20	7.6E-04
SGA1	YIL099W	1.22	7.6E-04
YOR381W-A	YOR381W-A	1.21	7.7E-04
SNO1	YMR095C	1.20	8.3E-04
YGR131W	YGR131W	1.20	8.4E-04
FYV12	YOR183W	1.20	8.5E-04
MET14	YKL001C	1.21	8.7E-04
OSW2	YLR054C	1.19	8.7E-04
YML007C-A	YML007C-A	1.19	8.8E-04
COX5B	YIL111W	1.16	8.9E-04
RNP1	YLL046C	1.20	9.1E-04
MFA1	YDR461W	1.19	9.2E-04
DCG1	YIR030C	1.20	9.2E-04
ECM11	YDR446W	1.18	9.6E-04
DIA3	YDL024C	1.18	9.6E-04
SMA1	YPL027W	1.18	9.8E-04
MLS1	YNL117W	1.22	1.0E-03
SPR28	YDR218C	1.16	1.1E-03
YLL053C	YLL053C	1.17	1.1E-03
SNA4	YDL123W	1.17	1.1E-03
YOR378W	YOR378W	1.15	1.1E-03

Symbol	ORF	stat. mean [log_2]	p value
YPL033C	YPL033C	1.15	1.2E-03
SOM1	YEL059C-A	1.15	1.2E-03
SER3	YER081W	1.10	1.2E-03
FRE4	YNR060W	1.14	1.2E-03
YOL047C	YOL047C	1.14	1.2E-03
SPR3	YGR059W	1.13	1.2E-03
YPR078C	YPR078C	1.13	1.2E-03
GPG1	YGL121C	1.13	1.3E-03
ATX1	YNL259C	1.11	1.4E-03
PCK1	YKR097W	1.13	1.4E-03
YGR201C	YGR201C	1.13	1.4E-03
BIO4	YNR057C	1.14	1.4E-03
GPM2	YDL021W	1.13	1.4E-03
NCE101	YJL205C	1.12	1.4E-03
BNA1	YJR025C	1.12	1.5E-03
MET2	YNL277W	1.09	1.6E-03
GND2	YGR256W	1.10	1.7E-03
YNR062C	YNR062C	1.08	1.7E-03
SNZ1	YMR096W	1.07	1.7E-03
BNA4	YBL098W	1.07	1.8E-03
YOL086W-A	YOL086W-A	1.08	1.8E-03
PCC1	YKR095W-A	1.07	1.8E-03
CRC1	YOR100C	1.09	1.9E-03
DYN2	YDR424C	1.08	1.9E-03
YBL059W	YBL059W	1.05	1.9E-03
SHC1	YER096W	1.05	1.9E-03
ECM8	YBR076W	1.05	2.1E-03
NQM1	YGR043C	1.05	2.1E-03
YOL162W	YOL162W	1.05	2.2E-03
YSY6	YBR162W-A	1.07	2.2E-03
SPS19	YNL202W	1.05	2.2E-03
DIT2	YDR402C	1.04	2.2E-03
ARO10	YDR380W	-1.13	4.0E-08
OXA1	YER154W	-1.11	1.3E-07
UBP5	YER144C	-1.03	3.6E-07
YER140W	YER140W	-1.05	4.1E-07
RTR1	YER139C	-0.95	2.5E-06
PEA2	YER149C	-0.92	2.7E-06
COG3	YER157W	-0.92	2.8E-06
SFG1	YOR315W	-0.93	3.0E-06
MEF1	YLR069C	-0.93	3.3E-06
YER156C	YER156C	-0.92	3.5E-06
CLB1	YGR108W	-0.93	4.5E-06
COX15	YER141W	-0.91	5.5E-06
DDI1	YER143W	-0.87	9.6E-06
PUT4	YOR348C	-0.86	1.3E-05
PCL1	YNL289W	-0.81	2.1E-05
TPO4	YOR273C	-0.83	2.1E-05

Symbol	ORF	stat. mean [log_2]	p value
MRP4	YHL004W	-0.81	2.3E-05
CTT1	YGR088W	-0.85	2.4E-05
CYT1	YOR065W	-0.82	2.7E-05
YDR222W	YDR222W	-0.79	2.9E-05
YER152C	YER152C	-0.79	3.1E-05
PET122	YER153C	-0.78	3.6E-05
YJL107C	YJL107C	-0.75	5.1E-05
YER064C	YER064C	-0.75	5.2E-05
HO	YDL227C	-0.73	7.9E-05
SPT15	YER148W	-0.72	9.5E-05
TMN2	YDR107C	-0.71	1.1E-04
SCC4	YER147C	-0.70	1.1E-04
AEP2	YMR282C	-0.69	1.4E-04
ROX1	YPR065W	-0.69	1.5E-04
SGM1	YJR134C	-0.69	1.5E-04
YLR455W	YLR455W	-0.68	1.7E-04
CLN1	YMR199W	-0.68	1.8E-04
YKL121W	YKL121W	-0.68	1.8E-04
UBP3	YER151C	-0.67	1.9E-04
NDI1	YML120C	-0.68	1.9E-04
QCR2	YPR191W	-0.67	2.2E-04
HMX1	YLR205C	-0.66	2.4E-04
YDR524W-C	YDR524W-C	-0.65	2.4E-04
BEM2	YER155C	-0.65	2.5E-04
CBP3	YPL215W	-0.67	2.5E-04
YGR110W	YGR110W	-0.65	2.7E-04
CLN2	YPL256C	-0.64	2.9E-04
YOL019W	YOL019W	-0.64	3.2E-04
ADR1	YDR216W	-0.63	3.9E-04
MRPL35	YDR322W	-0.63	4.2E-04
CSI2	YOL007C	-0.61	5.1E-04
GZF3	YJL110C	-0.61	5.1E-04
FTR1	YER145C	-0.61	5.2E-04
TAT1	YBR069C	-0.61	5.3E-04
CKI1	YLR133W	-0.60	5.7E-04
MPS3	YJL019W	-0.60	5.8E-04
PEF1	YGR058W	-0.60	5.9E-04
YLR108C	YLR108C	-0.60	6.5E-04
MOT3	YMR070W	-0.59	6.5E-04
PRM10	YJL108C	-0.60	6.8E-04
HAP4	YKL109W	-0.60	6.8E-04
MSY1	YPL097W	-0.58	7.2E-04
KEL2	YGR238C	-0.58	7.3E-04
TOS4	YLR183C	-0.58	7.5E-04
SKS1	YPL026C	-0.58	7.7E-04
CLB2	YPR119W	-0.58	7.8E-04
STE12	YHR084W	-0.58	8.0E-04
DEG1	YFL001W	-0.57	8.6E-04

Symbol	ORF	stat. mean [log_2]	p value
BCS1	YDR375C	-0.57	8.7E-04
CTM1	YHR109W	-0.57	8.9E-04
MDH2	YOL126C	-0.58	9.2E-04
CHA1	YCL064C	-0.57	9.5E-04
SPB4	YFL002C	-0.57	9.9E-04
YOX1	YML027W	-0.56	1.0E-03
YLR132C	YLR132C	-0.57	1.0E-03
SFP1	YLR403W	-0.56	1.1E-03
FUI1	YBL042C	-0.56	1.1E-03
YAL037C-A	YAL037C-A	-0.57	1.1E-03
ALT2	YDR111C	-0.56	1.2E-03
YLR264C-A	YLR264C-A	-0.58	1.2E-03
BUR6	YER159C	-0.43	1.3E-03
MDM20	YOL076W	-0.56	1.3E-03
YHL018W	YHL018W	-0.55	1.3E-03
BRE5	YNR051C	-0.54	1.3E-03
MSN2	YMR037C	-0.55	1.3E-03
MSK1	YNL073W	-0.54	1.4E-03
MRPL3	YMR024W	-0.54	1.5E-03
RHB1	YCR027C	-0.54	1.5E-03
BUR2	YLR226W	-0.54	1.6E-03
PCL2	YDL127W	-0.54	1.6E-03
SVS1	YPL163C	-0.53	1.6E-03
SLG1	YOR008C	-0.54	1.6E-03
YMR166C	YMR166C	-0.54	1.6E-03
COX10	YPL172C	-0.53	1.6E-03
NUT1	YGL151W	-0.53	1.7E-03
PET112	YBL080C	-0.54	1.7E-03

Table 3: Global expression level changes for the *dot1Δ* mutant.

List of all up-regulated genes resulting from the comparison of three biological replicates of *dot1Δ* (MRY1627) and wild-type (MRY1629) strains from the same diploid parent. For each gene, the relative expression level was defined as the $\log_2$-based expression level ratio of each mutant sample (the mean of three experiments) versus the mean of all three wild-type experiments. Both strains were *ade2Δ ura3Δ hmr*::*ADE2 URA3*-VIIL.

Symbol	ORF	stat. mean [log_2]	p value		Symbol	ORF	stat. mean [log_2]	p value
ADH4	YGL256W	2.53	0		SSE2	YBR169C	-0.81	5.5E-04
SPL2	YHR136C	1.76	0		COX15	YER141W	-0.88	6.2E-04
DAD4	YDR320C-A	1.60	0		TSL1	YML100W	-0.92	3.1E-04
URA3	YEL021W	1.51	4.7E-06		YER140W	YER140W	-0.92	5.6E-04
YSY6	YBR162W-A	1.50	3.4E-06		MDH2	YOL126C	-0.94	5.9E-04
SMX2	YFL017W-A	1.45	1.4E-05		YER158C	YER158C	-0.94	2.2E-04
DYN2	YDR424C	1.37	3.8E-05		GLC3	YEL011W	-0.95	5.9E-04
CGR1	YGL029W	1.33	3.2E-05		PHM7	YOL084W	-0.96	3.2E-04
HUB1	YNR032C-A	1.33	4.8E-05		NDI1	YML120C	-0.98	5.6E-04
SOM1	YEL059C-A	1.29	1.0E-04		UBP5	YER144C	-0.98	1.6E-04
ERI1	YPL096C-A	1.28	6.5E-05		HSP42	YDR171W	-0.98	4.1E-04
PCC1	YKR095W-A	1.27	1.2E-04		GSY1	YFR015C	-1.04	1.5E-04
QRI5	YLR204W	1.26	1.6E-04		SCC4	YER147C	-1.04	5.3E-04
SMD3	YLR147C	1.26	8.1E-05		OXA1	YER154W	-1.06	2.3E-04
NCE101	YJL205C	1.25	2.0E-04		RTN2	YDL204W	-1.06	1.5E-04
LSM3	YLR438C-A	1.24	1.5E-04		RTR1	YER139C	-1.07	1.0E-04
YOS1	YER074W-A	1.22	1.8E-04		DDI1	YER143W	-1.10	1.2E-04
TMA7	YLR262C-A	1.22	2.7E-04		PGM2	YMR105C	-1.13	6.7E-05
YCR075W-A	YCR075W-A	1.22	2.8E-04		SPI1	YER150W	-1.13	2.0E-04
YIL002W-A	YIL002W-A	1.21	2.5E-04		YPS6	YIR039C	-1.14	3.2E-04
YLR099W-A	YLR099W-A	1.21	2.7E-04		YRO2	YBR054W	-1.18	1.5E-04
SMX3	YPR182W	1.19	2.5E-04		YHR087W	YHR087W	-1.19	1.6E-04
LUG1	YCR087C-A	1.19	1.2E-04		GPH1	YPR160W	-1.20	4.1E-05
ATX1	YNL259C	1.16	4.7E-04		GAD1	YMR250W	-1.22	6.0E-05
DBP10	YDL031W	1.13	1.8E-04		YPL247C	YPL247C	-1.24	2.7E-04
EMI1	YDR512C	1.12	5.8E-04		YPK2	YMR104C	-1.28	4.5E-04
MRPS16	YPL013C	1.12	6.6E-04		ALD4	YOR374W	-1.28	1.1E-04
ALB1	YJL122W	1.11	1.7E-04		TPO4	YOR273C	-1.35	1.2E-04
RDS3	YPR094W	1.10	6.7E-04		GLK1	YCL040W	-1.38	7.0E-05
MED11	YMR112C	1.10	6.2E-04		MSC1	YML128C	-1.40	8.7E-06
RUB1	YDR139C	1.09	6.3E-04		HXK1	YFR053C	-1.50	4.8E-06
YOL086W-A	YOL086W-A	1.09	6.6E-04		CTT1	YGR088W	-1.51	7.3E-06
OST4	YDL232W	1.08	7.6E-04		PIR3	YKL163W	-1.56	6.3E-06
TFB5	YDR079C-A	1.08	7.3E-04		YOR302W	YOR302W	-1.86	1.9E-04
YJL047C-A	YJL047C-A	1.08	3.9E-04		YER152C	YER152C	-2.03	8.5E-06
GON7	YJL184W	1.07	8.4E-04		DOT1	YDR440W	-3.37	3.7E-08
TIM9	YEL020W-A	1.07	6.8E-04					
URM1	YIL008W	1.05	6.3E-04					
BUD20	YLR074C	1.01	5.4E-04					
YBL028C	YBL028C	1.01	4.6E-04					
YLR363W-A	YLR363W-A	1.00	8.0E-04					
PXR1	YGR280C	0.97	7.4E-04					
BUD22	YMR014W	0.97	4.1E-04					
SLX9	YGR081C	0.96	6.0E-04					
HPT1	YDR399W	0.96	4.0E-04					
BUD21	YOR078W	0.94	5.4E-04					
YMR230W-A	YMR230W-A	0.90	8.1E-04					
REI1	YBR267W	0.80	8.4E-04					

Table 4: Global expression level changes for the *pol30-8 dot1Δ* mutant.

List of all up-regulated genes resulting from the comparison of three biological replicates of *pol30-8 dot1Δ* (MRY1069) and wild-type (MRY1629) strains from the same diploid parent. For each gene, the relative expression level was defined as the $\log_2$-based expression level ratio of each mutant sample (the mean of three experiments) versus the mean of all three wild-type experiments. Both strains were *ade2Δ ura3Δ hmr*::*ADE2 URA3*-VIIL.

Symbol	ORF	stat. mean [log_2]	p value
YLR307C-A	YLR307C-A	2.57	0
PAU5	YFL020C	3.10	0
HUG1	YML058W-A	3.52	0
SPG4	YMR107W	2.17	0
ADH2	YMR303C	3.52	0
FRM2	YCL026C-A	2.94	1.3E-07
ANB1	YJR047C	2.82	2.0E-07
IRC18	YJL037W	2.66	3.4E-07
TIR1	YER011W	2.72	3.5E-07
YDR374C	YDR374C	2.61	5.7E-07
YNR064C	YNR064C	2.40	1.3E-06
DAN3	YBR301W	2.39	1.4E-06
FIT2	YOR382W	2.36	1.7E-06
YDR034W-B	YDR034W-B	2.34	2.0E-06
YGR066C	YGR066C	2.24	2.6E-06
YAL018C	YAL018C	2.07	9.8E-06
BNA2	YJR078W	1.84	1.8E-05
GAS4	YOL132W	1.83	2.0E-05
YOR387C	YOR387C	1.83	2.2E-05
YHR126C	YHR126C	1.81	2.2E-05
FIG1	YBR040W	1.75	2.7E-05
TAH1	YCR060W	1.73	3.1E-05
YMR317W	YMR317W	1.72	3.1E-05
ADH4	YGL256W	1.71	3.3E-05
CDA1	YLR307W	1.74	3.5E-05
GAL10	YBR019C	1.67	4.3E-05
SPS2	YDR522C	1.69	4.4E-05
DTR1	YBR180W	1.68	5.0E-05
ADH7	YCR105W	1.64	5.7E-05
RNR3	YIL066C	1.66	6.0E-05
SRX1	YKL086W	1.66	6.5E-05
TIR2	YOR010C	1.63	7.0E-05
THI73	YLR004C	1.60	7.3E-05
YCR045C	YCR045C	1.65	7.3E-05
MET16	YPR167C	1.57	7.6E-05
HXT9	YJL219W	1.56	9.3E-05
PAU2	YEL049W	1.55	1.1E-04
PRM2	YIL037C	1.54	1.2E-04
SNO1	YMR095C	1.50	1.4E-04
DIT1	YDR403W	1.50	1.5E-04
YOR214C	YOR214C	1.49	1.7E-04
SPO74	YGL170C	1.45	2.0E-04
MLS1	YNL117W	1.53	2.1E-04
PRM1	YNL279W	1.45	2.1E-04
YML007C-A	YML007C-A	1.42	2.4E-04
DMC1	YER179W	1.42	2.5E-04
YLR364W	YLR364W	1.39	2.5E-04
YMR118C	YMR118C	1.41	2.6E-04

Symbol	ORF	stat. mean [log_2]	p value
YLR031W	YLR031W	1.41	2.6E-04
AAC3	YBR085W	1.39	2.7E-04
DAD4	YDR320C-A	1.40	2.7E-04
MET14	YKL001C	1.37	3.1E-04
FMP46	YKR049C	1.33	3.1E-04
SRD1	YCR018C	1.36	3.2E-04
THI4	YGR144W	1.37	3.3E-04
PAI3	YMR174C	1.34	3.3E-04
MIP6	YHR015W	1.33	3.9E-04
HES1	YOR237W	1.34	3.9E-04
MUC1	YIR019C	1.34	4.0E-04
MAM1	YER106W	1.34	4.1E-04
SPR28	YDR218C	1.32	4.2E-04
YML083C	YML083C	1.33	4.5E-04
MFA1	YDR461W	1.32	4.6E-04
PCC1	YKR095W-A	1.26	4.7E-04
YNL195C	YNL195C	1.29	4.8E-04
YDL218W	YDL218W	1.30	5.0E-04
SNZ1	YMR096W	1.30	5.0E-04
PMA2	YPL036W	1.30	5.1E-04
SIP18	YMR175W	1.29	5.1E-04
ECM11	YDR446W	1.29	5.2E-04
YSY6	YBR162W-A	1.32	5.4E-04
YMR244W	YMR244W	1.27	5.8E-04
SOM1	YEL059C-A	1.29	5.8E-04
CRC1	YOR100C	1.31	6.0E-04
TIS11	YLR136C	1.27	6.0E-04
UBC11	YOR339C	1.26	6.2E-04
FIT3	YOR383C	1.25	6.3E-04
SPO21	YOL091W	1.26	6.4E-04
YGR131W	YGR131W	1.25	6.5E-04
PCK1	YKR097W	1.28	6.6E-04
DAL1	YIR027C	1.25	7.0E-04
ATX1	YNL259C	1.21	7.3E-04
YHL042W	YHL042W	1.24	7.6E-04
SPR3	YGR059W	1.22	7.7E-04
FMP23	YBR047W	1.21	8.3E-04
SMA1	YPL027W	1.22	8.4E-04
YJL045W	YJL045W	1.20	9.5E-04
DYN2	YDR424C	1.20	1.0E-03
FYV12	YOR183W	1.17	1.0E-03
OSW1	YOR255W	1.18	1.0E-03
FKS3	YMR306W	1.16	1.0E-03
YJL038C	YJL038C	1.18	1.1E-03
HOT13	YKL084W	1.14	1.1E-03
YOR381W-A	YOR381W-A	1.17	1.1E-03
YGR240C-A	YGR240C-A	1.15	1.2E-03
YEL057C	YEL057C	1.15	1.2E-03

Symbol	ORF	stat. mean [log_2]	p value
TKL2	YBR117C	1.17	1.2E-03
RNP1	YLL046C	1.14	1.2E-03
YPR078C	YPR078C	1.14	1.3E-03
PUG1	YER185W	1.14	1.3E-03
YOL086W-A	YOL086W-A	1.17	1.3E-03
YPL033C	YPL033C	1.13	1.3E-03
YSW1	YBR148W	1.13	1.4E-03
SHC1	YER096W	1.11	1.4E-03
SPS100	YHR139C	1.13	1.4E-03
YBL059W	YBL059W	1.10	1.4E-03
BNA1	YJR025C	1.12	1.5E-03
COX5B	YIL111W	1.09	1.6E-03
YER078W-A	YER078W-A	1.10	1.7E-03
YOL162W	YOL162W	1.09	1.7E-03
RNH203	YLR154C	1.07	1.7E-03
PES4	YFR023W	1.09	1.8E-03
MED11	YMR112C	1.06	1.8E-03
DAK2	YFL053W	1.06	1.8E-03
TIR3	YIL011W	1.09	1.8E-03
FLO1	YAR050W	1.07	1.9E-03
TMA7	YLR262C-A	1.12	1.9E-03
YGR201C	YGR201C	1.08	2.0E-03
ECM8	YBR076W	1.06	2.0E-03
NCE101	YJL205C	1.14	2.0E-03
TSA2	YDR453C	1.07	2.1E-03
DCG1	YIR030C	1.06	2.1E-03
DIA3	YDL024C	1.05	2.1E-03
YIL002W-A	YIL002W-A	1.08	2.1E-03
SMX2	YFL017W-A	1.15	2.2E-03
YOS1	YER074W-A	1.08	2.2E-03
DOT1	YDR440W	-3.54	1.4E-08
ARO10	YDR380W	-1.19	1.3E-06
OXA1	YER154W	-1.12	4.1E-06
YER140W	YER140W	-1.11	5.0E-06
CLB1	YGR108W	-1.07	5.3E-06
PUT4	YOR348C	-1.01	5.8E-06
YER152C	YER152C	-1.51	7.4E-06
TPO4	YOR273C	-1.04	1.2E-05
UBP5	YER144C	-1.00	1.2E-05
RTR1	YER139C	-0.94	2.2E-05
SFG1	YOR315W	-0.97	2.2E-05
PET122	YER153C	-1.08	2.5E-05
COX15	YER141W	-0.91	3.1E-05
CYT1	YOR065W	-0.91	3.5E-05
DDI1	YER143W	-0.92	3.8E-05
YER156C	YER156C	-0.92	4.0E-05
PEA2	YER149C	-0.85	5.4E-05
MRP4	YHL004W	-0.83	6.6E-05

Symbol	ORF	stat. mean [log_2]	p value
HMX1	YLR205C	-0.83	7.9E-05
YPK2	YMR104C	-1.35	8.1E-05
NDI1	YML120C	-0.89	9.8E-05
COG3	YER157W	-0.81	1.1E-04
YER064C	YER064C	-0.78	1.4E-04
CKI1	YLR133W	-0.77	1.6E-04
HO	YDL227C	-0.78	1.8E-04
SCC4	YER147C	-0.80	2.1E-04
ENT4	YLL038C	-0.95	2.1E-04
CLN1	YMR199W	-0.74	2.4E-04
MEF1	YLR069C	-0.68	3.5E-04
YKL121W	YKL121W	-0.65	4.1E-04
CLN2	YPL256C	-0.69	4.1E-04
YJL107C	YJL107C	-0.76	4.4E-04
QCR2	YPR191W	-0.70	4.7E-04
SPT15	YER148W	-0.67	5.2E-04
YOL019W	YOL019W	-0.71	5.8E-04
PHM8	YER037W	-0.66	6.2E-04
YDR222W	YDR222W	-0.64	6.5E-04
YOX1	YML027W	-0.72	7.0E-04
MRPL4	YLR439W	-0.67	7.0E-04
CTT1	YGR088W	-0.58	7.0E-04
FTR1	YER145C	-0.66	7.9E-04
YLR132C	YLR132C	-0.65	7.9E-04
TMN2	YDR107C	-0.66	7.9E-04
HAC1	YFL031W	-1.87	8.1E-04
HAP4	YKL109W	-0.60	8.5E-04
CSI2	YOL007C	-0.62	8.6E-04
TDP1	YBR223C	-0.72	8.8E-04
BEM2	YER155C	-0.60	8.8E-04
MSK1	YNL073W	-0.60	9.0E-04
YLR108C	YLR108C	-0.61	9.2E-04

Table 5: Most affected Gene Ontology (GO) pathways in the *pol30-8*, *dot1Δ* and *pol30-8 dot1Δ* mutants.

List of the five most significantly up- as well as down-regulated GO pathways in the *pol30-8* (MRY1071, top), *dot1Δ* (MRY1627, middle) and *pol30-8 dot1Δ* (MRY1069, bottom) mutants. For each gene, the relative expression level was defined as the $\log_2$-based expression level ratio of each mutant strain (the mean of three experiments) versus the mean of all three wild-type (MRY1629) experiments. Pathway analysis was performed using GAGE test statistics (Luo et al., 2009). The data was sorted according to the lowest p value. A total number of 5478 GO groups were used for the analysis.

pol30-8

GO process	stat. mean [log_2]	p value	set size
GO:0030435 sporulation resulting in formation of a cellular spore	5.79	3.2E-22	238
GO:0043934 sporulation	5.79	3.2E-22	238
GO:0030154 cell differentiation	5.15	2.8E-18	271
GO:0030476 ascospore wall assembly	4.65	1.3E-13	55
GO:0042244 spore wall assembly	4.65	1.3E-13	55

GO:0016773 phosphotransferase activity, alcohol group as acceptor	-5.16	1.4E-21	457
GO:0004672 protein kinase activity	-5.28	1.6E-21	326
GO:0007005 mitochondrion organization	-3.89	6.4E-21	357
GO:0032543 mitochondrial translation	-4.36	4.7E-19	102
GO:0007165 signal transduction	-5.14	4.8E-19	476

dot1Δ

GO process	stat. mean [log_2]	p value	set size
GO:0006364 rRNA processing	11.26	4.0E-82	378
GO:0005730 nucleolus	9.65	3.1E-61	285
GO:0030684 preribosome	7.69	3.1E-40	159
GO:0003735 structural constituent of ribosome	6.27	4.7E-35	367
GO:0042273 ribosomal large subunit biogenesis	5.79	1.8E-22	93

GO:0044262 cellular carbohydrate metabolic process	-7.26	2.7E-36	341
GO:0016773 phosphotransferase activity, alcohol group as acceptor	-5.52	3.8E-25	457
GO:0009628 response to abiotic stimulus	-5.77	3.6E-24	377
GO:0009408 response to heat	-5.59	1.6E-23	208
GO:0009266 response to temperature stimulus	-5.34	1.5E-21	235

pol30-8 dot1Δ

GO process	stat. mean [log_2]	p value	set size
GO:0030435 sporulation resulting in formation of a cellular spore	5.65	2.3E-21	238
GO:0043934 sporulation	5.65	2.3E-21	238
GO:0030154 cell differentiation	5.01	1.9E-17	271
GO:0030476 ascospore wall assembly	4.60	1.8E-13	55
GO:0042244 spore wall assembly	4.60	1.8E-13	55

GO:0016773 phosphotransferase activity, alcohol group as acceptor	-5.08	8.6E-21	457
GO:0004672 protein kinase activity	-4.99	7.9E-20	326
GO:0007165 signal transduction	-4.62	5.9E-16	476
GO:0007242 intracellular signaling cascade	-4.61	1.9E-15	303
GO:0006468 protein amino acid phosphorylation	-4.25	6.5E-15	270

previous study of *cac2Δ* or *asf1Δ* cells synchronized in G2/M did not find any bias of gene expression changes towards telomeres (Zabaronick and Tyler, 2005). Re-analyzing replicates of this dataset revealed a similar phenotype for these two mutants to that observed for *pol30-8* or *pol30-8 dot1Δ*, but not the *dot1Δ* mutant (Figures 16C and 16D; raw data files for a duplicate data set for wild type, *cac2Δ* and *asf1Δ* were kindly provided by Dr. Jessica Tyler, The University of Texas, Houston, TX). Intriguingly, genome-wide up-regulated genes in *pol30-8* cells were those expressed at low levels in wild-type cells (Figure 17A), while there was no such bias when comparing the *dot1Δ* mutant or single wild-type replicates to the average wild-type signal (Figures 17B, 17C and 17D). The same correlation was seen for *cac2Δ* and *asf1Δ* mutants (Tyler laboratory dataset; Figures 18A, 18B and 18C). In agreement with the up-regulation of poorly expressed gene in wild-type cells, the top up-regulated Gene Ontology (GO) processes in *pol30-8* cells concern sporulation, a process normally suppressed in vegetative cells by the transcriptional repressor Sum1 (Table 5; Pierce et al., 2003).

In the microarray analysis we observed down-regulation (or abrogation) of gene expression in a 40-kb region on chromosome V (chromosome coordinates 450558 - 490573) common to all three mutant strains tested (Figure 19). This region contains 20 open reading frames (ORFs), four dubious ORFs, two tRNA genes and one long terminal repeat (LTR; Figure 20). Since the *pol30-8* mutation otherwise altered gene expression differently from the *dot1Δ* mutation, I did not further investigate this effect.

Figure 19: *dot1Δ* and *pol30-8* cells do not have a general telomere-specific silencing defect – part V.

log_2-based gene expression ratio in three biological replicates of *pol30-8* (MRY1071, top panel), *dot1Δ* (MRY1627, middle panel) and *pol30-8 dot1Δ* (MRY1069, bottom panel) compared to wild-type (MRY1629) strains along chromosome V. Vertical red dashed lines mark a 40 kb region of chromosomal coordinates 450,558 to 490,573. Note that one data point on V-L above the maximum y-axis value = 1.5 (but below 2.0) was removed in the plots for *pol30-8* and *pol30-8 dot1Δ* in order to not compact the data around 0.

Chromosome V

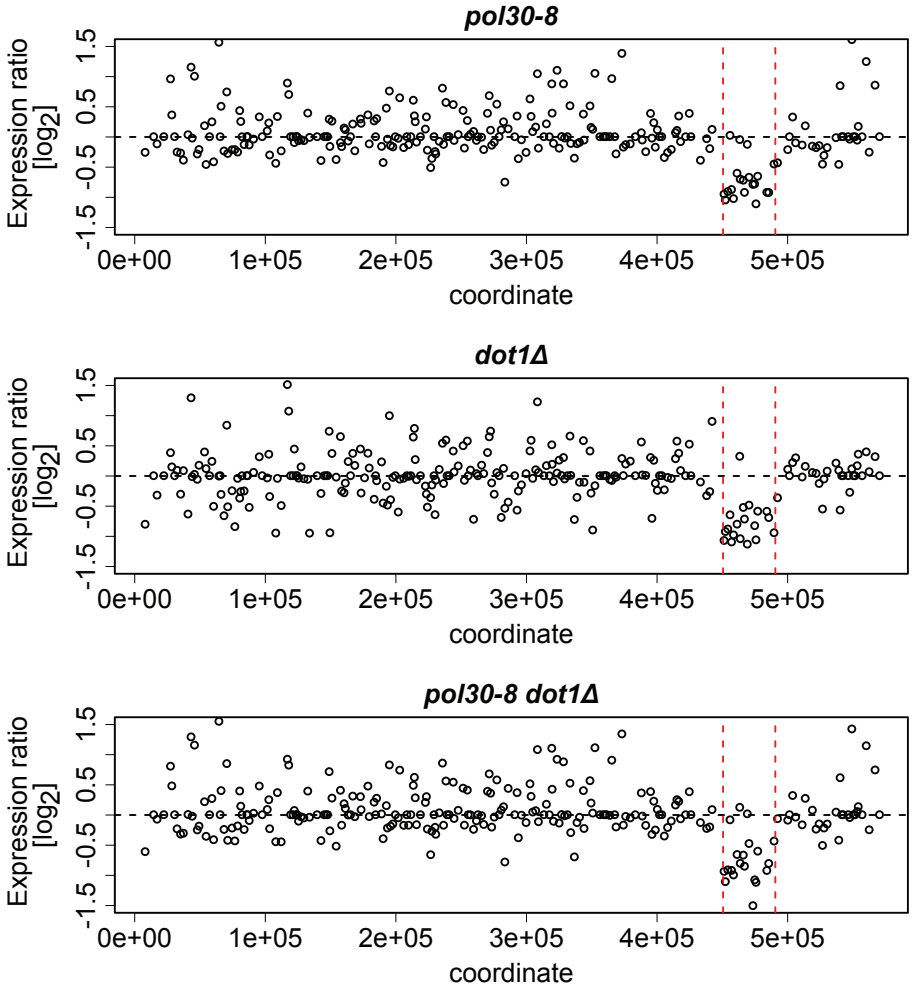

Figure 20: *dot1Δ* and *pol30-8* cells do not have a general telomere-specific silencing defect – part VI.

Snapshot from SGD database (www.yeastgenome.org) for coordinates 450,558 to 490,573 on chromosome V as of June 10, 2010. The centromere is indicated by a black circle. Within the magnified region, ORFs on Watson strands are depicted in red, those on Crick strands in blue, dubious ORFs in grey, tRNAs in green and LTRs of transposable elements in pink.

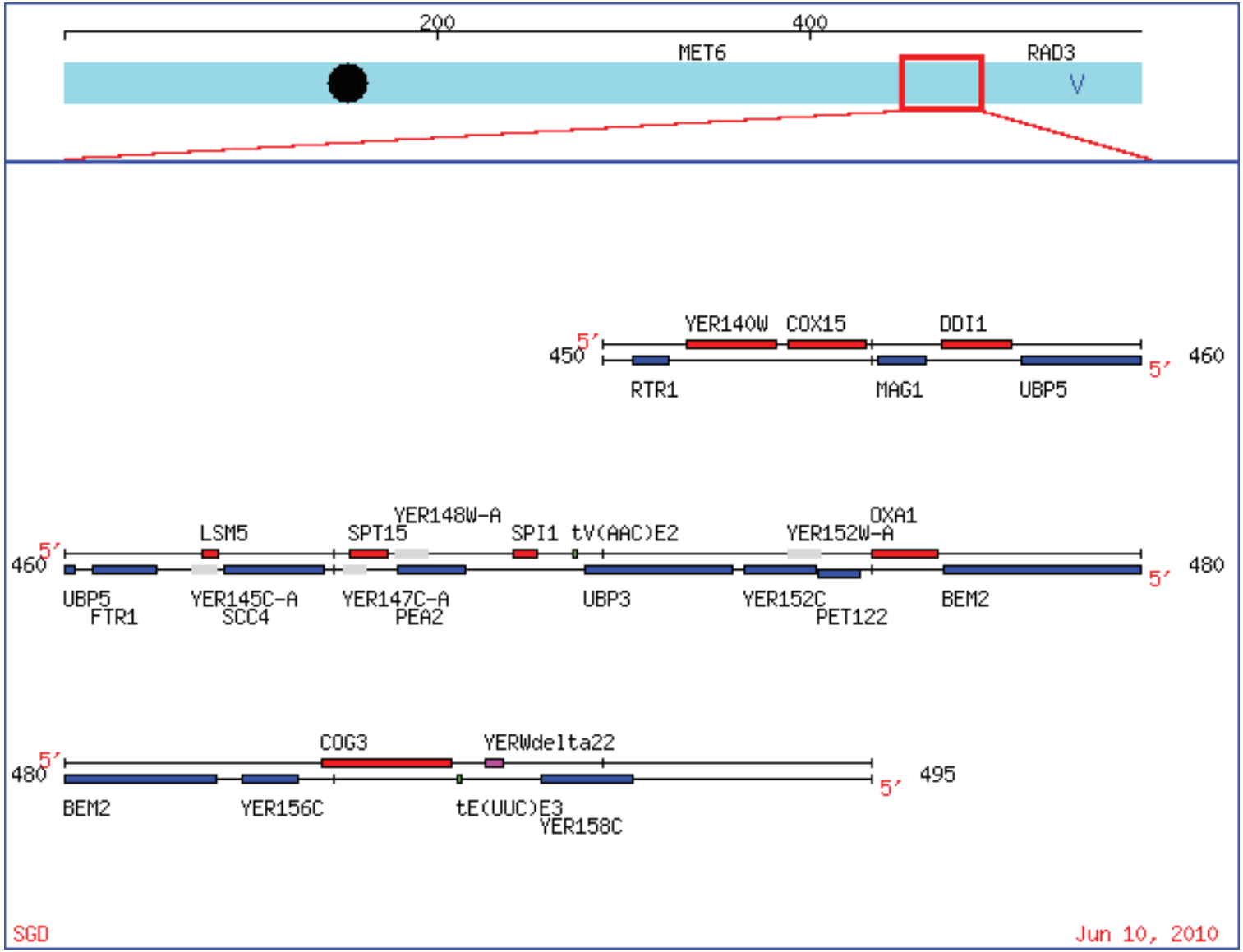
200
400
MET6
RAD3
V
450
5′
YER140W
COX15
DDI1
5′
460
RTR1
MAG1
UBP5
460
5′
LSM5
SPT15
YER148W-A
SPI1
tV(AAC)E2
OXA1
YER152W-A
5′
480
UBP5
FTR1
YER145C-A
SCC4
YER147C-A
PEA2
UBP3
YER152C
PET122
BEM2
480
5′
COG3
YERWdelta22
5′
495
BEM2
YER156C
tE(UUC)E3
YER158C
SGD
Jun 10, 2010

In summary these results indicate that neither mutation specifically affects telomeric silencing; the *pol30-8* mutation results in genes to be up-regulated that are expressed at low levels in wild-type cells, and the *dot1Δ* mutation only up-regulates expression of the *adh4*::*URA3*-VIIL locus.

2.15 Histone occupancy on DNA is reduced in *pol30-8* cells.

Tamburini et al. (2006) had previously observed histone H3 occupancy to be reduced in the *cac1Δ* mutant at *HMR*-E, telomere VI-R and also at an ORF located within euchromatin. Due to the genetic and physical interaction of *POL30* and *CAC1* I tested whether this could be also observed in the *pol30-8* mutant. Indeed, ChIP analysis showed less histone H3 bound in all chromosomal regions tested in *pol30-8* cells, including the *RNR2* (2.2-fold) and *RNR4* (3.7-fold) promoters, *PMA1* (6.2-fold), the *URA3*-VIIL promoter (15.7-fold), the *URA3* gene body (11-fold) as well as an intergenic region on the right arm of chromosome VIII (14.4-fold; Figure 21A and data not shown). Although no ChIP experiments for histone H4 were performed, the stable conformation of the histone H3-H4 tetramer leads me to propose that nucleosome occupancy is reduced in *pol30-8* cells. While total histone H3 levels were unaltered in *pol30-8* cells (Figures 21B and 21C), overexpression of *POL30* resulted in increased histone H3K56 acetylation levels, which is consistent with a previous report (Miller et al., 2008) as well as slightly increased total histone H4 levels (Figure 21B). This suggests that histone metabolism is not affected to an extent that could result in reduced histone H3 occupancy on chromatin. Of note, total histone H3 levels were

Figure 21: Histone occupancy on DNA is reduced in *pol30-8* cells.

(A) ChIP analysis for IgG and H3 followed by qPCR of wild-type (MRY1638) and *pol30-8* (MRY1647) *ura3Δ URA3*-VIIL strains. “p” indicates the promoter region. VIII ig: intergenic region on VIII-R between *AAP1* and *YHK8*. Error bars denote the SEM for two experiments.

(B) Western blot analysis of whole cell protein extracts from a *pol30-8* (MRY0828) strain transformed with pRS425, *POL30* or *CDC21*. #1 and #2 indicate independent transformants; “short” and “long” refer to exposure times.

(C) Western blot analysis of whole cell protein extracts from *MAT***a** and *MAT*α wild-type (MRY1075, 1073), *pol30-8* (MRY1068, 1064), *dot1Δ* (MRY1076, 1072) and *pol30-8 dot1Δ* (MRY1065, 1074) strains. A cross-reacting band from the antibody against H3K79me3 serves as a loading control.

A

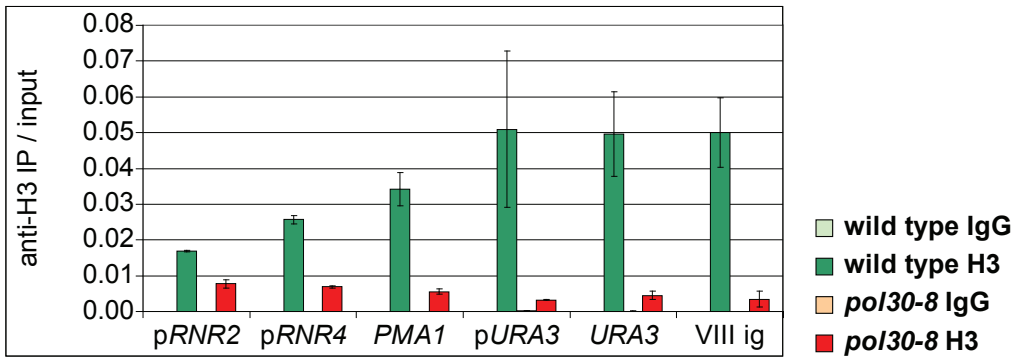

B

pol30-8 hmr::*ADE2 URA3*-VIIL
+

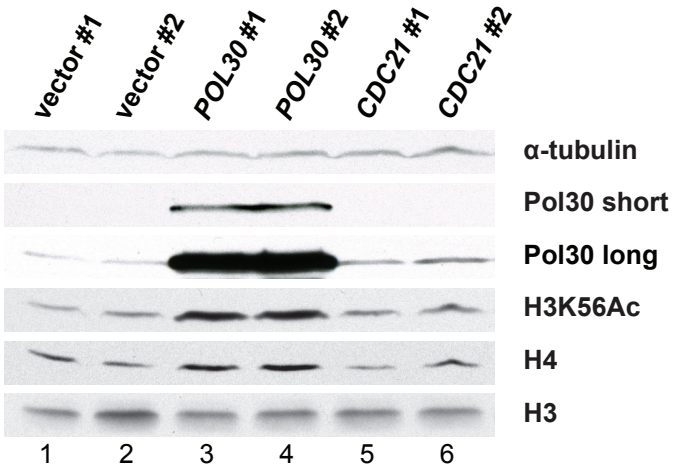

C

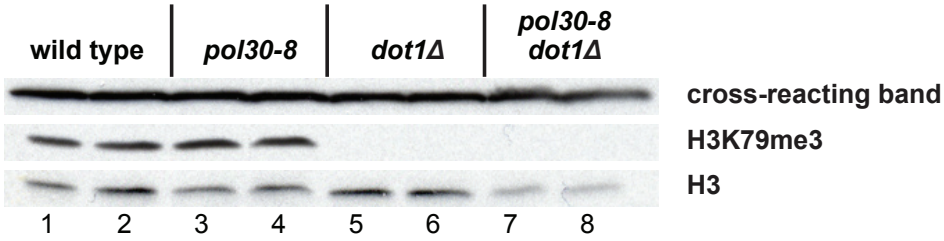

unchanged in *dot1Δ* cells, however, they seemed to be slightly reduced in the *pol30-8 dot1Δ* double mutant (Figure 21C). Sir4, which recruits Sir2 (Ghidelli et al., 2001; Hoppe et al., 2002), is itself tethered to chromatin via its interaction with histones H3 and H4 (Hecht et al., 1995). However, unlike in *cac1Δ* cells (Tamburini et al., 2006) I was unable to confirm reduced SIR protein occupancy in *pol30-8* cells (Sir2 and Sir3 were tested for, data not shown). The mostly less than 2-fold reduction of SIR occupancy in *cac1Δ* cells was derived from the quantification of conventional PCR products after running agarose gels. Hence, possibly the higher sensitivity and accuracy of qPCR might account for the differences observed (The Gene Expression Course, CSHL, 2009, personal communication).

The above data support the conclusion that the *pol30-8* mutation results in global up-regulation of genes expressed at low levels, likely due to lower histone density across the genome. The *dot1Δ* cells, however, specifically up-regulate the *ADH4* locus into which *URA3* was inserted for measuring TPEV. Thus, in both cases the *URA3*-VIIL reporter assay did not reflect a specific role for either of these genes in silencing of telomere-associated genes.

2.16 Ribonucleotide reductase levels are up-regulated in *pol30-8* cells.

The *pol30-8* mutation causes no telomere-specific silencing defect (Figures 16A, 16B and 17A), but strong 5-FOA sensitivity in the context of the *URA3*-VIIL reporter (Figures 9A, 10A, 10B). We hypothesized that these contrasting observations might be explained by the up-regulation of certain

genes in *pol30-8* cells that are poorly expressed in wild-type cells. The most up-regulated gene in *pol30-8* cells was *HUG1* (Table 2). This gene has been implicated in the Mec1-dependent DNA damage checkpoint response, is a target of Crt1/Ssn6-Tup1-mediated repression (Basrai et al., 1999) and was postulated to bind to Rnr2-Rnr4 (Lee et al., 2008). However, there is some doubt as to whether *HUG1* is a completely independent ORF or rather an upstream regulatory region of the *SML1* gene which lies just 417 bp downstream of *HUG1* in the same orientation on chromosome XIII (Dr. Andrei Chabes, personal communication). *HUG1* expression was up-regulated by 15-fold in *pol30-8* cells in a RT-qPCR analysis, confirming the microarray result. In contrast, expression of *SML1* - while expressed at 88-fold higher levels than *HUG1*, both relative to the internal *ACT1* control - was unaltered in *pol30-8* cells (Figure 22A), as it was in the microarray analysis. However, neither overexpression nor deletion of *HUG1*, *SML1* or both genes together in *pol30-8 URA3*-VIIL or in wild-type cells resulted in an alleviation or exacerbation of 5-FOA sensitivity, respectively (data not shown).

The microarray analysis for *pol30-8* mutant strains presented in Figures 15-20 as well as a previous microarray analysis (in the laboratories of Drs. Janet Leatherwood and Bruce Futcher, Stony Brook University, data not shown) revealed elevated expression of *RNR2*, *RNR4* (both 1.7-fold, data not shown) and *RNR3* (3.3-fold, Table 2). These genes encode subunits of RNR, which generates the four dNTPs required for DNA synthesis. The microarray results were confirmed by RT-qPCR (Figure 22B). In the case of *RNR2* and *RNR4*, the

Figure 22: Ribonucleotide reductase levels are up-regulated in *pol30-8* cells.

(A) Expression levels of *HUG1* and *SML1*, measured by RT-qPCR, in wild-type (MRY1629) or *pol30-8* (MRY1071) *ade2Δ ura3Δ hmr*::*ADE2 URA3*-VIIL strains. *ACT1*: reference. Error bars denote the SEM for three replicates per genotype, each tested with two primer pairs.

(B) Expression levels of *RNR1*, *RNR2*, *RNR3* and *RNR4*, measured by RT-qPCR, in wild-type (MRY1629) or *pol30-8* (MRY1071) *ade2Δ ura3Δ hmr*::*ADE2 URA3*-VIIL strains. *ACT1*: reference. Error bars denote the SEM for six strains per genotype tested.

(C) Western blot analysis of whole cell extracts from two wild-type (MRY1767, 1773) and two *pol30-8* (MRY1768, 1772) strains; lanes 7 and 8 show a wild-type strain (MRY1638), either left untreated or treated with 0.4 g/l 4-nitroquinoline 1-oxide (4-NQO) for 2 h.

(D) ChIP analysis for IgG and Ssn6 followed by qPCR of wild-type (MRY1551) and *pol30-8* (MRY1550) *URA3* strains. “p” indicates the promoter region. Error bars denote the SEM for two experiments.

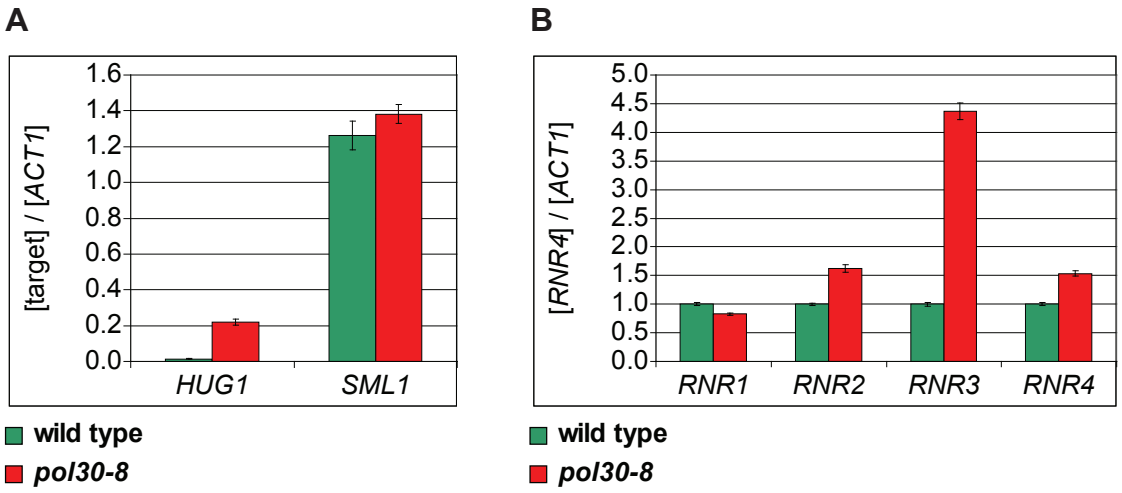
A
[target] / [ACT1]
1.6
1.4
1.2
1.0
0.8
0.6
0.4
0.2
0.0
HUG1
SML1
wild type
pol30-8
B
[RNR4] / [ACT1]
5.0
4.5
4.0
3.5
3.0
2.5
2.0
1.5
1.0
0.5
0.0
RNR1
RNR2
RNR3
RNR4
wild type
pol30-8

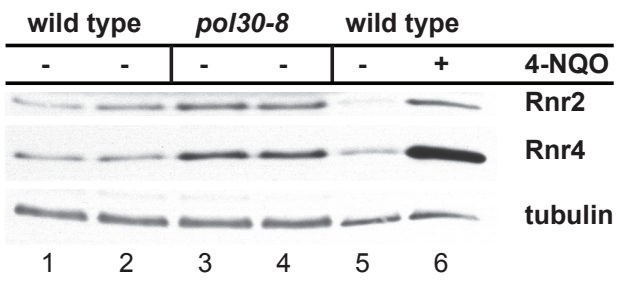
C
wild type
pol30-8
wild type
- - - - - +
4-NQO
Rnr2
Rnr4
tubulin
1 2 3 4 5 6

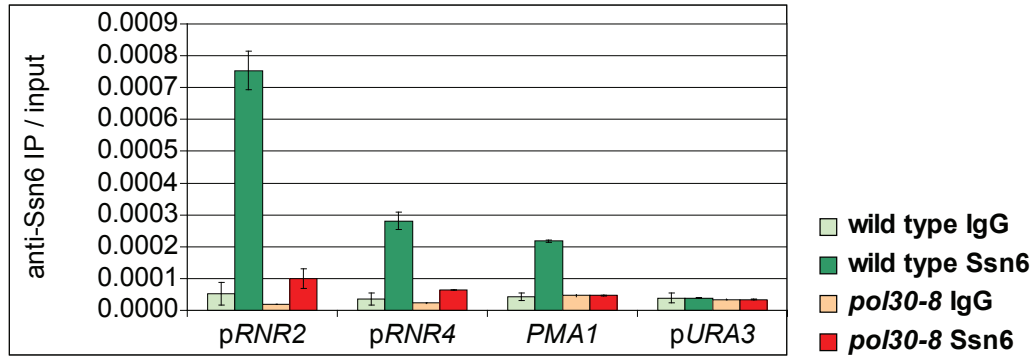
D
anti-Ssn6 IP / input
0.0009
0.0008
0.0007
0.0006
0.0005
0.0004
0.0003
0.0002
0.0001
0.0000
pRNR2
pRNR4
PMA1
pURA3
wild type IgG
wild type Ssn6
pol30-8 IgG
pol30-8 Ssn6

mild transcriptional up-regulation was reflected at the protein level (Figure 22C). However, likely due to the subtlety of this phenotype, dNTP levels did not significantly differ between wild-type in *pol30-8* cells (data not shown). One of the well described consequences of DNA damage is the derepression of the RNR genes (Figure 2; reviewed by Zegerman and Diffley, 2009). ChIP for Ssn6, a subunit of the transcriptional co-repressor complex Tup1-Ssn6 that together with Crt1 represses RNR transcription in the absence of DNA damage (Huang et al., 1998), showed a markedly reduced occupancy at the *RNR2* and *RNR4* promoters in *pol30-8* compared to wild-type cells (Figure 22D) while total Ssn6 levels were unaltered (data not shown). The result for wild-type cells agrees with previous ChIP data for Tup1 at the *RNR2* and *RNR3* promoters (Davie et al., 2002). I also observed a previously unreported binding of Ssn6 to the body of the *PMA1* gene. Interestingly, expression of *PMA2*, an isoform of *PMA1* was found to be 2.5-fold up-regulated in *pol30-8* compared to wild-type cells (Table 2). The localization of the Tup1-Ssn6 complex has been found to vary; while at the **a**-cell specific genes *STE2* and *STE6*, Tup1-Ssn6 seems to spread from the α2 repressor binding site into the coding region (Davie et al. 2002; Ducker and Simpson 2000), it is restricted to the promoter regions of *RNR2* and *RNR3* (Davie et al. 2002; Li and Reese 2001). In both cases these localizations coincide with histone hypoacetylation and, *in vivo*, Tup1-Ssn6 interacts physically with the class I HDACs Rpd3, Hos1, and Hos2, possibly with more than one of them at the same time (Davie et al. 2003). These data are in support of the

observed RNR up-regulation in *pol30-8* cells due to reduced binding of the co-repressor complex Tup1-Ssn6.

2.17 DNA damage checkpoint mutants rescue the silencing defect of *pol30-8*, but the suppressive function of *CDC21* is partially independent of the DNA damage response pathway.

Interestingly, a role in silencing of telomeric *ADE2*-VR and *URA3*-VIIL has been attributed to several components of the conserved DNA damage checkpoint pathway (Craven and Petes, 2000; Longhese et al., 2000), including CAF-1 dependent TPEV (Sharp et al., 2005). Moreover, *CDC21* has been implicated upstream of *DUN1* in the DNA damage checkpoint response pathway (Huang et al., 1998). In agreement with results for the *cac1Δ* mutant (Sharp et al., 2005), *rad53-K227A pol30-8 URA3*-VIIL cells grew at least 10,000-fold better on 5-FOA than *pol30-8* cells alone (Figure 23A, note: YPH strain background). The growth defect of *pol30-8 URA3*-VIIL on 5-FOA-containing medium was also alleviated in a *dun1Δ pol30-8 URA3*-VIIL strain, albeit to a much lesser extent (100 to 1,000-fold, Figure 23B). *CDC21* overexpression in *dun1Δ pol30-8 URA3*-VIIL cells led to further suppression of 5-FOA sensitivity (Figure 23B) while it did not significantly enhance 5-FOA resistance of a *pol30-8 rad53-K227A* strain (Figure 23C). Moreover, *RAD53* overexpression in *pol30-8 URA3*-VIIL cells reversed the *CDC21* overexpression, resulting in 5-FOA sensitivity indistinguishable from that of *pol30-8 URA3*-VIIL alone (Figure 23D). The attempt to generate a *cdc21-216 dun1Δ* strain revealed synthetic lethality between these

Figure 23: DNA damage checkpoint mutants rescue the silencing defect of *pol30-8*, but the suppressive function of *CDC21* is partially independent of the DNA damage response pathway.

(A) 10-fold serial dilution of *MAT***a** and *MAT*α wild-type (MRY0607, 0611), *pol30-8* (MRY0610, 0608), *rad53-K227A* (MRY0613, 0609) and *pol30-8 rad53-K227A* (MRY0614, 0612) *ADE2*-VR *URA3*-VIIL strains.

(B) 10-fold serial dilution of *MAT*α wild-type (MRY0919), *pol30-8* (MRY0921), *dun1Δ* (MRY0920) and *pol30-8 dun1Δ* (MRY0918) *hmr*::*ADE2 URA3*-VIIL strains transformed with pRS425 or *CDC21*.

(C) 10-fold serial dilution of *MAT*α wild-type (MRY0611), *pol30-8* (MRY0608), *rad53-K227A* (MRY0609) and *pol30-8 rad53-K227A* (MRY0612) *ADE2*-VR *URA3*-VIIL strains transformed with pRS425 or *CDC21*.

(D) 10-fold serial dilution of wild-type (MRY1097) and *pol30-8* (MRY1092) *ade2Δ ura3Δ hmr*::*ADE2 URA3*-VIIL strains transformed with indicated plasmids; vectors: pRS425 and pRS423.

(E) Tetrad analysis of a cross between *MAT***a** *pol30-8 dun1Δ hmr*::*ADE2 URA3*-VIIL (MRY0915) and *MAT*α *cdc21-216 rnr3*::*RNR3-URA3-LEU3* (Y235); white arrows indicate missing spores which should carry both the *cdc21-216* and the *pol30-8* mutations.

A

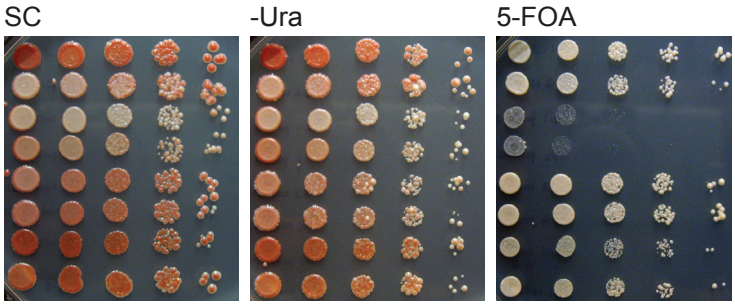
SC
-Ura
5-FOA
wild type *MAT***a**
wild type *MAT*α
*pol30-8 MAT***a**
*pol30-8 MAT*α
*rad53-K227A MAT***a**
*rad53-K227A MAT*α
*pol30-8 rad53-K227A MAT***a**
*pol30-8 rad53-K227A MAT*α

B

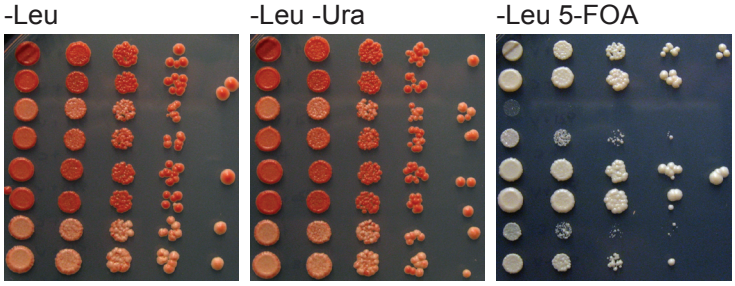
-Leu
-Leu -Ura
-Leu 5-FOA
wild type + vector
wild type + *CDC21*
pol30-8 + vector
pol30-8 + *CDC21*
dun1Δ + vector
dun1Δ + *CDC21*
pol30-8 dun1Δ + vector
pol30-8 dun1Δ + *CDC21*

C

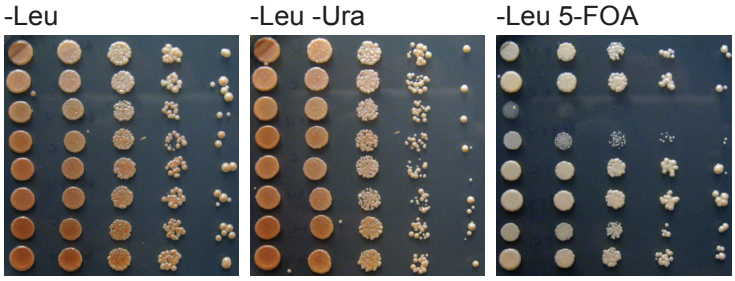
-Leu
-Leu -Ura
-Leu 5-FOA
wild type + vector
wild type + *CDC21*
pol30-8 + vector
pol30-8 + *CDC21*
rad53-K227A + vector
rad53-K227A + *CDC21*
pol30-8 rad53-K227A + vector
pol30-8 rad53-K227A + *CDC21*

D

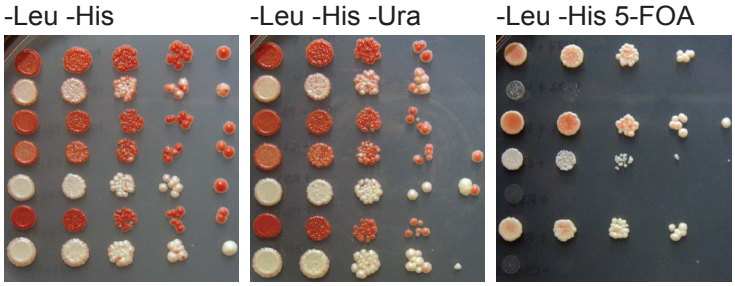
-Leu -His
-Leu -His -Ura
-Leu -His 5-FOA
wild type + vectors
pol30-8 + vectors
pol30-8 + *POL30*
pol30-8 + *CDC21*
pol30-8 + *RAD53*
pol30-8 + *POL30* + *RAD53*
pol30-8 + *CDC21* + *RAD53*

E

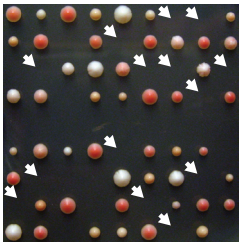

two mutations (Figure 23E). These results suggest a role for *CDC21* in 5-FOA sensitivity in a pathway separate from the *RAD53-DUN1* checkpoint response, but possibly in a pathway that is also controlled by *RAD53*.

2.18 The *pol30-8* mutant is mildly sensitive to DNA damage.

The increased RNR expression in *pol30-8* cells (Figure 22A) and the rescue of *pol30-8 URA3*-VIIL 5-FOA sensitivity by *rad53-K227A* (Figure 23A) together suggest the possibility that in *pol30-8* cells the DNA damage checkpoint response is activated, leading to induction of RNR and a specific inability to silence *URA3*-VIIL but not *HIS3*-VIIL expression. As previously reported for bleomycin (BLM; Martin et al., 1999), wild-type *URA3*-VIIL cells exhibited increased 5-FOA sensitivity upon treatment with either BLM, MMS or 4-nitroquinoline 1-oxide (4-NQO; Figures 24A, 24B and data not shown). For *URA3*-VIIL strains mutant for *pol30-8* or *cac1Δ* I could confirm their sensitivity to MMS, BLM and 4-NQO (Ayyagari et al., 1995; Li et al., 2009; Linger and Tyler, 2005; Tyler et al., 1999); BLM treatment, however, only resulted in less than 10-fold decreased growth of these mutants compared to wild type (Figures 24A, 24B and data not shown). In the presence of these DNA damaging agents their sensitivity to 5-FOA was maximal. These results support the hypothesis that DNA damage occurring in a *pol30-8 URA3*-VIIL mutant might lead to increased 5-FOA sensitivity. Interestingly, in *asf1Δ URA3*-VIIL cells 5-FOA sensitivity was not increased compared to wild type in the presence of DNA damage whereas 5-

Figure 24: The *pol30-8* mutant is mildly sensitive to DNA damage.

(A) 10-fold serial dilution of *MAT*α wild-type (MRY0656), *pol30-8* (MRY0654), *asf1Δ* (MRY0662), *hir1Δ* (MRY0660), *asf1Δ hir1Δ* (MRY0659), *pol30-8 asf1Δ* (MRY0658) and *pol30-8 asf1Δ hir1Δ* (spore 5-3) *hmr*::*ADE2 URA3*-VIIL strains. BLM = Bleomycin [3 U/l].

(B) 10-fold serial dilution of *MAT*α wild-type (MRY0827, 0832) or *pol30-8* (MRY0828) *hmr*::*ADE2 URA3*-VIIL strains transformed with pRS425 or *CDC21*. BLM = Bleomycin [6 U/l].

A

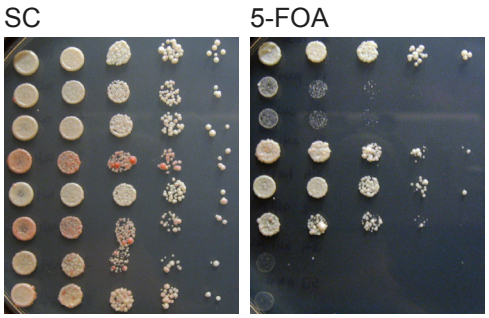
SC
5-FOA
MATα
MATα pol30-8
MATα cac1Δ
MATα asf1Δ
MATα hir1Δ
MATα asf1Δ hir1Δ
MATα asf1Δ pol30-8
MATα asf1Δ hir1Δ pol30-8

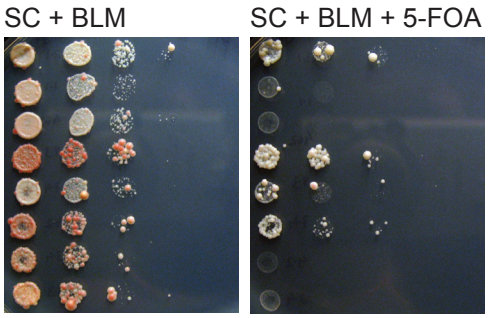
SC + BLM
SC + BLM + 5-FOA
MATα
MATα pol30-8
MATα cac1Δ
MATα asf1Δ
MATα hir1Δ
MATα asf1Δ hir1Δ
MATα asf1Δ pol30-8
MATα asf1Δ hir1Δ pol30-8

B

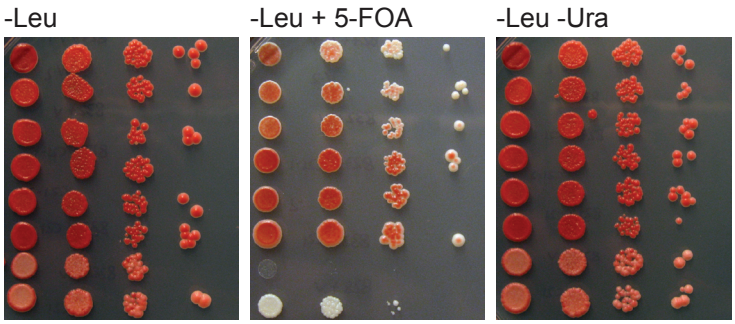
-Leu
-Leu + 5-FOA
-Leu -Ura
wild type #1 + vector #1
wild type #1 + vector #2
wild type #2 + vector
wild type #1 + CDC21 #1
wild type #1 + CDC21 #2
wild type #2 + CDC21
pol30-8 + vector
pol30-8 + CDC21

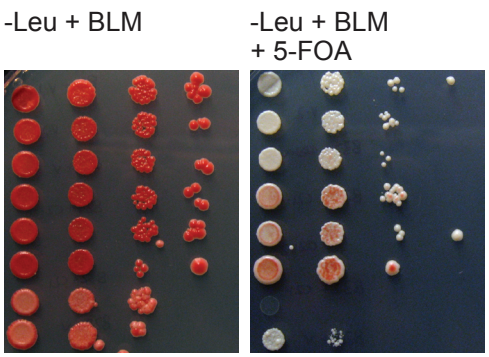
-Leu + BLM
-Leu + BLM
+ 5-FOA
wild type #1 + vector #1
wild type #1 + vector #2
wild type #2 + vector
wild type #1 + CDC21 #1
wild type #1 + CDC21 #2
wild type #2 + CDC21
pol30-8 + vector
pol30-8 + CDC21

FOA sensitivity was maximal in this assay with the combined inactivation of the *ASF1*/*HIR1* and *POL30*/CAF-1 pathways (Figure 24A).

Overexpression of *CDC21* could suppress the 5-FOA sensitivity of wild-type *URA3*-VIIL cells in the presence of BLM or MMS only marginally, but that of *pol30-8 URA3*-VIIL by at least 100-fold in the case of BLM (Figure 24B and data not shown). Thus, while part of the 5-FOA sensitivity of *pol30-8* mutants might be due to DNA damage, *CDC21* might have additional and genetically separable functions.

2.19 The DNA damage response only has a minor contribution to the elevated *URA3*-VIIL levels in *pol30-8* cells.

In gene expression microarray analyses, both, *URA3* and *HIS3* gene expression were shown to be altered by DNA damaging agents; whereas *HIS3* expression was up-regulated by 3.4- to 4.2-fold, that of endogenous *URA3* was 2.7-fold down-regulated (Jelinsky et al., 2000; Jelinsky and Samson, 1999). To directly address gene expression changes at the telomeric reporters upon DNA damage, wild-type, *pol30-8* or *sir3Δ* cells carrying *URA3*, *HIS3* or *kanMX6* at telomere VII-L were grown in rich medium and treated with MMS. Subsequently, expression levels of *URA3*-VIIL, *HIS3*-VIIL and *kanMX6*-VIIL as well as *RNR4* as a control for DNA damage checkpoint activation were determined by RT-qPCR. Of note, expression levels for *URA3*-VIIL in wild-type cells compared to *ACT1* as internal control were 16-fold lower than *HIS3*-VIIL expression levels, which in turn were 26-fold lower than *kanMX6*-VIIL expression levels (Figure 25A). In wild-type

Figure 25: The DNA damage response only has a minor contribution to the elevated *URA3*-VIIL levels in *pol30-8* cells.

(A) Expression levels of *URA3*, *HIS3* and *kanMX6*, measured by RT-qPCR, in wild-type, *pol30-8* and *sir3Δ* strains carrying *ura3Δ URA3*-VIIL (MRY1082, 1086, 1100), *his3Δ HIS3*-VIIL (MRY1418, 1414, 1415) or *kanMX6*-VIIL (MRY1749, 1751, 1763), which where either left untreated or treated with 0.05 % MMS for 2 h. Data from one representative experiment are shown. The top right panel leaves out the *sir3Δ* results for better visualization of those for wild-type and *pol30-8*. Middle right panel: *RNR4* expression levels in all strains harvested for this experiment with error bars denoting the SEM.

(B) Western blot analysis of whole cell protein extracts from wild-type (MRY1111) and *pol30-8* (MRY1104, 1108, 1105) strains either left untreated or treated with 0.4 g/l 4-NQO for 2 h.

A

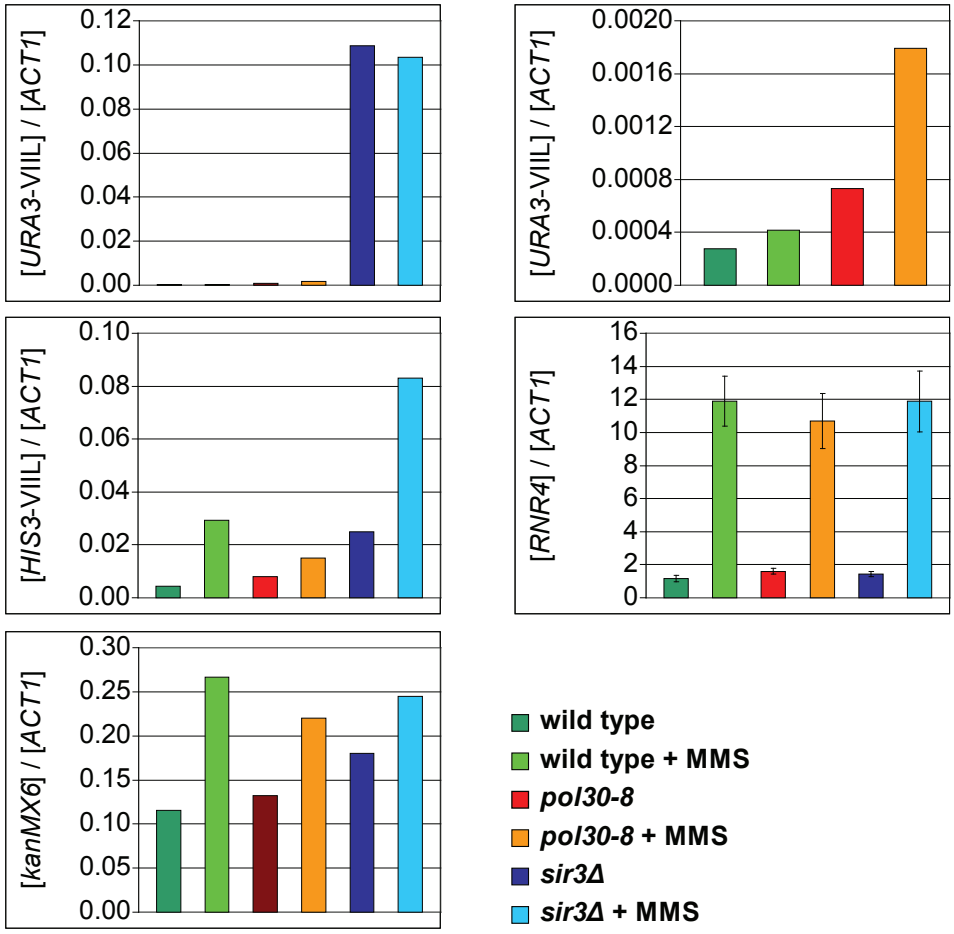
[URA3-VIIL] / [ACT1]
0.12
0.10
0.08
0.06
0.04
0.02
0.00
[URA3-VIIL] / [ACT1]
0.0020
0.0016
0.0012
0.0008
0.0004
0.0000
[HIS3-VIIL] / [ACT1]
0.10
0.08
0.06
0.04
0.02
0.00
[RNR4] / [ACT1]
16
14
12
10
8
6
4
2
0
[kanMX6] / [ACT1]
0.30
0.25
0.20
0.15
0.10
0.05
0.00
wild type
wild type + MMS
pol30-8
pol30-8 + MMS
sir3Δ
sir3Δ + MMS

B

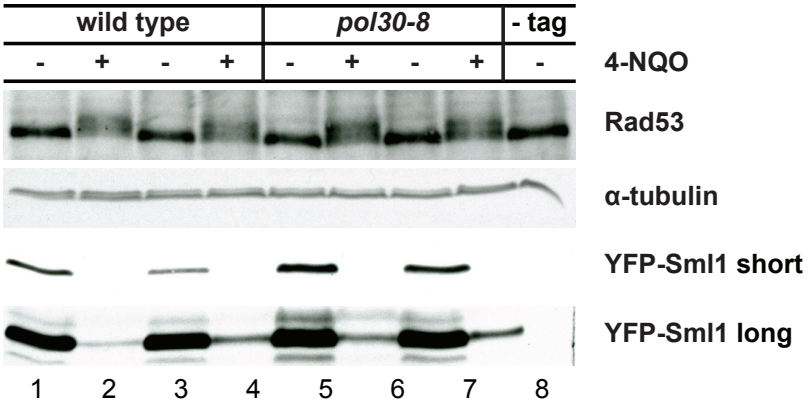
wild type
pol30-8
- tag
- + - + - + - + -
4-NQO
Rad53
α-tubulin
YFP-Sml1 short
YFP-Sml1 long
1 2 3 4 5 6 7 8

cells, MMS treatment resulted in 1.5-fold up-regulation of *URA3*-VIIL, 6.6-fold up-regulation of *HIS3*-VIIL and 2.3-fold up-regulation of *kanMX6*-VIIL expression (Figure 25A). In *pol30-8* cells, basal *URA3*-VIIL, *HIS3*-VIIL and *kanMX6*-VIIL expression was up-regulated 2.6-, 1.8- and 1.1-fold, respectively. While *HIS3*-VIIL expression upon MMS treatment was up-regulated less (1.9-fold), the results for *URA3*-VIIL (2.5-fold elevated) and *kanMX6*-VIIL expression (1.7-fold elevated) were similar to wild type (Figure 25A). These results indicate that expression of the poorly expressed *URA3* and HIS3 genes at telomere VII-L responded similarly to DNA damage in wild-type and *pol30-8* cells. Interestingly, in *sir3Δ* cells, basal *URA3*-VIIL expression was up-regulated 393-fold compared to wild type (see also Figure 6C) and could not be further induced by MMS, whereas that of *HIS3*-VIIL was only up-regulated 5.6-fold compared to wild-type cells. These results indicate that *URA3*-VIIL is especially prone to transcriptional activation.

In support of the above results, the DNA damage checkpoint response, as assessed by Rad53 hyper-phosphorylation and YFP-Sml1 degradation was not overtly activated in the *pol30-8* mutant, and could be stimulated by treatment with 4-NQO to a similar extent as in wild-type cells (Figure 25B). I conclude that the up-regulation of *URA3*-VIIL and the resulting 5-FOA sensitivity in *pol30-8* cells is unlikely due to an intrinsic DNA damage response, even though RNR levels are elevated and compromising components of the DNA damage response pathway suppresses the effect of *pol30-8* on *URA3*-VIIL gene expression.

2.20 Inhibition of ribonucleotide reductase rescues 5-FOA sensitivity of *pol30-8 URA3*-VIIL cells.

Since inhibition of the DNA damage response pathway led to rescue of growth of *pol30-8 URA3*-VIIL cells on 5-FOA (Figures 23A and 23B) although the DNA damage checkpoint response was not overtly activated (Figure 25B), I wondered whether the increased RNR activity in *pol30-8 URA3*-VIIL cells could directly contribute to 5-FOA sensitivity. The toxicity caused by 5-FOA stems from a product generated by its conversion to fluoroorotidine monophosphate (5-FOMP) and further decarboxylation to 5-fluorouridine monophosphate (5-FUMP) by OMPdecase, encoded by *URA3*. After phosphorylation, the diphosphate (5-FUDP) can be either incorporated into RNA as 5-fluorouridine triphosphate (5-FUTP) or it can be reduced by RNR to the deoxy-diphosphate (5-FdUDP), which is either phosphorylated (to 5-FdUTP) and used for DNA synthesis or dephosphorylated to 5-fluorodeoxyuridine monophosphate (5-FdUMP). 5-FdUMP forms a covalent complex with Cdc21 and the methyl donor MTHF, inhibiting the enzymatic methylation reaction of dUMP to dTMP (Figure 26A; Hardman et al., 2001; Jones and Fink, 1982; Longley et al., 2003). I asked whether directly interfering with RNR function could also rescue the 5-FOA sensitivity phenotype. Hydroxyurea has been shown to inhibit RNR activity by quenching the free radical at the active site of Rnr2 (Harder and Follmann, 1990). Indeed, hydroxyurea at sublethal concentrations (Laman et al., 1995) rescued the 5-FOA sensitivity of *pol30-8* or *cac1Δ* strains about 10,000-fold, but not that of *asf1Δ pol30-8*, *hir1Δ pol30-8* or *asf1Δ hir1Δ pol30-8* strains (Figure 26B). These results

Figure 26: Inhibition of ribonucleotide reductase rescues 5-FOA sensitivity of *pol30-8 URA3*-VIIL cells.

(A) Schematic overview of 5-fluorouracil (5-FU) metabolism in the cell (modified from Hardman et al., 2001); added on is the metabolism of 5-FOA (Jones and Fink, 1982). For abbreviations see text.

(B) 10-fold serial dilution of wild-type (MRY0656), *pol30-8* (MRY0041), *cac1Δ* (MRY0462), *pol30-8 asf1Δ* (MRY0658), *pol30-8 hir1Δ* (MRY0661) and *pol30-8 asf1Δ hir1Δ* (MRY0655). HU = hydroxyurea.

A

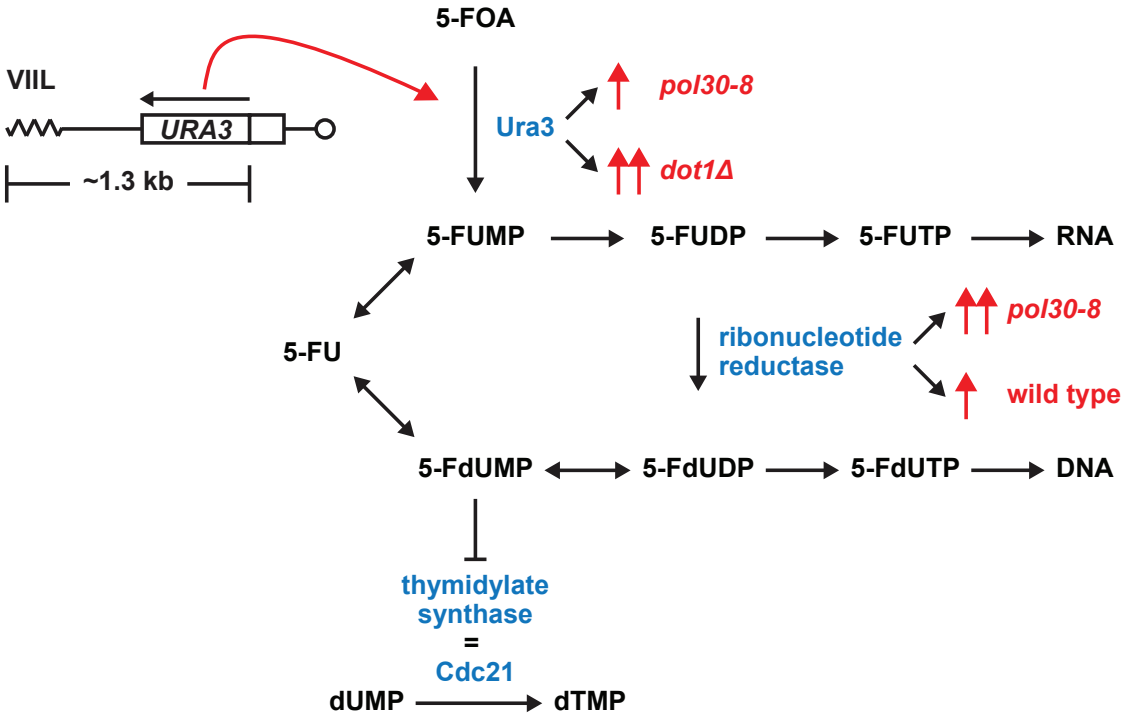
5-FOA
VIIL
URA3
~1.3 kb
Ura3
pol30-8
dot1Δ
5-FUMP
5-FUDP
5-FUTP
RNA
5-FU
ribonucleotide reductase
pol30-8
wild type
5-FdUMP
5-FdUDP
5-FdUTP
DNA
thymidylate synthase = Cdc21
dUMP
dTMP

B

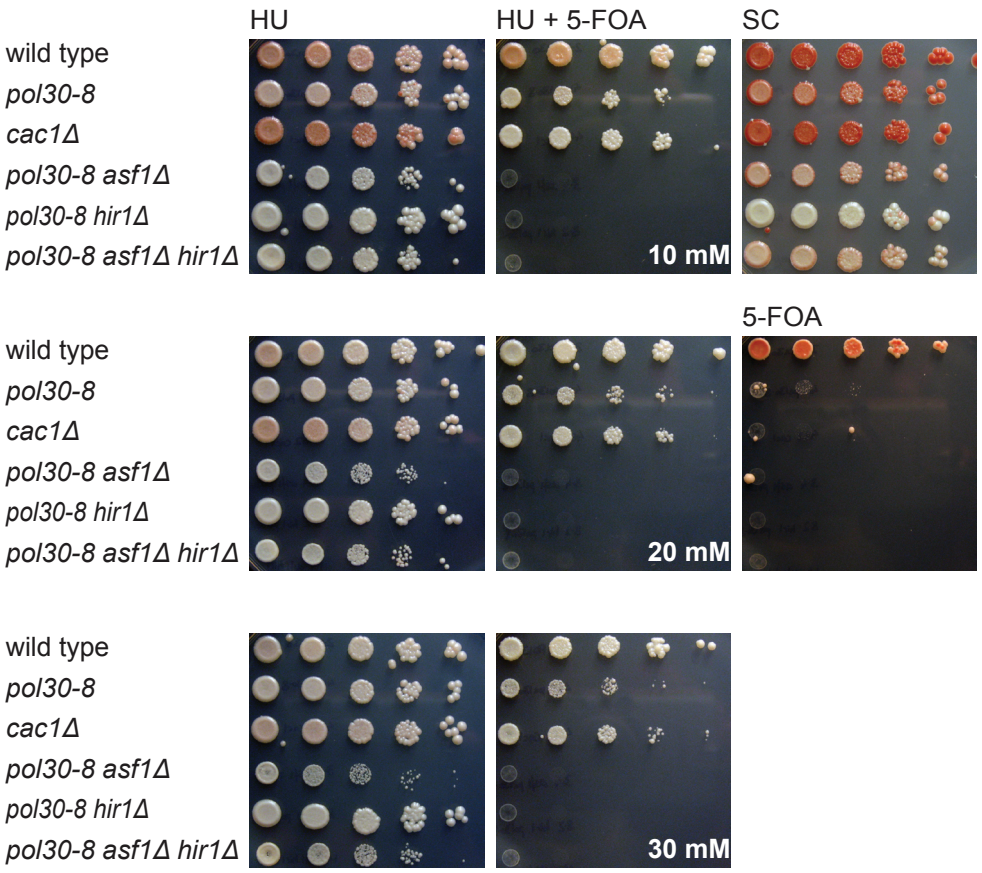
HU
HU + 5-FOA
SC
wild type
pol30-8
cac1Δ
pol30-8 asf1Δ
pol30-8 hir1Δ
pol30-8 asf1Δ hir1Δ
10 mM
5-FOA
wild type
pol30-8
cac1Δ
pol30-8 asf1Δ
pol30-8 hir1Δ
pol30-8 asf1Δ hir1Δ
20 mM
wild type
pol30-8
cac1Δ
pol30-8 asf1Δ
pol30-8 hir1Δ
pol30-8 asf1Δ hir1Δ
30 mM

indicate that elevated RNR contributes to 5-FOA sensitivity of *pol30-8 URA3*-VIIL cells.

2.21 5-FOA treatment induces RNR transcription.

The striking effect of hydroxyurea in the presence of a rather mild up-regulation of *RNR2*, *RNR3* and *RNR4* expression in the *pol30-8* mutant prompted the question whether 5-FOA itself could stimulate RNR transcription. When treating logarithmically growing wild-type and *pol30-8 URA3*-VIIL cells with 5-FOA (or DMSO as a control) for up to four hours, I indeed observed a marked increase in RNR transcript levels. For *RNR3*, transcript levels were raised by 4.1- and 4.5-fold, respectively, with final levels being 2.5-fold higher in *pol30-8 URA3*-VIIL cells. For *RNR4*, transcript levels increased 3.3- and 5.8-fold, respectively, with final levels being 2.4-fold higher in *pol30-8 URA3*-VIIL cells (Figure 27A, Experiments 1 and 2). For *RNR2* I obtained similar results as for *RNR4* (data not shown). It should be noted that there was some variability between the two experiments shown which represent data from one *MAT***a** (Figure 27A, left) and one, otherwise isogenic, *MAT*α (Figure 27A, right) strain. However, for another *MAT*α *pol30-8*/wild-type pair, I observed *RNR4* levels to be up-regulated 1.9-fold in *pol30-8* cells which increased a further 3-fold three hours after adding 5-FOA (Figure 27A, Experiment 3).

Importantly, while overexpression of *POL30* only marginally lowered *URA3*-VIIL expression in *pol30-8* cells (Figure 7A), it lowered Rnr4 protein levels, while *CDC21* overexpression did not (Figure 27B). These results indicate that 5-

Figure 27: 5-FOA treatment induces RNR transcription.

(A) Upper panel: two independent experiments showing expression levels, of *RNR3* and *RNR4*, measured by RT-qPCR, in wild-type (MRY1082, 1090) and *pol30-8* (MRY1086, 1101) *ura3Δ URA3*-VIIL strains. *PGK1*: reference. Results were normalized to wild-type *RNR4* levels before treatment. Lower panel: expression levels of *RNR4*, measured by RT-qPCR, in wild-type (MRY1097) and *pol30-8* (MRY1092) *ade2Δ ura3Δ hmr*::*ADE2 URA3*-VIIL strains. *ACT1*: reference.

(B) Western blot analysis of whole cell protein extracts from a *pol30-8 hmr*::*ADE2 URA3*-VIIL strain (MRY0828) transformed with pRS425, *POL30* or *CDC21*. #1 and #2 indicate independent transformants; “short” and “long” refer to exposure times.

A

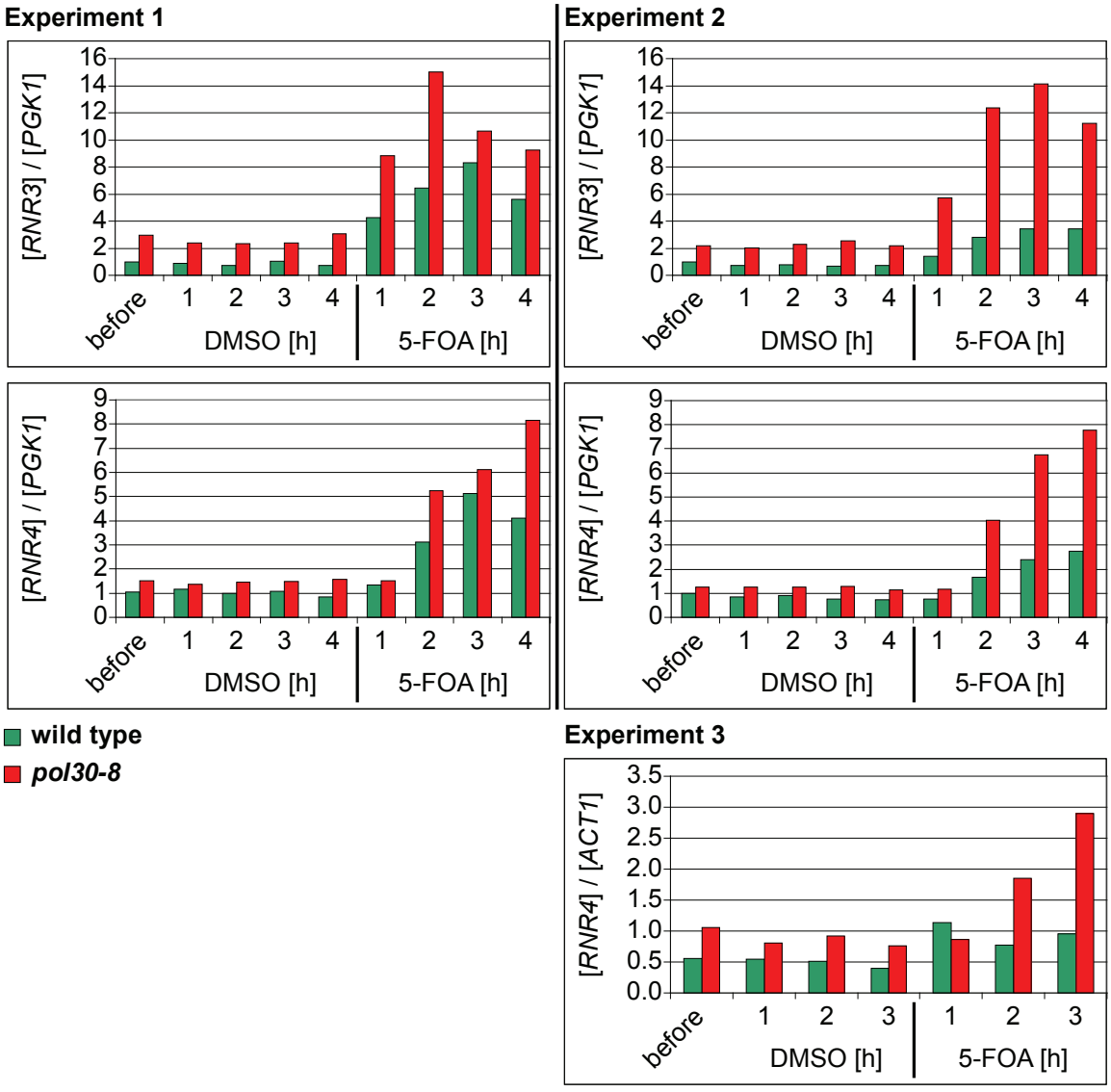
Experiment 1
Experiment 2
[RNR3] / [PGK1]
[RNR4] / [PGK1]
before
DMSO [h]
5-FOA [h]
wild type
pol30-8
Experiment 3
[RNR4] / [ACT1]

B

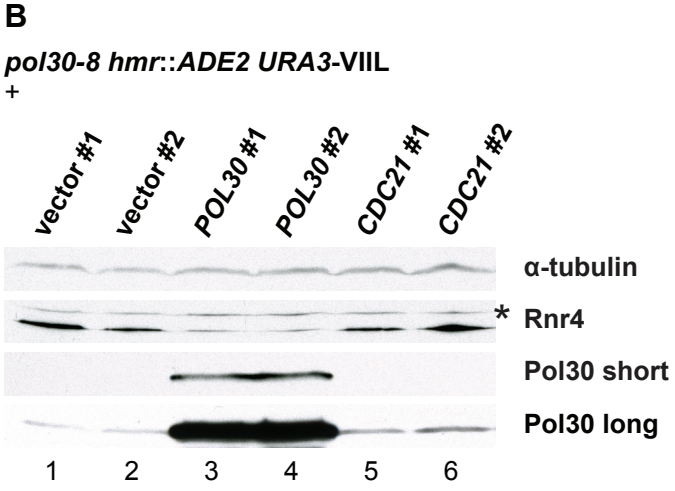
pol30-8 hmr::ADE2 URA3-VIIL
+
vector #1
vector #2
POL30 #1
POL30 #2
CDC21 #1
CDC21 #2
α-tubulin
Rnr4
*
Pol30 short
Pol30 long
1 2 3 4 5 6

FOA causes a DNA damage response and thereby exacerbates the transcriptional up-regulation of RNR genes in *pol30-8* mutant cells. Of note, overexpression of just *RNR2* in wild-type *URA3*-VIIL cells did not increase their 5-FOA sensitivity (data not shown). Moreover, segregants from a cross between a strain carrying the allosteric site mutant *rnr1-D57N* leading to ~2-fold increased dNTP levels (AC23; Chabes et al., 2003) and *pol30-8 hmr*::*ADE2 URA3*-VIIL neither displayed altered 5-FOA sensitivity in a *RAD5* (W1588-4C) nor in a *rad5-535* (W303) genetic background (data not shown). Thus, up-regulation of RNR alone might not be sufficient, but together with mild up-regulation of *URA3*-VIIL expression is likely the reason for their markedly increased 5-FOA sensitivity in *pol30-8* cells. The latter can be either overcome by overexpressing *CDC21*, reducing RNR activity, reducing the DNA damage response pathway or overexpressing *POL30*.

2.22 Altered nucleotide metabolism in *dot1Δ URA3*-VIIL cells contributes to 5-FOA sensitivity.

dot1Δ URA3-VIIL cells did not show general up-regulation of telomeric gene expression, but in contrast, elevated expression occurred primarily at the *adh4*::*URA3*-VIIL locus (Figure 15). Thus, it was surprising that deletion of *ASF1*, a histone chaperone described to be involved in nucleosome assembly, partially rescued *dot1Δ URA3*-VIIL 5-FOA sensitivity (Figure 11C). *asf1Δ* rescued the growth of *ppr1Δ URA3*-VIIL cells on medium lacking uracil (Figure 10A) and showed up-regulation of poorly expressed genes, including those at chromosome

ends similar to *pol30-8* or *cac2Δ* mutants (Figures 16C, 16D and 18B). However, *asf1Δ URA3*-VIIL cells were not sensitive to 5-FOA themselves (Figure 10A; Tyler et al., 1999). Hence, *asf1Δ* might partially rescue *dot1Δ URA3*-VIIL 5-FOA sensitivity by a mechanism independent of heterochromatin assembly but instead due to a failure to increase RNR levels in this strain. To test this idea I compared whole cell protein extracts from wild-type, *asf1Δ*, *dot1Δ* and *asf1Δ dot1Δ* strains either untreated or treated with 4-NQO for Rnr2 and Rnr4 protein levels. While basal Rnr2 and Rnr4 protein levels seemed to be elevated (below 2-fold) in *asf1Δ* cells, I could only detect a mild increase (again below 2-fold) upon DNA damage treatment (Figure 28A). This is surprising, since checkpoint signaling has previously been found to be unaffected in *asf1Δ* mutants (Emili et al., 2001). A similar RNR regulation was observed in *asf1Δ dot1Δ* cells as well as *asf1Δ pol30-8* cells (Figure 28A and data not shown), but not in *dot1Δ* cells. These observations further support the hypothesis that up-regulation of RNR expression upon 5-FOA treatment is a main component of 5-FOA sensitivity (Figure 26A). *CDC21* overexpression did not cause an additional growth advantage of *asf1Δ dot1Δ URA3*-VIIL mutants on 5-FOA (Figure 11C). I conclude that the 5-FOA assay in the context of low *URA3*-VIIL expression can function as an indicator for RNR levels (Figure 26A); failure to up-regulate RNR can counteract 5-FOA metabolism so that overexpression of the target of 5-FdUMP, *CDC21*, is without effect.

Figure 28: Altered nucleotide metabolism in *dot1Δ URA3*-VIIL cells contributes to 5-FOA sensitivity.

(A) Western blot analysis of whole cell protein extracts from wild-type (MRY1807), *asf1Δ* (MRY1811), *dot1Δ* (MRY1802) and *asf1Δ dot1Δ* (MRY1797) strains, either left untreated or treated with 0.4 g/l 4-NQO for 2 h.

(B) Expression level of *hmr*::*ADE2*, measured by RT-qPCR, in four biological replicates each of wild-type (MRY1066, 1629), *pol30-8* (MRY1071), *dot1Δ* (MRY1627) and *pol30-8 dot1Δ* (MRY1069) strains as well as two biological replicates of a *sir3Δ* strain (MRY1080). All strains were *ade2Δ ura3Δ hmr*::*ADE2 URA3*-VIIL. *ACT1*: reference. Results were normalized to wild-type *ADE2* levels. Error bars denote the SEM for all strains and/or replicates per genotype tested.

(C) Patches of four tetrads from a diploid strain heterozygous for *pol30-8 ard1Δ hmr*::*ADE2 URA3*-VIIL (MRY1726). White arrows indicate *ard1Δ hmr*::*ADE2* strains, white/pink arrows indicate *pol30-8 ard1Δ hmr*::*ADE2* strains.

(D) 10-fold serial dilution of wild-type (MRY1081), *bas1Δ pho2Δ* (MRY1866, 1867), *dot1Δ* (MRY1063) and *dot1Δ bas1Δ pho2Δ* (MRY1871, 1872) *ade2Δ ura3Δ hmr*::*ADE2 URA3*-VIIL strains (upper panel) as well as wild-type (MRY1081), *bas1Δ pho2Δ* (MRY1866, 1867), *pol30-8* (MRY1098) and *pol30-8 bas1Δ pho2Δ* (MRY1868, 1869) strains (lower panel). All strains were *ade2Δ ura3Δ hmr*::*ADE2 URA3*-VIIL. #1 and #2 indicate independent isogenic strains.

A

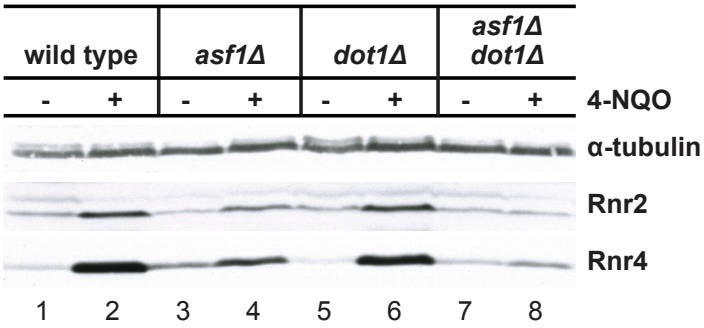
wild type
asf1Δ
dot1Δ
asf1Δ dot1Δ
- + - + - + - +
4-NQO
α-tubulin
Rnr2
Rnr4
1 2 3 4 5 6 7 8

B

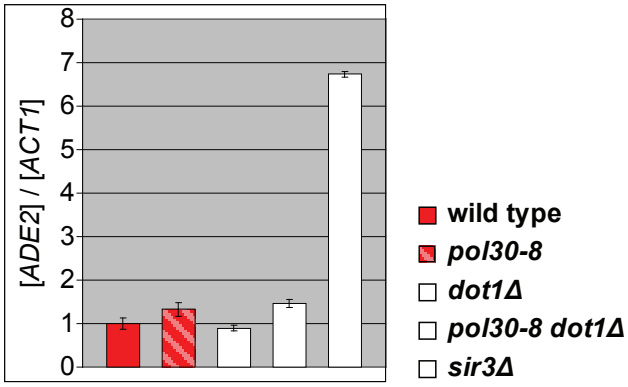
[ADE2] / [ACT1]
0 1 2 3 4 5 6 7 8
wild type
pol30-8
dot1Δ
pol30-8 dot1Δ
sir3Δ

C

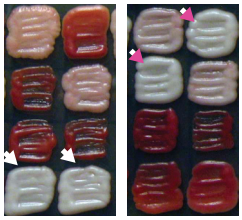

D

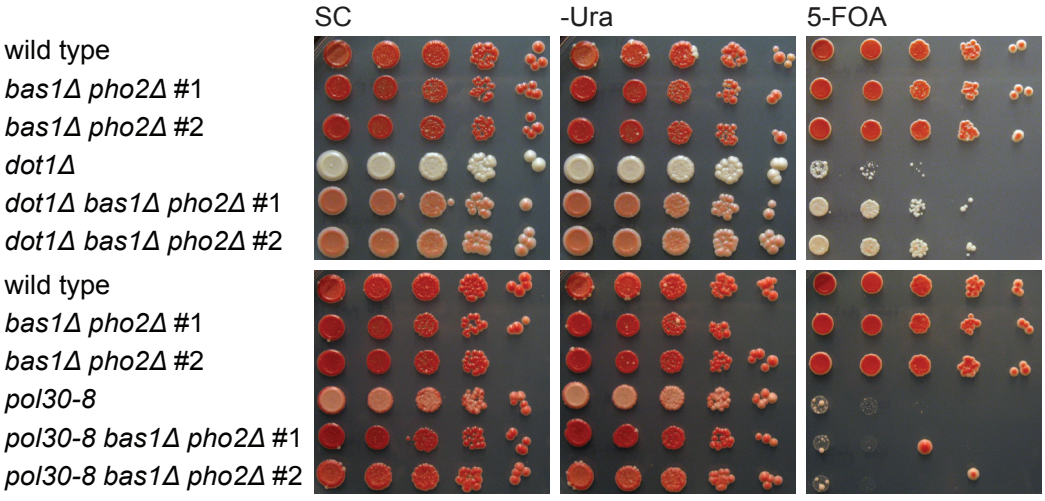
SC
-Ura
5-FOA
wild type
bas1Δ pho2Δ #1
bas1Δ pho2Δ #2
dot1Δ
dot1Δ bas1Δ pho2Δ #1
dot1Δ bas1Δ pho2Δ #2
wild type
bas1Δ pho2Δ #1
bas1Δ pho2Δ #2
pol30-8
pol30-8 bas1Δ pho2Δ #1
pol30-8 bas1Δ pho2Δ #2

Since *dot1Δ* cells did not have a general telomeric silencing defect, I wondered whether the derepressed *hmr*::*ADE2* reflected the apparent role of *DOT1* in heterochromatin formation at *HMR*. During the analysis of *hmr*::*ADE2* expression levels I noticed that despite the relatively white appearance of *dot1Δ hmr*::*ADE2* colonies that is almost indistinguishable from *sir3Δ hmr*::*ADE2* colonies, the *ADE2* expression levels were elevated by almost 7-fold in *sir3Δ*, but not at all in *dot1Δ* strains grown in synthetic complete (SC) medium containing 20 mg/l adenine (Figure 28B). Moreover, *ard1Δ*, a mutant with a role in the *dot1Δ*-dependent genetic silencing pathway (van Welsem et al., 2008) that was shown to have no silencing defect at *HMR* (Mullen et al., 1989; Whiteway et al., 1987) also grew as a completely white colony (Figure 28C). Interestingly, I observed that *ard1Δ* mutants in a wild-type W303 background (containing the *ade2-1* allele) were of a rusty red colony color and grew poorly in rich medium. This growth defect was rescued in the presence of *hmr*::*ADE2* (data not shown).

Together these phenotypes raised the possibility that purine (adenine) and pyrimidine (uracil) synthesis were inter-connected. Cross-regulation of purine and pyrimidine pathways was suggested because deletion of either of two transcription factors *BAS1* or *PHO2* required for *de novo* purine synthesis almost abolished *URA3* transcription in conditions limiting for purines (Denis et al., 1998). This led me to test whether decreasing the activity of the purine synthesis pathway by deleting these two transcriptional activators would also lead to lowered *URA3*-VIIL expression. Indeed this was the case, since a *dot1Δ bas1Δ pho2Δ URA3*-VIIL mutant grew about 1,000-fold better on 5-FOA than *dot1Δ*

alone (Figure 28D, upper panel). The effect was specific to *dot1Δ* cells, since 5-FOA sensitivity of *pol30-8* cells was unchanged by deletion of *BAS1* and *PHO2* (Figure 28D, lower panel). These results confirm a co-regulation of *ADE2* and *URA3* and thus call into question the independence of the two prototophic markers at different heterochromatic loci. They also further underscore that different mechanisms cause 5-FOA sensitivity in the *dot1Δ* and the *pol30-8 URA3*-VIIL mutants.

2.23 The role of additional confirmed high-copy suppressors of the 5-FOA sensitivity phenotype of *pol30-8*

MCM1

The most frequently isolated (29 times, Table 1) high-copy suppressor candidate, *MCM1* suppressed the *pol30-8 URA3*-VIIL 5-FOA sensitivity by about 1,000-fold, while it did not suppress the 5-FOA sensitivity of a Ura^+ strain (Figure 29A). Cells carrying a mutation in the gene minichromosome maintenance 1 (*MCM1*) lose their ability to propagate plasmids containing ARSs, the yeast origins of replication (Maine et al., 1984). Subsequently, Mcm1 was found to be a member of the MADS box transcription factor family. With 69 % identical residues its DNA binding/dimerization domain, Mcm1 shows highest similarity to the human serum response factor (SRF; Norman et al., 1988). A diverse set of genes with roles in cell type specification, cell cycle progression, biosynthesis of cell wall and membrane structures and metabolic functions (Kuo and Grayhack,

Figure 29: The role of additional confirmed high-copy suppressors of the 5-FOA sensitivity phenotype of *pol30-8*: *MCM1*.

(A) 10-fold serial dilution of a *pol30-8 hmr*::*ADE2 URA3*-VIIL strain (MRY0041) transformed with YEp13M4, pRS425, *POL30*/YEp213, *POL30*/pR425, genomic *MCM1* or cloned *MCM1*. #1 and #2 indicate independent transformants.

(B) 10-fold serial dilution of *MAT***a** or *MAT*α wild-type (MRY0830, 0827) or *pol30-8* (MRY0834, 0828) *hmr*::*ADE2 URA3*-VIIL strains transformed with pRS425 or *MCM1*.

(C) 10-fold serial dilution of *MAT***a** or *MAT*α wild-type (MRY0830, 0827) or *pol30-8* (MRY0834, 0828) *hmr*::*ADE2 URA3*-VIIL strains as well as diploid wild-type (MRY903, 0906) or *pol30-8* (MRY909, 0912) strains homozygous or heterozygous for *hmr*::*ADE2* and *URA3*-VIIL.

(D) 10-fold serial dilution of diploid wild-type (MRY0903) or *pol30-8* (MRY0909) strains homozygous for *hmr*::*ADE2* and *URA3*-VIIL transformed with pRS425 or *MCM1*; *-8* = *pol30-8*.

A

pol30-8
hmr*::*ADE2
***URA3*-VIIL**
+

library vector
cloning vector
POL30/YEp213
POL30/cloning vector
library *MCM1* #1
library *MCM1* #2
cloned *MCM1* #1
cloned *MCM1* #2

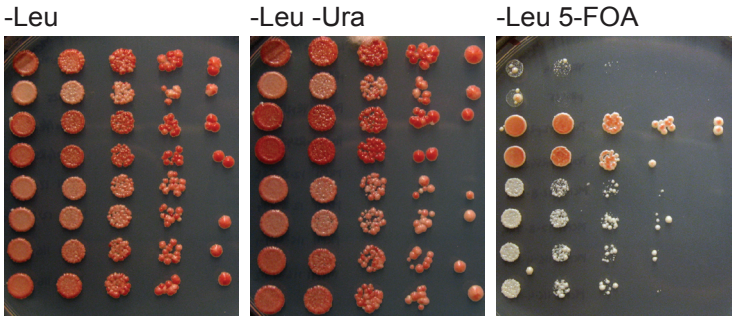

B

*MAT***a** + vector
*MAT***a** + *MCM1*
*MAT*α + vector
*MAT*α + *MCM1*
*MAT***a** *pol30-8* + vector
*MAT***a** *pol30-8* + *MCM1*
*MAT*α *pol30-8* + vector
*MAT*α *pol30-8* + *MCM1*

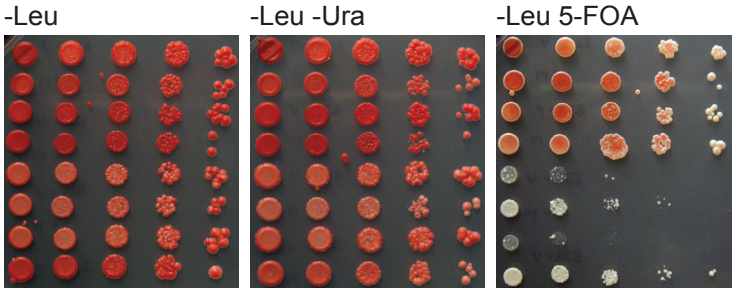

C

*MAT***a**
*MAT*α
*MAT***a** *pol30-8*
*MAT*α *pol30-8*
*MAT***a**/*MAT*α HOM
*MAT***a**/*MAT*α HET
*MAT***a**/*MAT*α *pol30-8*/*pol30-8* HOM
*MAT***a**/*MAT*α *pol30-8*/*pol30-8* HET

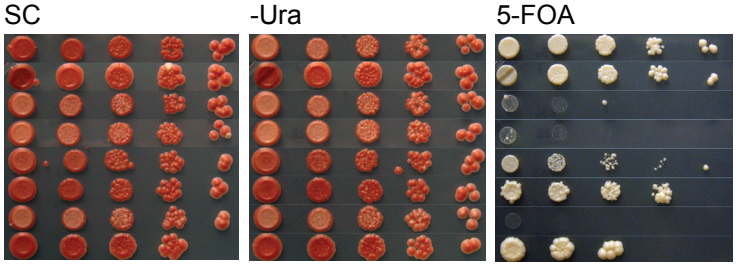

D

*MAT***a**/*MAT*α HOM + vector
*MAT***a**/*MAT*α HOM + *MCM1*
*MAT***a**/*MAT*α *-8*/*-8* HOM + vector
*MAT***a**/*MAT*α *-8*/*-8* HOM + *MCM1*

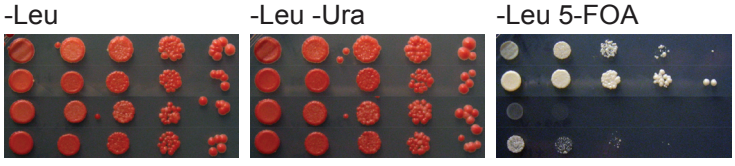

1994) contain upstream *MCM1* control elements (MCEs). In *MAT*α cells, genes encoding a cell type functions are repressed by Mcm1 together with the α2 transcription factor in a cooperative manner at the α2-Mcm1 operator (Johnson and Herskowitz, 1985; Keleher et al., 1988). Interestingly, this repression requires the global transcriptional co-repressor complex Tup1-Ssn6 (Keleher et al., 1992; Williams et al., 1991). More recently, Abraham and Vershon (2005) reported the non-essential N-terminus of Mcm1 to be required for expression of a subset of cell wall genes and cell wall integrity.

Due to the role of *MCM1* in repression of **a**-specific genes, I tested the effect of *MCM1* overexpression in *pol30-8* cells of both mating types. Interestingly, *MCM1* was able to suppress the 5-FOA sensitivity of *MAT*α *pol30-8* *URA3*-VIIL cells 10-fold better than those of *MAT***a** mating type (Figure 29B), indicating that part of its function in this process might be through its role as a repressor of **a**-specific genes. In extending the analysis to diploid strains, I noticed that wild-type diploid cells homozygous for *URA3*-VIIL grew 100-fold more poorly on 5-FOA than their haploid counterparts (Figure 29C). The improved growth of wild-type and *pol30-8* diploids heterozygous for *URA3*-VIIL likely resulted from loss of the *URA3*-VIIL reporter, possibly due to recombination between homologous telomeres proximal to the *adh4*::*URA3* locus, since those 5-FOA resistant colonies were Ura^- auxotrophs (data not shown). As in *MAT***a** cells, overexpression of *MCM1* had only a very small suppressive effect on 5-FOA sensitivity of diploid *pol30-8* cells homozygous for *URA3*-VIIL (Figure 29D). In summary, while these experiments indicate that mating type specificity and or

regulation of cell wall genes might be part of the effect of *MCM1* overexpression on 5-FOA sensitivity, they do not exclude the possibility that the 2-fold higher *URA3*-VIIL levels in wild-type and *pol30-8* diploid cells compared to those in haploid cells contribute to the effect.

MSA2

After my identification of *YKR077W* as a high-copy suppressor of the *pol30-8 hmr*::*ADE2 URA3*-VIIL phenotype, the protein product of this gene was found to interact with the heterodimeric transcription factor MBF (MluI cell-cycle box binding factor) and SBF (Swi4/6 cell-cycle box binding factor), both of which are responsible for G1 phase gene transcription to initiate the cell cycle. *YKR077W* was thus renamed *MSA2* (for “MBF and SBF associated”; Ashe et al., 2008). While the neighboring ORF *YKR078W* within the originally identified genomic library insert was not able to suppress 5-FOA sensitivity of *pol30-8 URA3*-VIIL, *YKR077W* did so to about 1,000 - 10,000-fold (note: YPH strain background), which only slightly differs from the library insert itself (Figure 30A). Interestingly, *MSA2* overexpression was slightly less able to suppress 5-FOA sensitivity of *cac1Δ URA3*-VIIL strains (Figure 30B). Using Orc3, a subunit of ORC with an established role in heterochromatin silencing (Bell et al., 1993; Foss et al., 1993; Micklem et al., 1993b), as a bait in a yeast-two hybrid assay, Msa2 was found as an interacting protein (Matsuda et al., 2007). In the same work also Cac1 was shown to interact with Orc3. Thus, it could be possible that Msa2 is in

Figure 30: The role of additional confirmed high-copy suppressors of the 5-FOA sensitivity phenotype of *pol30-8*: *MSA2*.

(A) 10-fold serial dilution of a *pol30-8 ADE2*-VR *URA3*-VIIL strain (MRY0388) transformed with YEp13M4, pRS425, *POL30*/pR425, genomic *MSA2* and the neighboring ORF *YKR078W*, cloned *MSA2* and cloned *YKR078W*. #1 and #2 indicate independent transformants.

(B) 10-fold serial dilution of a *cac1Δ hmr*::*ADE2 URA3*-VIIL strain (MRY0462) transformed with *CAC1*/pRS425, YEp13M4, pRS425, genomic *MSA2* and the neighboring ORF *YKR078W* and cloned *MSA2*. #1 and #2 indicate independent transformants.

(C) 10-fold serial dilution of a *pol30-8 hmr*::*ADE2 URA3*-VIIL strain (MRY0041) transformed with pRS425, *POL30*, *MSA2* and *YOR066W*.

(D) 10-fold serial dilution of wild-type (MRY0436), *pol30-8* (MRY0438), *msa2Δ* (MRY0440, 0442) and double mutant (MRY0445, 0446) *hmr*::*ADE2 URA3*-VIIL strains.

A

pol30-8
hmr*::*ADE2
***URA3*-VIIL**
+

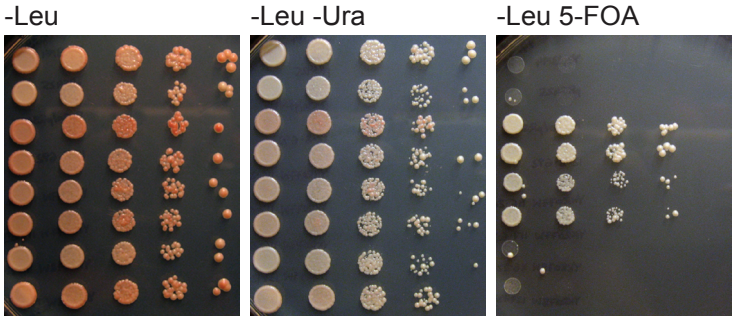

B

cac1Δ
hmr*::*ADE2
***URA3*-VIIL**
+

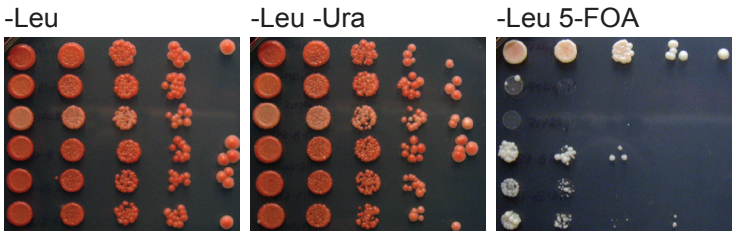

C

pol30-8
hmr*::*ADE2
***URA3*-VIIL**
+

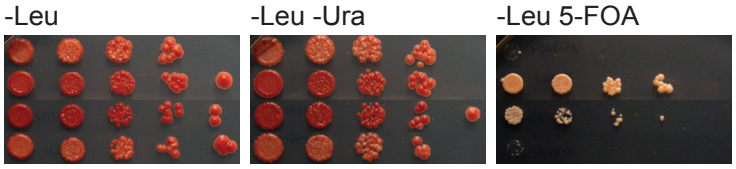

D

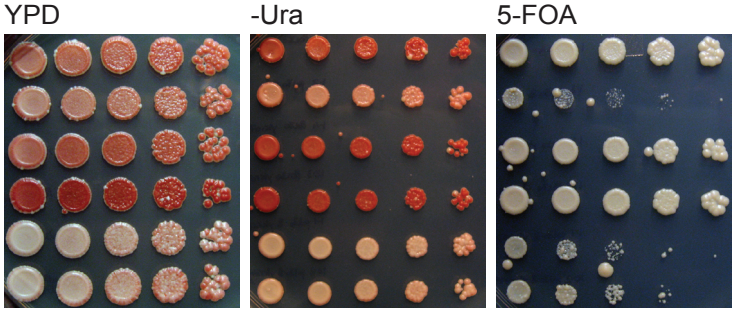

a complex with Cac1 and requires Cac1 for its suppressive effect on 5-FOA sensitivity in the *pol30-8 URA3*-VIIL mutant.

It is unlikely that the suppressive effect of *MSA2* overexpression is caused by titrating away binding sites for MBF (MCB) and SBF (SCB) that are present in the *MSA2* promoter, since overexpression of just arrays of either four MCBs or four SCBs did not suppress *pol30-8 URA3*-VIIL 5-FOA sensitivity (data not shown). Msa1, a homolog of Msa2 that was identified in the same mass spectrometry approach as Msa2, shares 28 % amino acid identity and 43 % similarity to *MSA2* (Ashe et al., 2008). However, overexpression of *MSA1* was not able to suppress *pol30-8 URA3*-VIIL 5-FOA sensitivity (Figure 30C). While deletion of *MSA2* did not lead to an alteration of *hmr*::*ADE2* expression or sensitivity to 5-FOA in the context of *URA3*-VIIL, spores carrying both, *msa2Δ* and *pol30-8* were more defective in repressing *hmr*::*ADE2* than either mutation alone, resulting in very light pink colored colonies (Figure 30D). However, 5-FOA sensitivity was not altered (Figure 30D). Thus, albeit this phenotype is not very strong, it suggests a genetic interaction of *MSA2* with the *POL30*/CAF-1 pathway outside of 5-FOA metabolism.

CRT1

RFX1 or *CRT1* (*C*onstitutive *R*NR *T*ranscription, the latter name is used throughout this work) is a negative regulator of DNA damage inducibility (Zhou and Elledge, 1992). Based on its homology to the mammalian RFX family of DNA-binding proteins, it was found to bind to a conserved 13-nucleotide long

motif (X box) in the *RNR2* and *RNR3* promoters of as well as its own promoter. Repression of Crt1 target genes in undamaged cells is achieved by recruiting the products of two other CRT genes, the global Tup1-Ssn6 co-repressor complex, via a direct interaction with Ssn6 (Huang et al., 1998). In a previous study, *CRT1* overexpression did not suppress 5-FOA sensitivity of a *cac1Δ URA3*-VIIL strain (Sharp et al., 2005). While there was variability in its suppressive effect also in my experiments, I found 5-FOA sensitivity of *pol30-8 URA3*-VIIL cells to be suppressed by only 100-fold by *CRT1* when overexpressed under its own promoter (either 831 or 1473 bp upstream regulatory region) in comparison to empty vector (Figure 31A). This comparatively weak effect is in agreement with it being downstream of *RAD53* and *DUN1* within the DNA damage checkpoint pathway (compare with Figures 23A and 23B). Overexpression of *TUP1*, *SSN6* or *HDA1* did not suppress 5-FOA sensitivity of *pol30-8 URA3*-VIIL cells (data not shown). Of note, a role for Hda1 in mediating Tup1-dependent repression has also previously been debated (Davie et al., 2003; Green and Johnson, 2004; Wu et al., 2001; Zhang and Reese, 2004). Surprisingly, deletion of *TUP1* rescued the 5-FOA sensitivity of *pol30-8 URA3*-VIIL cells by 100-fold (Figure 31B). These results are in contrast to the effect produced by *CRT1* overexpression and might be due to the general growth defect in *tup1Δ* cells (Laman et al., 1995). Alternatively, they might point to a more complex role of Tup1-Ssn6 as a transcriptional repressor and activator (Proft and Struhl, 2002).

Figure 31: The role of additional confirmed high-copy suppressors of the 5-FOA sensitivity phenotype of *pol30-8*: *CRT1*.

(A) 10-fold serial dilution of a *pol30-8 hmr*::*ADE2 URA3*-VIIL strain (MRY0828) transformed with *POL30*/pR425, YEp13M4, pRS425, genomic *CRT1* and cloned *CRT1* with either a shorter (831 bp) or a longer (1473 bp) promoter. #1 and #2 indicate independent transformants.

(B) 10-fold serial dilution of *pol30-8 ppr1Δ* (MRY0180), *pol30-8 ppr1Δ tup1Δ* (MRY0788), *ppr1Δ* (MRY0191), *ppr1Δ tup1Δ* (MRY0792, 0793), *pol30-8* (MRY0041) and *pol30-8 tup1Δ* (MRY0798, 0797) *hmr*::*ADE2 URA3*-VIIL strains. #1 and #2 indicate independent isogenic strains.

A

pol30-8
hmr*::*ADE2
***URA3*-VIIL**
+

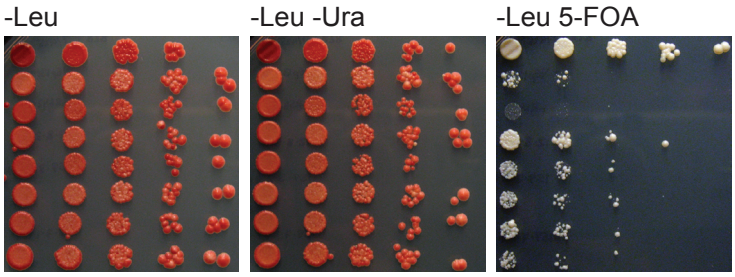

POL30 library vector
cloning vector
library *CRT1*
cloned *CRT1* short #1
cloned *CRT1* short #2
cloned *CRT1* long #2
cloned *CRT1* long #2

B

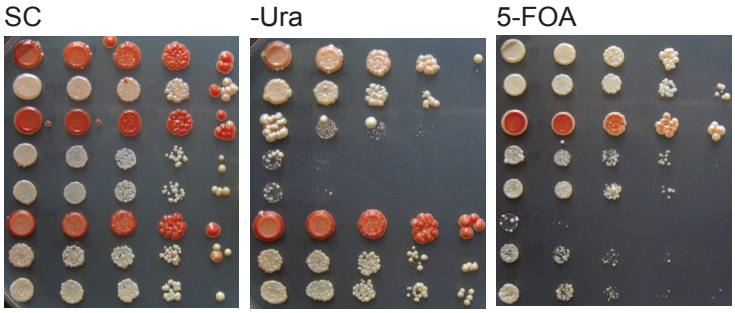

pol30-8 ppr1Δ
pol30-8 ppr1Δ tup1Δ
ppr1Δ
ppr1Δ tup1Δ #1
ppr1Δ tup1Δ #2
pol30-8
pol30-8 tup1Δ #1
pol30-8 tup1Δ #2

UBS1

Ubiquitin (Ub)-conjugating enzyme suppressor 1 (*UBS1*) was identified as a high copy suppressor of the growth defect of an allele of the G1-cell cycle stage-specific Ub-conjugating enzyme *CDC34*. Overexpression of *UBS1* not only suppresses the cell cycle defect of *cdc34-2* mutants at the restrictive temperature, but also can partially restore the degradation of the Cdc34 target Gcn4, a transcriptional activator for genes involved in amino acid biosynthesis (Prendergast et al., 1996). *UBS1* overexpression only suppressed the *pol30-8 URA3*-VIIL 5-FOA sensitivity by 100-fold (Figure 32A). A similar small and variable effect was seen when in the place of *pol30-8* the mutant *pol30-8-K164R*, which prevents this residue from ubiquitylation or sumoylation, was expressed (Figure 32B). When encountering DNA lesions during DNA replication, Pol30 can be either mono- or polyubiquitylated at this residue which triggers the error-prone translesion synthesis pathway or the error-free bypass pathway, respectively (Hoege et al., 2002). Moreover, sumoylation of the same residue in an unperturbed S phase prevents deleterious recombination through interaction of the anti-recombinogenic helicase Srs2 with Pol30 (Papouli et al., 2005; Pfander et al., 2005). However, while a small effect of *UBS1* on 5-FOA sensitivity in *pol30-8 URA3*-VIIL cells was reproducible, it was not robust enough to warrant further investigation.

Figure 32: The role of additional confirmed high-copy suppressors of the 5-FOA sensitivity phenotype of *pol30-8*: *UBS1*.

(A) 10-fold serial dilution of a *pol30-8 hmr*::*ADE2 URA3*-VIIL strain (MRY0041) transformed with *POL30*/YEp213, *POL30*/pR425, pRS425, genomic *ARL1* and the neighboring ORF *UBS1*, cloned *ARL1* and cloned *UBS1*. #1 and #2 indicate independent transformants.

(B) 10-fold serial dilution of a *pol30Δ hmr*::*ADE2 URA3*-VIIL strain carrying *pol30-8*/pRS314 (MRY0036) transformed with *pol30-8*, *POL30*, *pol30-K127R*, *pol30-K164R*, *pol30-K127/164R*, *pol30-8-K127R*, *pol30-8-K164R*, *pol30-8-K127/164R*, all in pRS415, after plasmid shuffle to eliminate *pol30-8*/pRS314.

A

pol30-8
hmr*::*ADE2
***URA3*-VIIL**
+

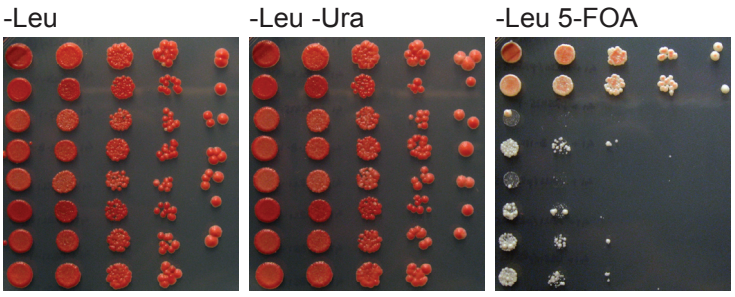

POL30/YEp213
POL30/cloning vector
cloning vector
library *ARL1-UBS1*
cloned *ARL1* #1
cloned *ARL1* #2
cloned *UBS1* #1
cloned *UBS1* #2

B

pol30Δ
hmr*::*ADE2
***URA3*-VIIL**
+

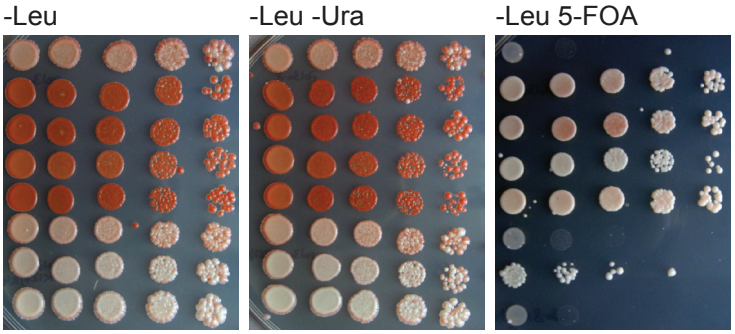

pol30-8
POL30
pol30-K127R
pol30-K164R
pol30-K127/164R
pol30-8-K127R
pol30-8-K164R
pol30-8-K127/164R

3. DISCUSSION

Epigenetically heritable gene expression states of the cell are an important component of development and disease. There are examples for developmental and disease states being associated with particular chromatin signatures, but it is not clear whether these chromatin signatures are heritable through cell division or re-established after mitosis (Kaufman and Rando, 2010; Ptashne, 2007). The use of *S. cerevisiae* as a genetic model organism has greatly advanced our understanding of the factors and molecular mechanisms involved in the formation, maintenance and inheritance of distinct (mostly silent) chromatin states. These processes include specific roles for DNA replication as well as histone modifying enzymes. However, in the study of telomeric heterochromatin formation and maintenance, research has mostly focused on truncated telomeres with the majority of studies employing *URA3* as a reporter gene because of its amenability to counter-selection. This dissertation work reveals the surprising finding that for two different mutants, *pol30-8*, encoding an allele of PCNA, an essential and central protein in DNA replication, and *dot1Δ*, lacking the only histone H3K79 methyltransferase, their previously demonstrated direct roles in heterochromatin formation and maintenance at telomeres do not withstand more detailed analysis, because the results are influenced by the assay employed.

pol30-8, the DNA damage response and 5-FOA sensitivity

How the *pol30-8* mutation affects heterochromatin distinctly and differently from euchromatin, has not been clear. The microarray data I obtained demonstrated that *pol30-8* cells globally up-regulate expression of genes that are normally poorly expressed, including, but not biased, to those located at telomeres. This phenotype stands in contrast to the pronounced 5-FOA sensitivity of *pol30-8* cells that harbor the *URA3*-VIIL gene. This study attributes the increased 5-FOA sensitivity of *pol30-8 URA3*-VIIL cells to a combination of low histone occupancy throughout the genome, which leads to an increased transcription of RNR genes as downstream targets of the DNA damage response and in turn an altered 5-FOA metabolism, as well as a specific up-regulation of *URA3* transcription. I conclude that the *URA3*-VIIL reporter does not reflect heterochromatin formation and that it is not possible to infer from studies using *URA3*-VIIL that PCNA has a role in telomeric heterochromatin formation.

It has previously been demonstrated that treatment of wild-type cells with the DSB-inducing HO endonuclease causes SIR proteins to relocalize from telomeres to the site of DNA damage (Martin et al., 1999; Mills et al., 1999). In this setting, Sir3/Sir4 occupancy at telomere VI-R was reduced by 2-fold (Martin et al., 1999). A very similar redistribution of SIR proteins was reported in *cac1Δ* mutants at the same telomere (Tamburini et al., 2006). *pol30-8* as well as *cac1Δ* mutants show increased sensitivity to DNA damaging agents as well as (to a lesser extent) UV treatment while no growth defect and - for *pol30-8* - no reduced

interaction with RFC or DNA polymerase δ could be detected (Ayyagari et al., 1995; Linger and Tyler, 2005). In light of the seemingly unaffected DNA replication, an impairment of specific interactions with DNA repair proteins in these mutants was suggested (Ayyagari et al., 1995). Pol30-8 was shown to have reduced interaction with Cac1 *in vitro*, and chromatin-bound Cac1 levels were reduced in this PCNA mutant background (Zhang et al., 2000). Thus, while we cannot exclude a subtle DNA repair defect in *pol30-8* cells, activation of downstream targets of the DNA damage response might occur via a reduction in global histone density due to a defect in recruiting the CAF-1 complex to chromatin.

What could be the molecular basis of the inappropriate activation of DNA damage response genes? Tup1 is a component of the transcriptional co-repressor complex Tup1-Ssn6 and binds to histone H3 and H4 N-terminal tails *in vitro* (Edmondson et al., 1996). Combined mutation and truncation of H3 and H4 tails was shown to derepress several genes regulated by the Tup1-Ssn6 complex, including an *RNR2*-LacZ reporter by 9-fold (Edmondson et al., 1996; Huang et al., 1997). Thus, reduced histone density could lead to less binding of the Tup1-Ssn6 complex, leading to derepression of target genes such as *RNR2*, *RNR3* and *RNR4*. Indeed, I observed a 7.5- and 4.3-fold reduced Ssn6 occupancy at the promoters of *RNR2* and *RNR4* in *pol30-8* cells, respectively. In another study, Wyrick and colleagues (1999) studied the global effects of nucleosome depletion by a galactose-glucose shut-off experiment with cells that carried just one histone H4 copy. While 75 % of the genes were unaffected after

6 h of histone H4 depletion, 15 % showed more than 3-fold up-regulation. While the comparison of our data set with that of Wyrick and colleagues has not yet been completed, I noticed that out of the top 31 up-regulated genes in *pol30-8*, 17 were also up-regulated after 6 h of histone H4 depletion (this study and Wyrick et al., 1999). With respect to telomeres, I observed that not only telomeric *HIS3* but also *URA3* transcription was up-regulated by MMS treatment in wild-type cells. This is in contrast to what has been observed for endogenous *URA3* (Jelinsky et al., 2000). Thus, telomeric genes are prone to be transcriptionally activated by DNA damage, and this tendency is further exacerbated in mutants with an even slightly activated DNA damage response.

However, 5-FOA sensitivity is not only a read-out for transcription at *URA3*-VIIL as a consequence of an activated DNA damage checkpoint, but also influenced by processes involved in metabolism of the drug. The latter in turn are intricately intertwined with the DNA damage response pathway through RNR activity. My data show that down-regulation of the increased RNR levels, either genetically or by hydroxyurea, could suppress the 5-FOA sensitivity of *pol30-8* and *cac1Δ URA3*-VIIL mutants, revealing an important link between RNR activity and 5-FOA metabolism. Interestingly, these findings are paralleled by studies of human colorectal xenografts in mice in which resistance to 5-fluorouracil (5-FU), which like 5-FOA is converted to the toxic 5-FUMP, is accompanied by an almost 5-fold reduced RNR activity (Fukushima et al., 2001). 5-FU is a prodrug with widespread use in head and neck, breast and colon cancer, the latter of which it affects the strongest (IMPACT investigators, 1995).

It is intriguing that RNR can be induced by 5-FOA treatment in wild-type cells, similarly to 4-NQO and MMS treatment. It was previously reported that in approximately 50 % of a wild-type cell population the *URA3*-VIIL gene was repressed (Aparicio et al., 1991; Enomoto et al., 1997). This “repression” was determined by measuring the cells’ resistance to 5-FOA. Hence, up-regulated RNR could be a reason for at least a fraction of wild-type cells being sensitive to 5-FOA.

A question for further investigation would be whether the elevated RNR transcription in 5-FOA treated cells reflects a general DNA damage response. DNA damage induced by 5-FU in human cells is thought to occur either as a consequence of the incorporation of the deoxyribonucleotide analogue 5-FdUTP into DNA or by inhibition of thymidylate synthase leading to imbalanced dNTP pools. dNTP imbalances in turn cause misincorporation of dATP, dCTP, dTTP (or dUTP instead) and dGTP into DNA due to reduced fidelity of DNA polymerases (Echols and Goodman, 1991) and thus replication fork stalling. Therefore it is difficult to distinguish a DNA damage effect from an acute effect on RNR in these experiments. To my knowledge, 5-FOA effects have not been examined in microarray studies. However, 5-FU has been studied in its effects on gene expression in cancer cells, specifically breast cancer cell lines of luminal or basal origin (Maxwell et al., 2003; Troester et al., 2004; Tsao et al., 2010) and cultured primary breast cancer cells (Tsao et al., 2010). While two of these studies found genes of the DNA damage response, including the p53-regulated gene

p21$^{WAF1/CIP1}$, which acts as an inhibitor of PCNA, as well as GADD45, up-regulated, RNR gene expression was not elevated (Troester et al., 2004).

Although it has not been formally tested, I expect that the induction of RNR upon addition of 5-FOA is dependent on the Rad53-Dun1-Crt1 pathway. Mutation or deletion of *RAD53* and *DUN1*, respectively, and overexpression of *CRT1* was able to rescue the 5-FOA sensitivity of the *pol30-8 URA3*-VIIL strain. The decrease in potency of the more "downstream" components of the DNA damage response pathway might correlate with their effect on RNR transcription. In Northern blots Huang and Elledge (1997) showed that induction of *RNR4* transcription was severely impeded in *rad53-1* cells compared to wild-type cells upon treatment with hydroxyurea or MMS (91 % reduction). In comparison, *dun1Δ* mutants could still induce *RNR4* transcription quite well (52 % reduction). These results are supported by genome-wide expression data by Gasch and colleagues (2001) who found higher induction of *RNR2* and *RNR4* in *dun1Δ* compared to *mec1Δ* mutant strains. Interestingly, in the same study, deletion of *CRT1* did not result in an induction of many genes that were *MEC1*/*DUN1*-dependent with the exception of *RNR2* and *RNR4* (Gasch et al., 2001). However, only genes induced more than 2-fold were considered in this study. While the number of common targets between *MEC1* and *CRT1* might be larger when considering a lower cutoff value (Zaim et al., 2005), this could mean that either the role of *CRT1* is only revealed under DNA damage conditions or, alternatively, that it might have other upstream regulators. One could also postulate that

overexpression of *CRT1* might target the protein to other promoters than just those of DNA damage inducible genes.

Sharp et al. (2005) suggested that the DNA checkpoint pathway contributes to telomeric heterochromatin formation even in the absence of exogenous DNA damage by controlling the sequestration of Asf1 in the Rad53-Asf1 complex. However, my work suggests that the role that these proteins play in telomeric heterochromatin formation needs to be revisited. Nevertheless, 5-FOA sensitivity might still be a useful assay to monitor the contribution of the DNA damage checkpoint pathway to RNR transcription. However, post-transcriptional modification of RNR protein activity might not influence 5-FOA sensitivity in the context of *URA3*-VIIL. For instance, deletion of the RNR protein inhibitor *SML1* leads to an approximately 2.5-fold increase in dNTP levels (Chabes et al., 1999; Zhao et al., 1998). In the context of *URA3*-VIIL, however, deletion of *SML1* alone or in combination with *rad53*, *mec1*, *cac1Δ* or *pol30-8* mutants did not change 5-FOA sensitivity (Longhese et al., 2000; Sharp et al., 2005 and data not shown), and also overexpression of *SML1* did not suppress *pol30-8 URA3*-VIIL 5-FOA sensitivity (data not shown).

An alternative explanation for the lack of a *SML1* effect could be the presence of a paralog of *SML1*, *DIF1*, derived from an ancestral gene duplication event (Lee et al., 2008). Dif1 also has a Sml domain and, like Sml1, is a direct substrate of the Dun1 kinase. Thus, Dif1 might compensate for a lack of Sml1 function in the context of 5-FOA sensitivity of *URA3*-VIIL strains.

Interestingly, Dif1 binds to the Rnr2-Rnr4 R2 subunit and facilitates its nuclear transport in the absence of DNA damage (Lee et al., 2008), preventing it from forming an active RNR complex with the R1 subunit in the cytoplasm. Rnr2 and Rnr4, normally anchored in the nucleus by Wtm1 (Lee and Elledge, 2006), can also shuttle out of the nucleus (Yao et al., 2003) and they do so increasingly upon DNA damage. Of note, Asf1 not only associates with Rad53 and Hir3 but also with Rnr2 and Rnr4 (Gavin et al., 2002). In summary, altered localization of Rnr2/4 in the cell might be of additional importance for 5-FOA sensitivity of *URA3*-VIIL strains and might explain why only a subtle elevation of RNR in *pol30-8* cells has a large effect on cell growth in the presence of this drug.

Why does *asf1Δ* rescue 5-FOA sensitivity of *dot1Δ* but not *pol30-8 URA3*-VIIL cells? On one hand, *asf1Δ* results in reduced induction of RNR in presence of DNA damage. On the other hand, Asf1 influences nucleosome density, since the latter was slightly reduced (on centromeric plasmids) in *asf1Δ* mutants as indicated by loss of negative supercoiling (Prado et al., 2004). More importantly, Asf1/H3/H4 complexes have been shown to stimulate chromatin assembly in the presence of PCNA-binding defective CAF-1 mutants (Krawitz et al., 2002). In the absence of Pol30/CAF-1-mediated chromatin assembly Asf1 might therefore still replace some CAF-1 function. Thus, in *asf1Δ pol30-8 URA3*-VIIL mutants, the lack of Asf1 might lead to very low global histone occupancy at promoters, likely outweighing the positive effect of reduced RNR levels.

Is the *HM* phenotype of *pol30-8* cells due to a silencing defect?

Does the previously reported pink-white sectoring phenotype (Zhang et al., 2000) reflect an epigenetic heterochromatin silencing defect and do *pol30-8* mutants have a heterochromatin silencing defect at *HM* loci?

Epigenetic inheritance at the replication fork

Unstable inheritance of transcriptional expression states has been previously reported, both at the *HML* (Mahoney et al., 1991; Pillus and Rine, 1989) and the *HMR* locus (Sussel et al., 1993), yet without a detailed molecular mechanism as to how they occur. Epigenetic states could be inherited through a self-perpetuating cycle of chromatin modification, in which an inherited mark such as histone H4K16 hypoacetylation on one or both strands of the DNA recruits enzymes that make additional marks in conjunction with DNA replication. This could then be coupled to a chromatin assembly process which distinguishes between specific histone marks in certain chromosomal regions. Marks like acetylation of histone H3K56 generated by Rtt109/Asf1 indeed greatly stimulate chromatin assembly activity of the replication-dependent histone chaperones CAF-1 and Rtt106 (Han et al., 2007; Li et al., 2008; Recht et al., 2006; Tsubota et al., 2007). Several lines of evidence, however, argue for the existence of mechanisms that are active throughout the cell cycle to perpetuate chromatin states. Early experiments analyzing chromatin in CsCl density gradients indicated a random distribution of nucleosomes onto replicated daughter strands (Jackson and Chalkley, 1985; Jackson et al., 1975). Also, Deal and colleagues

(2010) recently showed by biotin-coupled metabolic labeling of H3-H4 tetramers in *D. melanogaster* S2 cells that the mean lifetime of nucleosomes on chromatin is approximately 1.5 h at sites of repressive H3K27 methylation while this cell line has a doubling time of 40 h (Ceriani, 2007). These results argue against DNA replication to be the sole process required for the inheritance of active and repressed chromatin.

The *HM* phenotype of *pol30-8* cells

Neither *pol30-8* nor *cac1Δ* mutants have a mating defect (Huang et al., 2005; Sharp et al., 2001) which indicates wild-type levels of *HML* repression. Moreover, *TRP1* in *pol30-8 hmrΔa*::*TRP1* strains was silenced as well as in corresponding wild-type strains (data not shown). In strains carrying GFP at *hmr* under the control of the *URA3* promoter, *cac1Δ* cells were completely repressed (Huang et al., 2005 and data not shown), while two populations could be observed for *sir1Δ*, roughly in the same distribution as previously observed in the "shmoo-farming" experiment by Pillus and Rine (1989). *sir3Δ* mutants completely derepressed *hmr*::GFP (data not shown). A cold-sensitive mutation in *POL30*, *pol30-52*, is defective in DNA replication *in vitro* and the resulting protein exists as a monomer in solution (Ayyagari et al., 1995). This allele and those of some other genes with a role in DNA replication tested in this assay were shown to increase silencing of a modified and thus derepressed *HMR*-E silencer, *HMR***a**-*e***, with mutated binding sites for Abf1 and Rap1, leaving only the ACS as a functional silencer region (Ehrenhofer-Murray et al., 1999). Although no specific

mechanism of how these mutations might achieve repression could be elucidated, the authors argued against an indirect effect of slowing down the cell cycle, because only some DNA replication mutants had these repressing abilities. Therefore they favored a model in which these specific DNA replication proteins would interact with heterochromatin assembly proteins. An alternative possibility would be, however, that the identified factors could be rate-limiting for the processivity of DNA replication. A slowed-down DNA replication would not only be conceivable for *pol30-52* but also for the rate-limiting factor *CDC45* (Broderick and Nasheuer, 2009). A mutant of *CDC45*, *cdc45-1*, was identified in the *HMR***a**-*e*** screen, however, no mutants for the seven genes encoding the MCM complex, which genetically and physically interacts with Cdc45, were uncovered in the screen (Moir et al., 1982; Zou and Stillman, 2000).

A combination of *pol30* alleles 8 and 79 to create the *pol30-879* allele, while by itself not mating-defective, exhibited synergistic loss in shmoo formation when combined with a deletion of *SAS2* (17 % in *pol30-879 sas2Δ* compared to 66.3 % in *sas2Δ*; Huang et al., 2005). *SAS2* encodes the acetyltransferase responsible for creating the histone H4K16 acetyl mark that is removed by Sir2 (Suka et al., 2002). A mutant of *SAS2* was originally identified in the same *HMR***a**-*e*** screen discussed above (Axelrod and Rine, 1991; Ehrenhofer-Murray et al., 1997). Surprisingly, deletion of *SAS2* also causes pronounced 5-FOA sensitivity in the context of *URA3*-VIIL. This would be not expected for the loss of a histone acetyltransferase in context of SIR-dependent silencing and suggests

that, as for *pol30-8* and *dot1Δ* mutants, for *sas2Δ* mutants the 5-FOA assay might not report heterochromatin formation.

Why are *pol30-8 hmr*::*ADE2* mutants showing a pink-white sectored phenotype? The microarray analysis might hint at a potential reason. Apart from up-regulated genes that are normally repressed by the Tup1-Ssn6 co-repressor complex another group of up-regulated genes is the target of Sum1. *SUM1* represses middle-sporulation specific genes during the budding yeast mitotic life cycle (Xie et al., 1999). Of the 162 genes derepressed in *sum1Δ* (Andrew Vershon, personal communication; Pierce et al., 2003), I found 128 to be also up-regulated in *pol30-8* cells. This might be not surprising, since in general those genes are expressed at low levels in wild-type cells and thus may be sensitive to up-regulation in *pol30-8* cells due to lower histone density along their sequences. However, *SUM1* has been ascribed a function also in silencing *HM* loci. An allele of *SUM1*, *sum1-1*, is thought to be recruited to the *HMR*-E and *HMR*-I ACS due to an increased affinity for ORC, which in turn induces it to spread along these loci in a Hst1-dependent manner (Lynch et al., 2005; Rusche and Rine, 2001; Sutton et al., 2001). Moreover, deletion of *SUM1*, while exhibiting no or only a mild effect on 5-FOA sensitivity of a *URA3*-VIIL strain (Chi and Shore, 1996 and data not shown), shows a pink-white sectoring phenotype at *hmr*::*ADE2* which looks very similar to that of *pol30-8 hmr*::*ADE2* and *sum1Δ pol30-8 hmr*::*ADE2* double mutant colonies (data not shown). Interestingly, Sum1 could not be located to the silencers at *HM* loci (Dr. Laura Rusché, personal communication; Rusche and Rine, 2001) and *sum1Δ* mutants mate normally. Thus, one might

speculate that it is the derepressed transcription of *ADE2* rather than some action at the silencers that causes the *sum1Δ* sectoring phenotype.

Dot1 has no role in telomeric silencing

Two lines of evidence speak against a role for Dot1 in telomeric silencing. Initial genetic experiments employing telomere VII-L pointed to the specific up-regulation of *URA3* expression at the truncated telomere VII-L in *dot1Δ* mutants. However, an unbiased microarray analysis surveying the genome for gene expression changes in *dot1Δ URA3*-VIIL cells revealed that the lack of the only histone H3K79 methyltransferase in yeast is associated with very few gene expression changes on a global level. We surveyed 125 telomeric genes and found that most were mildly down-regulated with respect to wild type. Interestingly, expression of the artificial *adh4*::*URA3* locus at telomere VII-L was elevated the highest.

It was suggested that Dot1 preferably methylates histone H3K79 residues in euchromatin, thereby preventing SIR proteins which are limiting in the cell from binding promiscuously throughout chromatin and confining them to telomeres (van Leeuwen et al., 2002; van Welsem et al., 2008). For the majority of the genome, a mutual exclusiveness of histone H3K79 di- and trimethylation has been reported, the former of which has been correlated with low gene expression (Schulze et al., 2009). This especially pertains to genes regulating the G1/S transition (Pokholok et al., 2005; Schulze et al., 2009). Regarding telomere VI-R, I observed a drop in histone H3K79 trimethylation between 7 kb and 600 bp from

the telomere (data not shown) as previously also reported for histone H3K79 dimethylation (Ng et al., 2002). Hence, assuming an equal accessibility of the H3K79 di- and trimethyl antibodies to the respective residues within telomeric heterochromatin, telomeric nucleosomes indeed seem to be less accessible for Dot1. Interestingly, *DOT1* overexpression in wild-type cells resulted in 98 % of all H3K79 being methylated with 90 % of those showing trimethylation (van Leeuwen et al., 2002). These cells displayed a telomeric silencing phenotype at *URA3*-VIIL which was dependent on the methyltransferase activity of Dot1. In light of the data presented here, this trimethylation activity of Dot1 must be directly or indirectly responsible for the transcriptional repression of the *adh4*::*URA3* locus. Of note, the truncated C-terminal fragment of *ADH4* at the *adh4*::*URA3*-VIIL locus contains an ATG with a potential TATA box lent by the *URA3* promoter that allows for a 120-aa long protein to be synthesized until its natural stop codon. *ADH4* expression is up-regulated by *ZAP1*, a Zinc-responsive transcription factor (Lyons et al., 2000; Yuan, 2000). However, amongst the few up-regulated genes in *dot1Δ* cells I could not find any other genes known to be controlled by *ZAP1*. The specific context of *URA3* adjacent to the 5' end of the truncated *ADH4* gene at telomere VII-L must be important for the transcriptional up-reguation of *URA3* as well, since a *dot1Δ HMR*::*URA3* strain shows wild-type levels of 5-FOA resistance (Osborne et al., 2009).

In my own experiments with an antibody against Dot1 from the Gottschling laboratory (van Leeuwen et al., 2002), I could observe two isoforms of Dot1, one of which was not detectable when carrying a 9xMyc-tag at its N-terminus (data

not shown). Recently, two isoforms of Dot1 were reported due to leaky scanning by the ribosome (Frederiks et al., 2009). While both isoforms rescued 5-FOA sensitivity as well as lack of histone H3K79 methylation in *dot1Δ* cells to the same extent, the long Dot1 isoform was implicated in cell wall metabolism, mediated through its N-terminal 16 amino acids (Frederiks et al., 2009). Overexpression of the *D. melanogaster* homologue of *DOT1*, *grappa*, caused adult flies to become more resistant to oxidative or caloric stress, although no induction of genes in these pathways could be detected (List et al., 2009). Together, these two studies hint towards more complex roles of Dot1. Future studies will be needed to determine whether and how exactly *ADH4* expression is linked to *DOT1*.

What about the role of Dot1 in silencing of the *HM* loci? Even if assuming that an "all-or-none" process of transcriptional activation determines the accumulation of red pigment or its absence, it is difficult to explain the difference between *dot1Δ* and *sir3Δ* cells, whose *hmr*::*ADE2* phenotypes are similar but different from the one observed in *pol30-8* cells. Furthermore, *dot1Δ* cells of either mating type mated normally (San-Segundo and Roeder, 2000; van Welsem et al., 2008 and data not shown). In a pedigree assay assessing the establishment of a silenced state in single cells twice as many cells deleted for *DOT1* established silencing at *HML*α within one cell division compared to wild-type cells (Osborne et al., 2009). However, a specific transcriptional up-regulation of *hmr*::*ADE2* in *dot1Δ* cells is supported by the observation that

deletion of the transcriptional activators of *ADE2*, *BAS1* and *PHO2* can increase 5-FOA sensitivity in *dot1Δ URA3*-VIIL strains. Bas1 and Pho2 are required for all ten steps of inosine monophosphate (IMP) *de novo* synthesis and the two steps of its conversion to adenosine monophosphate (AMP), and it is thought that Bas1 recruits Pho2 to the promoters of the relevant genes (Denis et al., 1998; Som et al., 2005). Moreover, intermediates from the IMP synthesis pathway, such as phosphoribosylaminoimidazole carboxamide (AICAR) and succinyl-AICAR (SAICAR) likely modulate transcriptional activity of Bas1 and Pho2 (Pinson et al., 2009). Interestingly, the purine synthesis pathway is co-regulated with the histidine synthesis pathway by these transcription factors. This co-regulation could be observed in my experiments using a *HIS3*-VIIL reporter strain on 3-AT-containing media. The more severely the strain was impaired in its ability to express *HIS3*-VIIL, the whiter it became, possibly due to an inability to sufficiently activate transcription of the genes whose products produce precursors upstream of the “Ade2-1 step” (these strains did not carry *hmr*::*ADE2*). In this light, multiple other targets of Bas1 and/or Pho2 have been identified (Denis et al., 1998; Denis and Daignan-Fornier, 1998). One example is *PHO5* which is derepressed by the action of Pho2 in conjunction with Pho4, and, interestingly, nucleosome disassembly by Asf1 is required for its activation (Adkins et al., 2004; Kramer and Andersen, 1980). Thus, it might be that the nucleosome disassembly rather than chromatin assembly activity of Asf1 is relevant for its synthetic genetic phenotype with *pol30-8* at *hmr*::*ADE2*.

Repression of *URA3* transcription was predominantly seen in *bas1Δ* or *pho2Δ* single mutants under conditions of adenine starvation (Denis et al., 1998). All 5-FOA sensitivity assays in this work were done with medium containing 20 mg/l adenine which is not a limiting concentration. Thus, either “starvation” is defined by increased transcription of *ADE2* for any reason, or *dot1Δ* cells, like *ard1Δ* cells, are under some sort of metabolic constraint requiring the increased transcription of *hmr*::*ADE2*. I conclude that for the investigation of these phenotypes the present strain background W303 is not suitable for further studies since it carries mutations in genes required for purine, pyrimidine and amino acid biosynthesis.

PPR1

POL30 was able to suppress the elevated *URA3*-VIIL expression levels in the *pol30-8* mutant although it conferred resistance to 5-FOA. Moreover, overexpression of *PPR1*, the trans-activator of *URA3*, was not able to overcome *URA3*-VIIL repression by *POL30* overexpression. Thus, *POL30*, which recently has been found to interact with the Elp3 transcriptional elongator complex (Li et al., 2009), might have a specialized role in *URA3* transcription which directly intersects with that of *PPR1*. The role of *PPR1* in trans-activating *URA3*-VIIL within the chromatin context is not clear. While it was essential for *URA3* expression at telomere VII-L, it was generally not required when *URA3* was placed at native telomeres (Pryde and Louis, 1999) or within *HMR* heterochromatin (Lin et al., 2008). Of note, as described for the purine pathway,

the pyrimidine synthesis pathway also has metabolic intermediates that function as transcriptional co-factors: pyrimidine starvation leads to intracellular accumulation of dihydroorotic acid (DHO) above a threshold which results in 3- to 5-fold transcriptional activation of *URA3* (Losson and Lacroute, 1983). Ppr1 function requires cells to go through S phase, and possibly DNA replication (Aparicio and Gottschling, 1994) or a related process such as replication induced damage. Intriguingly, I found promoter occupancy of Ssn6 at the *RNR2* and *RNR4* genes to be reduced in *ppr1Δ* cells. Together with the observation that *ppr1Δ* is synthetically sick or lethal with *rtt109Δ* (Fillingham et al., 2008; Lin et al., 2008) this suggests an involvement of *PPR1* in the DNA damage response. Although I could not see that *ppr1Δ* differs from wild-type cells with respect to *RNR2* or *RNR4* levels (data not shown), I observed specific cleavage products of Ppr1-13Myc upon DNA damage and in *pol30-8* or *asf1Δ* cells. This suggests that the genetic interaction between *ASF1*, which functions together with *RTT109* (Recht et al., 2006; Tsubota et al., 2007), and the PCNA/CAF-1 pathway with *PPR1* might also be relevant in the context of the DNA damage response.

Cdc21 and telomeric silencing

In the *URA3*-VIIL system, there are likely two related reasons why *CDC21* overexpression increases 5-FOA resistance: (1) its role in the DNA damage response in a pathway distinct from the one mediated by *DUN1* and (2) the covalent binding of 5-FdUMP to Cdc21. *CDC21* overexpression on a 2-µm plasmid did not result in resistance to 5-FOA of a strain carrying endogenous

URA3. Hence, the suppressive function of *CDC21* only reveals itself in the context of low levels of *URA3* transcription (as in *URA3*-VIIL) when even slightly elevated RNR levels in *pol30-8* cells might lead to a shift from a 5-FUDP incorporation into RNA to its reduction to 5-FdUDP (Figure 26A). On the other hand, *CDC21* has been initially identified in a screen for factors that bring about constitutive *RNR3* transcription (Zhou and Elledge, 1992) and might act upstream of *dun1Δ* (Figure 2; Huang et al., 1998). We noticed that *CDC21* overexpression was able to slightly decrease 5-FOA sensitivity in wild-type *URA3*-VIIL strains treated with DNA damaging agents (as well as reduce *HIS3*-VIIL expression in wild-type cells by 2-fold). These effects might reflect its true contribution within the DNA damage response. Thus, the effects of *CDC21* on 5-FOA sensitivity might be the sum of its involvement in DNA damage and 5-FOA metabolism.

A previous study identified two ts alleles of the *S. pombe* homologue of thymidylate synthase, *tds1*, in a screen for heterochromatin spreading beyond the silent mating type *mat2,3* boundaries and thus repression of the marker genes *ade6* and *ura4* (Singh and Klar, 2008). As discussed above for the DNA replication mutants *pol30-52* and *cdc45-1*, the effect could be indirect since the two *tds1* alleles have growth defects and arrest at the G1-S transition at the restrictive temperature. Slower progression through S phase has been found to increase repression of a silencing-defective *HMR* locus in *rap1* mutants in budding yeast (Laman et al., 1995). It has been speculated that this will allow

cells more time to establish a silenced state, although this question has not yet been resolved (Osborne et al., 2009).

Why does Cdc21 only have a mild impact on dNTP levels? The catalytic activity of Cdc21 depends on the amount of the substrate, dUMP. dUMP in turn will be supplied by RNR and by dCMP deaminase, which are both allosterically inhibited by dTTP (Kunz et al., 1994). On the other hand, higher dTTP levels should also allosterically up-regulate other dNTP levels which we did not observe. I speculate that a 1.8-fold elevation of dTTP might be not enough to do so. More detailed studies of metabolites in the dNTP synthesis pathway would be required to address this question. In addition, the small effect could be due to the population being heterogeneous with regard to Cdc21 activity (Nordlund and Reichard, 2006). Alternatively, dNTP levels could be elevated in subcellular compartments (Chabes and Thelander, 2003), which may not be reflected in global measurements.

Reporter assays for telomeric silencing in budding yeast

Previous work by Pryde and Louis (1999) suggested that phenotypes at native telomeres in wild-type cells differed from those at truncated telomeres marked with reporter genes. In particular, this work establishes that the reporter gene *URA3* itself does not necessarily reflect presence or absence of a heterochromatin state.

Interestingly, with a few exceptions, all screens or assays employed to delineate a telomeric silencing defect of a mutant/overexpressed gene made use of the *URA3*-VIIL or the *ADE2*-VR reporter constructs initially described by Gottschling and colleagues (Gottschling et al., 1990). In some cases, *URA3* was also inserted into other telomeres (Craven and Petes, 2000; Pryde and Louis, 1999). Despite the availability of other constructs such as *HIS3* or *TRP1*, the *URA3* and *ADE2* reporters likely have been popular due to their counter-selectability and potential for immediate phenotyping. Also, in the structure-function analysis of Sir3 in telomeric silencing, especially its BAH domain which it shares with Orc1, *URA3*-VIIL counter-selection with 5-FOA has been useful (Buchberger et al., 2008; Norris et al., 2008; Sampath et al., 2009; Stone et al., 2000). However, in my hands deletion of *SIR3* caused *URA3* at telomere VII-L to be derepressed by an order of magnitude higher than *HIS3* at the same telomere. This difference could be the reason for the small phenotypic variance observed by Buchberger and colleagues (2008): While almost all their *sir3* *URA3*-VIIL *hmr*Δ*e*::*TRP1* alleles exhibited maximum sensitivity towards 5-FOA, their growth phenotype was more differential on medium lacking Trp.

In another context, when *URA3* was placed at an *HMR* locus containing a Gal4 binding site at the *HMR*-E silencer replacing the ACS, a mating assay could recapitulate the results from a 5-FOA assay. However, this was only shown for *sir1* mutants (Dhillon and Kamakaka, 2000). Despite a specific effect on *URA3* expression in heterochromatin contexts also seen in *sir* mutants, 5-FOA

sensitivity probably largely reflects their heterochromatin phenotype. However, the SIR genes might be an exception for this assay.

A different screen design was originally described by Enomoto and colleagues (1994), in which they made use of plasmid instability caused by the concomitant presence of both centromeric DNA (CEN) and telomeric DNA (TEL) sequences on the same plasmid lacking an ARS. This instability could be alleviated by mutant alleles of the SIR genes as well as *NAT1* and *ARD1*. When combining this assay with a search for disruptors of the telomeric localization of Rap1, they identified several mutants including one of *CAC1* (Enomoto et al., 1997). However, since the molecular mechanism of CEN-TEL antagonism was not elucidated, it is not clear that this screen indeed was suitable to identify genes specifically involved in heterochromatin formation. Another group employed a microscopic screen to isolate mutants from the yeast deletion set that influence nuclear architecture by screening for abnormal nucleolar patterns and those of nuclear pore complexes. While this might be indeed a good strategy to look at genes affecting higher order chromatin structure (albeit it might have to be combined with a secondary screen such as one for condensation), they did not notice a significant overlap between the performance of the isolated mutants in their assay and their performance in “conventional” silencing assays including 5-FOA sensitivity in presence of *URA3*-VIIL (Teixeira et al., 2002).

In conclusion, this work should caution against the use of reporter genes, in particular that of *URA3* and *ADE2*, to assess subtle phenotypes such as heterochromatin formation. While reporters are useful for the pursuit of genetic

screens, unknown changes in metabolism caused by the drugs employed and the mutants being studied can affect the outcome as in the case of *pol30-8* and 5-FOA; DNA damage and nucleotide metabolism. Instead, the focus should be on the assays for endogenous silencing properties. However, for telomeres currently no assay amenable to high-throughput screening is available.

4. MATERIAL AND METHODS

Media and growth conditions

Standard yeast genetic methods were used and media were prepared as described with noted exceptions (Amberg et al., 2005; Guthrie and Fink, 2002). YPD medium was prepared with 10 g/l Bacto yeast extract, 20 g/l Bacto peptone and 20 g/l glucose. Agar plates contained granulated Difco agar (Becton, Dickinson and Co., Franklin Lakes, NJ) at 21 g/l final concentration. For drug marker cassette selection, geneticin (GIBCO, Carlsbad, CA), nourseothricin (clonNAT, WERNER BioAgents, Jena, Germany) or hygromycin B (Invitrogen, Carlsbad, CA) were added to YPD agar to a final concentration of 0.3 g/l, 0.1 g/l or 0.3 g/l, respectively. Synthetic complete (SC) medium was prepared as described (Amberg et al., 2005) with the exception that filter-sterilized adenine and uracil were added after autoclaving to a final concentration of 20 mg/l and 100 mg/l (or 20 mg/l for SC 5-FOA [5-fluoroorotic acid] media), respectively. SC 5-FOA media contained 1 g/l of 5-FOA (US Biologicals, Swampscott, MA; for liquid cultures see below) except for the high-copy suppressor screen (2 g/l) and in experiments testing strains carrying *URA3* at its endogenous locus (0.2, 0.4 and 0.6 g/l). 5-Fluoroanthranilic acid (5-FAA; Sigma-Aldrich, St. Louis, MO) for counter-selection of the *TRP1*-containing plasmid pBL230-8 was added to SC agar to a final concentration of 1 g/l (Toyn et al., 2000). 3-amino-1,2,4-triazole (3-AT; Sigma-Aldrich) was added to SC -His agar from a 1-M stock solution to final

concentrations of 5 mM, 10 mM, 30 mM and 50 mM. Bleomycin (Sigma-Aldrich) was added to SC agar from a 1-U/ml stock solution to final concentrations of 3 U/l and 6 U/l. Hydroxyurea (Sigma-Aldrich) was added to SC agar from a 1-M stock solution to final concentrations of 10 mM, 20 mM and 30 mM. Yeast strains were grown at 30 ˚C unless otherwise indicated. Liquid cultures were agitated at 250 rpm.

Plasmids

All plasmids used in this study are listed in Table 6. Primers used for cloning and mutageneses are listed in Table 7. Plasmid pMR1 was generated by subcloning the *pol30-8* (*pol30-RD61,63AA*) ORF plus 194 bp up- and 165 bp downstream sequence from pBL230-8 (Ayyagari et al., 1995) into pRS306 (integrating, *URA3*; Sikorski and Hieter, 1989) with *Kpn*I and *Not*I. Plasmid pBL230-8 was digested with *Kpn*I, the overhang filled in with Klenow fragment from *E. coli* DNA Polymerase I and dNTPs, followed by digestion with *Pst*I, liberating the same genomic *pol30-8* fragment which was ligated into pRS415 digested with *Sma*I and *Pst*I to yield pMR2. Plasmid pBL211 containing the entire *POL30* ORF plus 194 bp up- and 1,070 bp downstream sequence was digested with *Hind*III, then blunted with Klenow fragment and dNTPs, digested with *Bam*HI and ligated to *Sal*I-digested, blunted and *Bam*HI-digested YEp213 to result in pMR3. For pMR4 and pMR5, the *POL30* fragment from pBL211 digested with *Hind*III followed by *Bam*HI was ligated into pRS425 (2-µm, *LEU2*; Christianson et al., 1992) and pRS415 (CEN6, ARSH4, *LEU2*; Sikorski and Hieter, 1989),

respectively. To obtain pMR6, pBL211 was digested with *Aat*II, 5' overhangs were filled in as above, and *Bam*HI digestion ensued; the liberated genomic *POL30* fragment was subcloned into pRS423 sequentially digested with *Sma*I and *Bam*HI. Plasmids pMR2 and pMR5 were PCR-mutagenized to generate pMR7, pMR8 or pMR9 and pMR10, pMR11, or pMR12, respectively. Mutagenesis followed the QuikChange Site-Directed Mutagenesis Kit (Stratagene, La Jolla, CA) protocol with the following modifications: 50-µl reactions contained 100 ng of plasmid template, 1 x PfuUltra reaction buffer, 1 µM each of forward and reverse primers, 0.2 mM dNTPs and 2.5 U PfuUltra DNA polymerase (Stratagene, #600380). PCR products were directly digested with *Dpn*I and transformed into XL10-Gold ultracompetent cells (Stratagene). A 2.9-kb *CAC1 Eco*RI-*Bam*HI fragment was subcloned from pPK98 (Kaufman et al., 1997) via pRS313 into pRS424 with *Not*I and *Sal*I to generate pMR13. For *in vitro* pull-down assays, *POL30*/pGEX-6P-1 (pMR14; pGEX-6P-1: GE Healthcare, Piscataway, NJ) and *cac1(259-1287)*/pET21a (pMR15; pET21a: EMD Chemicals, Gibbstown, NJ) were PCR-cloned from W303-1a genomic DNA. Typical PCR reactions contained 100 ng genomic DNA, 1 x Herculase reaction buffer (Stratagene), 0.5 µM each of forward and reverse primers, 1 mM dNTPs, 1 µl DMSO and 5 U Herculase DNA polymerase (Stratagene) in a total volume of 20 µl.

The genomic library (LL1) was a generous gift from Dr. Michael Wigler of Cold Spring Harbor Laboratory (CSHL, Vojtek et al., 1991). It was constructed from *S. cerevisiae* strain SP1 (*MAT***a** *leu2 his3 ura3 trp1 ade8 can1*; CSHL

collection) by partial *Sau*A3 restriction digest and fragments of an average size of 5 kb were cloned into the unique *Bam*HI site of the 2-µm vector YEp13M4 (*LEU2*).

High-copy suppressors were confirmed after cloning into 2-µm vectors of the pRS42x series (Christianson et al., 1992). The *CDC21* ORF with 124 bp up- and 21 bp downstream regions was PCR-cloned into pRS425 with *Pst*I and *Spe*I to generate pMR25. We noticed that *CDC21* when cloned with a larger upstream region (498 bp) from either W303-1a or the genomic library clone pMR19 into pRS425 was toxic to bacteria. Furthermore, bacterial transformants carrying *CDC21*/pRS425 with 124-bp upstream sequence originating from 3 different PCR products carried the same $T_{850}TG \rightarrow T_{850}CG$ = Leu → Ser mutation (starting at 850 bp in the *CDC21* ORF). We suspected that this was a polymorphism in *CDC21* between the W303-1a and the S288C (of which the sequence has been published) strains. However, when PCR-cloning *CDC21* with 498 bp up- and 21 bp downstream sequence into pRS306 with *Not*I and *Spe*I (pMR31), the *CDC21* ORF corresponded to the S288C sequence published in the SGD database and did not contain the $T_{850}TG \rightarrow T_{850}CG$ mutation. The consistent results between the library clone containing *CDC21* and cloned *CDC21* speak in favor of this mutation not grossly affecting the phenotype seen. The *ΔEUK1* mutation in *CDC21* (pMR26) was generated from pMR25 in two steps by PCR-mediated site-directed mutagenesis. The predicted catalytic site mutation C177A in *CDC21* (pMR27) was generated from pMR25 following the same protocol. An *Xho*I-*Spe*I fragment containing the entire *CDC21* ORF plus up- and downstream sequences

was subcloned from pMR25 into pRS423 to obtain pMR28. The upstream 885 bp and 124 bp of *CDC21* were amplified by PCR using primers flanked with *Sal*I and *Not*I restriction sites for cloning into pRS425 to generate pMR29 and pMR30, respectively. pMR31 (described above) was mutagenized by PCR to yield the *cdc21-G139D* mutation, creating pMR32. For pMR33, the *CDC21* ORF was amplified by PCR from W303-1a genomic DNA and cloned into pGEX-6P-1 using the restriction sites *Xho*I and *Not*I. Sequencing this construct revealed a silent $A_{877}AT \rightarrow A_{877}AC$ mutation. *MCM1*, *MSA2*, *YKR078W*, *YOR066W*, *CRT1*, *ARL1*, *UBS1*, *PPR1* and *DOT1* including their upstream regions (see Tables 6 and 7) were PCR-cloned from W303-1a genomic DNA as above into pRS425 using *Bam*HI and *Not*I to generate pMR34, pMR35, pMR36, pMR37, pMR38/39, pMR40, pMR41, pMR42, and pMR43, respectively. For *CRT1*, two constructs comprising different lengths of upstream regions (pMR38 and pMR39) were cloned. The putative PIP box mutation in *DOT1* (*dot1-QINFY516-520AANAA*) was generated in two steps by PCR-mediated mutagenesis of pMR43 as described above to yield pMR44. To transfer *DOT1* or *dot1-pip* into a centromeric plasmid, the *Bam*HI-*Not*I fragment from pMR43 or pMR44 was subcloned into pRS415 to generate pMR45 or pMR46, respectively. For *in vitro* transcription/translation of *DOT1*, the *DOT1* ORF was cloned by PCR into pET21a digested with *Bam*HI and *Not*I. The *RAD53* ORF together with 438 bp up- and 44 bp downstream sequence were PCR-amplified with *Eco*RI- and *Not*I-containing primers and cloned into pRS416 (CEN6, ARSH4, *URA3*; Sikorski and Hieter, 1989). From several attempts, only one clone grown at RT was free of

mutations (pMR48). From this construct, the *Eco*RI-*Not*I fragment was subcloned into pRS423 (*HIS3*), thus obtaining pMR49; this plasmid was always amplified at RT.

Yeast strains

For a complete list of *S. cerevisiae* strains used in this study see Table 8. Yeast strains were in the W303 (Thomas and Rothstein, 1989), W1588-4C (Zhao et al., 1998) as well as YPH (Sikorski and Hieter, 1989) backgrounds. A *pol30-8* strain (*pol30-RD61,63AA*) was generated by replacing the endogenous *POL30* gene in W303-1A by *pol30-8* via integration of pMR1 digested with *Bcl*I, backcrossing to W303-1B for 2:2 segregation of *URA3* and 5-FOA counter-selection, resulting in MRY0031. Subsequently, this strain was crossed to a segregant from a cross between RS1295 (from R. Sternglanz, Zhang et al., 2000) and PKY090 (Kaufman et al., 1997) that carries *hmr*::*ADE2* and *URA3*-VIIL to obtain MRY0041. MRY0041 was again backcrossed to W303-1A which resulted in diploid MRY0803. To generate strains used for *URA3*-VIIL ChIP or RT-qPCR, the *ade2-1* and *ura3-1* alleles were deleted from a diploid of W303-1A and W303-1B. An *ade2Δ ura3Δ* segregant was then crossed to a *pol30-8 hmr*::*ADE2 adh4*::*URA3*-VIL segregant from MRY0803 to obtain MRY0948. This strain was sporulated and two *ade2Δ ura3Δ* segregants were crossed to obtain MRY0999 which is homozygous for *ade2Δ ura3Δ* and heterozygous for *pol30-8 hmr*::*ADE2 adh4*::*URA3*-VIIL. A *kanMX6*-VIIL strain was generated by replacing *URA3*-VIIL with its entire 222-bp upstream sequence contained in the

adh4::*URA3*-VIIL fusion (up to the *Hind*III site, Gottschling et al., 1990) by the *kanMX6* cassette (Longtine et al., 1998) in MRY0999 to obtain MRY1446. *SIR3* was subsequently deleted from this diploid strain, resulting in MRY1606. An *adh4*::*URA3*-*HIS3*-VIIL strain was generated by integrating plasmid pYAHISTEL (Bourns et al., 1998) digested with *Pvu*II into MRY0031 crossed to W303-1B. Integration was confirmed by Southern Blot. A *MAT*α *pol30-8 adh4*::*URA3*-*HIS3*-VIIL segregant from this diploid was again backcrossed to W303-1B. A *pol30-8 adh4*::*URA3*-VIIL *ADE2*-VR strain in the YPH background was generated by integrating pMR1 digested with *Bcl*I into YPH500 (from Dr. Daniel Gottschling, Sikorski and Hieter, 1989), 5-FOA counter-selection and crossing to UCC3505 (Singer et al., 1998); segregants included MRY0388. The *pol30-8* mutation can be diagnosed by PCR of a 1227-bp fragment containing the entire ORF with primers 5'*POL30*-272u and 3'*POL30*-178d (Table 7) followed directly by digestion with *Nsi*I which in the case of the *pol30-8* PCR product generates a 772-bp and a 455-bp fragment.

High-copy suppressor screen

Strain MRY0041 was transformed with the LL1 genomic library and plated onto SC -Leu medium to select for cells containing the *LEU2*-marked library plasmids. After two days of growth, colonies were replica-plated onto SC -Leu medium containing 2 g/l 5-FOA and incubated at 30 ˚C for five days. 5-FOA resistant colonies were re-streaked twice onto SC -Leu medium for color assessment. Transformants containing *POL30*, empty vector (YEp13M4) or

GFA1, the most common false positive suppressor, were excluded by colony PCR. Plasmids were rescued from the rest of suppressor strains as described (Hoffman and Winston, 1987) with the modification that the DNA in the aqueous phase was purified by ethanol precipitation before transformation. The identity of the inserts was determined by sequencing from both ends of YEp13M4 with primers M13(-40)-fw and YEp13M4-45-rv. Empty vectors were identified 79 times (Table 1), we speculate mostly due to the not completely penetrant phenotype of the *pol30-8* mutation.

Serial dilutions

Overnight (ON) cultures were adjusted to OD_{600} = 1.0, except for experiments including *ppr1Δ* strains where cultures were grown ON to saturation. OD-adjusted cultures were 10-fold serially diluted six times and 5 µl of each dilution was spotted onto indicated media. When grown at 30 ˚C, 5-FOA plates were incubated for five days, whereas all other plates were shifted to 4 ˚C after three to five days (depending on colony size). For experiments carried out at RT, 5-FOA plates were transferred to 4 ˚C after seven days, all other plates after five days. Plates were photographed after at least three days of incubation at 4 ˚C. Pictured are the first five spots.

DNA damage experiments

ON cultures were diluted to OD_{600} ~ 0.1 and grown until OD_{600} ~ 0.4. Cultures were then treated for 2 h with either 4-nitroquinoline 1-oxide (4-NQO;

Sigma-Aldrich) or methyl methanesulfonate (MMS; Sigma-Aldrich, #M4016) to a final concentration of 0.2 mg/l and 0.05 %, respectively. Untreated or treated cells were harvested at a cell density of 1.8 - 2.2 x 10^7 cells/ml (as determined by OD_{600}) and processed for either RNA or protein extraction.

Liquid 5-FOA culture experiments

ON cultures in SC medium containing 20 mg/l uracil were diluted 1:130 and grown until OD_{600} ~ 0.2, when they were again diluted 2-fold. At OD_{600} ~ 0.2, 40 ml culture was harvested for RNA preparation, after which cultures were split and treated with a 100 x 5-FOA solution (Zymo Research, Orange, CA) to a final concentration of 1 g/l or the equivalent amount of the solvent DMSO. Samples for RNA preparation were harvested after 1, 2, 3 and 4 h.

Determination of gene expression

Total RNA was extracted from 10 ml of cells harvested at a density of 2 x 10^7 cells/ml (unless otherwise noted in this section) using the hot acidic phenol method as described with two chloroform extractions (Collart and Oliviero, 2001). Briefly, cultures were harvested over crushed ice for 5 min at 2,750 x g, 4 ˚C. Cells were transferred to an Eppendorf tube, and after spinning for 10 s at 20,800 x g, 4 ˚C, the pellet was frozen in liquid nitrogen. Cell pellets were resuspended in 400 µl of TES solution (10 mM Tris-Cl, pH 7.5, 10 mM EDTA, 0.5 % SDS). 400 µl of phenol solution (saturated with 0.1 M citrate buffer, pH 4.3, Sigma) was added and samples were incubated at 65 ˚C for 1 h with short vortexing every 10

min. After 5 min of incubation on ice total RNA was extracted twice with phenol-chloroform-isoamyl alcohol (PCI), followed by two chloroform extractions. After ethanol precipitation, pellets were briefly dried at RT and resuspended in 50 µl of nuclease-free water (Ambion, Austin, TX). RNA was DNase-I treated (amplification grade, Invitrogen or DNA-*free*^{TM}, Ambion) and 0.75 µg - ~1 µg was used for RT-PCR (TaqMan kit, Applied Biosystems, Austin, TX). 1/20 of this reaction was used per quantitative PCR (qPCR) reaction in a LightCycler 480 (Roche Diagnostics Corporation, Indianapolis, IN) using the manufacturer's reagents and protocol. Primers used are listed in Table 7. qPCR reactions were performed in triplicate to assess technical variation. Pooled results were normalized to wild-type expression levels.

Preparation of whole cell protein extracts and immunoblotting

5 ODs of logarithmically growing cells at a density ~2 x 10^7 cells/ml (as determined by OD_{600}) were harvested, washed once with ice-cold purified and deionized (Milli-Q) water, transferred to an Eppendorf tube, and the pellet was frozen in liquid nitrogen. Depending on the protein of interest, protein extraction was either done just with mild alkali lysis (Cdc21, Dot1, histones, Pol30, Rnr, α-tubulin; modified from Kushnirov, 2000) or alkali lysis followed by TCA precipitation (Rad53, Rnr, α-tubulin, YFP-Sml1; modified from Kushnirov, 2000). Alkali lysis: Upon thawing on ice, pellets were resuspended in 100 µl of Milli-Q water, 300 µl of 0.2 M NaOH and β-mercaptoethanol was added to a final concentration of 5 %. After incubation on ice for 10 min, the sample was pelleted

for 10 min in a microcentrifuge at 20,900 x g at 4 ˚C, resuspended in 50 µl of 1 x SDS sample buffer (SB) and boiled for 10 min. 6 µl of this extract were used for SDS-PAGE followed by immunoblot analysis. Alkali lysis/TCA precipitation: Upon thawing on ice, pellets were resuspended in 100 µl of TCA buffer (1.85 M NaOH, 7.4 % β-mercaptoethanol) and incubated on ice for 10 min. 100 µl of 20 % ice-cold TCA was added, the tubes inverted and samples incubated on ice for a further 10 min. The mixture was centrifuged for 2 min at 17,900 x g at 4 ˚C, washed with 1 ml acetone, centrifuged as before and the dried pellet was resuspended in 50 µl of 0.1 M NaOH and 50 µl of 2 x SDS SB. After boiling as above, 12 µl per sample was used for SDS-PAGE followed by immunoblot analysis. Of note, for histone immunoblots whole cell protein extracts separated by SDS-PAGE were transferred onto Immobilon-P polyvinylidene fluoride (PVDF) membranes (pore size 0.45 µm, Millipore, Temecula, CA) prepared as per the manufacturer's instructions (soaked for 15 s in 100 % methanol, then washed for 2 min in Milli-Q water followed by equilibrating for 5 min in transfer buffer) at 22 V (fixed; ~160 mAmp) for 60 - 90 min. For all other immunoblots transfer was onto Protran BA85 nitrocellulose membranes (pore size 0.45 µm, Whatman) at ~500 mAmp (fixed) for 1 h. All transfers took place in sodium carbonate buffer (1x sodium carbonate from a 40 x stock at pH 9.5, 20 % methanol) at RT.

Standard immunoblotting techniques were used. Antibodies were anti-Cdc21 (CS2796, rabbit) at 1:5,000, anti-Dot1 (gift from Dr. Daniel Gottschling) at 1:2,000, anti-GFP (#11814460001, Roche Diagnostics Corporation, Indianapolis, IN) at 1:1,000, anti-H3 (C-terminus, ab1791, Abcam, Cambridge, MA) at 1:5,000,

anti-H4 (05-858, Millipore) at 1:1,000, anti-H3K4Me3 (ab8580, Abcam) at 1:5,000, anti-H3K56Ac (07-677, Millipore) at 1:2,000, anti-H3K79Me1 (ab2886, Abcam) at 1:500, anti-H3K79Me2 (ab3594, Abcam) at 1:500, anti-H3K79Me3 (ab2621, Abcam) at 1:1,000, anti-Pol30 (CS871, rabbit) at 1:6,000, anti-Rad53 (yC-19, Santa Cruz Biotechnology, Inc., Santa Cruz, CA) at 1:500, anti-Rnr2/Rnr4/α-tubulin (YL1/2, Santa Cruz) at 1:1,000.

Chromatin immunoprecipitation

Chromatin immunoprecipitation was done with some modifications to published procedures. ON cultures were diluted to OD_{600} = 0.15 and grown until a density of about 1.7 x 10^7 cells/ml (as determined by OD_{600}; OD_{600} = 0.78 - 0.84). 50 ml of cell culture was treated for 30 min with freshly prepared 1 % paraformaldehyde (from prills, Electron Microscopy Sciences, Fort Washington, PA), slowly rotating at RT. Crosslinking was stopped with Glycine added to a final concentratoin of 0.22 M. Cells were then harvested for 5 min at 2,750 x g, 4 ˚C, washed twice in ice-cold 1 x PBS and the pellets were frozen in liquid nitrogen. Cross-linked cells from a 50-ml culture were resuspended in 800 µl FA-lysis buffer (50 mM HEPES-NaOH pH 7.5, 150 mM NaCl, 0.5 % SDS, 0.1 % sodium deoxycholate, 1 % Triton X-100, 1 mM EDTA, and freshly added 5 mM NaF, 1 mM DTT, 1:25 Complete, EDTA-free [Roche], 660 µM Pefabloc SC PLUS [Roche]) and bead-beat in a Mini-Beadbeater-8 (BioSpec Products Inc., Bartlesville, OK) for 9 x 40 s with 2-min recovery on ice-water in-between. Sonication of lysates was performed for 12 cycles (five at a time with cooling in-

between) in a Bioruptor UCD-200 waterbath sonicater (Diagenode, Sparta, NJ) generating a mean DNA fragment size of 0.5 kb (range 0.1 - 1 kb). The DNA fragment size was checked for each input after reversal of cross-links (see below) by running 5 - 10 % on a 2 % agarose gel. Chromatin lysates were clarified twice for 2 min and 20 min at 25,000 x g, 4 ˚C. Immunoprecipitations were carried out with either 2 µg rabbit α-H3 (ab1791, Abcam) per 70 µg of chromatin, 8 µl rabbit α-Sir2 (CS1102; Zhang et al., 2002), or 8 µl rabbit α-Sir4 (CS1098; Zhang et al., 2002) per 90 µg of chromatin or 20 µl rabbit α-Ssn6 (a generous gift from Dr. Sharon Dent; Davie et al., 2003) per 120 µg of chromatin in a total volume of 1 ml. A control was performed with 2 µg normal rabbit IgG (Invitrogen). A pre-clearing step with 10 µl Protein A sepharose beads (4 Fast Flow; GE Healthcare) for 2 h at 4 ˚C was followed by ON incubation with antibody pre-bound to Protein A sepharose beads at 4 ˚C. Immunocomplexes were washed for 5 min each once with 1 ml of FA-lysis buffer, twice with 1 ml of FA-lysis buffer/500 mM NaCl, once with 1ml of 10mM Tris-Cl pH 8.0, 0.25 M LiCl, 0.5 % NP-40, 0.5 % sodium deoxycholate, 1 mM EDTA and twice with 1 ml of TE buffer (10 mM Tris-Cl pH 8.0, 1 mM EDTA pH 8.0) with transfer into a fresh tubes before the last wash. Chromatin-antibody complexes were eluted off beads twice with 100 µl each of freshly prepared 100 mM sodium bicarbonate, 1 % SDS. After addition of 2 µg of RNase A (Abcam; ab52579) and NaCl to a final concentration of 300 mM, cross-links were reversed ON at 65 ˚C. Protein was digested with proteinase K (0.3 mg/ml) for 2 h at 42 ˚C. After extraction with PCI (input samples were extracted twice) and chloroform, DNA was ethanol-

precipitated in the presence of 20 µg glycogen and resuspended in 60 µl TE buffer. Per quantitative PCR reaction, 2 µl of 1/10 input samples and 2 µl of immunoprecipitated samples were used in a qPCR reaction in a LightCycler 480 (Roche) using the manufacturer's reagents and protocol. qPCR reactions were performed in duplicate to assess technical variation. Primers used are listed in Table 7.

Antigen preparation for generation of anti-Cdc21 antibody

GST-Cdc21 was obtained from BL21-CodonPlus (DE3)-RIL (Stratagene) cells transformed with plasmid pMR21 induced at OD_{600} ~ 0.6 with 0.4 mM IPTG for 6 h at RT. Pellets from 500 ml cultures were thawed on ice and resuspended in 12.5 ml lysis buffer (TN150 [20 mM Tris-Cl pH 7.4, 150 mM NaCl, 0.5 % NP-40, 5 % glycerol, 0.5 mM EDTA, 3 mM DTT, 1 mM PMSF, 1 µg/ml leupeptin, 1 µg/ml pepstatin, 2 µg/ml aprotinin, 0.2 mg/ml bacitracin, 2 mM benzamidine]), treated with lysozyme to a final concentration of 0.2 % [w/v] for 30 min at 4 ˚C and sonicated on ice-water 6 x 10 s (1 s on, 1 s off, with 1 min breaks in-between) at 40 % amplitude. After spinning lysates for 30 min in an SS34 rotor at 23,400 x g, 4 ˚C, supernatants were bound to 3 ml 1:1 slurry of Glutathione Sepharose 4 Fast Flow (GE Healthcare, Uppsala, Sweden) for 1 h rotating at 4 ˚C, then washed 2 times with lysis buffer TN150, followed by 2 times with lysis buffer TN600 (containing 600 mM NaCl), and again 2 times with lysis buffer TN150. GST-Cdc21 was eluted from beads on the column with 20 mM Glutathione/50 mM Tris-Cl at pH 8.0, dialyzed twice (2 h, ON) against lysis buffer

TN150, containing only 0.02 % NP-40. The protein concentration was determined using the Bradford assay and SDS-PAGE followed by Coomassie staining.

Untagged Cdc21 was prepared as above up to and including washing the bead-bound lysate. Then beads were washed twice with 30 column volumes of cleavage buffer (20 mM Tris-Cl pH 7.4, 150 mM NaCl, 0.02 % NP-40, 1 mM EDTA, 1 mM DTT), and cleaved with 240 U PreScission Protease (GE Healthcare, Piscataway, NJ) for 4 h at 4 ˚C. The cleaved protein was dialyzed twice (2 h, ON) against 20 mM Tris-Cl pH 7.4, 10 % glycerol, 0.2 mM EDTA. Dialyzed Cdc21 was ultracentrifuged for 30 min in an TLA100.3 rotor at ~416,033 x g, 4 ˚C, and the supernatant was applied to a Mono Q column (5 x 50 mm, Pharmacia Biotech) pre-equilibrated with start buffer (20 mM Tris-Cl pH 7.4, 10 % glycerol, 0.2 mM EDTA) at a flow rate of 0.5 ml/min on an ÄKTAexplorer 10 (Pharmacia Biotech). After the column was washed with two column volumes of start buffer, Cdc21 was eluted in 0.5-ml fractions with a 20-column volume linear gradient from 0 to 1 M KCl in start buffer. SDS-PAGE was used to determine the Cdc21-containing peak. The protein concentration was determined using the Bradford assay and SDS-PAGE, using bovine serum albumin as a standard. This purification yielded 5 mg of Cdc21 protein at a peak concentration of 5.1 mg/ml.

Generation of anti-Cdc21 antibody

Polyclonal anti-Cdc21 antibodies were generated by Covance (Princeton, NJ). One immunization of two New Zealand White (NZW) rabbits (CS2796 and CS2797) with 250 µg of GST-Cdc21 and Freund's complete adjuvant each was

followed by six boost immunizations (first boost after one month, the five remaining in three-week intervals) with 125 µg of Cdc21 and Freund's incomplete adjuvant each. A pre-bleed was obtained before the first immunization and Cdc21-specific antiserum was obtained ten days after each boost starting with the first boost. With increased boosting, the sensitivity of Cdc21-specific antiserum increased, so that for later experiments the last (sixth) production bleed was preferentially used. Both antibodies, CS2796 and CS2797, were used without further purification.

Purification of GST and GST-Pol30

GST and GST-Pol30 were prepared as GST-Cdc21 above with the alterations that the lysis buffer contained 20 mM Tris-Cl pH 7.5, 150 mM NaCl, 0.02 % NP-40, 10 % glycerol, 1 mM EDTA, 1 mM DTT, 0.5 mM PMSF, 1 µg/ml leupeptin, 1 µg/ml pepstatin, 1 µg/ml aprotinin, 100 µg/ml bacitractin and 0.5 mM benzamidine. After elution, both proteins were ultracentrifuged as above. GST was dialyzed twice (2 h, ON) against 20 mM Tris-Cl pH 7.5, 150 mM NaCl, 10 % glycerol, 1 mM EDTA, 0.5 mM PMSF. GST-Pol30 was loaded onto a Mono Q column (as above), pre-equilibrated with lysis buffer. The protein was eluted in 0.5-ml fractions of a linear 20-column volume gradient from 150 mM to 1 M NaCl in lysis buffer. This purification yielded 1 mg of GST-Pol30 protein at a peak concentration of 1 mg/ml.

In vitro transcription and translation

Reactions were performed using the TNT T7 Coupled Reticulocyte Lysate System (Promega Corporation, Madison, WI) according to the manufacturer's protocol. A 50-µl reaction contained 2.8 µg template DNA (pMR13 or pMR28), 25 µl rabbit reticulocyte lysate, 2 µl reaction buffer, 1 µl T7 RNA polymerase, 40 U Protector RNase inhibitor (Roche), 20 µM amino acid mixture minus methionine, and 20 µCi [^{35}S]methionine (1175 Ci/mmol; PerkinElmer, Waltham, MA). Reactions were incubated for 1.5 h at 30 °C and directly used in the GST pull-down assay.

Pull-down assay

50-µl *in vitro* transcription/translation reactions were diluted 1:5 in pull-down buffer (20 mM Tris-Cl pH 7.4, 150 mM NaCl, 5 mM magnesium acetate, 0.02 % NP-40, 5 % glycerol, 0.1 mM EDTA, 5 mM β-mercaptoethanol, 1 mM PMSF, 1 µg/µl leupeptin, 1 µg/ml pepstatin, 1 µg/ml aprotinin, 100 µg/ml bacitracin and 0.5 mM benzamidine) and 100 µl were incubated with 4 µg of purified GST or GST-Pol30 and 50 µl 1:1 slurry of Glutathione Sepharose 4 Fast Flow (GE Healthcare) in a total volume of 250 µl for 2.5 h rotating at 4 ˚C. After 5 washes with pull-down buffer, bound proteins were eluted with 30 µl 2 x SDS SB, boiled for 10 min and analyzed on 12 % SDS-polyacrylamide gels. Gels were stained with Coomassie Brilliant Blue R-250, quickly destained, dried and exposed to a PhosphorImager screen (FUJIX BAS 1000; Fujifilm, Stamford, CT)

for 24 h up to two weeks. The PhosphorImager screen was read in a FLA-5100 imaging system (Fujifilm).

Preparation of genomic DNA

Genomic DNA was prepared as described (Philippsen et al., 1991) with some modifications. 10 ml of culture in early stationary phase (~2 x 10^8 cells/ml) was harvested by spinning for 5 min at 3,750 x g, 4 ˚C, and washed once with Milli-Q water. Cells were resuspended in 0.5 ml of 0.9 M sorbitol, 25 mM Tris-Cl pH 7.5, 0.1 M EDTA, 50 mM DTT and 0.2 mg of Zymolyase T100 (Seikagaku Corporation, Tokyo, Japan) was added and incubated at 30 ˚C for 120 - 150 min. Spheroplasting was monitored by OD_{600} measurement in 10 % SDS as well as microscopy. Spheroplasts were pelleted for 2 min at 2,700 x g, RT, and resuspended thoroughly in 0.5 ml of 50 mM Tris-Cl pH 7.5, 50 mM EDTA pH 8.0. After addition of 25 ul 20 % SDS samples were mixed and incubated for 15 min in a 65-˚C waterbath. 160 µl of 5 M potassium acetate was added, the samples mixed and incubated for 15 min on ice followed by centrifugation for 15 min at 20,800 x g, RT. The supernatant was extracted with an equal volume of PCI until the interface was clear (about four extractions). Then the DNA and RNA were precipitated with isopropanol at an equal amount to that of the supernatant, incubated for a few minutes at RT and pelleted for 10 min at 14,000 rpm, RT. The pellets were resuspended in 100 µl of 10 mM Tris-Cl, pH 7.5, 1 mM EDTA pH 8.0 and 7.5 µl from a 2-mg/ml Rnase-A stock was added to each sample at incubate for 20 min at 37 ˚C. The DNA was extracted once with PCI followed by

chloroform extraction. After addition of potassium acetate to a final concentration of 0.3 M the genomic DNA was ethanol precipitated and resuspended in 125 µl of 1 x 10 mM Tris-Cl, pH 8.0, 1 mM EDTA pH 8.0. Its concentration was assessed by UV spectrophotometry.

Radioactive labeling of DNA fragments for Southern hybridization

A fragment containing 279 bp upstream of the *HIS3* ATG and the 5' 651 bp of the *HIS3* ORF (*HIS3* ORF = 663 bp) was PCR-amplified from pRS423, gel purified using the PCR Purification Kit (Qiagen) and digested with *Dde*I and *Bgl*I to release a 431-bp fragment which was gel purified as before. 25 - 50 ng of this fragment was labeled using the Rediprime II Random Prime Labelling System (GE Healthcare) according to the manufacturer's protocol except that after adding 5 µl [α-^{32}P]-dCTP (6000Ci/mmol, 20mCi/ml; Perkin Elmer, Waltham, MA) the mixed reaction was incubated for 45 min at 37 ˚C instead of just 10 min. Labeled probes were immediately spin-purified using MicroSpin G-50 columns (GE Healthcare) as per the manufacturer's protocol except that all spins were carried out for 2 min at 770 x g and that the columns were pre-spun twice with placing them into a fresh Eppendorf tube in-between to collect any residual storage buffer. The amount of radioactivity was measured by adding 2 µl of labeled probe to 3 ml of Betamax scintillation fluid (ICN Biomedicals, Irvine, CA) in a 1209 Rackbeta liquid scintillation counter (LKB-Wallac, now Perkin Elmer).

Southern transfer and hybridization

Southern transfer and hybridization were generally done as described (Sambrook and Russell, 2001; Southern, 1975). After electrophoresis of *Bgl*I-digested genomic DNA from different diploid *adh4*::*HIS3*-*URA3* transformants on 1.2-% agarose gels, the gels were photographed, rinsed in Milli-Q water and incubated (DNA side up) for 1 h in freshly prepared denaturation solution (87.66 g NaCl and 20 g NaOH per l Milli-Q water) with one exchange of the solution after 30 min. The Southern transfer was done as an upward capillary transfer onto Hybond-N+ nylon membranes (GE Healthcare). After transfering for 16 - 20 h at RT the membranes were UV-irradiated at 254 nm with 0.12 kJ/cm^2 in a Stratalinker UV Crosslinker 2400 (Stratagene) to immobilize the DNA onto the membrane. Membranes were kept light-protected at 4 ˚C in Saran wrap.

Membranes in roller bottles with the DNA-side facing the lumen were prehybridized in 15 ml of QuikHyb hybridization solution (Stratagene) containing 25 ul (corresponding to about 520 µg) of boiled and snap-cooled salmon sperm DNA (ssDNA; Sigma-Aldrich) for at least 1 h in a prewarmed hybridization oven at 68 ˚C. Hybridizations were carried out for 1 h at 68 ˚C in the same solution to which boiled and snap-cooled 2 x 10^6 cpm/ml labeled probe and 520 µg ssDNA were added. Washes were performed twice with 100 ml 2 x SSC, 0.1 % SDS for 15 min each, followed by twice with 100 ml 0.1 x SSC, 0.1 % SDS for 30 min each at 68 ˚C. Membranes were exposed to a FUJIX BAS 1000 PhosphorImager screen (Fujifilm) for about 24 h and read as above.

Microarray

ON cultures of three independent colonies per genotype were diluted to OD_{600} ~ 0.15 and grown to a cell density of about 1.7 x 10^7 cells/ml (OD_{600} = 0.78 - 0.84). RNA was prepared as described above from 10 ml cells. RNA quality was assessed using Series II RNA 6000 Pico chips on an Agilent 2100 Bioanalyzer (Agilent, Palo Alto, CA) and samples with an RNA Integrity number (RIN) score of 7.5 or greater were passed. Quantity was assessed by NanoDrop 1000 (NanoDrop products, Wilmington, DE). Total RNA was amplified by a modified Eberwine Technique, using a MessageAmp II aRNA Amplification Kit (Ambion) for 2 rounds of amplification (Van Gelder et al., 1990). aRNA smear analysis for 3' bias was performed on select samples using Series II RNA 6000 Pico chips on an Agilent 2100 Bioanalyzer (Agilent). Samples were then prepared for hybridization, hybridized onto Yeast Genome 2.0 GeneChips (Affymetrix, Santa Clara, CA), washed and scanned according to the manufacturer's instructions. Affymetrix QC metrics were used to pass the image data.

Data analysis

All raw data were processed by Dr. Weijun Luo (Bioinformatics Shared Resource, CSHL) using the FARMS method (Hochreiter et al., 2006) with a current probe set definition (Dai et al., 2005). The latest gene annotation information was retrieved from the Entrez Gene and Gene Ontology (GO) public databases. He analyzed differentially expressed individual genes or gene sets

between each mutant and wild-type replicate. Gene set or pathway analysis was done using “generally applicable gene-set enrichment” (GAGE; Luo et al., 2009). The most differentially regulated GO groups were selected with a false discovery rate q-value < 0.1. For assessment of regional gene expression level changes, 10-kb chromosome regions were defined which span the same segments starting from both ends (telomeres) to the center of all 16 chromosomes. It should be noted that different chromosome regions are comprised of a different number of genes. Furthermore, the 16 chromosomes differ in length and gene number within the same 10-kb region. Error bars represent the standard error of the mean (SEM) of three experiments per genotype. Overall differential expression in each chromosome region was quantified by using either GAGE or the average $\log_2$-based expression ratio of mutant versus wild type (with SEM). Differential expression of genes 20 kb off telomeres was also visualized using heatmaps.

For correlation of fold change in the mutants to absolute gene expression levels in wild-type cells, the $\log_2$-based fold change of gene expression in the average of mutant versus the average of wild-type replicates was plotted over the signal value of the average of the three wild-type replicates. A local weighted polynomial smoothing (Loess) curve (in red) was fitted to the data using a neighborhood = 0.2. All expression data are $\log_2$ transformed. Note that a few outlier points fell outside the uniform y axis limits, which were imposed for direct comparison across multiple panels.

Determination of dNTP pools

dNTP pools were determined by Olga Tsaponina, a graduate student in Dr. Andrei Chabes' laboratory, Umeå University, Sweden. Cells were grown in SC -Leu medium. 3.7 x 10^8 cells (as determined by OD_{600}) were harvested by filtration through 25 mm white AAWP mixed cellulose filters (0.8 µm, Millipore AB, Solna, Sweden). The filters were immersed in 700 µl of ice-cold extraction solution (12 % w/v trichloroacetic acid, 15 mM $MgCl_2$) in Eppendorf tubes. The following steps were carried out at 4 °C. The tubes were vortexed for 30 s, incubated for 15 min and vortexed again for 30 s. The filters were removed and the supernatants were collected after centrifugation at 20,000 x g for 1 min and added to 700 µl of ice-cold Freon-trioctylamine mixture (10 ml of Freon [1,1,2-trichlorotrifluoroethane, 99 %, Aldrich, Sigma-Aldrich Sweden AB, Stockholm, Sweden] and 2.8 ml of trioctylamine [>99 %, Fluka, Sigma-Aldrich Sweden AB, Stockholm, Sweden]). The samples were vortexed and centrifuged for 1 min at 20,000 x g. The aqueous phase was collected and added to 700 µl of ice-cold Freon-trioctylamine mixture. The samples were vortexed and centrifuged for 1 min at 20,000 x g. The 475-µl aliquots of the aqueous phase were pH adjusted with 1 M NH_4HCO_3 (pH 8.9), loaded onto boronate columns (Affi-Gel 601 [Bio-Rad Laboratories AB, Sundbyberg, Sweden]) and eluted with 50 mM NH_4HCO_3, pH 8.9, 15 mM $MgCl_2$ to separate dNTPs and NTPs. The eluates with purified dNTPs were adjusted to pH 3.4 with 6 M HCl, separated on a PartiSphere SAX HPLC column (4.6 x 125 mm, Whatman plc, Maidstone, UK) and quantified using a UV-2075 Plus detector (Jasco Scandinavia AB, Mölndal, Sweden). Nucleotides

were isocratically eluted using 0.36 M ammonium phosphate buffer (pH 3.4, 2.5 % v/v acetonitrile). The 47.5-µl aliquots of the aqueous phase were adjusted to pH 3.4 and used to quantify NTPs by HPLC in the same way as dNTPs. Results from dNTP measurements were normalized to NTP levels of the cells.

Table 6: Plasmids used in this study.

Plasmid	Description	Source/ Reference
pBL230-8	*pol30-8* (*pol30-RD61,63AA*) by mutagenesis of pBL230 (= pRS314 containing a *Pst*I-*Kpn*I fragment of pBL205 [= entire *POL30* ORF on a 1,136-bp *Mlu*I-*Xba*I fragment within pBL203])	(Ayyagari et al., 1995; Zhang et al., 2000)
pBL211	YCp50 containing a *Bam*HI-*Hind*III fragment of pBL203 (= entire *POL30* ORF on a 2,041-bp *Mlu*I fragment cloned into *Sal*I site of pUC19)	(Bauer and Burgers, 1990)
pPK98	5.6-kb *CAC1 Bam*HI fragment cloned from yeast cosmid 9513 (ATCC) into *Bam*HI site of pBSKS+	(Kaufman et al., 1997)
pRS306	pBluescript (KS, M13+), *URA3*	(Sikorski and Hieter, 1989)
pRS415	pBluescript, CEN6, ARSH4, *LEU2*	(Sikorski and Hieter, 1989)
pRS416	pBluescript, CEN6, ARSH4, *URA3*	(Sikorski and Hieter, 1989)
pRS423	pBluescript II SK+, 2-µm, *HIS3*	(Christianson et al., 1992)
pRS424	pBluescript II SK+, 2-µm, *TRP1*	(Christianson et al., 1992)
pRS425	pBluescript II SK+, 2-µm, *LEU2*	(Christianson et al., 1992)
YEp13M4	pUC18, 2-µm, *LEU2*	(Gift from Dr. Jeffrey Gerst, Gerst et al., 1991)
YEp213	pBR322, 2-µm, *LEU2*	Gift from Dr. David Stillman
LL1	*Sau*3A fragments (~5 kb) from S. cerevisiae strain SP1 (*MAT***a** *leu2 his3 ura3 trp1 ade8 can1*) ligated into unique *Bam*HI site of YEp13M4	(Gift from Dr. Michael Wigler, Vojtek et al., 1991)
pFA6a-kanMX6	*kanMX6* module for PCR-mediated gene deletion	(Longtine et al., 1998)
pFA6a-HIS3-kanMX6	this module for PCR-mediated gene deletion contains the *HIS3* gene from *S. kluyveri*, not *S. pombe his5*$^{+}$ (Dr. Aaron Neiman, personal communication)	(Longtine et al., 1998)
pFA6a-13Myc-kanMX6	module for PCR-mediated C-terminal protein tagging with 13xMyc epitope encoded by c-	(Longtine et al., 1998)

	myc	
pAG25	*natMX4* cassette for PCR-mediated gene deletion; selectable with nourseothricin	(Goldstein and McCusker, 1999)
pAG32	*hphMX4* cassette for PCR-mediated gene deletion; selectable with hygromycin B	(Goldstein and McCusker, 1999)
pMR1	*pol30-8* (*pol30-RD61,63AA*)/pRS306	This study
pMR2	*pol30-8*/pRS415	This study
pMR3	*POL30*/YEp213	This study
pMR4	*POL30*/pRS425	This study
pMR5	*POL30*/pRS415	This study
pMR6	*POL30*/pRS423	This study
pMR7	*pol30-K127R*/pRS415	This study
pMR8	*pol30-K164R*/pRS415	This study
pMR9	*pol30-K127,164RR*/pRS415	This study
pMR10	*pol30-8-K127R/pRS415*	This study
pMR11	*pol30-8-K164R/pRS415*	This study
pMR12	*pol30-8-K127,164RR*/pRS415	This study
pMR13	*CAC1*/pRS424 = ORF + 659 bp 5' + 426 bp 3'	This study
pMR14	*POL30*/pGEX-6P-1	This study
pMR15	*cac1(259-1287)*/pET21a	This study
pMR16 = 12-8-633	LL1 genomic insert carrying *GFA1* and partial *YKL105C* (chromosome XI, about 240,733 - 245,449 bp)	This study
pMR17 = 12-8-634	LL1 genomic insert carrying *SDT1*, *COG1*, *EDC1*, *NIF3*, *FRA2* as well as partial *VRG4* and *MDM34*/*YGL218W* (chromosome VII, about 77,662 - 83,920 bp)	This study
pMR18 = 12-8-773	LL1 genomic insert carrying *YCR023C* as well as partial *YCR022C* and *SLM5* (chromosome III, about 157,671 - 161,749 bp)	This study
pMR19 = 12-8-765	LL1 genomic insert carrying *SUF11*, *YOR072W-B*, *SGO1*, *CDC21*, *YOR073W-A* (chromosome XV, about 463,684 - 467,970 bp)	This study
pMR20 = 12-8-525	LL1 genomic insert carrying *ARA2*, *tF(GAA)M*, *ARG80*, *MCM1* as well as partial *YET2* and *IOC4* (chromosome XIII, about 350,589 - 356,314 bp)	This study
pMR21 = 12-8-744	LL1 genomic insert carrying *MCM1*, *IOC4* as well as partial YMRCdelta7 and YMRCTy1-3 (chromosome XIII, about 353,175 - 357,352 bp)	This study

pMR22 = 12-8-692	LL1 genomic insert carrying *MSA2*, *YKR078W* as well as partial *ECM4* and *TRZ1* (chromosome XI, about 582,268 - 586,579 bp)	This study
pMR23 = 12-8-310	LL1 genomic insert carrying *CBF5*, *CRT1* as well as partial *IDP20* and *YLR177W* (chromosome XII, about 505,748 - 511,591 bp)	This study
pMR24 = 12-8-114	LL1 genomic insert carrying *ARL1* and *UBS1* as well as partial *EXO5* and *TYR1* (chromosome II, about 565,846 - 570,589 bp)	This study
pMR25	*CDC21*/pRS425 = ORF + 124 bp 5' + 21 bp 3'	This study
pMR26	*cdc21-ΔEUK1*/pRS425	This study
pMR27	*cdc21-C177A*/pRS425	This study
pMR28	*CDC21*/pRS423	This study
pMR29	p_{885}*CDC21*/pRS425 = 885 bp 5' - 97 bp in *CDC21* ORF	This study
pMR30	p_{124}*CDC21*/pRS425 = 124 bp 5' - 97 bp in *CDC21* ORF	This study
pMR31	*CDC21*/pRS306 = ORF + 498 bp 5' + 21 bp 3'	This study
pMR32	*cdc21-216* (*cdc21-G139D*)/pRS306	This study
pMR33	*CDC21*/pGEX-6P-1	This study
pMR34	*MCM1*/pRS425 = ORF + 726 bp 5' + 51 bp 3'	This study
pMR35	*MSA2*/pRS425 = ORF + 801 bp 5' + 16 bp 3'	This study
pMR36	*YKR078W*/pRS425 = ORF + 689 bp 5' + 5 bp 3'	This study
pMR37	*YOR066W*/pRS425 = ORF + 879 bp 5' + 117 bp 3'	This study
pMR38	*CRT1*(pshort)/pRS425 = ORF + 831 bp 5' + 261 bp 3'	This study
pMR39	*CRT1*(plong)/pRS425 = ORF + 1,473 bp 5' + 261 bp 3'	This study
pMR40	*ARL1*/pRS425 = ORF + 366 bp 5' + 107 bp 3'	This study
pMR41	*UBS1*/pRS425 = ORF + 509 bp 5' + 69 bp 3'	This study
pMR42	*PPR1*/pRS425 = ORF + 624 bp 5' + 47 bp 3'	This study
pMR43	*DOT1*/pRS425 = ORF + 1,650 bp 5' + 14 bp 3'	This study
pMR44	*dot1-pip*(dot1-QINFY516-520AANAA)/ pRS425	This study
pMR45	*DOT1*/pRS415	This study
pMR46	*dot1-pip*(dot1-QINFY516-520AANAA)/ pRS415	This study

pMR47	*DOT1*/pET21a	This study
pMR48	*RAD53*/pRS416 = ORF + 438 bp 5' + 44 bp 3'	This study
pMR49	*RAD53*/pRS423 = ORF + 438 bp 5' + 44 bp 3'	This study

Table 7: Primers used in this study.

Primer	Sequence	Purpose
5'POL30-BamHI	5'-AAAAGAGGAGG'GATCCATGTTAGAAG CAAAATTTGAAGA-3'	*POL30*/ pGEX-6P-1 (= pMR6)
3'POL30-XhoI	5'-AAAAGAGGAGC'TCGAGTTATTCTTCGT CATTAAATTTAG-3'	
5'CAC1-259-BamHI-PP	5'-AAAAGAGGAGG'GATCCCTGGAGGTGC TGTTCCAGGGCCCCAAGCTTTTATGCTAC AAAAA-3'	*cac1(259-1287)*/pET21a (= pMR7)
3'CAC1-1287-SalI	5'-AAAAGAGGAGG'TCGACGCTGTCTAGA AACCCGTCAA-3'	
5'CDC21-124u-PstI	5'-AAAAGAGGAGCTGCA'GTTGACGCGTT TCCTGAAATA-3'	*CDC21*/ pRS425 (= pMR14)
3'CDC21-21d-SpeI	5'-AAAAGAGGAGA'CTAGTTGTTTCTCCTC GTGCTGTCA-3'	
5'cdc21-Δ99-110	5'-GTAATGGATCTCGTGAAGGAGATCTGG GGCCCG-3'	*cdc21-ΔEUK1* (= pMR15) PCR 1
3'cdc21-Δ99-110	5'-CGGGCCCCAGATCTCCTTCACGAGAT CCATTAC-3'	
5'cdc21-mut93-98	5'-GTTAAGATTTGGGACGAGTGGGCAGAT GAGAATGGAGATCTGGGGCC-3'	*cdc21-ΔEUK1* (= pMR15) PCR 2
3'cdc21-mut93-98	5'-GGCCCCAGATCTCCATTCTCATCTGCC CACTCGTCCCAAATCTTAAC-3'	
5'cdc21-C177A	5'-CAAAATGGCTTTGCCGCCAGCCCATAT TTTTTCACAGTTC-3'	*cdc21-C177A* (pMR16)
3'cdc21-C177A	5'-GAACTGTGAAAAAATATGGGCTGGCG GCAAAGCCATTTTG-3'	
5'CDC21-885u-SalI	5'-AAAAGAGGAGG'TCGACTCCTTTTCCG CATCACTCAT-3'	p_{885}*CDC21*/ pRS425 (= pMR18)
5'CDC21-124u-SalI	5'-AAAAGAGGAGG'TCGACTTGACGCGTT TCCTGAAATA-3'	p_{124}*CDC21*/ pRS425 (=pMR19)
3'CDC21-97-NotI	5'-AAAAGAGGAGGC'GGCCGCTGCCTGTT CTATCTGGCCTAA-3'	$p_{885+124}$*CDC21* /pRS425 (pMR18, 19)
5'CDC21-498u-NotI	5'-AAAAGAGGAGGC'GGCCGCCGGAGAT CTTTCCTTGTTGG-3'	*CDC21*/ pRS306 (= pMR20)
3'CDC21-21d-SpeI	5'-AAAAGAGGAGA'CTAGTTGTTTCTCCTC GTGCTGTCA-3'	
5'cdc21-G139D	5'-GCGATGACGACTATACTGGACAAGATA TTGATCAATTGAAACAGG-3'	*cdc21-G139D* (= pMR21)
3'cdc21-G139D	5'-CCTGTTTCAATTGATCAATATCTTGTC CAGTATAGTCGTCATCGC-3'	

5'CDC21-XhoI	5'-AAAAGAGGAGC'TCGAGATGACTATGG ACGGAAAAAAC-3'	*CDC21*/ pGEX-6P-1 (= pMR22)
3'CDC21-NotI	5'-AAAAGAGGAGGC'GGCCGCTTATACAC TCATTTTCATTTGAAT-3'	
5'MCM1-726u-BamHI	5'-AAAAGAGGAGG'GATCCGAGTAAGAGA TGCCCCACGA-3'	*MCM1*/ pRS425 (= pMR23)
3'MCM1-51d-NotI	5'-AAAAGAGGAGGC'GGCCGCGCTTTTTC CTCTTAATGCTCGT-3'	
5'MSA2-801u-BamHI	5'-AAAAGAGGAGG'GATCCCGACGACGAT CACAAGAAAA-3'	*MSA2*/ pRS425 (= pMR24)
3'MSA2-16d-NotI	5'-AAAAGAGGAGGC'GGCCGCCGAAAACC AAATGGACCTACTC-3'	
5'YKR078W-689u-BamHI	5'-AAAAGAGGAGG'GATCCCCGCTGATTC ACAGGGTAAT-3'	*YKR078W*/ pRS425 (= pMR25)
3'YKR078W-5d-NotI	5'-AAAAGAGGAGGC'GGCCGCCATATTCA TTGGCTTATGTGCTC-3'	
5'YOR066W-879u-BamHI	5'-AAAAGAGGAGG'GATCCTTTTTCGGCC ACCCTATTTA-3'	*YKR066W*/ pRS425 (= pMR25)
3'YOR066W-117d-NotI	5'-AAAAGAGGAGGC'GGCCGCTCAGCTCT GGGAAAATGCTT-3'	
5'CRT1-831u-BamHI	5'-AAAAGAGGAGG'GATCCGCAGCTCCAT GGTACCCTAT-3'	*CRT1*/pRS425 (pMR26, 27)
5'CRT1-1473u-BamHI	5'-AAAAGAGGAGG'GATCCCGGAAGGAGC AGTGTATGGT-3'	
3'CRT1-261d-NotI	5'-AAAAGAGGAGGC'GGCCGCCTGAAGAC GGTGATTCTGAGG-3'	
5'ARL1-366u-BamHI	5'-AAAAGAGGAGG'GATCCCGCACAAAAT CACGACAAAG-3'	*ARL1*/pRS425 (= pMR28)
3'ARL1-107d-NotI	5'-AAAAGAGGAGGC'GGCCGCTGTTTGGA TAGAGCTCCTTGA-3'	
5'UBS1-509u-SalI	5'-AAAAGAGGAGG'TCGACACCATCCAAA CCCAAAATCA-3'	*UBS1*/pRS425 (= pMR29)
3'UBS1-69d-NotI	5'-AAAAGAGGAGGC'GGCCGCACAAATGC CCATGCAAAAA-3'	
5'PPR1-624u-BamHI	5'-AAAAGAGGAGG'GATCCCACACATCGC TTCTTGCAGT-3'	*PPR1*/pRS425 (= pMR30)
3'PPR1-47d-NotI	5'-AAAAGAGGAGGC'GGCCGCTGGTGGC CCTACTTTCAATC-3'	
5'DOT1-1650u-BamHI	5'-AAAAGAGGAGG'GATCCTCCATTTGGC TGTTTGAGGT-3'	*DOT1*/pRS425 (= pMR31)
3'DOT1-14d-NotI	5'-AAAAGAGGAGGC'GGCCGCCCGTTCAA AGTGCCTCATCT-3'	
5'DOT1-FY519,520AA	5'-CTCACTTATCAGATCAACGCCGCCAAT GTTGAGAACATCTTC-3'	*dot1-pip* (= pMR32) PCR 1
3'DOT1-FY519,520AA	5'-GAAGATGTTCTCAACATTGGCGGCGTT GATCTGATAAGTGAG-3'	

5'DOT1-QI516,517AA	5'-AAGAAGCCTCACTTATGCGGCCAACGCCGCCAATGTTG-3'	*dot1-pip* (= pMR32) PCR 2
3'DOT1-QI516,517AA	5'-CAACATTGGCGGCGTTGGCCGCATAAGTGAGGCTTCTT-3'	
5'RAD53-438u-EcoRI	5'-AAAAGAGGAGG'AATTCTGAGATTTCAGCGTG AGGTG-3'	*RAD53*/ pRS423 (= pMR36)
3'RAD53-44d-NotI	5'-AAAAGAGGAGGC'GGCCGCTCTCTTAAAAAGGGGCAGCA-3'	
5'POL30-272u	5'-TCGCACAACTTATGCTGATT-3'	*POL30* colony PCR
3'POL30-178d	5'-ATGTGCTGTCTAGATTAATG-3'	
M13(-40)-fw	5'-GTTTTCCCAGTCACGAC-3'	Sequencing LL1 inserts
YEp13M4-45-rv	5'-AAGGCGCATTTTTCTTCAAA-3'	
5'HIS3-279u	5'-TGCCAGGTATCGTTTGAACA-3'	*HIS3* fragment Southern Blot
3'HIS3-651	5'-ACCTTTGGTGGAGGGAACAT-3'	
Primers for qPCR:		
5'ACT1-771	5'-TCCGGTGATGGTGTTACTCA-3'	*ACT1*
3'ACT1-851	5'-GGCCAAATCGATTCTCAAAA-3'	
5'ADE2-375	5'-TGTGGAACAAGCCAGTGAGA-3'	*ADE2*
3'ADE2-458	5'-GCCAAAGTCCTCGACTTCAA-3'	
5'ADE2-667	5'-TATGCGCCTGCTAGAGTTCC-3'	*ADE2*
3'ADE2-751	5'-CACAACCGGGAAAAGATTTG-3'	
5'ADE2-1214	5'-TTGGAATCATCATGGGATCA-3'	*ADE2*
3'ADE2-1297	5'-CAAATGGAACGCCAAAATCT-3'	
5'URA3-74	5'-TGCACGAAAAGCAAACAAAC-3'	*URA3*
3'URA3-163	5'-TTTTGGGACCTAATGCTTCA-3'	
5'URA3-230	5'-TAAAGGCATTATCCGCCAAG-3'	*URA3*
3'URA3-323	5'-CCCGCAGAGTACTGCAATTT-3'	
5'URA3-651	5'-TAGAACCGTGGATGATGTGG-3'	*URA3*
3'URA3-736	5'-CCTTAGCATCCCTTCCCTTT-3'	
5'HIS3-189	5'-CCATATGATACATGCTCTGG-3'	*HIS3*
3'HIS3-276	5'-GGTGTGATGGTCGTCTATGTG-3'	
5'HIS3-300	5'-CGGTCAAGCTTTTAAAGAGG-3'	*HIS3*
3'HIS3-392	5'-CTCTGGAAAGTGCCTCATCC-3'	
5'HIS3-496	5'-AGCTTTGCAGAGGCTAGCAG-3'	*HIS3*
3'HIS3-580	5'-TGAACGCACTCTCACTACGG-3'	
5'KanR-31	5'-CCGCGATTAAATTCCAACAT-3'	*kanMX6*
3'KanR-120	5'-TCGATAGATTGTCGCACCTG-3'	
5'KanR-166	5'-AAAGGTAGCGTTGCCAATGA-3'	*kanMX6*
3'KanR-254	5'-AAATGCTTGATGGTCGGAAG-3'	
5'KanR-640	5'-GATGTTGGACGAGTCGGAAT-3'	*kanMX6*
3'KanR-733	5'-GCCGTTTCTGTAATGAAGGAG-3'	
5'KanR-85	5'-GATAATGTCGGGCAATCAGG-3'	*kanMX6*

3'KanR-176	5'-ACGCTACCTTTGCCATGTTT-3'	
5'RNR4-922	5'-GCTACCGCTGGTAAGACCAC-3'	*RNR4*
3'RNR4-1016	5'-ATTTCCTTGGATGGGGTAGC-3'	
5'VI-269945	5'-TGGCAAGGGTAAAAACCAGT-3'	~200 bp from telomere VI-R
3'VI-270031	5'-CCATGACCCAGTCCTCATTT-3'	
5'VI-269554	5'-CGGCTGGACTACTTTCTGGA-3'	~600 bp from telomere VI-R
3'VI-269640	5'-CTGAACTGTGCATCCACTCG-3'	
5'VI-259457	5'-AATTTGGCCTACCGCTTTG-3'	~10.7 kb from telomere VI-R
3'VI-259549	5'-TTTTAGACTTTGGGCCTGGA-3'	
5'RNR2-473u	5'-AACCGTTTGGGGAAAGACC-3'	p*RNR2*
3'RNR2-394u	5'-CAGGGAGGTCTGGGTGTG-3'	
5'RNR4-790u	5'-GCGTCTATGTGATTTCGCTTC-3'	p*RNR4*
3'RNR4-734u	5'-GAGCGGGTTGAATAGTTTGC-3'	
5'PMA1-166	5'-GTCGACGACGAAGACAGTGA-3'	*PMA1*
3'PMA1-260	5'-CCGTAAGATGGGTCAGTTTG-3'	
5'URA3-30u	5'-ACAAAAACCTGCAGGAAACG-3'	p*URA3*
3'URA3-57	5'-GGCAGCAACAGGACTAGGAT-3'	
5'VIII-203155	5'-AAGCGGAAATGAAAAATCCA-3'	intergenic region, VIII-R
3'VIII-203241	5'-CTGGGAAACGGTTTGGTAAA-3'	
5'HUG1-78	5'-GAGCAACCGTGTCAACAAGA-3'	*HUG1*
3'HUG1-147	5'-GTTGGCAGAAGGAACGTGAT-3'	
5'HUG1-107	5'-CCGGCTACTTATTCCCCAAG-3'	*HUG1*
3'HUG1-163	5'-GTTCGACGGCAATGATGTT-3'	
5'SML1-43	5'-CAACAACAACAAGCCCCTTC-3'	*SML1*
3'SML1-95	5'-CTAAATTCCGCCATGGTCAC-3'	
5'SML1-78	5'-GACCATGGCGGAATTTAGAA-3'	*SML1*
3'SML1-157	5'-TGCCCATGGAGTTTTGAGTA-3'	
5'RNR1-2390	5'-CTGCAAACGCAACTATTCCA-3'	*RNR1*
3'RNR1-2466	5'-GCTACCTGTTGGAGCTGGAG-3'	
5'RNR2-767	5'-GAGGTATGATGCCCGGTTTA-3'	*RNR2*
3'RNR2-850	5'-ACAACAAGCATGCAAAGTCG-3'	
5'RNR3-2446	5'-TCGAGTGCCATGTCAAATGT-3'	*RNR3*
3'RNR3-2510	5'-ATTGTTTCCGTTGGAACTGC-3'	
5'PGK1-150	5'-TTTGGAACACCACCCAAGAT-3'	*PGK1*
3'PGK1-217	5'-CGTTTCTTTCACCGTTTGGT-3'	

Table 8: *S. cerevisiae* strains used in this study.

Strain	Genotype	Source/ Reference
W303-1A	*MAT***a** *leu2-3,112 trp1-1 can1-100 ura3-1 ade2-1 his3-11,15 rad5-535*	(Thomas and Rothstein, 1989)
W303-1B	*MAT*α *leu2-3,112 trp1-1 can1-100 ura3-1 ade2-1 his3-11,15 rad5-535*	(Thomas and Rothstein, 1989)
W1588-4C	*MAT***a** *ade2-1 can1-100 his3-11,15 leu2-3,112 trp1-1 ura3-1 RAD5*	(Zhao et al., 1998)
YPH499	*MAT***a** *ura3-52 lys2-801_amber ade2-101_ochre trp1-Δ63 his3-Δ200 leu2-Δ1*	Dr. Daniel Gottschling, (Sikorski and Hieter, 1989)
YPH500	*MAT*α *ura3-52 lys2-801_amber ade2-101_ochre trp1-Δ63 his3-Δ200 leu2-Δ1*	Dr. Daniel Gottschling, (Sikorski and Hieter, 1989)
MRY0031	(W303) *MAT***a** *pol30-8*	This study
RS1295 = YLS409	(W303) *MAT*α, *hmr*::*ADE2*	Dr. Rolf Sternglanz (Sussel et al., 1993; Zhang et al., 2000)
PKY090	(W303) *MAT***a** *adh4*::*URA3*-VIIL	(Kaufman et al., 1997)
MRY0803	(W303) *MAT***a**/α *pol30-8*/*POL30 hmr*::*ADE2*/*HMR adh4*::*URA3*-VIIL/VIIL	This study
MRY0948	(W303) *MAT***a**/α *pol30-8*/*POL30 ade2Δ*::*natMX4*/*ade2-1 ura3Δ*::*hphMX4*/*ura3-1 hmr*::*ADE2*/*HMR adh4*::*URA3*-VIIL/VIIL	This study
MRY0999	(W303) *MAT***a**/α *pol30-8*/*POL30 ade2Δ*::*natMX4*/*ade2Δ*::*natMX4 ura3Δ*::*hphMX4*/*ura3Δ*::*hphMX4 hmr*::*ADE2*/*HMR adh4*::*URA3*-VIIL/VIIL	This study
UCC3505	(YPH) *ppr1*::*HIS3 adh4*::*URA3*-VIIL *ADE2*-VR	(Singer et al., 1998)
Figure 3:		
AC437	(W1588-4C) *MAT***a** *URA3*::pGAL	(Chabes and Stillman, 2007)
Figures 4, 9, 21, 24, 26, 27, 29, 30, 31, 32, Table 1:		
MRY0828[1]	(W303) *MAT*α *pol30-8 hmr*::*ADE2*	This study

	adh4::*URA3*-VIIL	
MRY0041	(W303) *MAT*α *pol30-8 hmr*::*ADE2 adh4*::*URA3*-VIIL	This study
Figure 5:		
MRY1448	(W303) *MAT***a**/α *pol30-8*/*POL30 cdc21-216*/*CDC21 hmr*::*ADE2*/*HMR adh4*::*URA3*-VIIL/VIIL	This study
Segregants:		
MRY1655	(W303) *MAT***a** *hmr*::*ADE2 adh4*::*URA3*-VIIL	This study
MRY1657	(W303) *MAT*α *hmr*::*ADE2 adh4*::*URA3*-VIIL	This study
MRY1653	(W303) *MAT***a** *pol30-8 hmr*::*ADE2 adh4*::*URA3*-VIIL	This study
MRY1652	(W303) *MAT*α *pol30-8 hmr*::*ADE2 adh4*::*URA3*-VIIL	This study
MRY1656	(W303) *MAT***a** *cdc21-216 hmr*::*ADE2 adh4*::*URA3*-VIIL	This study
MRY1651	(W303) *MAT*α *cdc21-216 hmr*::*ADE2 adh4*::*URA3*-VIIL	This study
MRY1654	(W303) *MAT***a** *pol30-8 cdc21-216 hmr*::*ADE2 adh4*::*URA3*-VIIL	This study
MRY1650	(W303) *MAT*α *pol30-8 cdc21-216 hmr*::*ADE2 adh4*::*URA3*-VIIL	This study
Figures 6, 7, 23, 28:		
MRY0709	(W303) *MAT***a** *hmr*::*ADE2 adh4*::*URA3-HIS3*-VIIL	This study
MRY0712	(W303) *MAT*α *hmr*::*ADE2 adh4*::*URA3-HIS3*-VIIL	This study
MRY0704	(W303) *MAT***a** *cac1Δ*::*kanMX6 hmr*::*ADE2 adh4*::*URA3-HIS3*-VIIL	This study
MRY0713	(W303) *MAT*α *cac1Δ*::*kanMX6 hmr*::*ADE2 adh4*::*URA3-HIS3*-VIIL	This study
Segregants from the same cross		
MRY0700	(W303) *MAT*α *pol30-8 adh4*::*URA3-HIS3*-VIIL	This study
MRY1527[2]	(W303) *MAT***a** *his3Δ*::*natMX4 adh4*::*URA3-HIS3*-VIIL	This study
MRY1532[2]	(W303) *MAT***a** *sir3Δ*::*kanMX6 his3Δ*::natMX4 *adh4*::*URA3-HIS3*-VIIL	This study
MRY1081[3]	(W303) *MAT***a** *ade2Δ*::*natMX4 ura3Δ*::*hphMX4 hmr*::*ADE2 adh4*::*URA3*-VIIL	This study
MRY1097[3]	(W303) *MAT*α *ade2Δ*::*natMX4 ura3Δ*::*hphMX4 hmr*::*ADE2 adh4*::*URA3*-VIIL	This study
MRY1098[3]	(W303) *MAT***a** *pol30-8 ade2Δ*::*natMX4 ura3Δ*::*hphMX4 hmr*::*ADE2 adh4*::*URA3*-VIIL	This study
MRY1092[3]	(W303) *MAT*α *pol30-8 ade2Δ*::*natMX4*	This study

	ura3Δ::*hphMX4 hmr*::*ADE2 adh4*::*URA3*-VIIL	
MRY1084[3]	(W303) nm (*MAT***a**) *sir3Δ*::*kanMX6 ade2Δ*::*natMX4 ura3Δ*::*hphMX4 hmr*::*ADE2 adh4*::*URA3*-VIIL	This study
MRY1080[3]	(W303) *MAT*α *sir3Δ*::*kanMX6 ade2Δ*::*natMX4 ura3Δ*::*hphMX4 hmr*::*ADE2 adh4*::*URA3*-VIIL	This study
MRY1088[3]	(W303) nm (*MAT***a**) *pol30-8 sir3Δ*::*kanMX6 ade2Δ*::*natMX4 ura3Δ*::*hphMX4 hmr*::*ADE2 adh4*::*URA3*-VIIL	This study
MRY1102[3]	(W303) *MAT*α *pol30-8 sir3Δ*::*kanMX6 ade2Δ*::*natMX4 ura3Δ*::*hphMX4 hmr*::*ADE2 adh4*::*URA3*-VIIL	This study
Figures 7, 25:		
MRY1418[4]	(W303) *MAT*α *his3Δ*::*natMX4 adh4*::*URA3-HIS3*-VIIL	This study
MRY1414[4]	(W303) *MAT*α *pol30-8 his3Δ*::*natMX4 adh4*::*URA3-HIS3*-VIIL	This study
Figures 8, 22:		
MRY1607[5], 1615[5]	(W303) *MAT***a** *ade2Δ*::*natMX4 ura3Δ*::*hphMX4 hmr*::*ADE2 kanMX6*-VIIL	This study
MRY1612[5], 1610[5]	(W303) *MAT*α *ade2Δ*::*natMX4 ura3Δ*::*hphMX4 hmr*::*ADE2 kanMX6*-VIIL	This study
MRY1611[5], 1613[5]	(W303) *MAT***a** *pol30-8 ade2Δ*::*natMX4 ura3Δ*::*hphMX4 hmr*::*ADE2 kanMX6*-VIIL	This study
MRY1617[5], 1619[5]	(W303) *MAT*α *pol30-8 ade2Δ*::*natMX4 ura3Δ*::*hphMX4 hmr*::*ADE2 kanMX6*-VIIL	This study
MRY1609[5], 1622[5]	(W303) nm (*MAT***a**) *sir3Δ*::*CgTRP1 ade2Δ*::*natMX4 ura3Δ*::*hphMX4 hmr*::*ADE2 kanMX6*-VIIL	This study
MRY1614[5], 1620[5]	(W303) *MAT*α *sir3Δ*::*CgTRP1 ade2Δ*::*natMX4 ura3Δ*::*hphMX4 hmr*::*ADE2 kanMX6*-VIIL	This study
MRY1616[5], 1618[5]	(W303) nm (*MAT***a**) *pol30-8 sir3Δ*::*CgTRP1 ade2Δ*::*natMX4 ura3Δ*::*hphMX4 hmr*::*ADE2 kanMX6*-VIIL	This study
MRY1621[5]	(W303) *MAT*α *pol30-8 sir3Δ*::*CgTRP1 ade2Δ*::*natMX4 ura3Δ*::*hphMX4 hmr*::*ADE2 kanMX6*-VIIL	This study
MRY1608[5]	(W303) nm *pol30-8 sir3Δ*::*CgTRP1 ade2Δ*::*natMX4 ura3Δ*::*hphMX4 hmr*::*ADE2 kanMX6*-VIIL	This study
MRY1551, 1556	(W303) *MAT***a** *URA3*	This study
MRY1549, 1554	(W303) *MAT*α *URA3*	This study

MRY1550, 1557, 1558	(W303) *MAT***a** *pol30-8 URA3*	This study
MRY1555	(W303) *MAT*α *pol30-8 URA3*	This study
MRY1547	(W303) *MAT***a** *ppr1*::*HIS3 URA3*	This study
MRY1552	(W303) *MAT*α *ppr1*::*HIS3 URA3*	This study
MRY1548	(W303) *MAT***a** *pol30-8 ppr1*::*HIS3 URA3*	This study
MRY1553	(W303) *MAT*α *pol30-8 ppr1*::*HIS3 URA3*	This study
Segregants from the same diploid parent		
Figures 9, 10, 31:		
MRY0814	(W303) *MAT*α *hmr*::*ADE2 adh4*::*URA3*-VIIL	This study
MRY0811	(W303) *MAT*α *ppr1*::*HIS3 hmr*::*ADE2 adh4*::*URA3*-VIIL	This study
MRY0812	(W303) *MAT*α *ppr1*::*HIS3 pol30-8 hmr*::*ADE2 adh4*::*URA3*-VIIL	This study
MRY0813	(W303) *MAT*α *cac1Δ*::*kanMX6 hmr*::*ADE2 adh4*::*URA3*-VIIL	This study
MRY0815	(W303) *MAT***a** *ppr1*::*HIS3 cac1Δ*::*kanMX6 hmr*::*ADE2 adh4*::*URA3*-VIIL	This study
MRY0810	(W303) *MAT*α *cac1Δ*::*kanMX6 pol30-8 hmr*::*ADE2 adh4*::*URA3*-VIIL	This study
MRY0816	(W303) *MAT***a** *ppr1*::*HIS3 cac1Δ*::*kanMX6 pol30-8 hmr*::*ADE2 adh4*::*URA3*-VIIL	This study
Segregants from the same cross		
MRY0191[6]	(W303) *MAT*α *ppr1*::*HIS3 hmr*::*ADE2 adh4*::*URA3*-VIIL	This study
MRY0180[6]	(W303) *MAT*α *ppr1*::*HIS3 pol30-8 hmr*::*ADE2 adh4*::*URA3*-VIIL	This study
MRY0731	(W303) *MAT*α *ppr1*::*HIS3 hmr*::*ADE2 adh4*::*URA3*-VIIL	This study
Figure 10:		
MRY1510	(W303) *MAT*α *hmr*::*ADE2 adh4*::*URA3*-VIIL	This study
MRY1513	(W303) *MAT*α *asf1Δ*::*CgTRP1 hmr*::*ADE2 adh4*::*URA3*-VIIL	This study
MRY1516	(W303) *MAT*α *pol30-8 hmr*::*ADE2 adh4*::*URA3*-VIIL	This study
MRY1502	(W303) *MAT*α *ppr1*::*HIS3 hmr*::*ADE2 adh4*::*URA3*-VIIL	This study
MRY1511	(W303) *MAT*α *asf1Δ*::*CgTRP1 pol30-8 hmr*::*ADE2 adh4*::*URA3*-VIIL	This study
MRY1508	(W303) *MAT*α *asf1Δ*::*CgTRP1 ppr1*::*HIS3 hmr*::*ADE2 adh4*::*URA3*-VIIL	This study
MRY1514	(W303) *MAT*α *pol30-8 ppr1*::*HIS3 hmr*::*ADE2 adh4*::*URA3*-VIIL	This study
MRY1505	(W303) *MAT*α *asf1Δ*::*CgTRP1 pol30-8 ppr1*::*HIS3 hmr*::*ADE2 adh4*::*URA3*-VIIL	This study

Segregants from the same cross		
MRY0183[6]	(W303) *MAT*α *hmr*::*ADE2 adh4*::*URA3*-VIIL	This study
MRY0181[6]	(W303) *MAT*α *pol30-8 hmr*::*ADE2 adh4*::*URA3*-VIIL	This study
MRY0178[6]	(W303) *MAT*α *sir1Δ*::*kanMX6 hmr*::*ADE2 adh4*::*URA3*-VIIL	This study
MRY0182[6]	(W303) *MAT*α *ppr1*::*HIS3 sir1Δ*::kanMX6 *hmr*::*ADE2 adh4*::*URA3*-VIIL	This study
MRY0190[6]	(W303) *MAT*α *pol30-8 sir1Δ*::*kanMX6 hmr*::*ADE2 adh4*::*URA3*-VIIL	This study
MRY0185[6]	(W303) *MAT***a** *ppr1*::*HIS3 pol30-8 sir1Δ*::*kanMX6 hmr*::*ADE2 adh4*::*URA3*-VIIL	This study
MRY1022	(W303) *MAT***a** *orc1Δ*::*hisG leu2*::*ORC1-LEU2 hmr*::*ADE2 adh4*::*URA3*-VIIL	This study
MRY1024	(W303) *MAT*α *orc1Δ*::*hisG leu2*::*ORC1-LEU2 hmr*::*ADE2 adh4*::*URA3*-VIIL	This study
MRY1025	(W303) *MAT***a** *orc1Δ*::*hisG leu2*::*ORC1-LEU2 ppr1*::*HIS3 hmr*::*ADE2 adh4*::*URA3*-VIIL	This study
MRY1023	(W303) *MAT*α *orc1Δ*::*hisG leu2*::*ORC1-LEU2 ppr1*::*HIS3 hmr*::*ADE2 adh4*::*URA3*-VIIL	This study
Segregants from the same cross		
MRY1030	(W303) *MAT***a** *orc1Δ*::*hisG leu2*::*orc1(Δ1-235)-LEU2 hmr*::*ADE2 adh4*::*URA3*-VIIL	This study
MRY1029	(W303) *MAT*α *orc1Δ*::*hisG leu2*::*orc1(Δ1-235)-LEU2 hmr*::*ADE2 adh4*::*URA3*-VIIL	This study
MRY1028	(W303) *MAT***a** *orc1Δ*::*hisG leu2*::*orc1(Δ1-235)-LEU2 ppr1*::*HIS3 hmr*::*ADE2 adh4*::*URA3*-VIIL	This study
MRY1034	(W303) *MAT*α *orc1Δ*::*hisG leu2*::*orc1(Δ1-235)-LEU2 ppr1*::*HIS3 hmr*::*ADE2 adh4*::*URA3*-VIIL	This study
Segregants from the same cross		
Figures 11, 13, 28:		
MRY1070[7]	(W303) *MAT***a** *ade2Δ*::*natMX4 ura3Δ*::*hphMX4 hmr*::*ADE2 adh4*::*URA3*-VIIL	This study
MRY1077[7]	(W303) *MAT***a** *pol30-8 ade2Δ*::*natMX4 ura3Δ*::*hphMX4 hmr*::*ADE2 adh4*::*URA3*-VIIL	This study
MRY1063[7]	(W303) *MAT***a** *dot1Δ*::*kanMX6 ade2Δ*::*natMX4 ura3Δ*::*hphMX4 hmr*::*ADE2 adh4*::*URA3*-VIIL	This study
MRY1062[7]	(W303) *MAT***a** *pol30-8 dot1Δ*::*kanMX6 ade2Δ*::*natMX4 ura3Δ*::*hphMX4 hmr*::*ADE2 adh4*::*URA3*-VIIL	This study
PKY969	(W303) *MAT***a** *hir1Δ*::*HIS3 asf1Δ*::*TRP1 adh4*::*URA3*-VIIL	(Sharp et al., 2001)

MRY1237	(W303) *MAT*α *hmr*::*ADE2 adh4*::*URA3*-VIIL	This study
MRY1224	(W303) *MAT*α *pol30-8 hmr*::*ADE2 adh4*::*URA3*-VIIL	This study
MRY1229	(W303) *MAT*α *asf1Δ*::*TRP1 hmr*::*ADE2 adh4*::*URA3*-VIIL	This study
MRY1222	(W303) *MAT*α *pol30-8 asf1Δ*::*TRP1 hmr*::*ADE2 adh4*::*URA3*-VIIL	This study
MRY1242	(W303) *MAT*α *dot1Δ*::*kanMX6 hmr*::*ADE2 adh4*::*URA3*-VIIL	This study
MRY1288	(W303) *MAT*α *asf1Δ*::*TRP1 dot1Δ*::*kanMX6 hmr*::*ADE2 adh4*::*URA3*-VIIL	This study
MRY1226	(W303) *MAT*α *pol30-8 asf1Δ*::*TRP1 dot1Δ*::*kanMX6 hmr*::*ADE2 adh4*::*URA3*-VIIL	This study
Segregants from the same diploid parent PKY969 x MRY0041 from which one *DOT1* allele was deleted		
Figures 14, 21:		
MRY1525[2]	(W303) *MAT*α *his3Δ*::*natMX4 adh4*::*URA3-HIS3*-VIIL	This study
MRY1530[2]	(W303) *MAT*α *dot1Δ*::*hphMX4 his3Δ*::*natMX4 adh4*::*URA3-HIS3*-VIIL	This study
MRY1521[2]	(W303) *MAT*α *pol30-8 his3Δ*::*natMX4 adh4*::*URA3-HIS3*-VIIL	This study
MRY1519[2]	(W303) *MAT*α *sir3Δ*::*kanMX6 his3Δ*::*natMX4 adh4*::*URA3-HIS3*-VIIL	This study
MRY1529[2]	(W303) *MAT*α *dot1Δ*::*hphMX4 pol30-8 his3Δ*::*natMX4 adh4*::*URA3-HIS3*-VIIL	This study
MRY1528[2]	(W303) *MAT*α *dot1Δ*::*hphMX4 sir3Δ*::*kanMX6 his3Δ*::*natMX4 adh4*::*URA3-HIS3*-VIIL	This study
MRY1523[2]	(W303) *MAT*α *pol30-8 sir3Δ*::*kanMX6 his3Δ*::*natMX4 adh4*::*URA3-HIS3*-VIIL	This study
MRY1533[2]	(W303) *MAT*α *dot1Δ*::*hphMX4 pol30-8 sir3Δ*::*kanMX6 his3Δ*::*natMX4 adh4*::*URA3-HIS3*-VIIL	This study
MRY1073[7]	(W303) *MAT*α *ade2Δ*::*natMX4 ura3Δ*::*hphMX4 adh4*::*URA3*-VIIL	This study
MRY1072[7]	(W303) *MAT*α *dot1Δ*::*kanMX6 ade2Δ*::*natMX4 ura3Δ*::*hphMX4 adh4*::*URA3*-VIIL	This study
Figures 15, 16, 17, 19, 22, 28, Tables 2, 3, 4, 5:		
MRY1629[7]	(W303) *MAT*α *ade2Δ*::*natMX4 ura3Δ*::*hphMX4 hmr*::*ADE2 adh4*::*URA3*-VIIL	This study
MRY1627[7]	(W303) *MAT*α *dot1Δ*::*kanMX6 ade2Δ*::*natMX4 ura3Δ*::*hphMX4 hmr*::*ADE2 adh4*::*URA3*-VIIL	This study

MRY1071[7]	(W303) *MAT*α *pol30-8 ade2Δ*::*natMX4 ura3Δ*::*hphMX4 hmr*::*ADE2 adh4*::*URA3*-VIIL	This study
MRY1069[7]	(W303) *MAT*α *pol30-8 dot1Δ*::*kanMX6 ade2Δ*::*natMX4 ura3Δ*::*hphMX4 hmr*::*ADE2 adh4*::*URA3*-VIIL	This study
Figure 21:		
MRY1638	(W303) *MAT***a** *PPR1-13MYC*::*kanMX6 ura3Δ*::*hphMX4 adh4*::*URA3*-VIIL	This study
MRY1647	(W303) *MAT***a** *pol30-8 PPR1-13MYC*::*kanMX6 ura3Δ*::*hphMX4 adh4*::*URA3*-VIIL	This study
Segregants from the same cross		
MRY1075[7]	(W303) *MAT***a** *ade2Δ*::*natMX4 ura3Δ*::*hphMX4 adh4*::*URA3*-VIIL	This study
MRY1068[7]	(W303) *MAT*α *pol30-8 ade2Δ*::*natMX4 ura3Δ*::*hphMX4 adh4*::*URA3*-VIIL	This study
MRY1064[7]	(W303) *MAT*α *pol30-8 ade2Δ*::*natMX4 ura3Δ*::*hphMX4 adh4*::*URA3*-VIIL	This study
MRY1076[7]	(W303) *MAT***a** *dot1Δ*::*kanMX6 ade2Δ*::*natMX4 ura3Δ*::*hphMX4 adh4*::*URA3*-VIIL	This study
MRY1065[7]	(W303) *MAT***a** *pol30-8 dot1Δ*::*kanMX6 ade2Δ*::*natMX4 ura3Δ*::*hphMX4 adh4*::*URA3*-VIIL	This study
MRY1074[7]	(W303) *MAT*α *pol30-8 dot1Δ*::*kanMX6 ade2Δ*::*natMX4 ura3Δ*::*hphMX4 adh4*::*URA3*-VIIL	This study
Figure 22:		
MRY1767[1], 1773[1]	(W303) *MAT***a** *adh4*::*URA3*-VIIL	This study
MRY1768[1], 1772[1]	(W303) *MAT***a** *pol30-8 adh4*::*URA3*-VIIL	This study
Figure 23:		
YLL410	(YPH) *MAT***a** *adh4*::*URA3*-VIIL *ADE2*-VR *rad53K227A*::*kanMX4*	(Longhese et al., 2000)
MRY0607	(YPH) *MAT***a** *adh4*::*URA3*-VIIL *ADE2*-VR	This study
MRY0611	(YPH) *MAT*α *adh4*::*URA3*-VIIL *ADE2*-VR	This study
MRY0610	(YPH) *MAT***a** *pol30-8 adh4*::*URA3*-VIIL *ADE2*-VR	This study
MRY0608	(YPH) *MAT*α *pol30-8 adh4*::*URA3*-VIIL *ADE2*-VR	This study
MRY0613	(YPH) *MAT***a** *rad53K227A*::*kanMX4 adh4*::*URA3*-VIIL *ADE2*-VR	This study
MRY0609	(YPH) *MAT*α *rad53K227A*::*kanMX4 adh4*::*URA3*-VIIL *ADE2*-VR	This study

MRY0614	(YPH) *MAT***a** *pol30-8 rad53K227A*::*kanMX4 adh4*::*URA3*-VIIL *ADE2*-VR	This study
MRY0612	(YPH) *MAT*α *pol30-8 rad53K227A*::*kanMX4 adh4*::*URA3*-VIIL *ADE2*-VR	This study
Segregants from the same cross (YLL410 x MRY0388)		
MRY0919[8]	(W303) *MAT*α *hmr*::*ADE2 adh4*::*URA3*-VIIL	This study
MRY0921[8]	(W303) *MAT*α *pol30-8 hmr*::*ADE2 adh4*::*URA3*-VIIL	This study
MRY0920[8]	(W303) *MAT*α *dun1Δ*::*natMX4 hmr*::*ADE2 adh4*::*URA3*-VIIL	This study
MRY0918[8]	(W303) *MAT*α *pol30-8 dun1Δ*::*natMX4 hmr*::*ADE2 adh4*::*URA3*-VIIL	This study
Y235	(W303) *MAT*α *rnr3*::*RNR3-URA3-LEU2*, *crt9-216* (=*cdc21-216*) + pZZ13 [=*HIS3* CEN4 ARS1 *RNR3*-lacZ]	(Zhou and Elledge, 1992)
MRY0915[8]	(W303) *MAT***a** *pol30-8 dun1Δ*::*natMX4 hmr*::*ADE2 adh4*::*URA3*-VIIL	This study
Figures 24, 26, 29:		
MRY0656[9]	(W303) *MAT*α *hmr*::*ADE2 adh4*::*URA3*-VIIL	This study
MRY0654[9]	(W303) *MAT*α *pol30-8 hmr*::*ADE2 adh4*::*URA3*-VIIL	This study
MRY0662[9]	(W303) *MAT*α *asf1Δ*::*TRP1 hmr*::*ADE2 adh4*::*URA3*-VIIL	This study
MRY0660[9]	(W303) *MAT*α *hir1Δ*::*HIS3 hmr*::*ADE2 adh4*::*URA3*-VIIL	This study
MRY0659[9]	(W303) *MAT*α *asf1Δ*::*TRP1 hir1Δ*::*HIS3 hmr*::*ADE2 adh4*::*URA3*-VIIL	This study
MRY0658[9]	(W303) *MAT*α *pol30-8 asf1Δ*::*TRP1 hmr*::*ADE2 adh4*::*URA3*-VIIL	This study
spore 5-3[9]	(W303) *MAT*α *pol30-8 asf1Δ*::*TRP1 hir1Δ*::*HIS3 hmr*::*ADE2 adh4*::*URA3*-VIIL	This study
MRY0827[1]	(W303) *MAT*α *hmr*::*ADE2 adh4*::*URA3*-VIIL	This study
MRY0832[1]	(W303) *MAT*α *hmr*::*ADE2 adh4*::*URA3*-VIIL	This study
Figures 25, 27:		
MRY1082[3]	(W303) *MAT*α *ade2Δ*::*natMX4 ura3Δ*::*hphMX4 adh4*::*URA3*-VIIL	This study
MRY1086[3]	(W303) *MAT*α *pol30-8 ade2Δ*::*natMX4 ura3Δ*::*hphMX4 adh4*::*URA3*-VIIL	This study
MRY1100[3]	(W303) nm *sir3Δ*::*kanMX6 ade2Δ*::*natMX4 ura3Δ*::*hphMX4 adh4*::*URA3*-VIIL	This study
MRY1415[4]	(W303) nm (*MAT*α) *sir3Δ*::*kanMX6 his3Δ*::*natMX4 adh4*::*URA3-HIS3*-VIIL	This study
MRY1749[5]	(W303) *MAT*α *ade2Δ*::*natMX4 ura3Δ*::*hphMX4 hmr*::*ADE2 kanMX6*-VIIL	This study
MRY1751[5]	(W303) *MAT*α *pol30-8 ade2Δ*::*natMX4*	This study

	ura3Δ::*hphMX4 hmr*::*ADE2 kanMX6*-VIIL	
MRY1763[5]	(W303) nm *sir3Δ*::*CgTRP1 ade2Δ*::*natMX4 ura3Δ*::*hphMX4 hmr*::*ADE2 kanMX6*-VIIL	This study
MRY1111	(W303) *MAT***a** *PPR1-13MYC*::*kanMX6 adh4*::*URA3*-VIIL	This study
MRY1104	(W303) *MAT*α *pol30-8 PPR1-13MYC*::*kanMX6 adh4*::*URA3*-VIIL	This study
MRY1108	(W303) *MAT***a** *pol30-8 PPR1-13MYC*::*kanMX6 adh4*::*URA3*-VIIL	This study
MRY1105	(W303) *MAT***a** *pol30-8 adh4*::*URA3*-VIIL	This study
Segregants from the same diploid parent		
Figures 26, 30:		
MRY0661[9]	(W303) *MAT*α *pol30-8 hir1Δ*::*HIS3 hmr*::*ADE2 adh4*::*URA3*-VIIL	This study
MRY0655[9]	(W303) *MAT*α *pol30-8 asf1Δ*::*TRP1 hir1Δ*::*HIS3 hmr*::*ADE2 adh4*::*URA3*-VIIL	This study
MRY0462	(W303) *MAT*α *cac1Δ*::*kanMX6 hmr*::*ADE2 adh4*::*URA3*-VIIL	This study
Figure 27:		
MRY1090[3]	(W303) *MAT***a** *ade2Δ*::*natMX4 ura3Δ*::*hphMX4 adh4*::*URA3*-VIIL	This study
MRY1101[3]	(W303) *MAT***a** *pol30-8 ade2Δ*::*natMX4 ura3Δ*::*hphMX4 adh4*::*URA3*-VIIL	This study
Figure 28:		
MRY1807	(W303) *MAT***a** *PPR1-13MYC*::*kanMX6 ura3Δ*::*hphMX4 hmr*::*ADE2 adh4*::*URA3*-VIIL	This study
MRY1811	(W303) *MAT***a** *asf1Δ*::*TRP1 PPR1-13MYC*::*kanMX6 ura3Δ*::*hphMX4 hmr*::*ADE2 adh4*::*URA3*-VIIL	This study
MRY1802	(W303) *MAT***a** *dot1Δ*::natMX4 *PPR1-13MYC*::*kanMX6 ura3Δ*::*hphMX4 hmr*::*ADE2 adh4*::*URA3*-VIIL	This study
MRY1797	(W303) *MAT***a** *asf1Δ*::*TRP1 dot1Δ*::*natMX4 PPR1-13MYC*::*kanMX6 ura3Δ*::*hphMX4 hmr*::*ADE2 adh4*::*URA3*-VIIL	This study
Segregants from the same diploid parent		
MRY1066[7]	(W303) *MAT*α *ade2Δ*::*natMX4 ura3Δ*::*hphMX4 hmr*::*ADE2 adh4*::*URA3*-VIIL	This study
MRY1726	MRY0999 *ard1Δ*::*CgTRP1*/*ARD1*	This study
MRY1866, 1867	MRY1081 *bas1Δ*::*CgTRP1 pho2Δ*::*SkHIS3*	This study
MRY1871, 1872	MRY1063 *bas1Δ*::*CgTRP1 pho2Δ*::*SkHIS3*	This study
MRY1868, 1869	MRY1098 *bas1Δ*::*CgTRP1 pho2Δ*::*SkHIS3*	This study

Figure 29:		
MRY0830[1]	*MAT***a** *hmr*::*ADE2 adh4*::*URA3*-VIIL	This study
MRY0834[1]	*MAT***a** *pol30-8 hmr*::*ADE2 adh4*::*URA3*-VIIL	This study
MRY0903	(W303) *MAT***a**/MATα *hmr*::*ADE2*/*hmr*::*ADE2 adh4*::*URA3*-VIIL/*adh4*::*URA3*-VIIL	This study
MRY0906	(W303) *MAT***a**/MATα *hmr*::*ADE2*/*HMR adh4*::*URA3*-VIIL/VIIL	This study
MRY0909	(W303) *MAT***a**/MATα *pol30-8*/*pol30-8 hmr*::*ADE2*/*hmr*::*ADE2 adh4*::*URA3*-VIIL/*adh4*::*URA3*-VIIL	This study
MRY0912	(W303) *MAT***a**/MATα *pol30-8*/*pol30-8 hmr*::*ADE2*/*HMR adh4*::*URA3*-VIIL/VIIL	This study
Figure 30:		
MRY0388	(YPH) *MAT*α *pol30-8 ADE2*-VR *adh4*::*URA3*-VIIL	This study
MRY0436	(W303) *MAT*α *hmr*::*ADE2 adh4*::*URA3*-VIIL	This study
MRY0438	(W303) *MAT***a** *pol30-8 hmr*::*ADE2 adh4*::*URA3*-VIIL	This study
MRY0440	(W303) *MAT*α *msa2Δ*::*kanMX6 hmr*::*ADE2 adh4*::*URA3*-VIIL	This study
MRY0442	(W303) *MAT*α *msa2Δ*::*kanMX6 hmr*::*ADE2 adh4*::*URA3*-VIIL	This study
MRY0445	(W303) *MAT***a** *msa2Δ*::*kanMX6 pol30-8 hmr*::*ADE2 adh4*::*URA3*-VIIL	This study
MRY0446	(W303) *MAT*α *msa2Δ*::*kanMX6 pol30-8 hmr*::*ADE2 adh4*::*URA3*-VIIL	This study
Segregants from the same diploid parent		
Figure 31:		
MRY0788	MRY0180 *tup1Δ*::*kanMX6*	This study
MRY0792	MRY0191 *tup1Δ*::*kanMX6*	This study
MRY0793	MRY0191 *tup1Δ*::*kanMX6*	This study
MRY0798	MRY0041 *tup1Δ*::*kanMX6*	This study
MRY0797	MRY0041 *tup1Δ*::*kanMX6*	This study
Figure 32:		
MRY0036	(W303) *MAT*α *pol30Δ*::*hisG hmr*::*ADE2 adh4*::*URA3*-VIIL + pBL230-8	This study

[1] Segregants of MRY0041 x W303-1A
[2] Segregants from the same diploid parent
[3] Segregants from the same diploid parent
[4] Segregants from the same diploid parent
[5] Segregants from the same diploid parent MRY1606 (see Material and Methods)
[6] Segregants from the same diploid parent
[7] Segregants from the same diploid parent
[8] Segregants from the same diploid parent
[9] Segregants from the same cross

REFERENCES

Abraham, D.S., and Vershon, A.K. (2005). N-terminal arm of Mcm1 is required for transcription of a subset of genes involved in maintenance of the cell wall. Eukaryot Cell *4*, 1808-1819.

Abraham, J., Nasmyth, K.A., Strathern, J.N., Klar, A.J., and Hicks, J.B. (1984). Regulation of mating-type information in yeast. Negative control requiring sequences both 5' and 3' to the regulated region. J Mol Biol *176*, 307-331.

Adkins, M.W., Howar, S.R., and Tyler, J.K. (2004). Chromatin disassembly mediated by the histone chaperone Asf1 is essential for transcriptional activation of the yeast PHO5 and PHO8 genes. Mol Cell *14*, 657-666.

Albertsen, M., Bellahn, I., Kramer, R., and Waffenschmidt, S. (2003). Localization and function of the yeast multidrug transporter Tpo1p. J Biol Chem *278*, 12820-12825.

Amberg, D.C., Burke, D.J., and Strathern, J.N. (2005). Methods in Yeast Genetics: A Cold Spring Harbor Laboratory Course Manual (Cold Spring Harbor, NY, Cold Spring Harbor Laboratory Press).

Andrulis, E.D., Neiman, A.M., Zappulla, D.C., and Sternglanz, R. (1998). Perinuclear localization of chromatin facilitates transcriptional silencing. Nature *394*, 592-595.

Aparicio, O.M., Billington, B.L., and Gottschling, D.E. (1991). Modifiers of position effect are shared between telomeric and silent mating-type loci in S. cerevisiae. Cell *66*, 1279-1287.

Aparicio, O.M., and Gottschling, D.E. (1994). Overcoming telomeric silencing: a *trans*-activator competes to establish gene expression in a cell cycle-dependent way. Genes Dev *8*, 1133-1146.

Arias, E.E., and Walter, J.C. (2006). PCNA functions as a molecular platform to trigger Cdt1 destruction and prevent re-replication. Nat Cell Biol *8*, 84-90.

Ashe, M., de Bruin, R.A., Kalashnikova, T., McDonald, W.H., Yates, J.R., 3rd, and Wittenberg, C. (2008). The SBF- and MBF-associated protein Msa1 is required for proper timing of G1-specific transcription in Saccharomyces cerevisiae. J Biol Chem *283*, 6040-6049.

Astrom, S.U., Okamura, S.M., and Rine, J. (1999). Yeast cell-type regulation of DNA repair. Nature *397*, 310.

Axelrod, A., and Rine, J. (1991). A role for CDC7 in repression of transcription at the silent mating-type locus HMR in Saccharomyces cerevisiae. Mol Cell Biol *11*, 1080-1091.

Ayyagari, R., Impellizzeri, K.J., Yoder, B.L., Gary, S.L., and Burgers, P.M. (1995). A mutational analysis of the yeast proliferating cell nuclear antigen indicates distinct roles in DNA replication and DNA repair. Mol Cell Biol *15*, 4420-4429.

Bairoch, A., Bucher, P., and Hofmann, K. (1997). The PROSITE database, its status in 1997. Nucleic Acids Res *25*, 217-221.

Bannister, A.J., Zegerman, P., Partridge, J.F., Miska, E.A., Thomas, J.O., Allshire, R.C., and Kouzarides, T. (2001). Selective recognition of methylated lysine 9 on histone H3 by the HP1 chromo domain. Nature *410*, 120-124.

Bashkirov, V.I., Bashkirova, E.V., Haghnazari, E., and Heyer, W.D. (2003). Direct kinase-to-kinase signaling mediated by the FHA phosphoprotein recognition domain of the Dun1 DNA damage checkpoint kinase. Mol Cell Biol *23*, 1441-1452.

Basrai, M.A., Velculescu, V.E., Kinzler, K.W., and Hieter, P. (1999). NORF5/HUG1 is a component of the MEC1-mediated checkpoint response to DNA damage and replication arrest in Saccharomyces cerevisiae. Mol Cell Biol *19*, 7041-7049.

Bauer, G.A., and Burgers, P.M. (1990). Molecular cloning, structure and expression of the yeast proliferating cell nuclear antigen gene. Nucleic Acids Res *18*, 261-265.

Baur, J.A., Zou, Y., Shay, J.W., and Wright, W.E. (2001). Telomere position effect in human cells. Science *292*, 2075-2077.

Bazett-Jones, D.P., Li, R., Fussner, E., Nisman, R., and Dehghani, H. (2008). Elucidating chromatin and nuclear domain architecture with electron spectroscopic imaging. Chromosome Res *16*, 397-412.

Bell, S.P., and Dutta, A. (2002). DNA replication in eukaryotic cells. Annu Rev Biochem *71*, 333-374.

Bell, S.P., Kobayashi, R., and Stillman, B. (1993). Yeast origin recognition complex functions in transcription silencing and DNA replication. Science *262*, 1844-1849.

Boeke, J.D., LaCroute, F., and Fink, G.R. (1984). A positive selection for mutants lacking orotidine-5'-phosphate decarboxylase activity in yeast: 5-fluoro-orotic acid resistance. Mol Gen Genet *197*, 345-346.

Bourns, B.D., Alexander, M.K., Smith, A.M., and Zakian, V.A. (1998). Sir proteins, Rif proteins, and Cdc13p bind Saccharomyces telomeres in vivo. Mol Cell Biol *18*, 5600-5608.

Bowman, G.D., O'Donnell, M., and Kuriyan, J. (2004). Structural analysis of a eukaryotic sliding DNA clamp-clamp loader complex. Nature *429*, 724-730.

Braunstein, M., Rose, A.B., Holmes, S.G., Allis, C.D., and Broach, J.R. (1993). Transcriptional silencing in yeast is associated with reduced nucleosome acetylation. Genes Dev *7*, 592-604.

Bravo, R., and Celis, J.E. (1980). A search for differential polypeptide synthesis throughout the cell cycle of HeLa cells. J Cell Biol *84*, 795-802.

Bravo, R., Fey, S.J., Bellatin, J., Larsen, P.M., Arevalo, J., and Celis, J.E. (1981). Identification of a nuclear and of a cytoplasmic polypeptide whose relative proportions are sensitive to changes in the rate of cell proliferation. Exp Cell Res *136*, 311-319.

Brennan, M.B., and Struhl, K. (1980). Mechanisms of increasing expression of a yeast gene in Escherichia coli. J Mol Biol *136*, 333-338.

Broderick, R., and Nasheuer, H.P. (2009). Regulation of Cdc45 in the cell cycle and after DNA damage. Biochem Soc Trans *37*, 926-930.

Buchberger, J.R., Onishi, M., Li, G., Seebacher, J., Rudner, A.D., Gygi, S.P., and Moazed, D. (2008). Sir3-nucleosome interactions in spreading of silent chromatin in Saccharomyces cerevisiae. Mol Cell Biol *28*, 6903-6918.

Bustin, M., Catez, F., and Lim, J.H. (2005). The dynamics of histone H1 function in chromatin. Mol Cell *17*, 617-620.

Bylund, G.O., and Burgers, P.M. (2005). Replication protein A-directed unloading of PCNA by the Ctf18 cohesion establishment complex. Mol Cell Biol *25*, 5445-5455.

Byun, T.S., Pacek, M., Yee, M.C., Walter, J.C., and Cimprich, K.A. (2005). Functional uncoupling of MCM helicase and DNA polymerase activities activates the ATR-dependent checkpoint. Genes Dev *19*, 1040-1052.

Ceriani, M.F. (2007). Basic protocols for Drosophila S2 cell line: maintenance and transfection. Methods Mol Biol *362*, 415-422.

Chabes, A., Domkin, V., and Thelander, L. (1999). Yeast Sml1, a protein inhibitor of ribonucleotide reductase. J Biol Chem *274*, 36679-36683.

Chabes, A., Georgieva, B., Domkin, V., Zhao, X., Rothstein, R., and Thelander, L. (2003). Survival of DNA damage in yeast directly depends on increased dNTP levels allowed by relaxed feedback inhibition of ribonucleotide reductase. Cell *112*, 391-401.

Chabes, A., and Stillman, B. (2007). Constitutively high dNTP concentration inhibits cell cycle progression and the DNA damage checkpoint in yeast Saccharomyces cerevisiae. Proc Natl Acad Sci U S A *104*, 1183-1188.

Chabes, A., and Thelander, L. (2003). DNA building blocks at the foundation of better survival. Cell Cycle *2*, 171-173.

Chen, L., and Widom, J. (2005). Mechanism of transcriptional silencing in yeast. Cell *120*, 37-48.

Cherry, J.M., Ball, C., Weng, S., Juvik, G., Schmidt, R., Adler, C., Dunn, B., Dwight, S., Riles, L., Mortimer, R.K.*, et al.* (1997). Genetic and physical maps of Saccharomyces cerevisiae. Nature *387*, 67-73.

Chi, M.H., and Shore, D. (1996). SUM1-1, a dominant suppressor of SIR mutations in Saccharomyces cerevisiae, increases transcriptional silencing at telomeres and HM mating-type loci and decreases chromosome stability. Mol Cell Biol *16*, 4281-4294.

Christianson, T.W., Sikorski, R.S., Dante, M., Shero, J.H., and Hieter, P. (1992). Multifunctional yeast high-copy-number shuttle vectors. Gene *110*, 119-122.

Chuang, L.S., Ian, H.I., Koh, T.W., Ng, H.H., Xu, G., and Li, B.F. (1997). Human DNA-(cytosine-5) methyltransferase-PCNA complex as a target for $p21^{WAF1}$. Science *277*, 1996-2000.

Collart, M.A., and Oliviero, S. (2001). Preparation of yeast RNA. Curr Protoc Mol Biol *Chapter 13*, Unit13 12.

Craven, R.J., and Petes, T.D. (2000). Involvement of the checkpoint protein Mec1p in silencing of gene expression at telomeres in Saccharomyces cerevisiae. Mol Cell Biol *20*, 2378-2384.

Dai, M., Wang, P., Boyd, A.D., Kostov, G., Athey, B., Jones, E.G., Bunney, W.E., Myers, R.M., Speed, T.P., Akil, H.*, et al.* (2005). Evolving gene/transcript definitions significantly alter the interpretation of GeneChip data. Nucleic Acids Res *33*, e175.

Davie, J.K., Edmondson, D.G., Coco, C.B., and Dent, S.Y. (2003). Tup1-Ssn6 interacts with multiple class I histone deacetylases in vivo. J Biol Chem *278*, 50158-50162.

Davie, J.K., Trumbly, R.J., and Dent, S.Y. (2002). Histone-dependent association of Tup1-Ssn6 with repressed genes in vivo. Mol Cell Biol *22*, 693-703.

Deal, R.B., Henikoff, J.G., and Henikoff, S. (2010). Genome-wide kinetics of nucleosome turnover determined by metabolic labeling of histones. Science *328*, 1161-1164.

Denis, V., Boucherie, H., Monribot, C., and Daignan-Fornier, B. (1998). Role of the myb-like protein bas1p in Saccharomyces cerevisiae: a proteome analysis. Mol Microbiol *30*, 557-566.

Denis, V., and Daignan-Fornier, B. (1998). Synthesis of glutamine, glycine and 10-formyl tetrahydrofolate is coregulated with purine biosynthesis in Saccharomyces cerevisiae. Mol Gen Genet *259*, 246-255.

DeRisi, J.L., Iyer, V.R., and Brown, P.O. (1997). Exploring the metabolic and genetic control of gene expression on a genomic scale. Science *278*, 680-686.

Dhillon, N., and Kamakaka, R.T. (2000). A histone variant, Htz1p, and a Sir1p-like protein, Esc2p, mediate silencing at HMR. Mol Cell *6*, 769-780.

Diede, S.J., and Gottschling, D.E. (1999). Telomerase-mediated telomere addition in vivo requires DNA primase and DNA polymerases alpha and delta. Cell *99*, 723-733.

Dimitri, P., Caizzi, R., Giordano, E., Carmela Accardo, M., Lattanzi, G., and Biamonti, G. (2009). Constitutive heterochromatin: a surprising variety of expressed sequences. Chromosoma *118*, 419-435.

Dubey, D.D., Davis, L.R., Greenfeder, S.A., Ong, L.Y., Zhu, J.G., Broach, J.R., Newlon, C.S., and Huberman, J.A. (1991). Evidence suggesting that the ARS elements associated with silencers of the yeast mating-type locus HML do not function as chromosomal DNA replication origins. Mol Cell Biol *11*, 5346-5355.

Echols, H., and Goodman, M.F. (1991). Fidelity mechanisms in DNA replication. Annu Rev Biochem *60*, 477-511.

Edmondson, D.G., Smith, M.M., and Roth, S.Y. (1996). Repression domain of the yeast global repressor Tup1 interacts directly with histones H3 and H4. Genes Dev *10*, 1247-1259.

Ehrenhofer-Murray, A.E., Kamakaka, R.T., and Rine, J. (1999). A role for the replication proteins PCNA, RF-C, polymerase epsilon and Cdc45 in transcriptional silencing in Saccharomyces cerevisiae. Genetics *153*, 1171-1182.

Ehrenhofer-Murray, A.E., Rivier, D.H., and Rine, J. (1997). The role of Sas2, an acetyltransferase homologue of Saccharomyces cerevisiae, in silencing and ORC function. Genetics *145*, 923-934.

Emili, A., Schieltz, D.M., Yates, J.R., 3rd, and Hartwell, L.H. (2001). Dynamic interaction of DNA damage checkpoint protein Rad53 with chromatin assembly factor Asf1. Mol Cell *7*, 13-20.

Enomoto, S., Longtine, M.S., and Berman, J. (1994). TEL+CEN antagonism on plasmids involves telomere repeat sequences tracts and gene products that interact with chromosomal telomeres. Chromosoma *103*, 237-250.

Enomoto, S., McCune-Zierath, P.D., Gerami-Nejad, M., Sanders, M.A., and Berman, J. (1997). RLF2, a subunit of yeast chromatin assembly factor-I, is required for telomeric chromatin function in vivo. Genes Dev *11*, 358-370.

Fanti, L., Giovinazzo, G., Berloco, M., and Pimpinelli, S. (1998). The heterochromatin protein 1 prevents telomere fusions in Drosophila. Mol Cell *2*, 527-538.

Feldman, J.B., Hicks, J.B., and Broach, J.R. (1984). Identification of sites required for repression of a silent mating type locus in yeast. J Mol Biol *178*, 815-834.

Feng, Q., Wang, H., Ng, H.H., Erdjument-Bromage, H., Tempst, P., Struhl, K., and Zhang, Y. (2002). Methylation of H3-lysine 79 is mediated by a new family of HMTases without a SET domain. Curr Biol *12*, 1052-1058.

Ferguson, B.M., and Fangman, W.L. (1992). A position effect on the time of replication origin activation in yeast. Cell *68*, 333-339.

Fillingham, J., Recht, J., Silva, A.C., Suter, B., Emili, A., Stagljar, I., Krogan, N.J., Allis, C.D., Keogh, M.C., and Greenblatt, J.F. (2008). Chaperone control of the activity and specificity of the histone H3 acetyltransferase Rtt109. Mol Cell Biol *28*, 4342-4353.

Foss, M., McNally, F.J., Laurenson, P., and Rine, J. (1993). Origin recognition complex (ORC) in transcriptional silencing and DNA replication in S. cerevisiae. Science *262*, 1838-1844.

Fox, C.A., Ehrenhofer-Murray, A.E., Loo, S., and Rine, J. (1997). The origin recognition complex, *SIR1*, and the S phase requirement for silencing. Science *276*, 1547-1551.

Franco, A.A., Lam, W.M., Burgers, P.M., and Kaufman, P.D. (2005). Histone deposition protein Asf1 maintains DNA replisome integrity and interacts with replication factor C. Genes Dev *19*, 1365-1375.

Franklin, R.E., and Gosling, R.G. (1953). Molecular configuration in sodium thymonucleate. Nature *171*, 740-741.

Frederiks, F., Heynen, G.J., van Deventer, S.J., Janssen, H., and van Leeuwen, F. (2009). Two Dot1 isoforms in Saccharomyces cerevisiae as a result of leaky scanning by the ribosome. Nucleic Acids Res *37*, 7047-7058.

Fujioka, A., Terai, K., Itoh, R.E., Aoki, K., Nakamura, T., Kuroda, S., Nishida, E., and Matsuda, M. (2006). Dynamics of the Ras/ERK MAPK cascade as monitored by fluorescent probes. J Biol Chem *281*, 8917-8926.

Fukushima, M., Fujioka, A., Uchida, J., Nakagawa, F., and Takechi, T. (2001). Thymidylate synthase (TS) and ribonucleotide reductase (RNR) may be involved in acquired resistance to 5-fluorouracil (5-FU) in human cancer xenografts in vivo. Eur J Cancer *37*, 1681-1687.

Gaillard, P.H., Martini, E.M., Kaufman, P.D., Stillman, B., Moustacchi, E., and Almouzni, G. (1996). Chromatin assembly coupled to DNA repair: a new role for chromatin assembly factor I. Cell *86*, 887-896.

Game, J.C., and Kaufman, P.D. (1999). Role of Saccharomyces cerevisiae chromatin assembly factor-I in repair of ultraviolet radiation damage in vivo. Genetics *151*, 485-497.

Gao, H., Cervantes, R.B., Mandell, E.K., Otero, J.H., and Lundblad, V. (2007). RPA-like proteins mediate yeast telomere function. Nat Struct Mol Biol *14*, 208-214.

Garcia-Cao, M., O'Sullivan, R., Peters, A.H., Jenuwein, T., and Blasco, M.A. (2004). Epigenetic regulation of telomere length in mammalian cells by the Suv39h1 and Suv39h2 histone methyltransferases. Nat Genet *36*, 94-99.

Gardner, K.A., Rine, J., and Fox, C.A. (1999). A region of the Sir1 protein dedicated to recognition of a silencer and required for interaction with the Orc1 protein in saccharomyces cerevisiae. Genetics *151*, 31-44.

Gasch, A.P., Huang, M., Metzner, S., Botstein, D., Elledge, S.J., and Brown, P.O. (2001). Genomic expression responses to DNA-damaging agents and the regulatory role of the yeast ATR homolog Mec1p. Mol Biol Cell *12*, 2987-3003.

Gavin, A.C., Bosche, M., Krause, R., Grandi, P., Marzioch, M., Bauer, A., Schultz, J., Rick, J.M., Michon, A.M., Cruciat, C.M*., et al.* (2002). Functional organization of the yeast proteome by systematic analysis of protein complexes. Nature *415*, 141-147.

Genome Reference Consortium (2009). Human Genome Assembly Information: Assembly Statistics for GRCh37

Gerst, J.E., Ferguson, K., Vojtek, A., Wigler, M., and Field, J. (1991). CAP is a bifunctional component of the Saccharomyces cerevisiae adenylyl cyclase complex. Mol Cell Biol *11*, 1248-1257.

Ghidelli, S., Donze, D., Dhillon, N., and Kamakaka, R.T. (2001). Sir2p exists in two nucleosome-binding complexes with distinct deacetylase activities. EMBO J *20*, 4522-4535.

Giannattasio, M., Lazzaro, F., Plevani, P., and Muzi-Falconi, M. (2005). The DNA damage checkpoint response requires histone H2B ubiquitination by Rad6-Bre1 and H3 methylation by Dot1. J Biol Chem *280*, 9879-9886.

Gilbert, C.S., Green, C.M., and Lowndes, N.F. (2001). Budding yeast Rad9 is an ATP-dependent Rad53 activating machine. Mol Cell *8*, 129-136.

Gilljam, K.M., Feyzi, E., Aas, P.A., Sousa, M.M., Muller, R., Vagbo, C.B., Catterall, T.C., Liabakk, N.B., Slupphaug, G., Drablos, F*., et al.* (2009). Identification of a novel, widespread, and functionally important PCNA-binding motif. J Cell Biol *186*, 645-654.

Goldstein, A.L., and McCusker, J.H. (1999). Three new dominant drug resistance cassettes for gene disruption in Saccharomyces cerevisiae. Yeast *15*, 1541-1553.

Gotta, M., Laroche, T., Formenton, A., Maillet, L., Scherthan, H., and Gasser, S.M. (1996). The clustering of telomeres and colocalization with Rap1, Sir3, and Sir4 proteins in wild-type Saccharomyces cerevisiae. J Cell Biol *134*, 1349-1363.

Gottschling, D.E. (1992). Telomere-proximal DNA in Saccharomyces cerevisiae is refractory to methyltransferase activity in vivo. Proc Natl Acad Sci USA *89*, 4062-4065.

Gottschling, D.E., Aparicio, O.M., Billington, B.L., and Zakian, V.A. (1990). Position effect at S. cerevisiae telomeres: reversible repression of Pol II transcription. Cell *63*, 751-762.

Green, S.R., and Johnson, A.D. (2004). Promoter-dependent roles for the Srb10 cyclin-dependent kinase and the Hda1 deacetylase in Tup1-mediated repression in Saccharomyces cerevisiae. Mol Biol Cell *15*, 4191-4202.

Grenon, M., Costelloe, T., Jimeno, S., O'Shaughnessy, A., Fitzgerald, J., Zgheib, O., Degerth, L., and Lowndes, N.F. (2007). Docking onto chromatin via the Saccharomyces cerevisiae Rad9 Tudor domain. Yeast *24*, 105-119.

Gulbis, J.M., Kelman, Z., Hurwitz, J., O'Donnell, M., and Kuriyan, J. (1996). Structure of the C-terminal region of p21(WAF1/CIP1) complexed with human PCNA. Cell *87*, 297-306.

Gunjan, A., and Verreault, A. (2003). A Rad53 kinase-dependent surveillance mechanism that regulates histone protein levels in S. cerevisiae. Cell *115*, 537-549.

Guthrie, C., and Fink, G.R., eds. (2002). Guide to Yeast Genetics and Molecular and Cellular Biology (San Diego, Academic Science).

Han, J., Zhou, H., Horazdovsky, B., Zhang, K., Xu, R.M., and Zhang, Z. (2007). Rtt109 acetylates histone H3 lysine 56 and functions in DNA replication. Science *315*, 653-655.

Harder, J., and Follmann, H. (1990). Identification of a free radical and oxygen dependence of ribonucleotide reductase in yeast. Free Radic Res Commun *10*, 281-286.

Hardman, J.G., Limbird, L.E., and Goodman Gilman, A., eds. (2001). Goodman and Gilman's the pharmacological basis of therapeutics, 10th edn (New York, McGraw-Hill).

Hartwell, L.H., Culotti, J., and Reid, B. (1970). Genetic control of the cell-division cycle in yeast. I. Detection of mutants. Proc Natl Acad Sci U S A *66*, 352-359.

Hartwell, L.H., Mortimer, R.K., Culotti, J., and Culotti, M. (1973). Genetic Control of the Cell Division Cycle in Yeast: V. Genetic Analysis of cdc Mutants. Genetics *74*, 267-286.

Hawthorne, D.C. (1963). A Deletion in Yeast and Its Bearing on the Structure of the Mating Type Locus. Genetics *48*, 1727-1729.

Hecht, A., Laroche, T., Strahl-Bolsinger, S., Gasser, S.M., and Grunstein, M. (1995). Histone H3 and H4 N-termini interact with SIR3 and SIR4 proteins: a molecular model for the formation of heterochromatin in yeast. Cell *80*, 583-592.

Heitz, E. (1928). Das Heterochromatin der Moose. Jb Wiss Bot *69*, 762-818.

Herskowitz, I. (1988). The Hawthorne deletion twenty-five years later. Genetics *120*, 857-861.

Ho, L., and Crabtree, G.R. (2010). Chromatin remodelling during development. Nature *463*, 474-484.

Hochreiter, S., Clevert, D.A., and Obermayer, K. (2006). A new summarization method for Affymetrix probe level data. Bioinformatics *22*, 943-949.

Hoege, C., Pfander, B., Moldovan, G.L., Pyrowolakis, G., and Jentsch, S. (2002). RAD6-dependent DNA repair is linked to modification of PCNA by ubiquitin and SUMO. Nature *419*, 135-141.

Hoek, M., and Stillman, B. (2003). Chromatin assembly factor 1 is essential and couples chromatin assembly to DNA replication in vivo. Proc Natl Acad Sci U S A *100*, 12183-12188.

Hoffman, C.S., and Winston, F. (1987). A ten-minute DNA preparation from yeast efficiently releases autonomous plasmids for transformation of Escherichia coli. Gene *57*, 267-272.

Holliday, R. (1987). The inheritance of epigenetic defects. Science *238*, 163-170.

Hoppe, G.J., Tanny, J.C., Rudner, A.D., Gerber, S.A., Danaie, S., Gygi, S.P., and Moazed, D. (2002). Steps in assembly of silent chromatin in yeast: Sir3-independent binding of a Sir2/Sir4 complex to silencers and role for Sir2-dependent deacetylation. Mol Cell Biol *22*, 4167-4180.

Hu, F., Alcasabas, A.A., and Elledge, S.J. (2001). Asf1 links Rad53 to control of chromatin assembly. Genes Dev *15*, 1061-1066.

Huang, L., Zhang, W., and Roth, S.Y. (1997). Amino termini of histones H3 and H4 are required for a1-alpha2 repression in yeast. Mol Cell Biol *17*, 6555-6562.

Huang, M., and Elledge, S.J. (1997). Identification of RNR4, encoding a second essential small subunit of ribonucleotide reductase in Saccharomyces cerevisiae. Mol Cell Biol *17*, 6105-6113.

Huang, M., Zhou, Z., and Elledge, S.J. (1998). The DNA replication and damage checkpoint pathways induce transcription by inhibition of the Crt1 repressor. Cell *94*, 595-605.

Huang, S., Zhou, H., Katzmann, D., Hochstrasser, M., Atanasova, E., and Zhang, Z. (2005). Rtt106p is a histone chaperone involved in heterochromatin-mediated silencing. Proc Natl Acad Sci U S A *102*, 13410-13415.

Huang, S., Zhou, H., Tarara, J., and Zhang, Z. (2007). A novel role for histone chaperones CAF-1 and Rtt106p in heterochromatin silencing. EMBO J *26*, 2274-2283.

Imai, S., Armstrong, C.M., Kaeberlein, M., and Guarente, L. (2000). Transcriptional silencing and longevity protein Sir2 is an NAD-dependent histone deacetylase. Nature *403*, 795-800.

investigators, I.M.P.A.o.C.C.T.I. (1995). Efficacy of adjuvant fluorouracil and folinic acid in colon cancer. Lancet *345*, 939-944.

Jackson, V., and Chalkley, R. (1985). Histone segregation on replicating chromatin. Biochemistry *24*, 6930-6938.

Jackson, V., Granner, D.K., and Chalkley, R. (1975). Deposition of histones onto replicating chromosomes. Proc Natl Acad Sci U S A *72*, 4440-4444.

Jelinsky, S.A., Estep, P., Church, G.M., and Samson, L.D. (2000). Regulatory networks revealed by transcriptional profiling of damaged Saccharomyces cerevisiae cells: Rpn4 links base excision repair with proteasomes. Mol Cell Biol *20*, 8157-8167.

Jelinsky, S.A., and Samson, L.D. (1999). Global response of Saccharomyces cerevisiae to an alkylating agent. Proc Natl Acad Sci U S A *96*, 1486-1491.

Johnson, A.D., and Herskowitz, I. (1985). A repressor (MAT alpha 2 Product) and its operator control expression of a set of cell type specific genes in yeast. Cell *42*, 237-247.

Jones, E.W., and Fink, G.R. (1982). Regulation of Amino Acid and Nucleotide Biosynthesis in Yeast. In The Molecular Biology of the Yeast Saccharomyces Metabolism and Gene Expression, J.N. Strathern, E.W. Jones, and J.R. Broach, eds. (Cold Spring Harbor, Cold Spring Harbor Laboratory Press).

Kaufman, P.D., Cohen, J.L., and Osley, M.A. (1998). Hir proteins are required for position-dependent gene silencing in Saccharomyces cerevisiae in the absence of chromatin assembly factor I. Mol Cell Biol *18*, 4793-4806.

Kaufman, P.D., Kobayashi, R., and Stillman, B. (1997). Ultraviolet radiation sensitivity and reduction of telomeric silencing in Saccharomyces cerevisiae cells lacking chromatin assembly factor-I. Genes Dev *11*, 345-357.

Kaufman, P.D., and Rando, O.J. (2010). Chromatin as a potential carrier of heritable information. Curr Opin Cell Biol.

Keleher, C.A., Goutte, C., and Johnson, A.D. (1988). The yeast cell-type-specific repressor alpha 2 acts cooperatively with a non-cell-type-specific protein. Cell *53*, 927-936.

Keleher, C.A., Redd, M.J., Schultz, J., Carlson, M., and Johnson, A.D. (1992). Ssn6-Tup1 is a general repressor of transcription in yeast. Cell *68*, 709-719.

Kelman, Z. (1997). PCNA: structure, functions and interactions. Oncogene *14*, 629-640.

Kim, S.M., Dubey, D.D., and Huberman, J.A. (2003). Early-replicating heterochromatin. Genes Dev *17*, 330-335.

Kirchmaier, A.L., and Rine, J. (2001). DNA replication-independent silencing in S. cerevisiae. Science *291*, 646-650.

Koering, C.E., Pollice, A., Zibella, M.P., Bauwens, S., Puisieux, A., Brunori, M., Brun, C., Martins, L., Sabatier, L., Pulitzer, J.F.*, et al.* (2002). Human telomeric position effect is determined by chromosomal context and telomeric chromatin integrity. EMBO Rep *3*, 1055-1061.

Kong, X.P., Onrust, R., O'Donnell, M., and Kuriyan, J. (1992). Three-dimensional structure of the beta subunit of E. coli DNA polymerase III holoenzyme: a sliding DNA clamp. Cell *69*, 425-437.

Kornberg, R.D. (1974). Chromatin structure: a repeating unit of histones and DNA. Science *184*, 868-871.

Kramer, R.A., and Andersen, N. (1980). Isolation of yeast genes with mRNA levels controlled by phosphate concentration. Proc Natl Acad Sci U S A *77*, 6541-6545.

Krawitz, D.C., Kama, T., and Kaufman, P.D. (2002). Chromatin assembly factor I mutants defective for PCNA binding require Asf1/Hir proteins for silencing. Mol Cell Biol *22*, 614-625.

Krishna, T.S., Kong, X.P., Gary, S., Burgers, P.M., and Kuriyan, J. (1994). Crystal structure of the eukaryotic DNA polymerase processivity factor PCNA. Cell *79*, 1233-1243.

Krude, T. (1995). Chromatin assembly factor 1 (CAF-1) colocalizes with replication foci in HeLa cell nuclei. Exp Cell Res *220*, 304-311.

Kunz, B.A., Kohalmi, S.E., Kunkel, T.A., Mathews, C.K., McIntosh, E.M., and Reidy, J.A. (1994). International Commission for Protection Against Environmental Mutagens and Carcinogens. Deoxyribonucleoside triphosphate levels: a critical factor in the maintenance of genetic stability. Mutat Res *318*, 1-64.

Kuo, M.H., and Grayhack, E. (1994). A library of yeast genomic MCM1 binding sites contains genes involved in cell cycle control, cell wall and membrane structure, and metabolism. Mol Cell Biol *14*, 348-359.

Kushnirov, V.V. (2000). Rapid and reliable protein extraction from yeast. Yeast *16*, 857-860.

Lachner, M., O'Carroll, D., Rea, S., Mechtler, K., and Jenuwein, T. (2001). Methylation of histone H3 lysine 9 creates a binding site for HP1 proteins. Nature *410*, 116-120.

Lacoste, N., Utley, R.T., Hunter, J.M., Poirier, G.G., and Cote, J. (2002). Disruptor of telomeric silencing-1 is a chromatin-specific histone H3 methyltransferase. J Biol Chem *277*, 30421-30424.

Lacroute, F. (1968). Regulation of pyrimidine biosynthesis in Saccharomyces cerevisiae. J Bacteriol *95*, 824-832.

Laman, H., Balderes, D., and Shore, D. (1995). Disturbance of normal cell cycle progression enhances the establishment of transcriptional silencing in Saccharomyces cerevisiae. Mol Cell Biol *15*, 3608-3617.

Landry, J., Sutton, A., Tafrov, S.T., Heller, R.C., Stebbins, J., Pillus, L., and Sternglanz, R. (2000). The silencing protein SIR2 and its homologs are NAD-dependent protein deacetylases. Proc Natl Acad Sci U S A *97*, 5807-5811.

Laskey, R.A., Honda, B.M., Mills, A.D., and Finch, J.T. (1978). Nucleosomes are assembled by an acidic protein which binds histones and transfers them to DNA. Nature *275*, 416-420.

Lau, A., Blitzblau, H., and Bell, S.P. (2002). Cell-cycle control of the establishment of mating-type silencing in S. cerevisiae. Genes Dev *16*, 2935-2945.

Le, S., Davis, C., Konopka, J.B., and Sternglanz, R. (1997). Two new S-phase-specific genes from Saccharomyces cerevisiae. Yeast *13*, 1029-1042.

Lee, K.Y., Yang, K., Cohn, M.A., Sikdar, N., D'Andrea, A.D., and Myung, K. (2010). Human ELG1 regulates the level of ubiquitinated proliferating cell nuclear

antigen (PCNA) through Its interactions with PCNA and USP1. J Biol Chem *285*, 10362-10369.

Lee, S.E., Paques, F., Sylvan, J., and Haber, J.E. (1999). Role of yeast SIR genes and mating type in directing DNA double-strand breaks to homologous and non-homologous repair paths. Curr Biol *9*, 767-770.

Lee, S.J., Schwartz, M.F., Duong, J.K., and Stern, D.F. (2003). Rad53 phosphorylation site clusters are important for Rad53 regulation and signaling. Mol Cell Biol *23*, 6300-6314.

Lee, Y.D., and Elledge, S.J. (2006). Control of ribonucleotide reductase localization through an anchoring mechanism involving Wtm1. Genes Dev *20*, 334-344.

Lee, Y.D., Wang, J., Stubbe, J., and Elledge, S.J. (2008). Dif1 is a DNA-damage-regulated facilitator of nuclear import for ribonucleotide reductase. Mol Cell *32*, 70-80.

Levis, R., Hazelrigg, T., and Rubin, G.M. (1985). Effects of genomic position on the expression of transduced copies of the white gene of Drosophila. Science *229*, 558-561.

Li, Q., Fazly, A.M., Zhou, H., Huang, S., Zhang, Z., and Stillman, B. (2009). The elongator complex interacts with PCNA and modulates transcriptional silencing and sensitivity to DNA damage agents. PLoS Genet *5*, e1000684.

Li, Q., Zhou, H., Wurtele, H., Davies, B., Horazdovsky, B., Verreault, A., and Zhang, Z. (2008). Acetylation of histone H3 lysine 56 regulates replication-coupled nucleosome assembly. Cell *134*, 244-255.

Li, Y.C., Cheng, T.H., and Gartenberg, M.R. (2001). Establishment of transcriptional silencing in the absence of DNA replication. Science *291*, 650-653.

Lin, Y.Y., Qi, Y., Lu, J.Y., Pan, X., Yuan, D.S., Zhao, Y., Bader, J.S., and Boeke, J.D. (2008). A comprehensive synthetic genetic interaction network governing yeast histone acetylation and deacetylation. Genes Dev *22*, 2062-2074.

Linger, J., and Tyler, J.K. (2005). The yeast histone chaperone chromatin assembly factor 1 protects against double-strand DNA-damaging agents. Genetics *171*, 1513-1522.

Lingner, J., Hughes, T.R., Shevchenko, A., Mann, M., Lundblad, V., and Cech, T.R. (1997). Reverse transcriptase motifs in the catalytic subunit of telomerase. Science *276*, 561-567.

List, O., Togawa, T., Tsuda, M., Matsuo, T., Elard, L., and Aigaki, T. (2009). Overexpression of grappa encoding a histone methyltransferase enhances stress resistance in Drosophila. Hereditas *146*, 19-28.

Longhese, M.P., Paciotti, V., Neecke, H., and Lucchini, G. (2000). Checkpoint proteins influence telomeric silencing and length maintenance in budding yeast. Genetics *155*, 1577-1591.

Longley, D.B., Harkin, D.P., and Johnston, P.G. (2003). 5-fluorouracil: mechanisms of action and clinical strategies. Nat Rev Cancer *3*, 330-338.

Longtine, M.S., McKenzie, A., 3rd, Demarini, D.J., Shah, N.G., Wach, A., Brachat, A., Philippsen, P., and Pringle, J.R. (1998). Additional modules for versatile and economical PCR-based gene deletion and modification in Saccharomyces cerevisiae. Yeast *14*, 953-961.

Loo, S., and Rine, J. (1994). Silencers and domains of generalized repression. Science *264*, 1768-1771.

Losson, R., and Lacroute, F. (1983). Plasmids carrying the yeast OMP decarboxylase structural and regulatory genes: transcription regulation in a foreign environment. Cell *32*, 371-377.

Louis, E.J., Naumova, E.S., Lee, A., Naumov, G., and Haber, J.E. (1994). The chromosome end in yeast: its mosaic nature and influence on recombinational dynamics. Genetics *136*, 789-802.

Luger, K., Mader, A.W., Richmond, R.K., Sargent, D.F., and Richmond, T.J. (1997). Crystal structure of the nucleosome core particle at 2.8 A resolution. Nature *389*, 251-260.

Lundblad, V., and Blackburn, E.H. (1993). An alternative pathway for yeast telomere maintenance rescues est1- senescence. Cell *73*, 347-360.

Luo, W., Friedman, M.S., Shedden, K., Hankenson, K.D., and Woolf, P.J. (2009). GAGE: generally applicable gene set enrichment for pathway analysis. BMC Bioinformatics *10*, 161.

Lynch, P.J., Fraser, H.B., Sevastopoulos, E., Rine, J., and Rusche, L.N. (2005). Sum1p, the origin recognition complex, and the spreading of a promoter-specific repressor in Saccharomyces cerevisiae. Mol Cell Biol *25*, 5920-5932.

Lyons, T.J., Gasch, A.P., Gaither, L.A., Botstein, D., Brown, P.O., and Eide, D.J. (2000). Genome-wide characterization of the Zap1p zinc-responsive regulon in yeast. Proc Natl Acad Sci U S A *97*, 7957-7962.

Mahoney, D.J., Marquardt, R., Shei, G.J., Rose, A.B., and Broach, J.R. (1991). Mutations in the HML E silencer of Saccharomyces cerevisiae yield metastable inheritance of transcriptional repression. Genes Dev *5*, 605-615.

Maine, G.T., Sinha, P., and Tye, B.K. (1984). Mutants of S. cerevisiae defective in the maintenance of minichromosomes. Genetics *106*, 365-385.

Marcand, S., Brevet, V., Mann, C., and Gilson, E. (2000). Cell cycle restriction of telomere elongation. Curr Biol *10*, 487-490.

Martin, S.G., Laroche, T., Suka, N., Grunstein, M., and Gasser, S.M. (1999). Relocalization of telomeric Ku and SIR proteins in response to DNA strand breaks in yeast. Cell *97*, 621-633.

Martini, E., Roche, D.M., Marheineke, K., Verreault, A., and Almouzni, G. (1998). Recruitment of phosphorylated chromatin assembly factor 1 to chromatin after UV irradiation of human cells. J Cell Biol *143*, 563-575.

Martins-Taylor, K., Dula, M.L., and Holmes, S.G. (2004). Heterochromatin spreading at yeast telomeres occurs in M phase. Genetics *168*, 65-75.

Mathews, M.B., Bernstein, R.M., Franza, B.R., Jr., and Garrels, J.I. (1984). Identity of the proliferating cell nuclear antigen and cyclin. Nature *309*, 374-376.

Mathog, D., Hochstrasser, M., Gruenbaum, Y., Saumweber, H., and Sedat, J. (1984). Characteristic folding pattern of polytene chromosomes in Drosophila salivary gland nuclei. Nature *308*, 414-421.

Matsuda, K., Makise, M., Sueyasu, Y., Takehara, M., Asano, T., and Mizushima, T. (2007). Yeast two-hybrid analysis of the origin recognition complex of Saccharomyces cerevisiae: interaction between subunits and identification of binding proteins. FEMS Yeast Res *7*, 1263-1269.

Maxwell, P.J., Longley, D.B., Latif, T., Boyer, J., Allen, W., Lynch, M., McDermott, U., Harkin, D.P., Allegra, C.J., and Johnston, P.G. (2003). Identification of 5-fluorouracil-inducible target genes using cDNA microarray profiling. Cancer Res *63*, 4602-4606.

McCarroll, R.M., and Fangman, W.L. (1988). Time of replication of yeast centromeres and telomeres. Cell *54*, 505-513.

McClintock, B. (1938). The Production of Homozygous Deficient Tissues with Mutant Characteristics by Means of the Aberrant Mitotic Behavior of Ring-Shaped Chromosomes. Genetics *23*, 315-376.

McNally, F.J., and Rine, J. (1991). A synthetic silencer mediates SIR-dependent functions in Saccharomyces cerevisiae. Mol Cell Biol *11*, 5648-5659.

Mello, J.A., Sillje, H.H., Roche, D.M., Kirschner, D.B., Nigg, E.A., and Almouzni, G. (2002). Human Asf1 and CAF-1 interact and synergize in a repair-coupled nucleosome assembly pathway. EMBO Rep *3*, 329-334.

Melo, J., and Toczyski, D. (2002). A unified view of the DNA-damage checkpoint. Curr Opin Cell Biol *14*, 237-245.

Micklem, G., Rowley, A., Harwood, J., Nasmyth, K., and Diffley, J.F. (1993a). Yeast origin recognition complex is involved in DNA replication and transcriptional silencing. Nature *366*, 87-89.

Micklem, G., Rowley, A., Harwood, J., Nasmyth, K., and Diffley, J.F. (1993b). Yeast origin recognition complex is involved in DNA replication and transcriptional silencing. Nature *366*, 87-90.

Miller, A., Yang, B., Foster, T., and Kirchmaier, A.L. (2008). Proliferating cell nuclear antigen and ASF1 modulate silent chromatin in Saccharomyces cerevisiae via lysine 56 on histone H3. Genetics *179*, 793-809.

Miller, A.M., and Nasmyth, K.A. (1984). Role of DNA replication in the repression of silent mating type loci in yeast. Nature *312*, 247-251.

Miller, T., Krogan, N.J., Dover, J., Erdjument-Bromage, H., Tempst, P., Johnston, M., Greenblatt, J.F., and Shilatifard, A. (2001). COMPASS: a complex of proteins associated with a trithorax-related SET domain protein. Proc Natl Acad Sci U S A *98*, 12902-12907.

Mills, K.D., Sinclair, D.A., and Guarente, L. (1999). MEC1-dependent redistribution of the Sir3 silencing protein from telomeres to DNA double-strand breaks. Cell *97*, 609-620.

Milutinovic, S., Zhuang, Q., and Szyf, M. (2002). Proliferating cell nuclear antigen associates with histone deacetylase activity, integrating DNA replication and chromatin modification. J Biol Chem *277*, 20974-20978.

Mishra, K., and Shore, D. (1999). Yeast Ku protein plays a direct role in telomeric silencing and counteracts inhibition by rif proteins. Curr Biol *9*, 1123-1126.

Miyachi, K., Fritzler, M.J., and Tan, E.M. (1978). Autoantibody to a nuclear antigen in proliferating cells. J Immunol *121*, 2228-2234.

Moazed, D. (2009). Small RNAs in transcriptional gene silencing and genome defence. Nature *457*, 413-420.

Moir, D., Stewart, S.E., Osmond, B.C., and Botstein, D. (1982). Cold-sensitive cell-division-cycle mutants of yeast: isolation, properties, and pseudoreversion studies. Genetics *100*, 547-563.

Moldovan, G.L., Pfander, B., and Jentsch, S. (2007). PCNA, the maestro of the replication fork. Cell *129*, 665-679.

Monson, E.K., de Bruin, D., and Zakian, V.A. (1997). The yeast Cac1 protein is required for the stable inheritance of transcriptionally repressed chromatin at telomeres. Proc Natl Acad Sci U S A *94*, 13081-13086.

Moretti, P., Freeman, K., Coodly, L., and Shore, D. (1994). Evidence that a complex of SIR proteins interacts with the silencer and telomere-binding protein RAP1. Genes Dev *8*, 2257-2269.

Mullen, J.R., Kayne, P.S., Moerschell, R.P., Tsunasawa, S., Gribskov, M., Colavito-Shepanski, M., Grunstein, M., Sherman, F., and Sternglanz, R. (1989). Identification and characterization of genes and mutants for an N-terminal acetyltransferase from yeast. EMBO J *8*, 2067-2075.

Müller, H.J. (1938). The remaking of chromosomes. The Collecting Net *13*, 181-195,198.

Munro, E.M., Climie, S., Vandenberg, E., and Storms, R.K. (1999). Functional assessment of surface loops: deletion of eukaryote-specific peptide inserts in thymidylate synthase of Saccharomyces cerevisiae. Biochim Biophys Acta *1430*, 1-13.

Nakanishi, T., and Sekimizu, K. (2002). SDT1/SSM1, a multicopy suppressor of S-II null mutant, encodes a novel pyrimidine 5'-nucleotidase. J Biol Chem *277*, 22103-22106.

Nakayama, J., Rice, J.C., Strahl, B.D., Allis, C.D., and Grewal, S.I. (2001). Role of histone H3 lysine 9 methylation in epigenetic control of heterochromatin assembly. Science *292*, 110-113.

Ng, H.H., Ciccone, D.N., Morshead, K.B., Oettinger, M.A., and Struhl, K. (2003a). Lysine-79 of histone H3 is hypomethylated at silenced loci in yeast and mammalian cells: a potential mechanism for position-effect variegation. Proc Natl Acad Sci U S A *100*, 1820-1825.

Ng, H.H., Feng, Q., Wang, H., Erdjument-Bromage, H., Tempst, P., Zhang, Y., and Struhl, K. (2002). Lysine methylation within the globular domain of histone H3 by Dot1 is important for telomeric silencing and Sir protein association. Genes Dev *16*, 1518-1527.

Ng, H.H., Robert, F., Young, R.A., and Struhl, K. (2003b). Targeted recruitment of Set1 histone methylase by elongating Pol II provides a localized mark and memory of recent transcriptional activity. Mol Cell *11*, 709-719.

Nick McElhinny, S.A., Gordenin, D.A., Stith, C.M., Burgers, P.M., and Kunkel, T.A. (2008). Division of labor at the eukaryotic replication fork. Mol Cell *30*, 137-144.

Nordlund, P., and Reichard, P. (2006). Ribonucleotide reductases. Annu Rev Biochem *75*, 681-706.

Norman, C., Runswick, M., Pollock, R., and Treisman, R. (1988). Isolation and properties of cDNA clones encoding SRF, a transcription factor that binds to the c-fos serum response element. Cell *55*, 989-1003.

Norris, A., Bianchet, M.A., and Boeke, J.D. (2008). Compensatory interactions between Sir3p and the nucleosomal LRS surface imply their direct interaction. PLoS Genet *4*, e1000301.

Osborne, E.A., Dudoit, S., and Rine, J. (2009). The establishment of gene silencing at single-cell resolution. Nat Genet *41*, 800-806.

Pak, D.T., Pflumm, M., Chesnokov, I., Huang, D.W., Kellum, R., Marr, J., Romanowski, P., and Botchan, M.R. (1997). Association of the origin recognition complex with heterochromatin and HP1 in higher eukaryotes. Cell *91*, 311-323.

Palladino, F., Laroche, T., Gilson, E., Axelrod, A., Pillus, L., and Gasser, S.M. (1993). SIR3 and SIR4 proteins are required for the positioning and integrity of yeast telomeres. Cell *75*, 543-555.

Papouli, E., Chen, S., Davies, A.A., Huttner, D., Krejci, L., Sung, P., and Ulrich, H.D. (2005). Crosstalk between SUMO and ubiquitin on PCNA is mediated by recruitment of the helicase Srs2p. Mol Cell *19*, 123-133.

Pfander, B., Moldovan, G.L., Sacher, M., Hoege, C., and Jentsch, S. (2005). SUMO-modified PCNA recruits Srs2 to prevent recombination during S phase. Nature *436*, 428-433.

Philippsen, P., Stotz, A., and Scherf, C. (1991). DNA of Saccharomyces cerevisiae. Methods Enzymol *194*, 169-182.

Pierce, M., Benjamin, K.R., Montano, S.P., Georgiadis, M.M., Winter, E., and Vershon, A.K. (2003). Sum1 and Ndt80 proteins compete for binding to middle

sporulation element sequences that control meiotic gene expression. Mol Cell Biol *23*, 4814-4825.

Pillus, L., and Rine, J. (1989). Epigenetic inheritance of transcriptional states in S. cerevisiae. Cell *59*, 637-647.

Pinson, B., Vaur, S., Sagot, I., Coulpier, F., Lemoine, S., and Daignan-Fornier, B. (2009). Metabolic intermediates selectively stimulate transcription factor interaction and modulate phosphate and purine pathways. Genes Dev *23*, 1399-1407.

Pirrotta, V., and Gross, D.S. (2005). Epigenetic silencing mechanisms in budding yeast and fruit fly: different paths, same destinations. Mol Cell *18*, 395-398.

Pokholok, D.K., Harbison, C.T., Levine, S., Cole, M., Hannett, N.M., Lee, T.I., Bell, G.W., Walker, K., Rolfe, P.A., Herbolsheimer, E.*, et al.* (2005). Genome-wide map of nucleosome acetylation and methylation in yeast. Cell *122*, 517-527.

Poot, R.A., Bozhenok, L., van den Berg, D.L., Steffensen, S., Ferreira, F., Grimaldi, M., Gilbert, N., Ferreira, J., and Varga-Weisz, P.D. (2004). The Williams syndrome transcription factor interacts with PCNA to target chromatin remodelling by ISWI to replication foci. Nat Cell Biol *6*, 1236-1244.

Prado, F., Cortes-Ledesma, F., and Aguilera, A. (2004). The absence of the yeast chromatin assembly factor Asf1 increases genomic instability and sister chromatid exchange. EMBO Rep *5*, 497-502.

Prelich, G., Kostura, M., Marshak, D.R., Mathews, M.B., and Stillman, B. (1987a). The cell-cycle regulated proliferating cell nuclear antigen is required for SV40 DNA replication in vitro. Nature *326*, 471-475.

Prelich, G., Tan, C.K., Kostura, M., Mathews, M.B., So, A.G., Downey, K.M., and Stillman, B. (1987b). Functional identity of proliferating cell nuclear antigen and a DNA polymerase-delta auxiliary protein. Nature *326*, 517-520.

Prendergast, J.A., Ptak, C., Kornitzer, D., Steussy, C.N., Hodgins, R., Goebl, M., and Ellison, M.J. (1996). Identification of a positive regulator of the cell cycle ubiquitin-conjugating enzyme Cdc34 (Ubc3). Mol Cell Biol *16*, 677-684.

Proft, M., and Struhl, K. (2002). Hog1 kinase converts the Sko1-Cyc8-Tup1 repressor complex into an activator that recruits SAGA and SWI/SNF in response to osmotic stress. Mol Cell *9*, 1307-1317.

Pryde, F.E., and Louis, E.J. (1999). Limitations of silencing at native yeast telomeres. EMBO J *18*, 2538-2550.

Ptashne, M. (2007). On the use of the word 'epigenetic'. Curr Biol *17*, R233-236.

Pursell, Z.F., Isoz, I., Lundstrom, E.B., Johansson, E., and Kunkel, T.A. (2007). Yeast DNA polymerase epsilon participates in leading-strand DNA replication. Science *317*, 127-130.

Putnam, C.D., Jaehnig, E.J., and Kolodner, R.D. (2009). Perspectives on the DNA damage and replication checkpoint responses in Saccharomyces cerevisiae. DNA Repair (Amst) *8*, 974-982.

Qian, Z., Huang, H., Hong, J.Y., Burck, C.L., Johnston, S.D., Berman, J., Carol, A., and Liebman, S.W. (1998). Yeast Ty1 retrotransposition is stimulated by a synergistic interaction between mutations in chromatin assembly factor I and histone regulatory proteins. Mol Cell Biol *18*, 4783-4792.

Ransom, M., Dennehey, B.K., and Tyler, J.K. (2010). Chaperoning histones during DNA replication and repair. Cell *140*, 183-195.

Rea, S., Eisenhaber, F., O'Carroll, D., Strahl, B.D., Sun, Z.W., Schmid, M., Opravil, S., Mechtler, K., Ponting, C.P., Allis, C.D.*, et al.* (2000). Regulation of chromatin structure by site-specific histone H3 methyltransferases. Nature *406*, 593-599.

Recht, J., Tsubota, T., Tanny, J.C., Diaz, R.L., Berger, J.M., Zhang, X., Garcia, B.A., Shabanowitz, J., Burlingame, A.L., Hunt, D.F.*, et al.* (2006). Histone chaperone Asf1 is required for histone H3 lysine 56 acetylation, a modification associated with S phase in mitosis and meiosis. Proc Natl Acad Sci U S A *103*, 6988-6993.

Reifsnyder, C., Lowell, J., Clarke, A., and Pillus, L. (1996). Yeast SAS silencing genes and human genes associated with AML and HIV-1 Tat interactions are homologous with acetyltransferases. Nat Genet *14*, 42-49.

Renauld, H., Aparicio, O.M., Zierath, P.D., Billington, B.L., Chhablani, S.K., and Gottschling, D.E. (1993). Silent domains are assembled continuously from the telomere and are defined by promoter distance and strength, and by SIR3 dosage. Genes Dev *7*, 1133-1145.

Rivier, D.H., Ekena, J.L., and Rine, J. (1999). HMR-I is an origin of replication and a silencer in Saccharomyces cerevisiae. Genetics *151*, 521-529.

Rivier, D.H., and Rine, J. (1992). An origin of DNA replication and a transcription silencer require a common element. Science *256*, 659-663.

Robert, T., Dervins, D., Fabre, F., and Gangloff, S. (2006). Mrc1 and Srs2 are major actors in the regulation of spontaneous crossover. EMBO J *25*, 2837-2846.

Robyr, D., Suka, Y., Xenarios, I., Kurdistani, S.K., Wang, A., Suka, N., and Grunstein, M. (2002). Microarray deacetylation maps determine genome-wide functions for yeast histone deacetylases. Cell *109*, 437-446.

Rolef Ben-Shahar, T., Castillo, A.G., Osborne, M.J., Borden, K.L., Kornblatt, J., and Verreault, A. (2009). Two fundamentally distinct PCNA interaction peptides contribute to chromatin assembly factor 1 function. Mol Cell Biol *29*, 6353-6365.

Rusche, L.N., Kirchmaier, A.L., and Rine, J. (2002). Ordered nucleation and spreading of silenced chromatin in *Saccharomyces cerevisiae*. Mol Biol Cell *13*, 2207-2222.

Rusche, L.N., and Rine, J. (2001). Conversion of a gene-specific repressor to a regional silencer. Genes Dev *15*, 955-967.

Sambrook, J., and Russell, D.W. (2001). Molecular cloning: a laboratory manual, 3rd edn (Cold Spring Harbor, NY, Cold Spring Harbor Laboratory Press).

Sampath, V., Yuan, P., Wang, I.X., Prugar, E., van Leeuwen, F., and Sternglanz, R. (2009). Mutational analysis of the Sir3 BAH domain reveals multiple points of interaction with nucleosomes. Mol Cell Biol *29*, 2532-2545.

San-Segundo, P.A., and Roeder, G.S. (2000). Role for the silencing protein Dot1 in meiotic checkpoint control. Mol Biol Cell *11*, 3601-3615.

Sandell, L.L., and Zakian, V.A. (1993). Loss of a yeast telomere: arrest, recovery, and chromosome loss. Cell *75*, 729-739.

Schäfer, G., Smith, E.M., and Patterton, H.G. (2005). The Saccharomyces cerevisiae linker histone Hho1p, with two globular domains, can simultaneously bind to two four-way junction DNA molecules. Biochemistry *44*, 16766-16775.

Schubeler, D., Scalzo, D., Kooperberg, C., van Steensel, B., Delrow, J., and Groudine, M. (2002). Genome-wide DNA replication profile for Drosophila melanogaster: a link between transcription and replication timing. Nat Genet *32*, 438-442.

Schultz, J. (1947). The Nature of Heterochromatin. Cold Spring Harb Symp Quant Biol *12*, 179-191.

Schulz, L.L., and Tyler, J.K. (2006). The histone chaperone ASF1 localizes to active DNA replication forks to mediate efficient DNA replication. FASEB J *20*, 488-490.

Schulze, J.M., Jackson, J., Nakanishi, S., Gardner, J.M., Hentrich, T., Haug, J., Johnston, M., Jaspersen, S.L., Kobor, M.S., and Shilatifard, A. (2009). Linking cell cycle to histone modifications: SBF and H2B monoubiquitination machinery and cell-cycle regulation of H3K79 dimethylation. Mol Cell *35*, 626-641.

Sekinger, E.A., and Gross, D.S. (2001). Silenced chromatin is permissive to activator binding and PIC recruitment. Cell *105*, 403-414.

Shanower, G.A., Muller, M., Blanton, J.L., Honti, V., Gyurkovics, H., and Schedl, P. (2005). Characterization of the grappa gene, the Drosophila histone H3 lysine 79 methyltransferase. Genetics *169*, 173-184.

Sharp, J.A., Fouts, E.T., Krawitz, D.C., and Kaufman, P.D. (2001). Yeast histone deposition protein Asf1p requires Hir proteins and PCNA for heterochromatic silencing. Curr Biol *11*, 463-473.

Sharp, J.A., Rizki, G., and Kaufman, P.D. (2005). Regulation of histone deposition proteins Asf1/Hir1 by multiple DNA damage checkpoint kinases in Saccharomyces cerevisiae. Genetics *171*, 885-899.

Sherwood, P.W., Tsang, S.V., and Osley, M.A. (1993). Characterization of HIR1 and HIR2, two genes required for regulation of histone gene transcription in Saccharomyces cerevisiae. Mol Cell Biol *13*, 28-38.

Shibahara, K., and Stillman, B. (1999). Replication-dependent marking of DNA by PCNA facilitates CAF-1-coupled inheritance of chromatin. Cell *96*, 575-585.

Sikorski, R.S., and Hieter, P. (1989). A system of shuttle vectors and yeast host strains designed for efficient manipulation of DNA in Saccharomyces cerevisiae. Genetics *122*, 19-27.

Singer, M.S., and Gottschling, D.E. (1994). TLC1: template RNA component of Saccharomyces cerevisiae telomerase. Science *266*, 404-409.

Singer, M.S., Kahana, A., Wolf, A.J., Meisinger, L.L., Peterson, S.E., Goggin, C., Mahowald, M., and Gottschling, D.E. (1998). Identification of high-copy disruptors of telomeric silencing in Saccharomyces cerevisiae. Genetics *150*, 613-632.

Singh, G., and Klar, A.J. (2008). Mutations in deoxyribonucleotide biosynthesis pathway cause spreading of silencing across heterochromatic barriers at the mating-type region of the fission yeast. Yeast *25*, 117-128.

Singh, R.K., Kabbaj, M.H., Paik, J., and Gunjan, A. (2009). Histone levels are regulated by phosphorylation and ubiquitylation-dependent proteolysis. Nat Cell Biol *11*, 925-933.

Smith, J.S., Brachmann, C.B., Celic, I., Kenna, M.A., Muhammad, S., Starai, V.J., Avalos, J.L., Escalante-Semerena, J.C., Grubmeyer, C., Wolberger, C*., et al.* (2000). A phylogenetically conserved NAD+-dependent protein deacetylase activity in the Sir2 protein family. Proc Natl Acad Sci U S A *97*, 6658-6663.

Smith, J.S., Caputo, E., and Boeke, J.D. (1999). A genetic screen for ribosomal DNA silencing defects identifies multiple DNA replication and chromatin-modulating factors. Mol Cell Biol *19*, 3184-3197.

Smith, S., and Stillman, B. (1989). Purification and characterization of CAF-I, a human cell factor required for chromatin assembly during DNA replication in vitro. Cell *58*, 15-25.

Smith, S., and Stillman, B. (1991). Stepwise assembly of chromatin during DNA replication in vitro. EMBO J *10*, 971-980.

Sobel, R.E., Cook, R.G., Perry, C.A., Annunziato, A.T., and Allis, C.D. (1995). Conservation of deposition-related acetylation sites in newly synthesized histones H3 and H4. Proc Natl Acad Sci U S A *92*, 1237-1241.

Som, I., Mitsch, R.N., Urbanowski, J.L., and Rolfes, R.J. (2005). DNA-bound Bas1 recruits Pho2 to activate ADE genes in Saccharomyces cerevisiae. Eukaryot Cell *4*, 1725-1735.

Southern, E.M. (1975). Detection of specific sequences among DNA fragments separated by gel electrophoresis. J Mol Biol *98*, 503-517.

Spector, M.S., Raff, A., DeSilva, H., Lee, K., and Osley, M.A. (1997). Hir1p and Hir2p function as transcriptional corepressors to regulate histone gene transcription in the Saccharomyces cerevisiae cell cycle. Mol Cell Biol *17*, 545-552.

Steiner, S., and Philippsen, P. (1994). Sequence and promoter analysis of the highly expressed TEF gene of the filamentous fungus Ashbya gossypii. Mol Gen Genet *242*, 263-271.

Stillman, B. (1986). Chromatin assembly during SV40 DNA replication in vitro. Cell *45*, 555-565.

Stone, E.M., Reifsnyder, C., McVey, M., Gazo, B., and Pillus, L. (2000). Two classes of sir3 mutants enhance the sir1 mutant mating defect and abolish telomeric silencing in Saccharomyces cerevisiae. Genetics *155*, 509-522.

Suka, N., Luo, K., and Grunstein, M. (2002). Sir2p and Sas2p opposingly regulate acetylation of yeast histone H4 lysine16 and spreading of heterochromatin. Nat Genet *32*, 378-383.

Suka, N., Suka, Y., Carmen, A.A., Wu, J., and Grunstein, M. (2001). Highly specific antibodies determine histone acetylation site usage in yeast heterochromatin and euchromatin. Mol Cell *8*, 473-479.

Sussel, L., Vannier, D., and Shore, D. (1993). Epigenetic switching of transcriptional states: cis- and trans-acting factors affecting establishment of silencing at the HMR locus in Saccharomyces cerevisiae. Mol Cell Biol *13*, 3919-3928.

Sutton, A., Heller, R.C., Landry, J., Choy, J.S., Sirko, A., and Sternglanz, R. (2001). A novel form of transcriptional silencing by Sum1-1 requires Hst1 and the origin recognition complex. Mol Cell Biol *21*, 3514-3522.

Suzuki, M.M., and Bird, A. (2008). DNA methylation landscapes: provocative insights from epigenomics. Nat Rev Genet *9*, 465-476.

Taddei, A., Roche, D., Sibarita, J.B., Turner, B.M., and Almouzni, G. (1999). Duplication and maintenance of heterochromatin domains. J Cell Biol *147*, 1153-1166.

Talbert, P.B., and Henikoff, S. (2010). Histone variants--ancient wrap artists of the epigenome. Nat Rev Mol Cell Biol *11*, 264-275.

Tamburini, B.A., Carson, J.J., Linger, J.G., and Tyler, J.K. (2006). Dominant mutants of the Saccharomyces cerevisiae ASF1 histone chaperone bypass the need for CAF-1 in transcriptional silencing by altering histone and Sir protein recruitment. Genetics *173*, 599-610.

Tan, C.K., Castillo, C., So, A.G., and Downey, K.M. (1986). An auxiliary protein for DNA polymerase-delta from fetal calf thymus. J Biol Chem *261*, 12310-12316.

Teixeira, M.T., Dujon, B., and Fabre, E. (2002). Genome-wide nuclear morphology screen identifies novel genes involved in nuclear architecture and gene-silencing in Saccharomyces cerevisiae. J Mol Biol *321*, 551-561.

Thomas, B.J., and Rothstein, R. (1989). Elevated recombination rates in transcriptionally active DNA. Cell *56*, 619-630.

Tompa, R., and Madhani, H.D. (2007). Histone H3 lysine 36 methylation antagonizes silencing in Saccharomyces cerevisiae independently of the Rpd3S histone deacetylase complex. Genetics *175*, 585-593.

Toyn, J.H., Gunyuzlu, P.L., White, W.H., Thompson, L.A., and Hollis, G.F. (2000). A counterselection for the tryptophan pathway in yeast: 5-fluoroanthranilic acid resistance. Yeast *16*, 553-560.

Triolo, T., and Sternglanz, R. (1996). Role of interactions between the origin recognition complex and SIR1 in transcriptional silencing. Nature *381*, 251-253.

Troester, M.A., Hoadley, K.A., Sorlie, T., Herbert, B.S., Borresen-Dale, A.L., Lonning, P.E., Shay, J.W., Kaufmann, W.K., and Perou, C.M. (2004). Cell-type-specific responses to chemotherapeutics in breast cancer. Cancer Res *64*, 4218-4226.

Tsao, D.A., Chang, H.J., Lin, C.Y., Hsiung, S.K., Huang, S.E., Ho, S.Y., Chang, M.S., Chiu, H.H., Chen, Y.F., Cheng, T.L.*, et al.* (2010). Gene Expression Profiles for Predicting the Efficacy of the Anticancer Drug 5-Fluorouracil in Breast Cancer. DNA Cell Biol.

Tsubota, T., Berndsen, C.E., Erkmann, J.A., Smith, C.L., Yang, L., Freitas, M.A., Denu, J.M., and Kaufman, P.D. (2007). Histone H3-K56 acetylation is catalyzed by histone chaperone-dependent complexes. Mol Cell *25*, 703-712.

Tsukamoto, Y., Kato, J., and Ikeda, H. (1997). Silencing factors participate in DNA repair and recombination in Saccharomyces cerevisiae. Nature *388*, 900-903.

Tyler, J.K., Adams, C.R., Chen, S.R., Kobayashi, R., Kamakaka, R.T., and Kadonaga, J.T. (1999). The RCAF complex mediates chromatin assembly during DNA replication and repair. Nature *402*, 555-560.

Tyler, J.K., Collins, K.A., Prasad-Sinha, J., Amiott, E., Bulger, M., Harte, P.J., Kobayashi, R., and Kadonaga, J.T. (2001). Interaction between the Drosophila CAF-1 and ASF1 chromatin assembly factors. Mol Cell Biol *21*, 6574-6584.

Ushinsky, S.C., Bussey, H., Ahmed, A.A., Wang, Y., Friesen, J., Williams, B.A., and Storms, R.K. (1997). Histone H1 in Saccharomyces cerevisiae. Yeast *13*, 151-161.

Van Gelder, R.N., von Zastrow, M.E., Yool, A., Dement, W.C., Barchas, J.D., and Eberwine, J.H. (1990). Amplified RNA synthesized from limited quantities of heterogeneous cDNA. Proc Natl Acad Sci U S A *87*, 1663-1667.

van Leeuwen, F., Gafken, P.R., and Gottschling, D.E. (2002). Dot1p modulates silencing in yeast by methylation of the nucleosome core. Cell *109*, 745-756.

van Welsem, T., Frederiks, F., Verzijlbergen, K.F., Faber, A.W., Nelson, Z.W., Egan, D.A., Gottschling, D.E., and van Leeuwen, F. (2008). Synthetic lethal screens identify gene silencing processes in yeast and implicate the acetylated amino terminus of Sir3 in recognition of the nucleosome core. Mol Cell Biol *28*, 3861-3872.

Verreault, A., Kaufman, P.D., Kobayashi, R., and Stillman, B. (1996). Nucleosome assembly by a complex of CAF-1 and acetylated histones H3/H4. Cell *87*, 95-104.

Vojtek, A., Haarer, B., Field, J., Gerst, J., Pollard, T.D., Brown, S., and Wigler, M. (1991). Evidence for a functional link between profilin and CAP in the yeast S. cerevisiae. Cell *66*, 497-505.

Wach, A., Brachat, A., Pohlmann, R., and Philippsen, P. (1994). New heterologous modules for classical or PCR-based gene disruptions in Saccharomyces cerevisiae. Yeast *10*, 1793-1808.

Warbrick, E., Heatherington, W., Lane, D.P., and Glover, D.M. (1998). PCNA binding proteins in Drosophila melanogaster : the analysis of a conserved PCNA binding domain. Nucleic Acids Res *26*, 3925-3932.

Watson, J.D., and Crick, F.H. (1953). Molecular structure of nucleic acids; a structure for deoxyribose nucleic acid. Nature *171*, 737-738.

Watzele, G., and Tanner, W. (1989). Cloning of the glutamine:fructose-6-phosphate amidotransferase gene from yeast. Pheromonal regulation of its transcription. J Biol Chem *264*, 8753-8758.

Weinert, T.A., and Hartwell, L.H. (1988). The RAD9 gene controls the cell cycle response to DNA damage in Saccharomyces cerevisiae. Science *241*, 317-322.

Whiteway, M., Freedman, R., Van Arsdell, S., Szostak, J.W., and Thorner, J. (1987). The yeast ARD1 gene product is required for repression of cryptic mating-type information at the HML locus. Mol Cell Biol *7*, 3713-3722.

Wilkins, M.H., Stokes, A.R., and Wilson, H.R. (1953). Molecular structure of deoxypentose nucleic acids. Nature *171*, 738-740.

Williams, F.E., Varanasi, U., and Trumbly, R.J. (1991). The CYC8 and TUP1 proteins involved in glucose repression in Saccharomyces cerevisiae are associated in a protein complex. Mol Cell Biol *11*, 3307-3316.

Wright, J.H., Gottschling, D.E., and Zakian, V.A. (1992). Saccharomyces telomeres assume a non-nucleosomal chromatin structure. Genes Dev *6*, 197-210.

Wu, J., Suka, N., Carlson, M., and Grunstein, M. (2001). TUP1 utilizes histone H3/H2B-specific HDA1 deacetylase to repress gene activity in yeast. Mol Cell *7*, 117-126.

Wyrick, J.J., Holstege, F.C., Jennings, E.G., Causton, H.C., Shore, D., Grunstein, M., Lander, E.S., and Young, R.A. (1999). Chromosomal landscape of nucleosome-dependent gene expression and silencing in yeast. Nature *402*, 418-421.

Wysocki, R., Javaheri, A., Allard, S., Sha, F., Cote, J., and Kron, S.J. (2005). Role of Dot1-dependent histone H3 methylation in G1 and S phase DNA damage checkpoint functions of Rad9. Mol Cell Biol *25*, 8430-8443.

Xie, J., Pierce, M., Gailus-Durner, V., Wagner, M., Winter, E., and Vershon, A.K. (1999). Sum1 and Hst1 repress middle sporulation-specific gene expression during mitosis in Saccharomyces cerevisiae. EMBO J *18*, 6448-6454.

Xu, F., Zhang, Q., Zhang, K., Xie, W., and Grunstein, M. (2007). Sir2 deacetylates histone H3 lysine 56 to regulate telomeric heterochromatin structure in yeast. Mol Cell *27*, 890-900.

Xu, H., Zhang, P., Liu, L., and Lee, M.Y. (2001). A novel PCNA-binding motif identified by the panning of a random peptide display library. Biochemistry *40*, 4512-4520.

Yao, N., Turner, J., Kelman, Z., Stukenberg, P.T., Dean, F., Shechter, D., Pan, Z.Q., Hurwitz, J., and O'Donnell, M. (1996). Clamp loading, unloading and intrinsic stability of the PCNA, beta and gp45 sliding clamps of human, E. coli and T4 replicases. Genes Cells *1*, 101-113.

Yao, R., Zhang, Z., An, X., Bucci, B., Perlstein, D.L., Stubbe, J., and Huang, M. (2003). Subcellular localization of yeast ribonucleotide reductase regulated by the DNA replication and damage checkpoint pathways. Proc Natl Acad Sci U S A *100*, 6628-6633.

Ye, X., Franco, A.A., Santos, H., Nelson, D.M., Kaufman, P.D., and Adams, P.D. (2003). Defective S phase chromatin assembly causes DNA damage, activation of the S phase checkpoint, and S phase arrest. Mol Cell *11*, 341-351.

Yuan, D.S. (2000). Zinc-regulated genes in Saccharomyces cerevisiae revealed by transposon tagging. Genetics *156*, 45-58.

Yuan, G.C., Liu, Y.J., Dion, M.F., Slack, M.D., Wu, L.F., Altschuler, S.J., and Rando, O.J. (2005). Genome-scale identification of nucleosome positions in S. cerevisiae. Science *309*, 626-630.

Zabaronick, S.R., and Tyler, J.K. (2005). The histone chaperone anti-silencing function 1 is a global regulator of transcription independent of passage through S phase. Mol Cell Biol *25*, 652-660.

Zaim, J., Speina, E., and Kierzek, A.M. (2005). Identification of new genes regulated by the Crt1 transcription factor, an effector of the DNA damage checkpoint pathway in Saccharomyces cerevisiae. J Biol Chem *280*, 28-37.

Zegerman, P., and Diffley, J.F. (2009). DNA replication as a target of the DNA damage checkpoint. DNA Repair (Amst) *8*, 1077-1088.

Zhang, Z., Hayashi, M.K., Merkel, O., Stillman, B., and Xu, R.M. (2002). Structure and function of the BAH-containing domain of Orc1p in epigenetic silencing. EMBO J *21*, 4600-4611.

Zhang, Z., and Reese, J.C. (2004). Redundant mechanisms are used by Ssn6-Tup1 in repressing chromosomal gene transcription in Saccharomyces cerevisiae. J Biol Chem *279*, 39240-39250.

Zhang, Z., Shibahara, K., and Stillman, B. (2000). PCNA connexts DNA replication to epigenetic inheritance in yeast. Nature *408*, 221-225.

Zhao, X., Muller, E.G., and Rothstein, R. (1998). A suppressor of two essential checkpoint genes identifies a novel protein that negatively affects dNTP pools. Mol Cell *2*, 329-340.

Zhao, X., and Rothstein, R. (2002). The Dun1 checkpoint kinase phosphorylates and regulates the ribonucleotide reductase inhibitor Sml1. Proc Natl Acad Sci U S A *99*, 3746-3751.

Zhou, H., Madden, B.J., Muddiman, D.C., and Zhang, Z. (2006). Chromatin assembly factor 1 interacts with histone H3 methylated at lysine 79 in the processes of epigenetic silencing and DNA repair. Biochemistry *45*, 2852-2861.

Zhou, Z., and Elledge, S.J. (1992). Isolation of crt mutants constitutive for transcription of the DNA damage inducible gene RNR3 in Saccharomyces cerevisiae. Genetics *131*, 851-866.

Zou, L., and Elledge, S.J. (2003). Sensing DNA damage through ATRIP recognition of RPA-ssDNA complexes. Science *300*, 1542-1548.

Zou, L., and Stillman, B. (2000). Assembly of a complex containing Cdc45p, replication protein A, and Mcm2p at replication origins controlled by S-phase cyclin-dependent kinases and Cdc7p-Dbf4p kinase. Mol Cell Biol *20*, 3086-3096.